Tagging of the Type Three Secretion System Basal Apparatus of Enterohaemorrhagic *Escherichia coli* O157:H7

James Emmerson

B.Sc. (Durham)

Thesis presented for the degree of

Doctor of Philosophy

The University of Edinburgh

2008

Declaration

I hereby declare that this thesis is my own work and has not been submitted at any other University for any award. Where other sources of information have been used they have been acknowledged.

James Emmerson

Acknowledgments

I would like to thank my two supervisors Prof. David Gally and Prof. Mike Shipston for their support. Prof. Mike Shipston was always keen to meet and discuss the project. His expertise in imaging technologies and his unique perspective on the project provided endless assistance and encouragement. Prof. David Gally offered continual guidance, enthusiasm and advice throughout my project and has shown a genuine interest in my work and future career. Without Prof. Gally as my primary supervisor I doubt this project would have been completed!!

I would also like to thank the staff and students of the ZAP lab and the other Bacteriology groups based at the Medical School, whose help over these years has been greatly appreciated. I would like to separately thank Ms Denise Hutchison for providing excellent research assistance, including endless agar plates and interesting stories! A special thanks to Dr. Alison Low, who was patient and kind when teaching me microbiological techniques all those many years ago... Also special thanks to Luke Tysall, Dai Wang, Allen Flockhart, Bethan Lowder, Tracy Rosser, Tracy Dransfield, Pablo Nart, Karla Sanchez, Allison Wroe, Sean McAteer, Andy Roe, Nicola Holden, Ross Fitzgerald and the remaining LBEP girls (Jeanette, Nouri, Caitriona, Gill and Shruti) for making my PhD such an enjoyable experience. A massive thank you goes to Makrina Totsika for being 'joined at the hip' with me for four years! Becoming your friend has been the highlight of my time in the ZAP lab.

I would also like to thank all my friends who have supported me. Although the list would be too long to write here, I would like to separately mention Faye Gatenby, Alan Cox and Helen Yull for the positive influence they have had on my life over all these years.

Finally I would like to thank my family, Denise, Neil, Mark and Sarah. I owe my achievements to your continued support, love and understanding.

Contents

Common Abbreviations

A	Alanine
AAP	Antarctic alkaline phosphatase
ADP	Adenosine diphosphate
A/E	Attaching and effacing
Ala	Alanine
AMP	Adenosine monophosphate
Ap^R	Ampicillin resistance
APS	Ammonium persulfate
Asp	Aspartic acid
ATP	Adenosine triphosphate
bp	Base pairs
BSA	Bovine serum albumin
C1-INH	C1 esterase inhibitor
^oC	Degrees Celsius
Ces	Chaperone for *E. coli* secretion
CFP	Cyan fluorescent protein
CFTR	Cystic fibrosis transmembrane regulator chloride channel
CFU	Colony forming unit
cGMP	Cyclic guanosine monophosphate
CID	Centre for infectious diseases
Cm^R	Chloramphenicol resistance
CTAB	Hexadecyltrimethyl ammonium bromide
C terminus	Carboxy-terminus
D	Aspartic Acid
DAEC	Diffusely Adherent *E. coli*
dH_2O	Distilled water
DNA	Deoxyribonucleic acid
dNTP	Deoxyribonucleotide triphosphate

DMSO	Dimethyl sufoxide
DTT	Dithiothreitol
E	Glutamic acid
EAEC	Enteroaggregative *E. coli*
E. coli	*Escherichia coli*
ECL	Enhanced chemiluminescence
EDTA	Ethylenediamine tetraacetic acid
eGFP	Enhanced GFP
EHEC	Enterohaemorrhagic *Escherichia coli*
EIEC	Enteroinvasive *E. coli*
EPEC	Enteropathogenic *E. coli*
Esc	*E. coli* secretion protein
Esp	*E. coli* secreted protein
ETEC	Enterotoxigenic *E. coli*
F	Phenylalanine
FlhB	Flagellar gene (in flagellar region II within the chromosome)
FRET	Fluorescence resonance energy transfer
g	G-force
G	Glycine
Gb3	Globotriaosylceramide
GFP	Green fluorescent protein
Glu	Glutamic acid
Gly	Glycine
GrlA	Global regulator of LEE-activator
GrlR	Global regulator of LEE-repressor
H	Histidine
HA	Haemagglutinin
HC	Haemorrhagic colitis
hr	Hour(s)
His	Histidine

HRP	Horseradish peroxidase
HUS	Haemolytic uraemic syndrome
IHF	Integration host factor
H-NS	Histone-like non-structural proteins
IgG	Immunoglobulin G
IPTG	Isopropyl β-D-1-thiogalactopyranoside
K	Lysine
Kb	Kilobase(s)
kDa	KiloDalton(s)
Kn^R	Kanamycin resistance
L	Leucine
LB	Luria-Bertani
LBA	Luria-Bertani with ampicillin
LBC	Luria-Bertani with chloramphenicol
LBK	Luria-Bertani with kanamycin
LEE	Locus for Enterocyte Effacement
Ler	LEE regulator
LPS	Lipopolysaccharide
Lrp	Leucine-responsive regulatory protein
LT	Heat labile enterotoxin
M (following a number)	Molarity
M	Methionine
MEM-HEPES	Minimal essential media with HEPES modification
min	Minute(s)
ml	Millilitre(s)
MQ	Milli-Q water
mRNA	Messenger ribonucleic acid
µg	Microgram(s)
µl	Microlitre(s)

μM	MicroMolar
N	Asparagine
NAD	Nucleotide adenine dinucleotide
NEB	New England Biolabs
ng	Nanogram(s)
Nle	Non-LEE encoded
nm	Nanometer(s)
ns	Nanosecond(s)
OD_{600nm}	Optical density measured at 600nm wavelength
ORF	Open reading frame
P	Proline
PBS	Phosphate buffered saline
PCR	Polymerase chain reaction
PFA	Paraformaldehyde
pH	Power of hydrogen
PMSF	Phenylmethylsulphonyl fluoride
Pro	Proline
RAJ	Recto-anal-junction
REase	Restriction endonuclease
rfu	Relative fluorescence unit(s)
rpm	Revolution(s) per minute
S	Serine
SDS	Sodium dodecyl sulphate
SDS-PAGE	Sodium dodecyl sulphate-polyacrylamide gel electrophoresis
sec	Second(s)
Sep	Secretion of *E. coli* proteins
Ser	Serine
SOC	Salt-optimised and carbon
ST	Heat stable enterotoxin
STEC	Shiga-like toxin producing *E. coli*

Stx	Shiga-like toxin
T	Threonine
T2SS	Type II secretion system
T3S	Type III secretion
T3SS	Type III Secretion System
T_a	Annealing temperature
TBE	Tris-borate/EDTA
Tc^R	Tetracycline resistance
TCA	Trichloroactetic acid
TEMED	N,N,N',N'-Tetramethylethylene diamine
TFB	Transformation buffer
Tir	Translocated intimin receptor
Tris	Trishydroxymethylaminomethane
Tyr	Tyrosine
U	Enzyme unit
V (following a number)	Volt(s)
V	Valine
Val	Valine
VT	Vero cytotoxin
VTEC	Vero cytotoxin producing *E. coli*
Y	Tyrosine
YFP	Yellow fluorescent protein
Yrs	Years
Ysc	*Yersinia* secretion protein
ZAP	Zoonotic animal pathogens

List of Figures

List of Tables

Abstract

Like many Gram negative bacterial pathogens Enterohaemorrhagic *Escherichia coli* (EHEC) O157:H7 possesses a type III secretion system (T3SS). The T3SS translocates effector proteins into host cells during infection and consists of a basal apparatus that spans the inner and outer membranes and a needle and filament complex. The basal apparatus is composed of ~20 proteins that are highly conserved between bacterial species, but despite this homology little is known about the EHEC basal apparatus.

The aim of this project was to label inner membrane basal apparatus proteins with fluorescent markers or immunogenic tags in order to investigate their function, regulation and localization. Cloning strategies were designed to insert tags at the 3' end of eight genes encoding putative inner membrane proteins and to use these fusions to replace the wild type sequences by allelic exchange.

From the eight strategies, *escR* and *escU* were taken forward to produce five EHEC O157:H7 strains. One strain contained EscR labelled at the C-terminus with an HA (haemagglutinin) epitope tag and the other four strains contained different labelled versions of EscU. Work with these strains demonstrated that the T3SS could not be visualized using fluorescence microscopy. However, Western blot analysis did show that the EscU protein was cleaved into 30kDa and 10kDa peptides, both of which localized to the membrane fraction of the bacterial cell. This cleavage was most likely occurring at the conserved cleavage site NPTH, which is present in the homologous proteins YscU from *Yersinia pseudotuberculosis* and FlhB from the flagella basal apparatus of *Salmonella* Typhimurium.

Interestingly all the mutant strains constructed did not secrete a detectable level of EspD, apart from one fusion that had previously been shown to cleave the tag from EscU. This indicated that, despite the small size of the HA tag, all the tags interfered with the function of EscR or EscU. Fusions to the 10kDa fragment of EscU, along with a deletion of this domain, were used to elucidate its function in the T3SS. All the EscU mutants did

not form EspA filaments, secrete EspD at wild type levels or secrete detectable levels of Tir, while the expression from the LEE1-5 promoters remained unaffected. These phenotypes could not be restored upon supplying the 10kDa peptide *in trans*.

Based on these results and previous work with the EscU homologues; it is proposed that the uncleaved EscU protein is needed to secrete EscF. After a defined period EscU is cleaved (possibly auto-catalytically) and this allows the secretion of EspA, B and D. The lack of wild type EscU in the mutant strains may not allow EscF to be secreted or assembled correctly and this in turn leads to the inhibition of EspA, B and D translocation.

An anti EscF antibody was obtained and used to detect EscF in cell fractions of the mutant EscU strains. Western blot analysis with this antibody detected a protein of the estimated size for EscF; however, similar size bands were still detectable in a LEE4 deletion strain (containing no *escF*). Progression of the research requires EscF secretion to be measured in order to establish whether the carboxy-terminal of EscU is essential for EscF export in EHEC O157:H7.

In conclusion, the project utilized a complex strategy to produce single copy gene fusions to basal apparatus proteins. This approach was taken to elucidate the function, localization and interactions of basal apparatus proteins whilst causing minimal changes to sequence, expression and copy number. Even so, it was evident that even minimal changes were not tolerated and inhibited secretion by the system. Future research will have to proceed with either alternative target proteins or the generation of high affinity antibodies coupled with sensitive imaging technology.

Chapter 1
Introduction

1. Introduction

1.1 An introduction into *Escherichia coli*

The genus *Escherichia* is a member of the Enterobacteriaceaen family that have their principal habitat in the bowel of humans and animals. Commensal strains of *E. coli* usually colonise the gastrointestinal tract within a few hours of birth and rarely cause disease (Kaper, J., *et al* 2004).

E. coli are short, straight Gram negative bacilli. They are facultative anaerobes that can grow rapidly by respiratory metabolism and by fermentation (Nataro, J., *et al* 1998). Their serological characteristics depend on a number of antigens. The somatic lipopolysaccharide O-antigen, the flagella H-antigen, and the capsular K-antigen, form the basis of the modified Kauffmann typing scheme where a specific combination of O and H antigens defines the serotype of an isolate (Nataro, J., *et al* 1998, Orskov, I., *et al* 1977).

1.2 Diarrhoeagenic *E. coli*

As a pathogen *E. coli* has acquired colonisation and virulence factors, which allow it to cause disease in several body systems; including urinary tract infections, septicaemia, meningitis and diarrhoea. The *E. coli* that cause diarrhoea are categorised into six main pathogenicity groups depending on virulence properties, mechanisms of pathogenicity, clinical symptoms and serology (Kaper, J., *et al* 2004, Wasteson, Y., 2001).

1. **Enteroinvasive *E. coli* (EIEC)**
2. **Enterotoxigenic *E. coli* (ETEC)**
3. **Enteroaggregative *E. coli* (EAEC)**
4. **Diffusely Adherent *E. coli* (DAEC)**
5. **Enteropathogenic *E. coli* (EPEC)**
6. **Enterohaemorrhagic *E. coli* (EHEC/STEC/VTEC)**

1.2.1 Enteroinvasive *E. coli* (EIEC)

EIEC are associated with dysentery like disease, a disease involving the inflammation of the lining of the large intestine, causing stomach pains and diarrhoea. It is a large contributor to paediatric diarrhoea and has been associated with as much as 5% of diarrhoea and 20% of dysentery cases in developing countries (Pacheco-Gil, L., *et al* 2006). Where EIEC infections are common asymptomatic human excretors are found. In Western Europe EIEC is rarely isolated but the exact number of infections may be under estimated because of misdiagnoses due to its similarity with dysentery caused by *Shigella* (Beutin, L., *et al* 1997). The site of infection for EIEC is the colon and the diarrhoea tends to contain blood and mucus. EIEC is able to invade and multiply within the colonic epithelia cells (Kaper, J., *et al* 2004, Wasteson, Y., 2001).

1.2.2 Enterotoxigenic *E. coli* (ETEC)

ETEC strains are a major cause of disease in infants in developing countries and travellers. Worldwide ETEC is considered to be the most common cause of *E. coli* mediated diarrhoea. Its prevalence in the developing world results in 650 million cases a year and approximately 800,000 deaths (Turner, S., *et al* 2006). ETEC infection leads to a sudden onset of diarrhoea that can lead to severe dehydration and death. Where hygiene levels are high ETEC is not considered to be a significant pathogen, but it is a problem for travellers to the developing world and military personnel. ETEC also affects young animals such as calves, lambs and neonatal and post weaning piglets, leading to financial loss (Wasteson, Y., 2001). ETEC produces colonisation factors that allow the bacteria to attach to the intestinal mucosa. After the close contact is established ETEC produce one or more cytotoxin, which induce fluid secretion and/or inhibit absorption in the gut (Turner, S., *et al* 2006). These cytotoxins include:

1.2.2.1 Heat Labile Enterotoxin

The heat labile enterotoxin (LT) is the most characterised virulence factor of ETEC due to its similarity to the *Vibrio cholerae* enterotoxin (choleragen). Mature LT is 84kDa and consists of six subunits: one 28kDa A subunit and five 11.6kDa B subunits. Once in the

intestinal tract the B subunits mediate the entry of the A subunit into the host cell by binding to ganglioside receptors on the intestinal mucosal cell (enterocyte) membrane. Each B subunit binds to one receptor, when all five are bound the A subunit is internalised. Once inside the cell the A subunit is activated by proteolytic cleavage into two domains and becomes a functioning adenosine-ribosyl transferase. It acts by transferring ADP-ribose from nucleotide adenine dinucleotide (NAD) to the stimulatory guanine nucleotide-binding regulatory protein subunit of the adenylate cyclase system. This stimulates the adenylate cyclase system causing elevated levels of cyclic AMP, up to 100-fold of normal levels. This leads to increased secretion of calcium ions and impaired absorption of sodium ions, causing water to leave the cells due to osmotic effects, resulting in diarrhoea. There are two main subgroups of LT: LT-I and LT-II (with LT-I being most closely related to choleragen). These sub groups are distinguished by their different B subunits that bind to different ganglioside receptors (Sussman, M., 1997, Turner, S., *et al* 2006).

1.2.2.2 Heat Stable Enterotoxin

The heat stable enterotoxins (ST) can be categorized into two distinct groups: STa (STI) and STb (STII). Both types are synthesised as pre-pro-peptides of 72 amino acids that are processed during their export to an active toxin of just 18 or 19 amino acids (Turner, S., *et al* 2006). STa binds to host surface receptors and leads to an increase in intracellular cGMP levels, which activates the cystic fibrosis transmembrane conductance regulator chloride channel (CFTR). This activation enhances the secretion of water and salt and inhibits the absorption of sodium, causing secretory diarrhoea. STb, which is mostly associated with porcine infections, is also processed during translocation across the membrane from a 72 amino acid protein to a 48 amino acid toxin. The toxin binds to sulphatide and is internalised into the host cell where it causes an influx of calcium, which leads to the opening of ion channels (possibly CFTR) (Sussman, M., 1997, Turner, S., *et al* 2006).

1.2.3 Enteroaggregative *E. coli* (EAEC)

EAEC were first characterised in 1987 when stool cultures from Chilean children helped distinguish the EAEC strains from EPEC (Nataro, J., *et al* 1987). Their characteristic adherence is seen on HEp-2 cells where they bind in a 'stacked brick' formation. EAEC colonise the mucosa (most likely the colon) and enhance mucus secretion creating a mucus-bacterium biofilm. Their role as a causative agent of diarrhoea has been highly debated but studies have linked EAEC with diarrhoea in both developing and developed countries, particularly with persistent paediatric diarrhoea. Typically EAEC infection causes a watery, mucoid, secretory diarrhoea with low grade fever and little or no vomiting, but up to one third of all the cases can present with grossly bloody stools. Although some EAEC strains have been shown to contain toxins and adhesins, they are not found uniformly in all strains that cause diarrhoea (Wasteson, Y., 2001, Weintraub, A., 2007).

1.2.4 Diffusely Adherent *E. coli* (DAEC)

DAEC are named diffusely adherent due to their adherence to HEp-2 cells, where they do not produce microcolonies like EPEC. The association of DAEC with diarrhoea is not strong and only a few studies have been carried out on the clinical symptoms. However, there may be an age dependant susceptibility to DAEC and infection seems to manifests itself as watery diarrhoea with no blood in the stools (Nataro, J., *et al* 2004). Two fimbrial adhesins have been identified in DAEC which mediate the diffuse adherence; they are fimbrial adhesin F1845 and AIDA-I but the pathogenesis of the disease is still unknown (Torres, A., *et al* 2005).

1.2.5 Enteropathogenic *E. coli* (EPEC)

EPEC is responsible for significant mortality and morbidity worldwide as it is a leading cause of diarrhoea in infants under 2 years of age. It produces profuse watery diarrhoea, colonising the small intestine. Whilst the exact mechanism of diarrhoea remains obscure a three stage model of infection was proposed in 1992 by Donnenberg and Kaper (Donnenberg, M., *et al* 1992). This model used genetic evidence to upgrade the previous

two stage model and further dissected and separated EPEC's mode of action on epithelial cells. The model consists of a first stage of localized adherence, followed by a second stage of signal transduction and a final intimate adherence stage. Although vastly simplified it has proven to be robust enough to accommodate recent understandings of how EPEC utilises its virulence factors to colonise and cause diarrhoea (Clarke, S., *et al* 2003). The intimate attachment of EPEC to the intestinal epithelium, by the type III secretion system (T3SS), causes disruption of the ionic balance in the intestine by effacing microvilli. The effacement process requires three effector proteins (Map, EspF and Tir) and leads to the retention of detached microvillar material (Dean, P., *et al* 2006). The onset of diarrhoea in volunteers can occur as little as 2.9hr after ingestion of EPEC, indicating that active secretion is involved with a variety of intestinal ion transporters affected (Nataro, J., *et al* 1998).

1.3 Enterohaemorrhagic *E. coli* (EHEC/STEC/VTEC)

EHEC is the last of the six categories of diarrhoeagenic *E. coli* and is the organism studied in this project. To understand the different nomenclature (EHEC/STEC/VTEC) it is important to put the emergence and classification of EHEC/STEC/VTEC in chronological order. In 1977 Konowalchuk *et al* (Konowalchuk, J., *et al* 1977) found a cytotoxin present in culture filtrates in 10 of 136 *E. coli* strains. This toxin induced a cytotoxic response in Vero cells, distinct from the effect of the heat labile cytotoxin. Later in 1982 O'Brien *et al* (O'Brien, A., *et al* 1982) reported a cytotoxic effect of extracts from lysed *E. coli* on HeLa cells that was neutralised with anti-sera to shiga toxin from *S. dysenteriae* type I, this identified Shiga-like toxin producing *E. coli* (STEC) strains. The previous described assay (Konowalchuk, J., *et al* 1977) was then used by Karmali *et al* (Karmali, M., *et al* 1983b) in a study that linked sporadic cases of haemolytic uraemic syndrome (HUS) with faecal cytotoxins and cytotoxin-producing *E. coli*. Again, the cytotoxin was found to be active on Vero cells, less so on HeLa cells and inactive on W138 cells and termed Verotoxin (VT). The study found that 11 out of 15 (73%) of the HUS cases had evidence of infection by these VT positive *E. coli* (VTEC), suggesting a high association between the VT producing *E. coli* and the

disease. However, when O'Brien *et al* published again (O'Brien, A., *et al* 1983), they showed that a VTEC strain from the study by Konowalchuk *et al* in 1977 produced the Shiga-like toxin (Stx). After further analysis O'Brien *et al* deduced that the two toxins (the Verotoxin and the Shiga-like toxin) were the same toxin, having an identical molecular weight, subunit structure and cytotoxic effect on Vero cells. Late in 1983, Karmali *et al* (Karmali, M., *et al* 1983) proposed that it was the Verotoxin/Shiga-like toxin that was responsible for the clinical symptoms of haemorrhagic colitis (HC) and HUS and that both these conditions originated from the same disease – an infection with EHEC. From this publication history two terms emerged to describe the same strains of *E. coli*; Verotoxin producing *E. coli* (VTEC) and Shiga-like toxin producing *E. coli* (STEC) with EHEC classified as a VTEC/STEC strain that is associated with disease (particularly HC and HUS) and forms attaching and effacing (A/E) lesions. This is an important distinction as some strains of VTEC/STEC are not pathogenic, whilst by definition all strains of EHEC are capable of causing disease (Nataro, J., *et al* 1998).

Riley *et al* reported the first outbreaks of EHEC O157:H7 in 1983 after investigating two outbreaks in 1982, one in Oregon and one in Michigan. These outbreaks were of a gastrointestinal illness that affected at least 47 people. It was characterised by grossly bloody diarrhoea and little or no fever, symptoms that were termed haemorrhagic colitis (HC). Riley *et al* traced the outbreak back to the consumption of undercooked beef patty in a fast food restaurant chain. Stool analysis from the patients found 9 out of 12 samples contained the previously rarely isolated serotype of EHEC O157:H7, which was shed within 4 days of the onset of HC (Riley, L., *et al* 1983).

1982 and 1983 saw an eventful time for EHEC O157:H7, with the serotype being linked to outbreaks in America, where it was responsible for causing serious diseases. However, it was not until data published by the Public Health Laboratory (London, UK) was taken into account that the importance of these outbreaks could be interpreted. In 1983 Day *et al* (Day, N., *et al* 1983) reported that between 1978 and 1983 the Public Health Laboratory had catalogued 15,000 serotypes of *E. coli*, of which only 28 were of

the serotype O157 and only 1 of these was of the H type 7. Over the previous ten years (1973 – 1983) the Public Health Laboratory had received strains from 161 outbreaks of *E. coli* and non of them were attributed to O157. It could only be concluded that previous to 1983 O157:H7 was not an important cause of outbreaks or sporadic cases of diarrhoea in the UK. This conclusion was echoed in America and Canada after similar reviews of previously catalogued strains. It meant that in 1983 EHEC O157:H7 was a new emerging pathogen (Nataro, J., *et al* 1998).

1.3.1 Haemolytic Uraemic Syndrome (HUS)

Since 1982 the reported cases of EHEC infections have increased world wide, with large outbreaks in Japan, Scotland and the USA. In an EHEC surveillance and prevention meeting (WHO; Reilly, A., 1998) outbreaks were reported in USA, Canada, England and Wales, Scotland, Germany, Denmark, South America and in many of the African countries where diagnosis and serotyping was possible. Of these outbreaks 1-10% of all the cases develop HUS, a life threatening disease. Karmali *et al* (Karmali, M., *et al* 1983) linked the cause of HUS with the production of the Stx toxin and that link remains today, although the exact mechanism is still unknown. However, studies of the large outbreaks, such as the Sakai City outbreak in Japan in 1996, where over 9000 cases were reported, have led to treatment plans for patients presenting with HUS and can correlate the progression of an EHEC infection to the HUS complication (Honda, X., *et al* 1999, Yoshioka, K., *et al* 1999). Complete HUS is defined by three main symptoms:

1) Haemolytic anaemia (anaemia and fragmented red blood cells).
2) Thrombocytopenia (platelets, 100 000/μL or less).
3) Acute renal dysfunction (oliguria, anuria or increased serum creatine).

With the associated symptoms:

1) Central nervous system damage (loss of consciousness, convulsions, headaches etc).
2) Pancreatitis.

(Yoshioka, K., *et al* 1999)

Several risk factors have been identified that correlate with the progression of an EHEC infection to HUS, they include:

1) Age: either very young or very old.
2) Mental retardation.
3) The presence of bloody diarrhoea.
4) A weaker expression of P antigen on red blood cells.
5) Anti-motility agents and anti-diarrhoeal agents.
6) The use of antimicrobials.

(Honda, T., 1999)

The treatment regime of EHEC infections and HUS remains controversial, with the use of certain antibiotics making the illness worse. During the Sakai City outbreak the antibiotic fosfomycin was given to 84% of patients within 5 days of presenting with symptoms and found not to correlate with the progression to HUS (Honda, T., *et al* 1999). However, there are reports that fosfomycin causes a 13 to 16 fold increase of the amount of Stx in the supernatant of cultures grown in minimum inhibitory concentration (Yoh, M., *et al* 1997). It has been documented that antibiotics such as quinolones, that induce the bacterial 'SOS' response to DNA damage, cause an increase in the level of free faecal Stx in mice whilst decreasing the actual amount of faecal VTEC (Zhang, X., *et al* 2000). With antibiotics often prescribed before the cause of an infection has been ascertained there are concerns about the link between the antibiotic used and the onset of HUS. The use of anti-diarrhoeal agents and anti motility agents were also seen to increase the likelihood of developing HUS (Honda, T., 1999). The use of IgG, which contains antibodies to Stx1, and dialysis coupled with plasma exchange have yielded some success in treating both complete and incomplete forms of HUS (Yoshioka, K., *et al* 1999).

1.3.2 Epidemiology of EHEC O157:H7

1.3.2.1 Bovine Reservoir of EHEC O157:H7

In 1986 60 children and 14 adults visited a dairy farm in Southwest Ontario; of these 74 individuals, 48 became ill with abdominal cramps and watery diarrhoea. An EHEC O157:H7 infection was diagnosed in 43 of the cases, with significant association between infection and the consumption of unpasteurised milk on the farm. The faecal samples of 67 healthy cows from the farm were screened for the presence of EHEC, identifying 7 EHEC positive animals, two of which were positive for O157:H7, while the others were not serotyped. This was the first direct evidence that cattle were the primary reservoirs of EHEC O157:H7 and that colonised cattle were asymptomatic (Borczyk, A., *et al* 1987)

Cattle are considered the main reservoir for EHEC O157:H7, with 10% of cattle carrying EHEC O157:H7 in their faeces. Although EHEC O157:H7 could be detected in the faeces of cattle there was some debate as to its localization within the bovine host as it was infrequently found in the gastrointestinal tract. It was later found that EHEC O157:H7 has a specific tropism for the recto-anal-junction (RAJ) at the terminal rectum (Naylor, S., *et al* 2003). The main area colonised was 3-5cm proximal to the RAJ and explained its previous lack of detection, as this site had not been sampled before. Its colonisation at such high proximity to the anal opening also explained the observed faecal distribution of the bacteria, with more bacteria found on the surface of faeces compared to the core, indicating that EHEC O157:H7 lined the outside of the faeces during their final stages of compaction and excretion (Naylor, S., *et al* 2003). The RAJ localization was later confirmed with intact rectum samples from 267 cattle, where 35 animals were positive for EHEC O157:H7, with a region closest to the RAJ being the principle site for carriage. A high level of variation of the amount of EHEC O157:H7 detected in the faeces of individual animals was also observed, adding evidence to the existence of 'supershedders' (Low, J., *et al* 2005). These supershedders are identified by excretion of a high level of EHEC O157:H7 in their faeces ($>10^4 CFUmg^{-1}$) and have been identified in penned animals as the possible cause of infection of co-penned

animals (Cobbold, R., *et al* 2007). When considering EHEC O157:H7 epidemiology and infection control strategies, the supershedders are very important. In a mathematical model of an EHEC O157:H7 infected herd, supershedders account for only 20% of infected cattle but are responsible for 80% of the transmission of infection. Because these few supershedders are responsible for a disproportionate number of transmission events they provide a valid target for treatment. In fact, removing the suppershedding animals (5% of the herd) would control the spread of infection (Matthews, L., *et al* 2006). Interventions need only to stop this high bacterial carriage by capping bacterial carriage loads to below that of a supershedder (Matthews, L., *et al* 2006).

The easy access to the RAJ and the effect of eliminating high secretors from the herd in controlling the spread of infection has created the opportunity for easier prevention and detection techniques. One study used a direct application of an antiseptic to the RAJ, compared to orally treated calves, to great success, needing only one application to clear the EHEC O157:H7 infection. Swabs directly of the RAJ were used with a rapid immunochemical test kit, usually used for liquid cultures, at a sensitivity that would detect supershedders (Naylor, S., *et al* 2007). In conjunction these two methods can be used to identify supershedders in a herd and treat their infection to control the spread of EHEC O157:H7.

EHEC O157:H7 strains have been isolated from faeces or intestines of birds and animals but has only been shown as a causative agent of disease in cattle (calf dysentery) pigs (oedema disease) and dogs (Alabama rot), with a majority of animals carrying EHEC without disease (Wasteson, Y., 2001).

1.3.2.2 EHEC O157:H7 in the environment

In the USA there are an estimated 76 million cases of illnesses a year caused by food borne pathogens, costing the government approximately $6.7 billion. Of these illnesses more than 100,000 are estimated to be caused by EHEC O157:H7 and other shiga toxin producing *E. coli*, with EHEC O157:H7 causing over 250 deaths each year, although the

issue is made more complicated by the failure of many clinical laboratories to screen for this serotype (Mead, P., *et al* 1999, Natara, J., *et al* 1998, Tauxe, R., 2001). After being implicated in the outbreak in 1982 (Riley *et al* 1983) EHEC O157:H7 caused over 30 outbreaks in the USA in the following 10yrs. In 1993 a further 15 outbreaks were recorded and 20 outbreaks in the first half of 1994. With the increase in outbreaks more novel vehicles of transmission are starting to emerge. Ground beef, raw milk and person-to-person transmission still account for most cases, but acidic fruits, salad vegetables, yogurt and water have also been implicated (Feng, P., 1995).

There have been many cases of EHEC O157:H7 infection, some leading HUS, after consumption of unpasteurised apple cider. In 1996 in New Haven County, Connecticut 14 people were taken ill after consuming unpasteurised apple cider and five went on to develop HUS (Hilborn, E., *et al* 2000). In 1998 in Ontario, 66 people consumed contaminated apple cider with 10 people developing illness (Tamblyn, S., *et al* 1999). Both these cases are a result of the use of 'drop' apples to make apple cider. These apples have dropped from the tree onto the ground and cannot be marketed as fresh eating apples. Unfortunately, EHEC O157:H7 has been shown to persist in apple cider, which was previously thought to not be conducive to survival and growth of food pathogens due to its low pH (pH 4.0). However, EHEC O157:H7, whilst not growing can maintain its original population size in apple cider at pH3.7 and 8°C for 7-21 days. This timeframe can include the entire 2-3 week shelf life of apple cider (Zhao, T., *et al* 1993). It has also been shown that when faeces containing EHEC are deposited on grass the organism is transferred to the soil and can be detected after the faeces have decomposed. On soil with rooted grass EHEC O157:H7 was demonstrated to persist for several months (Wasteson, Y., 2001).

Recreational use of water can cause EHEC O157:H7 outbreaks. For example, in 1992 a children's paddling pool in Scotland became contaminated with EHEC O157:H7 by child defecation, the contaminated water infected two other children who infected others by person to person contact (Brewster, D., *et al* 1994). The first, but not the largest,

drinking water associated outbreak was in Missouri in 1989, where 243 people were infected, 32 hospitalised, 4 died and 2 developed HUS. It was traced to backflow during a water mains break (Swerdlow, D., *et al* 1992). The largest outbreak due to ingestion of contaminated water is still the outbreak in May 2000 in Walkerton, Ontario, Canada. The outbreak was caused by the towns drinking wells being contaminated by cattle faecal matter from a neighbouring farm following five days of heavy rainfall. 2,300 people were infected, 68 hospitalized with 4 confirmed fatalities (Hrudey, S., *et al* 2003). Any use of unchlorinated water as a supply for drinking water is a risk for EHEC O157:H7, this includes private drinking wells (most commonly found on small cattle farms) which are at risk for contamination with faeces from infected humans or animals due to sewage overflows, polluted storm water run off, or agricultural run off (Muniesa, M., *et al* 2006).

In 1985 chickens were put forward as a potential reservoir of EHEC O157:H7 for human infection. After challenging 1 day old chickens with EHEC O157:H7 the bacteria were still detectable in the cecae for 90 days post infection. Interestingly the infected chickens showed no physical response to the infection when compared to unchallenged birds. However, there was mild transient mucous membrane damage and A/E lesions were seen. The proximal end of the chicken cecae was the principle site of infection, which may possess specific receptors (Beery, J., *et al* 1985). Since then it has been shown that experimentally challenged chickens can shed EHEC O157:H7 up to 11 months post infection, possibly due to the bacteria penetrating and adhering to the epithelia of the ceca. EHEC O157:H7 was also detectable on 13.8% of eggs screened, coating the egg as the bacteria moved through the colon during faecal shedding (Schoeni, J., *et al* 1994). EHEC O157:H7 has also been shown to be present in intensive management hen farms in Southern Italy with 26 of the 720 samples from three different farms being positive for EHEC O157:H7 after swabs were taken from caged birds (Dipineto, L., *et al* 2006). This provides interesting evidence that poultry could have a role as a reservoir of EHEC O157:H7.

Due to its discovery in the 1980's, EHEC O157:H7 is considered to be an emerging pathogen. The discovery of cattle as a reservoir has meant that public health concerns must also include healthy animals and agricultural methods may need to be tightened due to the implication of contaminated fodder and water as a source of acquiring and transmitting EHEC O157:H7 amongst cattle (Tauxe, R., 1997). Since 1986 serological studies have suggested that the vast majority of cattle have been exposed to EHEC at some point in their lives. Although cattle appear to be the main environmental reservoir of O157:H7 epidemiological surveys have revealed that EHEC strains are also prevalent in the gastrointestinal tract of other domestic animals including sheep, pigs, goats, dogs and cats (Paton, J., *et al* 1998) and with the emergence of novel vehicles of infection this pathogen has become a serious threat to public heath.

1.3.3 Virulence factors of EHEC O157:H7

1.3.3.1 Shiga Toxin

As previously discussed EHEC O157:H7 can produce Shiga-like toxins (Stx), also known as Verotoxins (O'Brien, A., *et al* 1983). These toxins are the main virulence factor of EHEC and one of their defining characteristics. Stx is proposed to cause the clinical symptoms of an EHEC infection, which include: diarrhoea (lack of epithelium integrity in the intestine), HC (damage to endothelium of blood vessels in the intestine) and HUS (O'Brien, A., *et al* 1987). The severity of the EHEC infection and the clinical outcome depends largely on the type of Stx produced by the EHEC strain and the presence of the gene encoding intimin (Bielaszewska, M., *et al* 2006). The Stx family of toxins contain two major antigenically distinct groups, Stx1 and Stx2. In cross neutralisation experiments, with polyclonal antisera raised against the shiga toxin of *S. dysenteriae* type I, the toxic activity of Stx1 was neutralised, whilst Stx2 was not (Strockbine, N., 1986 *et al*). A single EHEC strain may express Stx1 or Stx2, both or even multiple forms of Stx2, with the toxin detectable in cell lysates and supernatants (Scotland, S., *et al* 1985, Strockbine, N., *et al* 1986). Stx1 from EHEC is homologous to the shiga toxin from *S. dysenteriae* type 1, while Stx2 has sequence variations. Whether a strain expresses Stx1 or Stx2 or both may play an important factor in clinical

management of an infection. Stx2 has been demonstrated to be more toxic when interacting with human intestinal microvascular endothelial cells (even though Stx1 binds at a higher affinity) and disruption of these cells may be the gateway to systemic circulation of Stx allowing it to reach the kidneys and brain (Jacewicz, M., *et al* 1999).

Due to the importance of Stx genes in the progression of EHEC O157:H7 infections to HUS it is important to limit the dissemination of the Stx genes through the induction of the phage that carries the gene. Treatment of EHEC infections with antibiotics that induce the bacterial 'SOS' response to DNA damage inadvertently increase the amount of Stx produced by inducing the phage, causing a greater likelihood of progression to HUS (Kimmit, P., *et al* 2000). This phage induction is also seen in antibiotics used in animal husbandry as growth promoters, where sub-inhibitory concentrations of antibiotics are used that lead to an increase of free phage particles in the intestine, which could promote the development of new VTEC pathotypes (Kohler, B., *et al* 2000). Free Stx2-encoding bacteriophages have been found in aquatic environments, but there is little information about the lysogenic strains and the bacteria in the environment susceptible to phage infection (Garcia-Aljaro, C., *et al* 2004). Even though it is conceivable that *E. coli* of any serotype can acquire the toxin genes it is believed the ability of the organism to produce the toxin alone does not confer pathogenicity, that a background of appropriate virulence factors is needed. In fact there is a strong association between Stx2 and the presence of the gene for intimin (*eae*) in strains of VTEC that cause human disease (Boerlin, P., *et al* 1999, Law, D., 2000).

The Stx family have a conserved basic A-B subunit structure. The receptor binding B subunits of Stx are arranged in a doughnut shaped pentamer and form a non polar pore that can be penetrated by the enzymatically active C terminus of the A subunit (Haddad, J., *et al* 1993). The single 32kDa A subunit is proteolytically nicked to yield a 28kDa peptide (A1) and a 4kDa peptide (A2), which remain linked by a disulphide bond. The A1 peptide has the enzymatic activity and the A2 peptide binds the A subunit to the pentamer of five identical 7.7kDa B subunits. The B pentamic ring encircles a helix at

the C terminus of the single A subunit (Paton, J., *et al* 1998) and binds the toxin to a specific glycolipid receptor, globotriaosylceramide (Gb3), which is present on the surface of certain eukaryotic cells (Lingwood, C., 1996). After binding the toxin it is internalised by receptor mediated endocytosis through coated pits and transported to the golgi apparatus and the endoplasmic reticulum (Sandvig, K., *et al* 1992). The A subunit is translocated to the cytoplasm and acts on the 60s ribosomal subunit, where the A1 peptide (a N-glycosidase) removes a single adenine residue from the 28S rRNA of eukaryotic ribosomes, inhibiting protein synthesis. The resulting disruption leads to cell death (Law, D., 2000, Lingwood, C., 1996).

Although very similar to the Shiga toxin from *S. dysenteriae* type 1, the Stx toxins from EHEC O157:H7 have some interesting structural differences which may account for their different mode of action and disease potential (Fraser, M., *et al* 2004). The Stx1 and Stx2 homopentameric B subunits also differ; when compared to Stx1, the Stx2 B subunit pentamer formation is less thermodynamically stable, with its assembly strongly dependent on temperature, subunit concentration and ionic strength. Its unstable nature may account for Stx2's perceived increase in toxicity (Kitova, E., *et al* 2005).

Stx translocates from the intestine into the blood stream and causes HUS by interacting with the Gb3 receptors on human renal tissue, particularly the Gb3 receptors found on blood vessels and capillaries (Nataro, J., *et al* 1998). To reach the susceptible tissues and cause the associated clinical symptoms of Stx positive VTEC infection, the Stx1 and Stx2 toxins must first cross the epithelial barrier and enter the blood stream (Paton *et al* 1998). *In vitro* Stx1, and to a lesser extent Stx2, can translocate across intestinal epithelium to reach the endothelial cell beds underneath. They translocate without having a cytotoxic effect on intestinal epithelium and finish the translocation process neither activated nor inactivated (Hurley, B., *et al* 1999). Evidence is conflicted in the significance of Stx in producing diarrhoea upon EHEC infection, Stx has been shown to preferentially target villus of the jejunum (due to their higher concentration of Gb3 receptors on the cell surface) in rabbit intestine, causing villus cell death and an

electrolyte imbalance (Kandel, G., *et al* 1989). However, it was also shown that the Stx toxins were not necessary to disrupt ion transport and cause diarrhoea, meaning other virulence factors must play a role in the onset of non-bloody diarrhoea (Li, Z., *et al* 1993).

In HUS immune interactions play an important role, with certain cytokines increasing the sensitivity of endothelial cells in the kidney to Stx (Kaye, S., *et al* 1993). In the brain, inflammatory cytokines increase the actual amount of Gb3 receptors present on human brain endothelial cells (Stricklett, P., *et al* 2002). It is also thought that there is a form of molecular mimicry, where Stx closely resembles CD36, a receptor present on platelets and microvascular endothelial cells. Antibodies for Stx are therefore cross reactive with CD36 and this cross reactivity may be the cause of platelet aggregation and kidney damage (Rock, G., *et al* 2005). In the bovine host EHEC O157:H7 does not cause infection, this may be part explained by the lack of vascular Gb3 receptors (Pruimboom-Brees, I., *et al* 2000) and the presence of the Gb3 receptor on crypt epithelial cells in the small and large intestine, which absorb Stx and limit its systemic effects (Hoey, D., *et al* 2002). Once in the crypt cells the toxin is destroyed in lysosomes (Hoey, D., *et al* 2003).

1.3.3.2. pO157

EHEC O157:H7 has a large 60MDa (9.2Kb) plasmid (pO157), which was shown to increase the strains adherence to Henle 407 intestinal and HEp-2 epithelial cell lines (Toth, I., *et al* 1990). In strains cured of the plasmid the growth, metabolic reactions and antibiotic resistance were identical to wild type strains. However, after oral administration to calves the cured strains survived passage through the bovine gastrointestinal tract better than the wild type strains but did not colonise the RAJ as well. This may indicate that cell lines are not an accurate representation of *in vivo* conditions (Lim, J., *et al* 2007). The presence of the plasmid encoded genes has been linked to adhesion and virulence. Originally the plasmid was thought to increase adherence by containing genes for fimbriae, but after sequencing no genes related to

known fimbriae were identified (Makino, K., *et al* 1998). Among the genes on the plasmid are genes for potential virulence factors, including: enterohaemolysin, (Schmidt, H., *et al* 1995), *toxB* which is homologous to Toxin B of *Clostridium difficile* and *efa-1* in non-O157:H7 EHEC strains (Stevens, M., *et al* 2004), *espP* which codes for a serine protease (Dziva, F., *et al* 2007), *stcE* a gene for a protease that cleaves C1 esterase inhibitor (Lathem, W., *et al* 2002) and genes that are homologous to the type II section system (T2SS) of other Gram negative bacteria (Schmidt, H., *et al* 1997).

1.3.3.2.1. Enterohaemolysin

Haemolysins belong to the RTX toxin family, named so because of the presence of nonomer repeats (repeats in toxin). The enterohaemolysin on the pO157 plasmid is toxic against human red blood cells (Bauer, M., *et al* 1996) but its involvement in virulence is still to be determined. The enterohaemolysin is found in all O157:H7 EHEC strains and sporadically in other EHEC serotypes, this may indicate an association between the gene and greater virulence and incidence of the EHEC strain (Law, D., *et al* 1995). Patients with HUS have antibodies in their sera reactive against the enterohaemolysin, however, very little of the toxin is secreted as its own secretion system is defective (Schmidt, H., *et al* 1995).

1.3.3.2.2 ToxB

ToxB shares 28% amino acid identity with EHEC Efa-1 (not present in O157:H7 serotypes), which is an important adherence factor to Chinese Hamster Ovary cells and 28% amino acid identity with the EPEC LifA, which has the ability to inhibit lymphocyte activation (Tatsuno, I., *et al* 2001). The *toxB* gene itself has been shown to be involved in full adherence to CaCo-2 cells and wild type levels of secretion and expression of proteins from the LEE (an important pathogenicity island in EHEC infection), however, a *toxB* mutant does not effect faecal shedding of 10-14 day old calves or 6 week old sheep (Stevens, M., *et al* 2004, Tatsuno, I., *et al* 2001).

1.3.3.2.3. EspP

EspP is a serine protease that cleaves pepsin and coagulation factor V. It has been shown to be important in the colonisation of calves by EHEC O157:H7 and adhesion to bovine rectal primary cells, although its mechanism of action is unclear (Dziva, F., *et al* 2007).

1.3.3.2.4 StcE

StcE is a zinc metalloprotease that specifically cleaves C1 esterase inhibitor (C1-INH) as well as mucin 7 and glycoprotein 340. The protein is secreted by the T2SS encoded on the pO157 plasmid and is involved in intimate adherence on HEp-2 cells (Grys, T., *et al* 2005). Its expression is also regulated by the LEE regulator Ler, indicating that it may be important during infection and colonisation at the same time as the genes on the LEE pathogenicity island (Lathem, W., *et al* 2002). Its mechanism is unclear, but it may degrade protective layers of mucin on host cells as well as anchoring the active C1-INH domain to the site of infection where C1-INH reduces inflammation and inhibits the activation of the complement immune system cascades (Grys, T., *et al* 2005).

1.3.3.2.5 Type II Secretion System (T2SS)

Thirteen genes closely related to the T2SS are found on pO157, named *etpC* to *etpO*. Although not a virulence factor, the pathway is used by Gram negative bacteria to secrete proteins, including toxins and has already been shown to be the mechanism by which StcE is translocated across the bacterial cell membrane (Schmidt, H., *et al* 1997, Lathem, W., *et al* 2002).

1.3.3.3 EAST1

The enteroaggregative *E. coli* heat stable enterotoxin 1 (EAST1) is only 38 amino acids long and 4.1kDa (Menard, L., *et al* 2004). EAST1 is encoded by the gene *astA*, has homology with the enterotoxic domain of STa and has been shown to increase cGMP levels in tissues that have been exposed to it (Savarino, S., *et al* 1993). The gene is not present in all EHEC strains but is present in EHEC O157:H7. Its link to disease has not been demonstrated in EHEC; however, atypical strains of EPEC with the *astA* gene are

more significantly associated with diarrhoea in children and are found in up to 15% of healthy cattle (Yuste, M., *et al* 2006).

1.3.3.4 Fimbriae

Although some fimbriae have been described and linked to adherence on tissue culture cell lines, such as Lpf1 and Lpf2 (Torres, A., *et al* 2002, Torres, A., *et al* 2004) not many have been visualised on EHEC O157:H7 or are functional. EHEC O157:H7 contains 16 recognisable fimbrial gene clusters, yet of 15 examined for expression only 4 expressed under a variety of conditions. This limited repertoire of expressed and functioning fimbrial genes may explain the RAJ tropism (Low, A., *et al* 2006b). One fimbrial operon (F9) does increase binding of K12 strains to bovine epithelial cells *in vitro*, but deletion of the fimbrial adhesin still leads to colonisation at the RAJ (Low, A., *et al* 2006). The regulation of the fimbrial operons and their influence on colonisation, still needs to be elucidated for the mechanism of tropism and adherence to be explained.

1.3.4 Type III Secretion System (T3SS)

The type III secretion system (T3SS) is used by many bacterial pathogens (such as *Yersinia, Salmonella, Shigella,* and *Pseudomonas*) to secrete proteins directly into host cells and is found exclusively amongst Gram negative bacteria (Heuck, C., 1998, Ghosh, P., 2004). EHEC uses the T3SS to translocate bacterial proteins into eukaryotic host cells to manipulate them during infection (Gruenheid, S., *et al* 2003). In EHEC, proteins with various functions are released through the T3SS that promote and sustain the unique interaction between the bacterium and the host cell (Deng, W., *et al* 2005). In cattle the T3SS of EHEC O157:H7 is required to maintain colonisation at the terminal rectum of the bovine gastrointestinal tract (Naylor, S., *et al* 2003).

The genes encoding the secretion apparatus are highly conserved among bacteria and may be products of horizontal transfer (Castillo, A., *et al* 2005). Much of what is known about the structure of the T3SS apparatus is based on extensive research investigating

the homologous flagellar assembly apparatus (Fig.2, C) and *Yersinia* T3SS (Blocker, A., *et al* 2003, Heuk, C., 1998).

1.3.4.1 Locus for Enterocyte Effacement and Attaching and Effacing Lesions

The genes for the EHEC and EPEC T3SS apparatus, and a series of secreted proteins including Tir and EspA, are situated on the locus for enterocyte effacement (LEE) (Goffaux, F., *et al* 2001). LEE sequences for EHEC and EPEC have been determined (Elliot, S., *et al* 1998, Perna, N., *et al* 2001, Goffaux, F., *et al* 1999), in EHEC the LEE is a large (~40Kb) genetic element (Perna, N., *et al* 1998). Secretion of the effector proteins encoded on the LEE, via the T3SS, is essential for signal transduction in host cells and the formation of attaching and effacing (A/E) lesions (Frankel, G., *et al* 1998, Knutton, S., *et al* 1998, Knutton, S., *et al* 1989). A/E lesions are a histopathological feature observed after infection with certain pathogens, including EHEC and EPEC (Naylor, S., *et al* 2005b). The A/E lesion is characterised by localised destruction (effacement) of the intestinal epithelial microvilli, intimate adherence between the bacterium and the epithelial cell membrane and the formation of an underlying pedestal-like structure in the host cell consisting of polymerised actin, alpha-actinin, ezrin, talin and myosin (Fig.1) (Finlay, B., *et al* 1996).

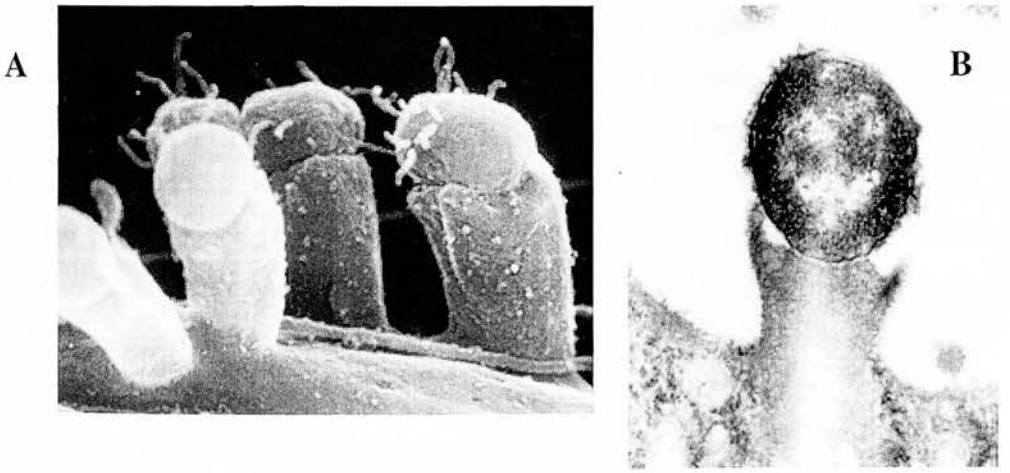

Fig.1. A/E lesions A) Scanning electron microscopy of EPEC pedestal formation on HEL cells (taken from Knutton, S., *et al* 1998) B) transmission electron microscopy of EHEC A/E lesion at the terminal region of infected cattle (taken from Naylor, S., *et al* 2005b).

It is worth noting that despite the LEE being highly conserved in diarrhoeagenic *E. coli* (Wieler, L., *et al* 1997) there are fundamental differences. For example; the LEE pathogenicity island of EHEC O157:H7 has high homology with the LEE of EPEC O127:H6, having the same genes in identical order and orientation. However, unlike EPEC, the LEE from EHEC is unable to form A/E lesions when cloned into an *E. coli* K-12 background, suggesting that there are unknown functional and/or regulatory differences (Elliot, S., *et al* 1999). These differences need to be considered as the majority of the literature concerning the T3SS in *E. coli* refers to strains of EPEC.

The LEE contains over 41 open reading frames (ORFs) of more than 50 amino acids, with at least five operons (LEE1-5) (Fig.2, A) (Elliot, S., *et al* 1998, Perna, N., *et al* 2001). Genes homologues to *Yersinia* T3SS genes are named '*E. coli* secretion' (*esc*) genes, genes without homology to *Yersinia* but with a defined role in secretion are named 'secretion of *E. coli*' proteins (*sep*) genes. Genes encoding secreted proteins and their chaperones are called *esp* (*E. coli* secreted proteins) and *ces* (chaperone for *E. coli* secretion) (Creasey, E., *et al* 2003). The remaining genes, like *eae* (that encodes the protein intimin) (Jerse, A., *et al* 1990), have either maintained their original name or are T3SS proteins with no homologues.

LEE1, 2 and 3 contain 22 ORFs and primarily encode proteins required for the basal apparatus of the T3SS, which spans the two bacterial membranes. LEE4 encodes EscF, SepL and the secreted proteins EspA, B, D, F (Mellies, J., *et al* 1999). These enable a translocon and pore to be formed, which secretes effector proteins into the host cell. The genes for the translocated intimin receptor (Tir), its chaperone (CesT) and intimin are located in LEE5. Other small operons and ORFs are also present, including one that encodes the mitochondrial associated protein, Map (ORF19) (Kenny, B., *et al* 2000).

A

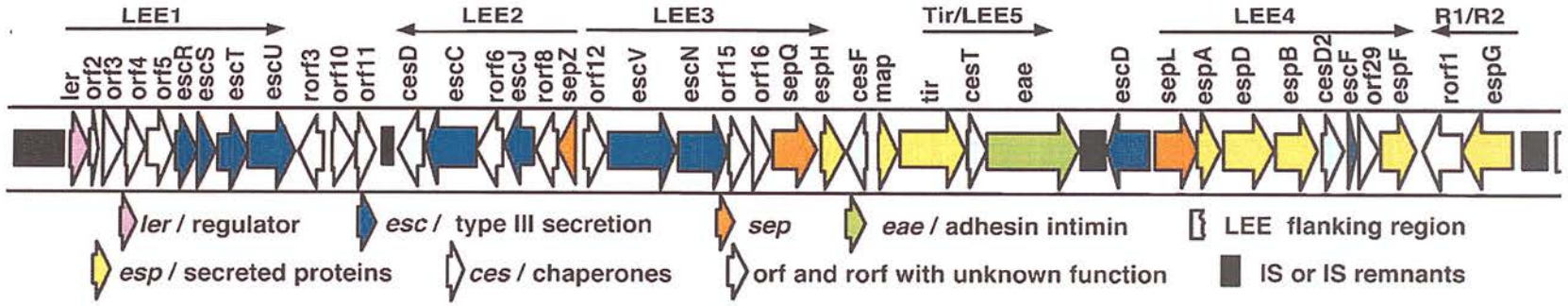
LEE1
LEE2
LEE3
Tir/LEE5
LEE4
R1/R2
ler
orf2
orf3
orf4
orf5
escR
escS
escT
escU
rorf3
orf10
orf11
cesD
escC
rorf6
escJ
rorf8
sepZ
orf12
escV
escN
orf15
orf16
sepQ
espH
cesF
map
tir
cesT
eae
escD
sepL
espA
espD
espB
cesD2
escF
orf29
espF
rorf1
espG
ler / regulator
esc / type III secretion
sep
eae / adhesin intimin
LEE flanking region
esp / secreted proteins
ces / chaperones
orf and rorf with unknown function
IS or IS remnants

B

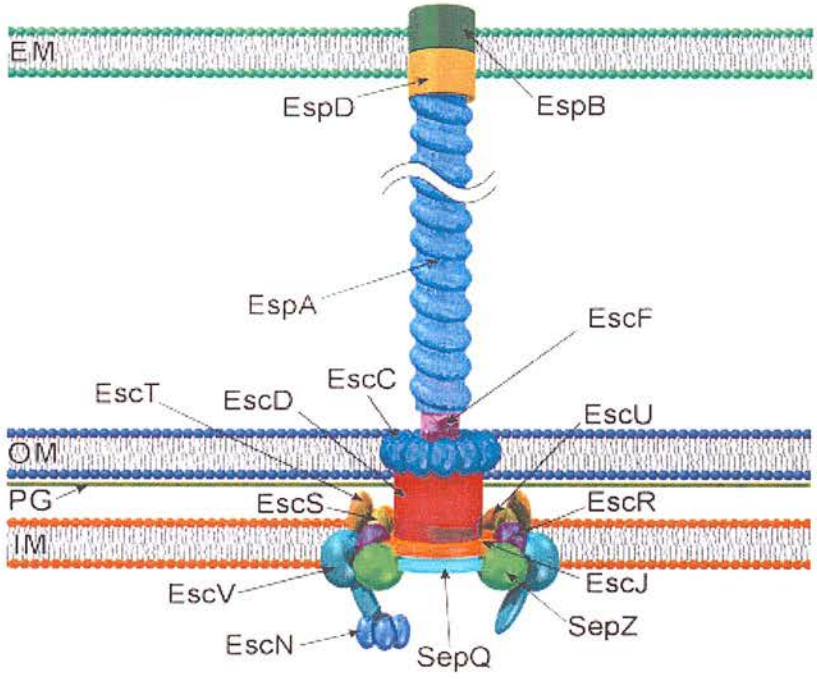
EM
EspD
EspB
EspA
EscF
EscT
EscD
EscC
EscU
OM
PG
EscS
EscR
IM
EscV
EscJ
SepZ
EscN
SepQ

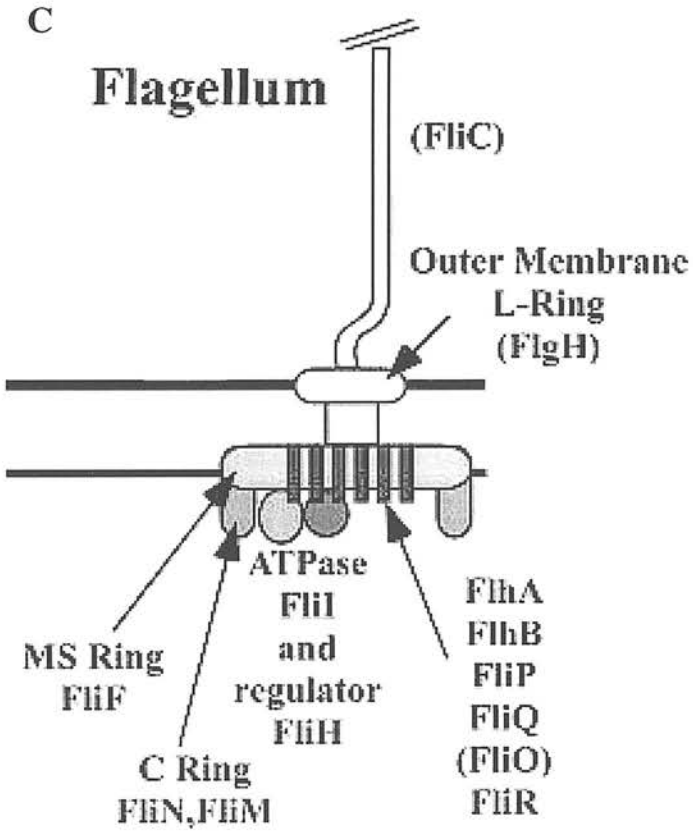

Fig.2 A) The genes present on the LEE from *Citrobacter rodentium* (taken from Deng, W., *et al* 2004), which are highly homologous to the EHEC and EPEC LEE genes. A semi-annotated picture of the LEE from EHEC (*ler* to *espF*) can be found in Pallen, M., *et al* 2005.
B) Diagram representing the T3SS apparatus of EHEC O157:H7 (taken from Pallen, M., *et al* 2005). EM, eukaryotic membrane, OM, outer membrane, PG, peptidoglycan layer, IM, inner membrane.
C) Diagram representing the flagellar apparatus of *Salmonella* (taken from Ghosh, P., 2004).

1.3.4.2 The Type III Secretion System Apparatus

The T3SS apparatus is composed of approximately 20 proteins (Blocker, A., *et al* 2003, Heuck, C., 1998, Ghosh, P., 2004). It consists of a basal apparatus that spans both the inner and the outer membrane with a short projecting needle composed of EscF (Sekiya, K., *et al* 2001). EscD, R, U, V, S and T, probably span the inner membrane and associate with a putative cytoplasmic ATPase EscN, required for the secretion of proteins. In EPEC, EscC is located in the outer membrane, where it is thought to form a large homomultimeric ring complex. Homology with *Shigella,* suggests the EscC ring is thought to project into the periplasm where it can interact with proteins to form the central rod (Gauthier, A., *et al* 2003b). The short projecting needle attached to the basal apparatus is composed of EscF, from which a filamentous structure composed of EspA extends (Ogino, T., *et al* 2006). The EspA filament interacts with EspB, which in turn interacts with EspD to form a pore in the host cell membrane (Fig.2, B) (Hartland, E., *et al* 2000, Ide, T., *et al* 2001).

Translocated proteins pass from the bacterial cytoplasm as fully translated proteins or are translated and translocated in a coupled step at the basal apparatus (Roe, A., *et al* 2003). They pass through the basal apparatus, the hollow needle and the EspA filament into the host cell via the EspB-EspD pore (Heuck, C., 1998).

The T3SS is essential for the translocation of effector proteins such as Tir, Map, EspF, EspH and EspG into the mammalian host cell (Shaw, R., *et al* 2005). Upon entering the host cell the effector proteins affect the brush borders and form A/E lesions.

1.3.5 LEE-Encoded Proteins

The majority of the proteins encoded on the LEE will now be discussed.

1.3.5.1 LEE-Encoded Regulator (Ler)

The LEE-Encoded Regulator (Ler) is a positive regulator of the LEE, homologous to Histone-like non-structural proteins (H-NS) (Pallen, M., *et al* 2005). H-NS binds

strongly to curved DNA and influences gene expression (Yamada, H., *et al* 1990). Ler has been shown to be essential for the expression of multiple LEE genes including *esp* and *esc* genes, *tir* and *eae*. Ler is also capable of activating the LEE operon promoters in a K-12 strain background (Elliott, S., *et al* 2000). The expression of *ler* has been shown to be influenced by a number of factors, including integration host factor (IHF), a DNA binding protein that bends DNA to form nucleoprotein complexes. IHF binds specifically upstream of the *ler* promoter, activating expression from *ler* (Friedberg, D., *et al* 1999). Quorum sensing has also been implicated in expression from *ler*. Quorum sensing is a mechanism by which bacteria can sense one another by detecting compounds called autoinducers. Fusions to *lacZ* have been used to show that the gene *luxS*, which produces the autoinducer AI-2, is important in increasing *ler* expression (Sperandio, V., *et al* 1999), as is QseA (an intermediary transcription factor in a quorum sensing signalling cascade) (Sharp, F., *et al* 2007). It would seem that multiple factors effect the expression from the *ler* promoter to relay environmental signals to the LEE and other genes, to assure correct timing of expression (Laaberki, M., *et al* 2006).

1.3.5.2 Orf2

Orf2 has homology with the *Yersinia* T3SS protein YscE and so it has been proposed to name it EscE (Pallen, M., *et al* 2005). YscE is needed for Yop secretion, as is Orf2 for T3S in *Citrobacter rodentium* (Allaoui, A., *et al* 1995, Deng, W., *et al* 2004). YscE is the smallest Ysc protein and is not broadly conserved amongst T3SS. It is a dimer in solution and its crystal structure has been elucidated (Phan, J., *et al* 2005). YscE interacts with YscG (thought to be the chaperone for YscE) and is not secreted out of the bacterial cell (Day, J., *et al* 2000). YscE was also shown to interact with TyeA, a homologue for the SepL protein in EHEC (Swietnicki, W., *et al* 2004), which indicates that EscE interacts with SepL (Pallen, M., *et al* 2005).

1.3.5.3 Orf3 (CesAB)

A yeast two-hybrid screen demonstrated an interaction between Orf3 (the protein from the uncharacterised *orf3*) and EspA and EspB (Creasey, E., *et al* 2003). Orf3 is now thought to be the chaperone for EspA and EspB and termed CesAB. A mutant in CesAB does not form A/E lesions, make EspA filaments or secrete EspB but expression from the LEE4 promoter is unaffected (Creasey, E., *et al* 2003b).

1.3.5.4 Orf4

Orf4 shows a homology to SsaK (Pallen, M., *et al* 2005). SsaK is a protein involved in the T3SS of *Salmonella*; it is thought to be hydrophilic with no predicted transmembrane helices (Hensel, M., *et al* 1997).

1.3.5.5 Orf5

Orf5 (EscL) shows homology with YscL from *Yersinia* T3SS and FliH from the flagellar system (Pallen, M., *et al* 2005). Two molecules of FliH bind to one molecule of FliI (the ATPase of the flagellar system, homologous to EscN in the EHEC T3SS) and down regulate the FliI ATPase activity (Auvray, F., *et al* 2002). YscL has a similar function as an ATPase regulator when it binds to YscN (ATPase of the *Yersinia* T3SS) it may also have a function in anchoring YscN to the T3SS (Blaylock, B., *et al* 2006).

1.3.5.6 EscR

EscR is predicted to be in the inner membrane basal apparatus of the EHEC T3SS (Ghosh, P., 2004). Little is known about EscR but it does interact with EscS, EscU, SepZ and EspD in yeast two-hybrid screens (Creasey, E., *et al* 2003). EscR is homologous to FliP in the flagella system and YscR in the *Yersinia* T3SS. FliP has been localised to the basal body of the flagellar secretion system (Fan, F., *et al* 1997) and undergoes cleavage of a signal peptide (Ohnishi, K., *et al* 1997).

1.3.5.7 EscS

EscS is predicted to be in the inner membrane, with a mass of ~10kDa (Ghosh, P., 2004) and interacts with EscR and EscD (Creasey, E., *et al* 2003). Its homologous protein in the flagellar basal body is FliQ (Pallen, M., *et al* 2005).

1.3.5.8 EscT

EscT is a predicted inner membrane protein of EHEC T3SS (Ghosh, P., 2004). Its homologous protein in the flagellar basal body is FliR (Pallen, M., *et al* 2005). In the *Salmonella* flagellar export system a FliR and FlhB (EscU homologue) fusion was made that could complement mutants of FliR and FlhB, indicating they interact with each other on a 1:1 ratio (Van Arnam, J., *et al* 2004). FliR has also been localised to the basal body of the flagellar secretion system (Fan, F., *et al* 1997).

1.3.5.9 EscU

EscU is a predicted inner membrane protein of the T3SS of EHEC (Ghosh, P., 2004). Its homologous proteins in the flagellar and *Yersinia* T3SS system are FlhB and YscU respectively. FlhB has an important role in determining hook length in flagellar (Hirano, T., *et al* 1994) through the interaction with a molecular ruler termed FliK (Kawagishi, I., *et al* 1996). During assembly, FlhB supports the export of rod-type and hook-type proteins but not filament proteins, then a hook length signal is transmitted to FlhB via FliK and filament proteins are secreted (Minamino, T., *et al* 1999). The cytoplasmic domain of FlhB ($FlhB_C$) is cleaved into two parts: $FlhB_{CN}$ and $FlhB_{CC}$, which retain the ability to interact with each other. The interaction of $FlhB_{CN}$ with $FlhB_{CC}$ gives different substrate specificity to the molecule than $FlhB_C$ (Minamino, T., *et al* 2000). The N terminus of FliK senses the length of the hook and turns into an active form that binds $FlhB_C$ (Minamino, T., *et al* 2004). This binding causes a conformational change in $FlhB_C$ required for the switch between hook and filament proteins. The model proposed is that hook assembly starts very fast and slows down after the autocleavage of $FlhB_C$ (a timing device) then the FliK molecule passes through the hook and senses its length, when the hook is of the correct size it binds the FliK N terminus leaving the C terminus

in close enough proximity to bind to $FlhB_C$:$FlhB_N$, the export specificity is changed and filament proteins are secreted (Moriya, N., *et al* 2006). YscU is proposed to act in a similar manner; it was shown to be necessary for T3S in *Yersinia* (Allaoui, A., *et al* 1994) and proteolytically cleaved like FlhB (Lavander, M., *et al* 2002). Its cleavage causes a conformational change that allows it to change substrate specificity (Sorg, I., *et al* 2007). YscP (FliK homologue in *Yersinia*) also has a role in needle subunit secretion (Edqvist, P., *et al* 2003) and needle length; acting as a molecular ruler (Journet, L., *et al* 2003).

1.3.5.10 rOrf3

rOrf3 is homologous to a group of enzymes known as lytic transglycosylases and so it has been proposed to rename it EtgA (*E. coli* transglycosylase) (Pallen, M., *et al* 2005). Specialized lytic transglycosylases degrade peptidoglycan in the bacterial cell allowing insertion of the secretion complexes into the membrane (Zahrl, D., *et al* 2005).

1.3.5.11 GrlR and GrlA

GrlR (global regulator of LEE-repressor) and GrlA (global regulator of LEE-activator) are LEE encoded LEE regulators that influence the expression of Ler (Deng, W., *et al* 2004). GrlR and GrlA interact with each other (Creasey, E., *et al* 2003) with the proposed mechanism for GrlR repression is binding GrlA, thereby not allowing GrlA to increase the expression of *ler* (Iyoda, S., *et al* 2006). There is a regulator loop, with *ler* required for GrlR and GrlA expression, which get transcribed together (Barba, J., *et al* 2005). GrlA also acts as a negative regulator for flagellar gene expression (Iyoda, S., *et al* 2006). The structure of GrlR shows that it is dimeric and contains a Glu-Asp-Glu-Asp motif, which is important for the GrlR-GrlA interaction (Jobichen, C., *et al* 2007).

1.3.5.12 CesD

CesD is the chaperone for EspD. Deletion of CesD leads to no secretion of EspD and a reduced detection of EspB in the supernatant. The EspB decrease has yet to be fully explained, it may be that EspB is less stable without EspD (Wainwright, L., *et al* 1998).

1.3.5.13 EscC

EscC is an outer membrane protein that forms a ring shaped structure (Ghosh, P., 2004). EscC enters the outer membrane in a Sec-dependent and T3SS dependent manner, with the proteins EscN and EscV needed for its correct insertion (Gauthier, A., *et al* 2003b). In the T3SS apparatus EscC is associated with EscF and EscD (Ogino, T., *et al* 2006). Its homologue in the *Yersinia* T3SS, YscC, forms a ~20nm oligmeric complex in the outer membrane with a central pore (Koster, M., *et al* 1997).

1.3.5.14 SepD

SepD interacts with SepL (Creasey, E., *et al* 2003) and is involved in a switching mechanism between translocator and effector proteins (Deng, W., *et al* 2005). A *sepD* deletion leads to no translocator proteins being secreted and an increase in the secretion of effector proteins (Deng, W., *et al* 2004).

1.3.5.15 EscJ

EscJ is predicted to be in the periplasm, where it forms a large 24 subunit ring sitting on the inner membrane (Yip, C., *et al* 2005) It belongs to a highly conserved YscJ/Prgk family of proteins, is required for T3S and is associated with EscF (Ogino, T., *et al* 2006, Yip, C., *et al* 2005).

1.3.5.16 rOrf8

rOrf8 is reported to have homology with PrJ, MxiI and YscI, creating a case to rename it EscI (Pallen, M., *et al* 2005). The homologue MxiI is a minor essential component of the T3SS of *Shigella*, forming the needle with MxiH (Sani, M., *et al* 2007).

1.3.5.17 SepZ/EspZ

EspZ is translocated into host cells via the T3SS of EPEC and accumulates in a subset of pedestals in regions where phosphorylated Tir has built up. Deletion of EspZ does not effect T3S or A/E lesion formation and its function is still unknown (Kanack, K., *et al* 2005).

1.3.5.18 Orf12

Orf12 is homologous to SsaM from the Salmonella SPI-2 system (Pallen, M., *et al* 2005). SsaM is a small protein that may interact with another SPI-2 protein (SpiC) to control the ordered secretion of translocators and effectors (Yu, X., *et al* 2004).

1.3.5.19 EscV

EscV is an inner membrane protein with seven predicted transmembrane domains and a large cytoplasmic tail (Ghosh, P., 2004). EscV is vital for T3S in EPEC, where an *escV* deletion fails to disrupt host cell signalling (Nadler, C., *et al* 2006). EscV is predicted to be 75kDa with a Sec-dependent signal sequence and is located to the inner membrane, even in an *escN* and *escC* mutant (Gauthier, A., *et al* 2003b). EscV is homologous to the FlhA protein in the flagellar basal body (Pallen, M., *et al* 2005). The crystal structure of FlhA has been deduced in a hope to further elucidate its function (Saijo-hamano, Y., *et al* 2005). If the large cytoplasmic domain of FlhA ($FlhA_C$) is over produced it inhibits motility and flagellar substrate export in *Salmonella*. $FlhA_C$ is thought to interact with FliH (the regulator of the ATPase in flagellar export) (Kihara, M., *et al* 2001), it is also involved in flagellar and virulence gene expression in *Campylobacter jejuni* (Carrillo, C *et al* 2004).

1.3.5.20 EscN

EscN is the cytoplasmic ATPase associated with the T3SS, providing the energy for assembly and secretion (Ghosh, P., 2004). EscN has been shown to directly interact with CesT and Tir, possibly providing the energy required for Tir secretion (Gauthier, A., *et al* 2003). EscN ATPase activity is dependent on oligomerization into a hexameric ring

(Zarivach, M., *et al* 2007) or dodecamers (two hexamers on top of one another) and requires the presence of magnesium ions (Andrade, A., *et al* 2007).

1.3.5.21 Orf15

Orf15 has no known homologous proteins (Pallen, M., *et al* 2005).

1.3.5.22 Orf16

Orf16 is in the same location on the LEE and has secondary structure similarities with the proteins FliK (flagellar secretion system) and YscP (*Yersinia* T3SS) (Pallen, M., *et al* 2005). YscP and FliK function as molecular rulers, determining the length of the T3SS needle and the flagellar hook, working in conjunction with YscU and FlhB, respectively (Agrain, C., *et al* 2005, Shibata, S., *et al* 2007). Experimental data is required to validate this theory due to the low sequence homology between YscP, FlhB and Orf16 (Pallen, M., *et al* 2005).

1.3.5.23 SepQ

SepQ is homologous with YscQ and FliN and it has been proposed to rename it EscQ (Pallen, M., *et al* 2005). Although little is known about SepQ, FliN is predicted to form a doughnut shaped tetramer that sits at the bottom of the C ring in the flagellar export machinery (the bottom of the flagellar basal body) (Paul, K., *et al* 2006, Fadouloglou, V., *et al* 2006). FliN is thought to be involved in switching between clockwise and counter-clockwise rotation of the flagellar and binding FliH (Paul, K., *et al* 2006b). This may mean that SepQ forms a ring within the T3SS basal body (Pallen, M., *et al* 2005).

1.3.5.24 EspH

EspH is a T3SS translocated effector protein that inhibits filopodia and promotes pedestal formation in A/E lesions in EHEC and EPEC (Tu, X., *et al* 2003). Despite this, EspH from EHEC is not needed for A/E lesion formation in infant rabbit intestine, but is required for full colonisation (Ritchie, J., *et al* 2005).

1.3.5.25 CesF

CesF is the chaperone for the translocated effector protein EspF and is required for full EspF function (Elliott, S., *et al* 2002).

1.3.5.26 Mitochondrial Associated Protein (Map)

Map is a T3SS translocated effector protein, which localizes to the mitochondria in the host cell (Kenny, B., *et al* 2000). It is not clear what the function of Map is at the mitochondria, but it does enter the mitochondria and appears to disrupt their morphology in yeast cells (Papatheodorou, P., *et al* 2006). It also stimulates the formation of filopodia in EPEC, a transient event that happens before the formation of pedestals (Kenny, B., *et al* 2002). EPEC is capable of invading cell culture lines, which requires Map, although it does not require the localization of Map to the mitochondria (Jepson, M., *et al* 2003).

1.3.5.27 Translocated Intimin Receptor (Tir)

Tir is an effector protein that is translocated through the T3SS. It enters the host cell where it localizes to the membrane, functioning as the receptor for the EHEC adhesin intimin (Devinney, R., *et al* 1999). The intimin:Tir interaction at the host-pathogen border leads to a cascade of signalling events in the host cell, which initiates cytoskeletal rearrangements promoting the formation of the pedestal and the creation of an A/E lesion (Goosney, D., *et al* 2001).

In eukaryotic cells a critical controller of actin polymerisation at the plasma membrane is a heptameric actin-related protein 2/3 (Arp2/3). The actin nucleation activity of Arp2/3 can be stimulated by Wiskott-Aldrich syndrome proteins (WASPs) (Galletta, B., *et al* 2008), a member of which is neuronal (N-) WASP.

EHEC pedestal formation does not rely on tyrosine phosphorylation or the Nck adaptor protein, as is the case for EPEC (Campellone, G., *et al* 2003). Instead three amino acid residues (NPY_{458}) in Tir are necessary for recruiting the T3SS translocated effector

protein EspFu (encoded on a cryptic prophage) (Brady, M., *et al* 2007). It is EspFu that directly binds and activates N-WASP, leading to actin polymerisation creating the pedestal (Campellone, K., *et al* 2006).

1.3.5.28 CesT

CesT is a chaperone required for the stable secretion of both Tir and Map (Abe, A., *et al* 1999, Creasey, E., *et al* 2003b). It interacts with Tir, bringing it to the T3SS in an EscN-dependent manner. It is also the chaperone for at least five other effector proteins including; SepZ, NleA, NleH, NleF and EspH (Thomas, N., *et al* 2005).

1.3.5.29 Intimin (*eae*)

Intimin binds to the receptor Tir to promote tight adherence and trigger the signalling events that lead to pedestal formation (Kenny, B., *et al* 1997, Kenny, B., *et al* 1997b). EHEC intimin is also capable of binding nucleolin (a protein involved in cell proliferation) that is presented on the surface of host cells (Sinclair, J., *et al* 2004).

1.3.5.30 EscD

EscD is a predicted inner membrane protein (Ghosh, P., 2004) and has been shown to interact with EscC (Creasey, E., *et al* 2003). It also interacts with EscJ and is thought to be located in the inner membrane with its C terminus in the periplasm where it can interact with EscC and EscJ to sustain the central rod (Ogino, T., *et al* 2006).

1.3.5.31 SepL

SepL interacts with SepD (Creasey, E., *et al* 2003) and is involved in a switching mechanism between translocator and effector proteins (Deng, W., *et al* 2005). A *sepL* deletion leads to no translocator proteins being secreted and an increase in the secretion of effector proteins, an identical phenotype to a *sepD* deletion (Deng, W., *et al* 2004). *SepL* is situated 58bp upstream of the start codon for *espA* and encodes a 351 amino acid protein with a predicted mass of 39.95kDa. Despite this close proximity *espA, espD* and *espB* genes may be transcribed as a single transcript without *sepL* (Beltrametti, F., *et al*

1999). However, work in our laboratory indicates that the transcript includes *sepL* and it is posttranscriptional cleavage that removes *sepL* mRNA from that of *espA, D* and *B*. The SepL protein is localized at the membrane and in the cytoplasm (Kresse, A., *et al* 2000). A recent hypothesis is that SepL and SepD form a complex at the T3SS pore and act as a gate. This gate only allows the export of translocon proteins but dissociates or changes, after cellular levels of calcium drop upon translocon completion and interaction with the host cell (Deng, W., *et al* 2005). The exact mechanism of the gating activity is still not known as there is no direct evidence that SepL or SepD bind to any of the translocon proteins. Work in our laboratory has shown that SepL can bind directly to Tir and that Tir is displaced from SepL when SepL binds to the basal apparatus protein EscD (unpublished data). This binding of SepL to Tir may have a role after the SepL-SepD complex has dissociated, proving important in the hierarchal secretion of proteins through the T3SS. In EHEC O157:H7 *sepL* mutants have a decreased in adherence to epithelial cells in mouse cecum and a decreased shedding period (Nagano, K., *et al* 2003).

1.3.5.32 EspA

EHEC produces a filamentous T3SS, as it contains a large filament made of polymerized EspA that extends from the needle structure (Daniell, S., *et al* 2001). The EspA filament is required for the formation of A/E lesions and full virulence, creating a direct link between the bacteria and the host cell (Abe, A., *et al* 1998, Knutton, S., *et al* 1998, Ebel, F., *et al* 1998). The EspA filament has polymorphisms that do not allow cross reactivity between antibodies raised against EspA from different strains (Neves, B., *et al* 2003b). This lack of reactivity was used to demonstrate that EspA filaments elongate from the tip of the growing filament (Crepin, V., *et al* 2005). The filaments are hollow conduits rising from the EscF needle of the T3SS to deliver bacterial proteins into the host cell (Crepin, V., *et al* 2005, Daniell, S., *et al* 2001b).

1.3.5.33 EspD and EspB

EspD and EspB form the pore in the target cell membrane at the tip of the EspA filament (Ide, T., *et al* 2001) and have a role in regulating EspA filament length (Daniell, S., *et al* 2001). Deletions in these proteins are unable to secrete Tir and produce A/E lesions (Lai, L., *et al* 1997) and they may have a role in initial adherence (Chiu, H., *et al* 2005). EspB is also translocated into the cytoplasm of host cells where it interacts with myosin in a step that is involved with effacing the microvilli in A/E lesions (Iizumi, Y., *et al* 2007).

1.3.5.34 CesD2

CesD2 is the second chaperone for EspD and is required for stabilization and secretion of EspD (Neves, B., *et al* 2003).

1.3.5.35 EscF

EscF forms the needle that protrudes from the basal body of the T3SS and from which the EspA filament extends (Sekiya, K., *et al* 2001, Wilson, R., *et al* 2001). The EscF needle also interacts with EscC and EscJ and may be part of the central rod that spans the periplasm (Ogino, T., *et al* 2006).

1.3.5.36 Orf29

Orf29 is homologous to the SsaI protein from the *Salmonella* T3SS, SsaI has yet to be characterized (Pallen, M., *et al* 2005).

1.3.5.37 EspF

EspF is a T3SS translocated effector protein that is involved in disrupting the tight junctions of epithelial cells (Viswanathan, V., *et al* 2004). EPEC EspF is targeted to the mitochondria in the host cell, here it disrupts the mitochondrial membrane potential and effects cell death, epithelial barrier dysfunction and uptake into macrophages (Nagai, T., *et al* 2005, Quitard, S., *et al* 2006).

1.3.5.38 rOrf1

rOrf1 has a domain that has homology with SdiA regulated proteins and it interacts with EspD (Pallen, M., *et al* 2005). SdiA is a signal receptor involved in quorum sensing (Ahmer, B., *et al* 2004), an SdiA homologue in *Salmonella* regulating genes on a virulence plasmid (Ahmer, B., *et al* 1998). Quorum sensing has already been linked to the expression from *ler* (Sperandio. V., *et al* 1999) and rOrf1 may be another way in which quorum sensing influences LEE encoded proteins.

1.3.5.39 EspG

EspG is a T3SS translocated effector protein with homology to the *Salmonella* protein VirA (Elliott, S., *et al* 2001, Pallen, M., *et al* 2005). Using *Citrobacter rodentium* in an animal model EspG was shown to interact with tubulin, modulating the host cell cytoskeleton by destroying microtubules and polymerising actin and having an accessory role in colonisation (Hardwidge, P., *et al* 2005).

1.3.6 Non-LEE Encoded Proteins

Several non-LEE encoded proteins use the T3SS to be delivered into the host cell (e.g. $EspF_U$) (Brady, M., *et al* 2007). However, only the Nle (Non-LEE encoded) proteins will be discussed.

1.3.6.1 Non-LEE Encoded (Nle) Effector Proteins

Some effector proteins have been identified that are not encoded on the LEE pathogenicity island, but are still secreted in a T3SS dependent manner and possibly influence colonisation and virulence. They have been termed non-LEE encoded (Nle) effector proteins (Deng, W., *et al* 2005). To date nine Nle proteins have been identified in LEE containing pathogens (NleABCDEFGHI), some by signature-tagged transposon mutagenesis (Dziva, F., *et al* 2004, Kelly, M., *et al* 2006) and some by increasing expression of effector proteins by deleting *sepD* or *sepL* (Deng, W., *et al* 2005, Li, M., *et al* 2006). Although NleB and NleE have been shown to be involved in colonisation in the mouse pathogen *Citrobacter rodentium* (Kelly, M., *et al* 2006, Wickham, M., *et al*

2007), NleD and NleC were not required for colonisation in lambs after infection with EHEC O157:H7 (Marches, O., *et al* 2005). It is clear that these proteins, under certain conditions, are translocated through the T3SS, but their contribution to virulence is still to be fully elucidated. This is highlighted by the fact that when the expression profiles of NleA,B,C,D and E were investigated, in a wild type EHEC O157:H7 strain, only *nleA* was expressed co-ordinately with EspA filamentation and detected in the supernatant (Roe, A., *et al* 2007).

1.4 Fluorescent and Immunogenic Tags

Green fluorescent protein (GFP) and Haemagglutinin (HA) tag fusions will be used in this project for fluorescence microscopy and Western blot analysis.

1.4.1 Green Fluorescent Protein (GFP)

GFP originates from the bioluminescent jellyfish *Aequorea Victoria*. It has long been of interest and in 1992 Prasher *et al* demonstrated that the visible green fluorescence was genetically encoded, the chromophore being derived from a Ser-Tyr-Gly sequence in the protein (Prasher, D., *et al* 1992). The chromophore is formed auto-catalytically by a unique series of reactions occurring intramolecularly, with oxygen needed for the final step (Sullivan, K., *et al* 1999).

Mature GFP is excited by photons of light with a wavelength of 395nm (ultraviolet light) and emits photons with a 508nm wavelength (green light) (Bongaerts, R., *et al* 2002). The ultraviolet light promotes the chromophore into an excited state and the excited GFP emits light with a fluorescence lifetime of 3.3ns (Sullivan, K., *et al* 1999).

The use of GFP has been optimised by the isolation and creation of GFP mutants with varied fluorescent half lives, lower and higher fluorescence quantum yields and shifted emission and absorbance spectra (e.g. enhanced GFP (eGFP), GFP+, YFP and CFP). These mutants have increased the variety of systems and techniques GFP can be applied to (Jung, G., *et al* 2005). The GFP protein can be used for monitoring gene expression in

both eukaryotes and prokaryotes as it requires no jellyfish specific cofactors or substrates (Cha, H., *et al* 1999, Southward, C., *et al* 2002). GFP fusions are also used to show protein localization and dynamics, allowing an insight into the spatial and temporal organisation of cellular processes (Mullineaux, C., *et al* 2006). To date numerous cytoplasmic protein fusions to GFP have been constructed and used *in vivo*, although export difficulties have limited its use in extra-cytoplasmic compartments. However, there has been success in the transport of functional GFP into the periplasm in bacteria using the twin arginine translocation system (Thomas, J., *et al* 2001).

The main considerations when using GFP or GFP variants are false readings due to artefact production or cell death caused by phototoxicity (from the production of reactive oxygen species) (Remington, S., *et al* 2006).

1.4.2 Haemagglutinin (HA) tag

The HA tag is based on a nine amino acid immunodominant sequence from the influenza haemagglutinin protein (Tyr Pro Tyr Asp Val Pro Asp Try Ala) (Green, N., *et al* 1982). Monoclonal antibodies with high specificity for the sequence can be purchased, including dye labelled anti HA antibodies that reduce immunolocalization methodology to a single step (Jarvik, J., *et al* 1998). The antibodies raised against the short peptide can often recognise the sequence when it is engineered into a folded protein (Niman, H., *et al* 1983). However, care needs to be taken with the position of the tag (Munro, S., *et al* 1984) as a drawback is the possibility of the loss of protein function *in vivo* (Kolodziej, P., *et al* 1991) or unexpected effects on protein localization and function, which only the presence of the correct controls can highlight (Brother, S., *et al* 2003).

1.5 Aims of the Thesis

Fluorescent markers and immunogenic tags will be used to tag the T3SS apparatus in the EHEC O157:H7 strain Walla3 (Ostroff, S., *et al* 1990). The Walla3 strain is from the Walla Walla outbreak in 1983, it is a Stx- strain (does not produce Stx) but work in our laboratory has shown that the strain can cause A/E lesions in cattle. This will make the work containment level 2.

Inner membrane components of the basal apparatus (EscR and EscU) will be labelled as full protein fusion with eGFP, GPF+ or the HA tag, to the C terminus with no linker region. These will be used in allelic exchange (Emmerson, J., *et al* 2007, Blomfield, I., *et al* 1991) to replace the native genes and allow visualisation of the basal apparatus using microscopy and detection by Western blot analysis. These new Walla3 strains will then be used as a tool to investigate the following:

1.5.1 Localization

- Determine how many basal apparatus are in each bacterial cell
- Examine whether novel non-LEE encoded proteins can be co-localised with the basal apparatus in order to ascertain whether they interact with the T3SS
- Whether the mRNA transcript of *espADB* can be localised to the basal apparatus
- Study what happens to the basal apparatus after intimate adherence has been achieved by EHEC
- Use fluorescence resonance energy transfer (FRET) be to measure the proximity of proteins with the basal apparatus
- Use transmission electron microscopy, with gold labelled anti HA antibody, to localize the HA tagged basal apparatus protein to either the bacterial inner membrane or outer membrane to confirm its position

1.5.2 Regulation

- Investigate whether EHEC strains that are considered to secrete a high level of effector proteins contain more T3SS basal apparatus units

- To elucidate whether basal apparatus are present in all EHEC cells grown in T3SS permissive conditions

1.5.3 Timing

- Examine whether the formation of basal apparatus be seen in real time

1.5.4 EscU Aims

The fusions of eGFP and HA to EscU will also be used to further elucidate the function and localization of EscU. The EscU specific aims of the thesis are:

- Determine at what stage the T3S ceases formation in the EscU mutants
- Investigate the effect of mutating EscU on secretion of EspD, EspA and Tir
- Elucidate the function of EscU cleavage
- Localise both fragments of EscU to a bacterial cell fraction
- Investigate the link between EscU and the secretion of EscF
- Investigate the link between EscU cleavage and secretion of EscF
- Determine whether an $EscU_{CC}$ deletion or an EscU fusion can be complemented *in trans* by $EscU_{CC}$

Chapter 2
Materials and Methods

2 Material and Methods

2.1 Bacterial Strains

All the bacterial strains used in this study, a description of their main characteristics and their source or reference are listed in alphabetical order in Table 1. For long term storage strains were cultured for 16hr in 5ml Luria-Bertani (LB) broth, 800µl of the culture was then mixed with 200µl 100% glycerol in a 1.5ml eppendorf and the strains catalogued and placed at -70°C.

2.2 Plasmid Constructs

All plasmids used in this study are listed in alphabetical order in Table 2. The commercial vectors were either obtained directly from the supplier or from existing laboratory stocks. Dr. I. Blomfield kindly supplied the pIB307 plasmid and the pGEM-*grlA* plasmid was supplied by Professor H. Ando. The plasmids with the prefix pJRE were created as part of this study and the remaining plasmids were provided by other researchers in the Zoonotic Animal Pathogens (ZAP) laboratory, Centre for Infectious Diseases, Edinburgh: pAJRs were constructed by Dr. Andrew Roe, pASLs by Dr. Alison Low, pDWs by Mr. Dai Wang, pHYs by Miss Helen Yull and pMTs by Dr. Makrina Totsika (where applicable a reference has been provided).

2.3 Bacterial Growth Conditions and Media

For the construction of strains and plasmids LB broth and LB agar (BDH Merck, Leicestershire, UK) were used. These were routinely supplemented with 50µg/ml Ampicillin (Amp), 25µg/ml Chloramphenicol (Cm), 10µg/ml Tetracycline (Tc), or 25µg/ml Kanamycin (Kn) when appropriate. Strains were also cultured in minimal essential medium with HEPES modification (MEM-HEPES; Sigma, Dorset, UK), a T3SS promoting media. This cell culture medium was supplemented with 2.5% glucose, micronutrients and 0.26µM ferric nitrate to facilitate bacterial growth with antibiotics added when necessary. All the bacterial cultures were grown at 37°C unless the bacteria contained the temperature sensitive plasmid pIB307, when cultures were grown at 28°C (42°C for plasmid integration in allelic exchange). All cultures in liquid media were placed in shaking incubators at 200rpm with static

incubators used for incubating LB agar plates. Incubation times, which varied from 42hr to 8hr, are stated in the relevant results sections.

Table 1: A description and the source of the strains used in this study. The symbol <> indicates a genetic substitution on the bacterial chromosome.

Strain	Description	Source/reference
148a	Partial deletion of EHEC T3SS apparatus structural proteins in strain EDL933. nucleotides 4,668,961 – 4,670,521 (8.9Kb and 15 ORFs) deleted	Campellone, K., *et al* 2004
AAEC185	F⁻ λ⁻ *supE44 hsdR17 mcrA endA1 thi-1 Δ(fimBEACDFGH) ΔrecA*	Blomfield, I., *et al* 1991
TOP10	One shot® TOP10 chemically-competent *E. coli* cells	Invitrogen™
Walla3	EHEC O157:H7 Stx2-, Nal^R	Supplied by Mary Reynolds, Atlanta. (Ostroff, S., *et al* 1990)
ZAP193Δ*escN*	*escN* deletion in strain ZAP193	Roe, A., *et al* 2007
ZAP632	Walla3 *escRSTU<>sac*/Kan complement strain	This Study
ZAP633	Walla3 *escU<>escU*$_{\Delta cc}$	``
ZAP634	Walla3 *escU<>escU*$_{cn::HA}$	``
ZAP635	Walla3 *escU<>escU*$_{cn::gfp+}$	``
ZAP636	Walla3 LEE4<>*sac*/Kan	``
ZAP637	Walla3 *escR<>escR::HA*	``
ZAP1140	Walla3 *escRSTU<>sac*/Kan	``
ZAP1141	Walla3 *escU<>escU*$_{cc::egp}$	``
ZAP1142	Walla3 *escU<>escU*$_{cc::gfp+}$	``

Table 2: A description and the source of all the plasmids used in this study.

Plasmid name	Description	Source/reference
pACYC184	Commercial cloning vector, Cm^R and Tc^R	New England Biolabs
pAJR70	pACYC184 digested with the REase *Bam*HI, *egfp* cloned using REases *Bam*HI and BglII	Roe, A *et al* 2003
pAJR71	pAJR70 digested with *Bam*HI and *Kpn*I; LEE1 promoter cloned in frame 5' to *egfp*	``
pAJR72	pAJR70 digested with *Bam*HI and *Kpn*I; LEE2 promoter cloned in frame 5' to *egfp*	``
pAJR73	pAJR70 digested with *Bam*HI and *Kpn*I; LEE3 promoter cloned in frame 5' to *egfp*	``
pAJR74	pAJR70 digested with *Bam*HI and *Kpn*I; LEE4 promoter cloned in frame 5' to *egfp*	``
pAJR75	pAJR70 digested with *Bam*HI and *Kpn*I, 442bp including LEE5 promoter cloned in frame 5' to *egfp*	Roe, A., *et al* 2004
pAJR145	pACYC184 with *rpsM::gfp+* transcriptional fusion	``
pASL10	pACYC184 based plasmid with *ler*	Supplied by Dr. Alison

	under the expression of the pTac promoter	Low, ZAP lab
pCR®4-TOPO®	Commercial cloning vector containing TOPO® cloning site and T3 and T7 priming sites, Amp^R and Kn^R	Invitrogen™
pDW06	pACYC184 based plasmid with LEE4 promoter and *sepL* fused to *egfp*	Supplied by Mr. Dai Wang, ZAP lab
pGEM-*grla*	pGEM-T-easy vector with *grlA* cloned under the expression of the T7 promoter	Ando, H., *et al* 2007
pHY10	pIB307 containing the *sacB*/Kan cassette and flanking regions for a LEE4 deletion	Naylor, S., *et al* 2005
pIB307	Allelic exchange temperature-sensitive vector, pSC101 replicon, Cm^R	Blomfield, I., *et al* 1991
pJRE01	pIB307*escRSTU*	This Study
pJRE02	pCR®4-TOPO®*escRSTU*	``
pJRE03	pIB307*escRSTU<>sacB*/Kan	``
pJRE04	pCR®4-TOPO®*escU* PCR1	``
pJRE05	pCR®4-TOPO®*escU* PCR 2	``
pJRE06	pCR®4-TOPO®*escU* PCR1 and 2	``
pJRE07	pCR®4-TOPO®$escU_{cc::egfp}$	``
pJRE08	pIB307$escRSTU_{cc::egfp}$	``
pJRE09	pCR®4-TOPO®$escU_{cc::gfp+}$	``
pJRE10	pIB307$escRSTU_{cc::gfp+}$	``
pJRE11	pIB307*escRSTU Age*I removal of *ler*	``
pJRE12	pIB307$escRSTU_{cn::gfp+}$ *Bst*EII	``
pJRE13	pIB307$escRSTU_{cn::HA}$ *Bst*EII	``
pJRE14	pIB307*escRSTU Pst*I site removed	``
pJRE15	pCR®4-TOPO®*escR* PCR 1	``
pJRE16	pCR®4-TOPO®*escR* PCR 2	``
pJRE17	pCR®4-TOPO®*escR* PCR 1 and 2	``
pJRE18	pCR®4-TOPO®*escR*::HA	``
pJRE19	pIB307*escR(::HA)STU*	``
pJRE20	pJRE10 digested with *Age*I to remove *ler* and the LEE1 promoter region then religated	``
pJRE21	pJRE20 digested with *Bst*EII and AatII, Klenow treated and religated	``
pJRE22	pJRE21 with the sequence from *Bst*EII to the cleavage site, to create an $escU_{cc}$ deletion	``
pJRE23	pKC21 containing $escU_{cc}$ sequence with a 5' HA tag, downstream of the pTac promoter	``
pJRE24	pKC21 containing the sequence for $escU_{cc}$, downstream of the pTac promoter	``
pKC21	pACYC184 based plasmid containing the pTac promoter. *Kpn*I and *Hind*III restriction sites are used for creating IPTG inducible clones of genes	Supplied by Miss Kirsteen Catherwood, ZAP lab
pMT01	pIB307 with *papI-A'* from CFT073 P1 fused to *egfp*	Holden, N., *et al* 2007

2.4 Molecular Techniques and Genetic Manipulations

Unless otherwise stated the procedures are essentially those described in Molecular Cloning: A laboratory Manual, 3rd edition (Sambrook, J., *et al* 2001).

2.4.1 CTAB DNA Extraction

The CTAB DNA extraction method (Murray, M., *et al* 1980) was used to extract Walla3 genomic DNA. The CTAB method uses hexadecyltrimethyl ammonium bromide (CTAB) that precipitates cell debris, proteins and polysaccharides to leave high-molecular weight DNA, which can be recovered by isopropanol precipitation. In brief a 1.5ml aliquot of a Walla3 culture grown in LB broth for 16hr was microcentrifuged at 13,000 *g* for 1min and the cell pellet suspended in 567µl TE buffer. To the suspension 30µl 10% sodium dodecyl sulphate (SDS) and 3µl 20mg/ml of proteinase K (QIAGEN, West Sussex, UK) were added, this mixture was then incubated at 37°C for 1hr. After the incubation 100µl of 5M sodium chloride (NaCl) was added and gently mixed, followed by 80µl 10% CTAB solution in 0.7M NaCl. The mixture was incubated at 65°C for 10min, then an equal volume of chloroform:isoamyl alcohol (24:1) was added followed by microcentrifugation at 13,000 *g* for 5min. The aqueous phase supernatant was removed and the chloroform:isoamyl alcohol step repeated. The genomic DNA was then precipitated from the remaining aqueous phase supernatant by adding 0.6 volumes of isopropanol and pelleted by microcentrifugation at 4°C and 13,000 *g* for 10min. The DNA pellet was washed with 0.5ml 70% ethanol and re-suspended in 50µl TE buffer. A 1:150 dilution of the extracted DNA was made with TE buffer for use as DNA template in Polymerase Chain Reactions (PCRs) and was stored, with the neat extraction, at -20°C.

2.4.2 Crude DNA Extractions from *E. coli*

To prepare crude extracts of DNA for PCR a 10µl plastic loop was used to uplift a colony of bacteria from an LB agar plate. The bacteria on the loop were suspended in a sterile 1.5ml eppendorf tube containing 100µl MQ water (Sigma, Dorset, UK). The lid of the eppendorf was closed and pierced with a fine syringe needle and the suspension heated in a 100°C water bath for 5min. The suspension was then

microcentrifuged at 13,000 *g* for 1min to pellet the bacterial cell debris and stored at -20°C. 1µl of the crude extract was used as the DNA template for PCR screens.

2.4.3 Polymerase Chain Reaction (PCR)

All PCR primers used in this study are listed in numerical order in Table 3. Sterile 0.2ml thin-walled PCR tubes were used, with a standard 50µl PCR reaction mixture containing:

DNA template	Approx. 1µg (1µl of stock solution)
5' Primer	2mM (from a 100mM stock solution)
3' Primer	2mM (from a 100mM stock solution)
dNTPs	16µM (from a 0.4mM stock solution)
10x PCR buffer	5µl (supplied with *Taq* DNA polymerase from Roche, Burgess Hill, UK)
Taq DNA polymerase	2.5 units (0.15µl of enzyme supplied by Roche, Burgess Hill, UK)
MQ water	39.85µl

The DNA template was either 1µl of 1:150 dilution of the CTAB extracted genomic DNA or 1µl of a crude DNA extraction. The tubes were placed in a Thermo-Hybaid PCR Express machine, which was programmed to cycle the PCR based on the following template:

Time	**Temperature**	**Number of Cycles**
4min	94°C (DNA denaturing step)	x1
45sec	94°C (DNA denaturing step)	x25/30
45sec	***X°C*** (T_a for primer pair)	
1min/Kb of DNA to be amplified	72°C (Extension)	
10min	72°C (Extension)	x1

Negative controls for the PCR reactions had the template DNA replaced by 1µl of MQ water. For PCR screens the volume of each PCR reaction was lowered from 50µl to 10µl, usually a master mix was made and 10µl aliquots were taken and added to 0.5µl of the DNA to be screened.

2.4.3.1 Expand Long Template PCR System

For PCR products used to construct clones a *Taq* DNA polymerase and *Tgo* DNA polymerase mix was used. This high-fidelity amplification was supplied in the Expand Long Template PCR System (Roche, Burgess Hill, UK) and used according to manufacturer's instructions. The high-fidelity is provided by the *Tgo* DNA polymerase enzyme that has proofreading activity, giving a lower error rate than *Taq* DNA polymerase. The reaction mixture for 50µl and the Thermo-Hybaid PCR Express machine cycling template are as follows:

DNA template	Approx. 1µg (1µl of stock solution)
5' Primer	2mM (from a 100mM stock solution)
3' Primer	2mM (from a 100mM stock solution)
dNTPs	17.6µM (from a 0.4mM stock)
10x PCR buffer	5µl (supplied with *Taq* DNA polymerase from Roche, Burgess Hill, UK)
Taq/Tgo DNA polymerase mix	3.75 units (0.75µl of enzyme mix)
MQ water	39.05µl

Time	**Temperature**	**No. of Cycles**
4min	94°C (DNA denaturing step)	x1
10sec	94°C (DNA denaturing step)	x10
30sec	***X°C*** (T_a for primer pair)	
1min/Kb of DNA to be amplified	68°C (Extension)	
10sec	94°C (DNA denaturing step)	x20
30sec	***X°C*** (T_a for primer pair)	
1min/Kb of DNA to be	68°C (Extension)	

amplified (+20sec every cycle)		
7min	68°C (Extension)	x1

2.4.3.2 Overlapping Site Directed Mutagenesis

For overlapping site directed mutagenesis the expand long template PCR system was used to produce two PCR products with overlapping ends. The two PCR products were produced separately using PCR primers that are sense and antisense versions of one another (primers c and b in Fig.3). The two PCR products are then purified, using the QIAquick PCR purification kit (QIAGEN, West Sussex, UK). The purified PCR products were used in a further expand long template PCR reaction as the DNA template – usually in varying concentrations to increase the chances of a successful PCR. Negative PCRs were set up with no DNA template and only one PCR product as DNA template. The second PCR was carried out with the outside primers (primers a and d from Fig.3). This created a PCR product, identical in sequence to the wild type DNA apart from the added mutation (contained in PCR primers b and c Fig.3).

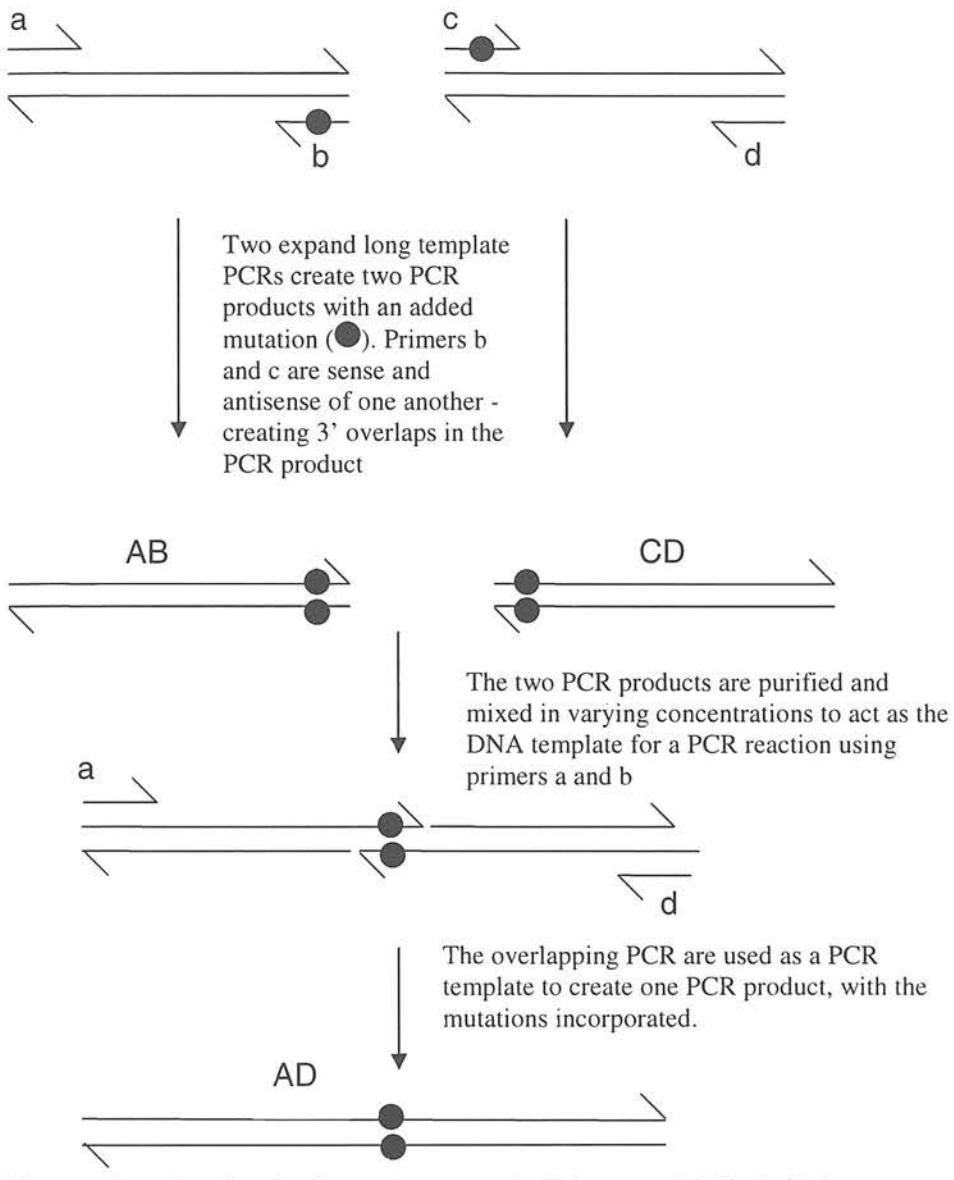

Fig.3 Diagram of overlapping site directed mutagenesis. Primers are labelled with lower case letters. PCR products are named by pairs of uppercase letters (corresponding to the primers used to generate them). Two PCR products are created, using primers (b and c) that are sense and antisense of one another. These primers are identical to the wild type sequence, except specific base changes to add a mutation. The two PCR products are purified and mixed. A further PCR reaction with the outside primers (a and d) create a final PCR product with the incorporated mutation(s).

Table 3: Table of the primers used in this study. In bold italics are the REase recognition sequences. NU = Not Used

Primer No.	PCR Product Name	Sequence	Paired primer	PCR size	T_a (°C)	5' / 3' primer	Additional Information
Primer 9	*escR* PCR 1	GTCACTGACTA***atgcat***TAC	12	957bp	59	5'	Situated over *Nsi*I site
Primer 10	*escR* PCR 2	GATTAATGACTGCA***ctgcag***CCATTACCTC	11	1.4Kb	56	3'	Situated over *Pst*I site
Primer 11	*escR* PCR 2	GGAGGCTGGCAAAAATT***atttaaat***TTCTGTTGG	10	1.4Kb	56	5'	Addition of *Swa*I site
Primer 12	*escR* PCR 1	CACCACCAACAGAA***atttaaat***AATTTTTGCCAGC	9	957bp	59	3'	Addition of *Swa*I site
Primer 13	*escS* PCR 2	CGATAATATTTGAAATG***cggccg***AAGGTGAACGGC	10	1Kb	56	5'	Addition of *Eag*I site
Primer 14	*escS* PCR 1	GCCGTTCACCTT***cggccg***CATTTCAAATATTATCG	9	1.2Kb	62	3'	Addition of *Eag*I site
Primer 15	*escT* PCR 1	CAATTATGTGTGCA***aacgtt***CTGG	18	1Kb	64	5'	Situated over *Acl*I site
Primer 16	*escT* PCR 2	CCTTTAATTTCAG***ggttacc***ATCCG	17	670bp	65	3'	Situated over *Bst*EII site
Primer 17	*escT* PCR 2	CTGACATAATTGATAFA***tgcgca***CCGAGCATG	16	670bp	65	5'	Addition of *Fsp*I site
Primer 18	*escT* PCR 1	CACTCATTAATCATGCTCGG***tgcgca***TCTATC	15	1Kb	64	3'	Addition of *Fsp*I site
Primer 19	*escU* PCR 1	CGAGAAGCCAAGGATACTGAT***ggtaacc***	22	346bp	56	5'	Situated over *Bst*EII site
Primer 20	*escU* PCR 2	GCAATATCAAGAATAAT***ggagacc***	21	572bp	63	3'	Situated over *Bsa*I site
Primer 21	*escU* PCR 2	GCGATAGACCTT***gacgtc***TAATCGATATTTGC	20	572bp	63	5'	Addition of *Aat*II site
Primer 22	*escU* PCR 1	GCAAATTATCGATTA***gacgtc***AAGGTCTATCGC	19	346bp	56	3'	Addition of *Aat*II site
Primer 23	*escRSTU*	TCCC***cccggg***GTTGGTCCTTCCTGATAAGGTCGC	24	6.3Kb	65	5'	*Xma*I site in tail for cloning
Primer 24	*escRSTU*	GC***tctaga***CTCAAGGCGCTTATAATGCAAATTACC	23	6.3Kb	65	3'	*Xba*I site in tail for cloning
Primer 25	Outside left flanking region	GAGTATAGTGAAACGGTTCAGC	27	3.4Kb	55	5'	Screening PCR for allelic exchange
Primer 26	*sacB* PCR	CAGCTCTTTGAACATCAACGG	27	230bp	55	5'	Screening for *sacB*
Primer 27	*sacB* PCR	CTTGGTAGCCATCTTCAGTTCC	26	230bp	55	3'	Screening for *sacB*
Primer 28	Inside left flanking region	CGAGGAGGAAATCGAAG	27	1.4Kb	55	5'	Screening PCR for allelic exchange
Primer No.	PCR Product Name	Sequence	Paired primer	PCR size	T_a (°C)	3' or 5' primer	Additional Information
Primer 29	pIB307 PCR	AGACAAATGGATCTCGTAAGCG	30	520bp	56	5'	Screening for pIB307
Primer 30	pIB307 PCR	GCTGTAACAAGTTGTCTCAGGTGT	29	520bp	56	3'	Screening for pIB307
Primer 31	*escR* PCR 3	AATTAATGACCATTGGCTCACAGC	32	270bp	66	5'	Screening for *escR*
Primer 32	*escR* PCR 3	CAGAGTCGGTATAATTGATTGGTTC	31	270bp	66	3'	Screening for *escR*
Primer 33	*escU egfp*	GGC***gacgtc***ATGGTGAGCAAGGGCGAGGAGC	34	723bp	58	5'	*egfp* for *escU Aat*II site

Primer 34	*escU egfp*	GCA***gacgtc***CTTGTACAGCTCGTCCATGC	33	723bp	58	3'	*egfp* for *escU* AatII site
Primer 35	*egfp*/HA AatII screen	GATTCGTATTGCGATAGACC	36	111bp	58	5'	Screen for insert (*Aat*II site)
Primer 36	*egfp*/HA AatII screen	GCAGTAGAACTCAGAAGG	35	111bp	58	3'	Screen for insert (*Aat*II site)
Primer 37	*escU gfp+*	GGC***gacgtc***ATGAGTAAAGGAGAAGAACTTTTC	38	732bp	57	5'	*gfp+* for *escU Aat*II site
Primer 38	*escU gfp+*	GGC***gacgtc***TTTGTAGAGCTCATCCATGC	37	732bp	57	3'	*gfp+* for *escU Aat*II site
Primer 39	*escU gfp+* BstEII	GGC***ggtaacc***CTATGAGTAAAGGAGAAGAACTTTTC	40	736bp	59	5'	*gfp+* for *escU Bst*EII site
Primer 40	*escU gfp+* BstEII	GGC***ggttacc***TTTGTAGAGCTCATCCATGC	39	736bp	59	3'	*gfp+* for *escU Bst*EII site
Primer 41	*gfp+*/HA BstEII screen	CATCGGCTCAGAAGATTAGTG	42	498bp		5'	Screen for insert (*Bst*EII site)
Primer 42	*gfp+*/HA BstEII screen	CTAAAGGTAATGGAGTCTCC	42	498bp		3'	Screen for insert (*Bst*EII site)
Primer 43	HA tag BstEII Oligo	GAA***ggtaacc***CTTATCCGTATGAT GTTCCTGATTATGCTAGC***ggtaacc***AAGG	44	-	-	-	Oligo for HA tag (*Bst*EII)
Primer 44	HA tag BstEII Oligo	CTT***ggttacc***GCTAGCATAATCAG GAACATCATACGGATAAG***ggttacc***TTC	43	-	-	-	Oligo for HA tag (*Bst*EII)
Primer 45	HA tag for *escR* SwaI	***atttaaat***ATCCGTATCCGTATGAT GTTCCTGATTATGCTTCATTTCTGTTGGTGG	10	1.4Kb	58	5'	HA tag in PCR tail for *escR* for *Swa*I site
Primer 46	HA *escR* SwaI screen	GGTATGATGATGGTATCGCCAGTAAC	47	121bp	58	5'	Screen for insert (*Swa*I site)
Primer 47	HA *escR* SwaI screen	CCAGTATCCATCAATTCACCACCAACAG	46	121bp	58	3'	Screen for insert (*Swa*I site)
Primer 48	BstEII – NPTH sequence	CCAAGGATACTGAT**ggtaac**	49	116bp	58	5'	Insertion of wild type sequence into pJRE21
Primer 49	BstEII – NPTH sequence	CG**ggttacc**GGGTTTTTAACAATAACGG	48	116bp	58	3'	Insertion of wild type sequence into pJRE21
Primer 50	$EscU_{CC}$ complement HA tag	GCC***ggtacc***ATGTATCCGTATGATGTTCCTGATTAT GCTAGCCCGACTCACATTGCGATTTGC	51	300	56	5'	Used to create the plasmid pJRE23
Primer 51	$EscU_{CC}$ complement	CCG***aagctt***TTAATAATCAAGGTCTATCGC	50	300	56	3'	Used to create the plasmids pJRE23/pJRE24
Primer 52	$EscU_{CC}$ complement no HA tag	GGCGGTACCATGCCGACTCACATTGCGATTTGC	50	273	56	5'	Used to create the plasmid pJRE24
Primer 53	*escF* screen	GGTGAAGTAGGTAAAACGCTG	54	182	55	5'	Screening for the presence of escF
Primer 54	*escF* screen	CGGTTAGAAATGGTTGAGACC	53	182	55	3'	Screening for the presence of escF

2.4.4 DNA Agarose Electrophoresis

PCR products were separated and visualised on agarose gels stained with ethidium bromide. Either medium (100ml) or small (50ml) agarose gels were made with 1x TBE buffer containing 0.7-1% agarose (depending on the size of the PCR product) and 1µl of 1M ethidium bromide. The Bio-rad (Hertfordshire, UK) electrophoresis system was used and electrophoresis was carried out at a constant 100v, until the dye front had migrated ¾ of the way down the gel. The gels were imaged by UV illumination in a Flowgen MultiImage™ light cabinet (Shenstone, UK) and pictures taken and stored using the ChemiImager 4000i v.4.04 software. The PCR product samples run on the gels contained 1x DNA loading buffer (Invitrogen, Paisley, UK) and were run alongside either the 100bp DNA ladder, the 1Kb DNA ladder or the λ HindIII DNA ladder (Invitrogen, Paisley, UK) for sizing.

2.4.4.1 Purification of DNA from Agarose Gels

Agarose gels were used to purify DNA from either a PCR or a plasmid DNA REase mixture. A 50ml 0.7% agarose gel was made using the Bio-rad system (Hertfordshire, UK). The comb used created wells that held 60µl of sample, allowing the whole PCR reaction/plasmid DNA REase mixture with loading buffer to be loaded. The gel was run as before and the band(s) excised with a scalpel after visualisation on a UV transilluminator (SLS, Nottingham, UK). The DNA was then extracted from the agarose gel using the QIAquick gel extraction kit (QIAGEN, West Sussex, UK) according to the manufacturer's instructions. The purified DNA was reconstituted in 30µl of MQ water.

2.4.5 Preparation of Plasmid DNA

For pACYC184, pCR4®-TOPO and pGEM-T-easy based plasmids (medium and high copy number plasmids) the plasmid DNA was extracted from bacterial cultures grown for 16hr at 37°C and 200rpm in 5ml LB broth with the appropriate antibiotic. The QIAprep™ spin plasmid miniprep kit (QIAGEN, West Sussex, UK) was used according to manufacturer's instructions (with all the buffers supplied with the kit) and the plasmid DNA was eluted in 50µl MQ water. For pIB307 based plasmids (low copy number plasmids) four 5ml LB cultures grown at 28°C and 200rpm for

16hr were pooled into a single QIAprep™ spin column and eluted in 35µl MQ water. Alternatively, if a large amount of the plasmid was required then the QIAGEN™ spin plasmid midiprep kit (QIAGEN, West Sussex, UK) was used according to manufacturer's instructions, which yielded 20-100ng of low copy plasmid DNA in 250µl of MQ water.

2.4.6 Restriction Enzyme Digestion

All the REases used in restriction digestions were purchased from New England Biolabs (NEB; Hertfordshire, UK) and used according to their instructions. Typically 2.5µl of the REase and 5µl of the corresponding NEB 10x enzyme buffer were added to a 50µl reaction volume that contained a varying concentration of DNA suspended in MQ water (depending on the concentration of DNA in the original sample). The reaction mixture was left for approximately 2.5hr at the recommended temperature for optimum enzyme activity (usually 37°C). In diagnostic digestions the reaction mixture volume was decreased to 20µl, of which 1µl was the REase and 2µl the corresponding NEB 10x enzyme buffer. After an hour incubation 2.2µl of 10x loading buffer (Invitrogen, Paisley, UK) was added and the whole sample loaded onto an agarose gel. When two REases were used which were compatible for a double digestion only 2µl of each were added to a 50µl reaction with 5µl of 10x bovine serum albumin (BSA; NEB, Hertfordshire, UK). For diagnostic digests 1µl of each REase was added and the reaction volume increased to 25µl with no BSA.

2.4.7 DNA Fragment Purification

DNA fragments from PCR (100bp – 10Kb) and DNA from 50µl REase digestion mixtures were purified from the reaction mixture using the QIAquick PCR purification kit (QIAGEN, West Sussex, UK) following the manufacturer's instructions. Purified DNA was eluted from the spin column in 30-50µl MQ water.

2.4.8 Klenow Treatment of Digested DNA

The DNA polymerase I, large (Klenow) fragment (NEB, Hertfordshire, UK) was used to form blunt ends after restriction enzyme digestion with REases that produced non compatible sticky ends. It was used according to manufacturer's instructions but briefly 2.5µl of Klenow was added to a 50µl reaction mixture containing the DNA suspended in MQ water, 5µl 10x NEB REase buffer 2 and 2µl 0.4mM dNTPs. After a 2.5hr incubation the reaction was stopped by either heat inactivation (75°C for 10min) or by using the QIAquick PCR purification kit (QIAGEN, West Sussex, UK) to purify the DNA from the reaction mixture.

2.4.9 Ligation of DNA Fragments

Vector and insert DNA were restricted with the appropriate REase(s) to form compatible ends for ligation. 1µl of Antarctic alkaline phosphatase (AAP; NEB, Hertfordshire, UK) was added to the REase reaction mixture containing the vector DNA for the final 30min of the incubation. This dephosphorylated 5' restricted termini to prevent the vector from religating. The digested vector and insert were visualised on an agarose gel with the λ HindIII DNA ladder, which was used to quantify the amount of DNA in the samples:

DNA ng/µl = Brightness factor x Size factor x ng of DNA in λ HindIII DNA band

Where the brightness factor is:

$$\text{Brightness factor} = \frac{\%\ \text{Brightness of insert or vector DNA band}}{\%\ \text{Brightness of DNA ladder band}}$$

and the size factor is:

$$\text{Size factor} = \frac{\text{Size of insert or vector DNA band}}{\text{Size of DNA ladder marker band}}$$

The amount of insert (ng) to be used in the ligation reaction with 50-100ng of vector DNA was calculated using the equation:

$$\text{Insert (ng)} = \frac{\text{ng of vector x size of insert (bp)}}{\text{Size of vector (bp)}} \times \text{Insert : Vector Ratio}$$

(Where the ratio of insert to vector is 3:1)

The DNA fragments (suspended in MQ water) were mixed with 1µl T4 DNA ligase (NEB, Hertfordshire, UK) and 1µl 10x ligase reaction buffer (NEB, Hertfordshire, UK) to a final volume of 10µl (made up with MQ water). For ligations with complementary sticky ends the ligation mixture was incubated at 4°C for 16hr and for blunt end ligations the mixture was incubated at 16°C for 16hr.

2.4.10 TOPO TA Cloning

The TOPO TA cloning® kit (Invitrogen, Paisley, UK) was used to clone PCR products for sequencing and for sub-cloning into low copy number vectors. The kit provides a method of non-directionally inserting a PCR product into the pCR4®-TOPO® vector, without the need for restriction digestion or purification of the insert DNA from the PCR mixture. *Taq* DNA polymerase has a non-template dependent terminal transferase activity that produces PCR products, which contain poly-A 3' overhangs (the addition of single deoxyadenosine (A) to the 3' end of PCR products). These overhangs are fragile and can easily be lost by mechanical shearing from procedures like purification from agarose gels. The PCR product with the poly-A 3' overhangs is ligated with linearized pCR4®-TOPO®, which contains poly-T 3' overhangs, by the enzyme topoisomerase. This ligation reaction was carried out according to manufacture's instructions with the kit containing the vector, enzyme and the buffer. PCR products generated by the expand long template system (Roche, Burgess Hill, UK) lack the poly-A 3' overhangs due to the proof reading activity of the *Tgo* DNA polymerase. Before these products can be TOPO TA cloned poly-A 3' overhangs are added after amplification by incubating the PCR reactions with 1 unit of *Taq* DNA polymerase and 2µl dNTP (0.4mM stock) at 72°C for 10min. The ligation mixtures were transformed into One shot® TOP10 chemically competent *E. coli* cells (Invitrogen, Paisley, UK).

2.5 Transformations

2.5.1 Preparation and Transformation of Chemically Competent Cells

5ml LB broth was inoculated with the *E. coli* K-12 strain to be made chemically competent. This was incubated for 16hr at 37°C and 200rpm and 1ml used to inoculate 100ml LB broth. The 100ml culture was grown under the same conditions until its optical density, measured at 600nm (OD_{600nm}), was 0.4-0.6. The culture was then centrifuged at 4°C and 3220 *g* for 10min. The cell pellet was gently suspended in 40ml (0.4 volume) ice-cold transformation buffer I (TFBI) and incubated on ice for at least 15min. After the incubation the cells were harvested by an 8min centrifugation at 4°C and 3220 *g*. The harvested cells were suspended in 1.6ml (0.04 volume) ice-cold transformation buffer II (TFBII). The cells were incubated on ice in TFBII for 15min before aliquoting into 100µl volumes and storing at -70°C.

To transform chemically competent cells, a 100µl aliquot of the cells was mixed by gentle pipetting with 1µl purified plasmid DNA or the 10µl of a ligation reaction mixture and incubated on ice for 30min. After the incubation the mixture was heat-shocked in a 42°C water bath for 45sec. The transformations were incubated on ice for 1min immediately after heat-shocking and then 350µl of room temperature Salt-Optimised and Carbon medium (SOC; Invitrogen, Paisley, UK) was added. Transformants containing the temperature sensitive plasmid pIB307 were incubated at 28°C and 80rpm for 2hr. For all other plasmids, transformants were recovered for 1hr at 37°C and 80rpm. After the recovery period a 200µl aliquot of the culture was plated on LB agar supplemented with the relevant antibiotic(s) and incubated for 16hr at the appropriate temperature (for pIB307 based plasmids a 48hr incubation at 28°C was often required before colonies could be seen).

2.5.2 Preparation and Transformation of Electro-Competent Cells

Electroporation was used to transform plasmids into all non laboratory strains. Firstly a 100ml culture of the bacteria was grown in LB broth in an identical manner to the preparation of chemically competent cells. The bacteria were pelleted out of the LB broth by centrifugation for 10min at 4°C and 3220 *g* and the pellet suspended in 100ml ice-cold MQ water. The centrifugation step was repeated for 8min and the

pellet washed with 50ml ice cold 10% glycerol (0.5 volume). The suspended bacteria were then harvested by another 3220 *g* centrifugation at 4°C for 8min and the pellet suspended in 25ml (0.05 volume) of ice-cold 10% glycerol. This suspension was centrifuged for a further 8min and the pellet suspended in 500µl (or less) ice-cold 10% glycerol, to produce a thick slurry. This suspension could be divided into 100µl aliquots and stored at -70°C, however electro-competent cells transformed at a higher efficiency if they were used on the same day they were prepared.

To transform electro-competent cells a 75µl aliquot of the cells was mixed with 1µl of purified plasmid DNA and incubated on ice for 1min. The mixture was then transferred to a 1.5ml ice-cold electroporation cuvette (Flowgen, Shenstone, UK). Before electroporating with a 2.5KV pulse the cuvette was wiped dry and air bubbles removed by tapping the bottom of the cuvette against the laboratory bench. After electroporating 1ml of room temperature SOC medium was immediately added. The SOC was mixed with the transformed cells by pipetting, removed and placed in a sterile 1.5ml eppendorf and recovered at 37°C for 1hr and 200rpm or 28°C for 2hr and 200rpm (depending on the plasmid being transformed). After the incubation a 200µl aliquot of the transformation mixture was plated onto an LB agar plate containing the relevant antibiotic(s) and incubated for 16hr at the appropriate temperature (for pIB307 based plasmids a 48hr incubation at 28°C was often required before colonies could be seen).

2.6 Allelic Exchange

All gene replacements and deletions in the Walla3 strain were created using a temperature-sensitive plasmid based allelic exchange system as described in Blomfield, I., *et al* 1991 and Emmerson, J., *et al* 2006 (which contains a detailed protocol).

Integral to the method is the *sac*/Kan cassette, a genetic element consisting of the *sacB* gene from *Bacillus subtilis* and the neomycin (Kn^R) gene from Tn5. This cassette was cloned between two homologous regions of flanking DNA (sequence either side of the region to be substituted on the chromosome) in the temperature

sensitive plasmid pIB307. This plasmid was electro-transformed into the strain to be manipulated. Incubation and successive passage at 42°C in LB broth (with chloramphenicol) promoted plasmid integration. This was followed by incubation and successive passage at 28°C in LB broth (with kanamycin) to promote plasmid backbone excision. This produced a mixed population of bacteria, some of which had excised the pIB307 plasmid in an event that had substituted the genetic material on the chromosome for the *sac*/Kan cassette. These bacteria were kanamycin resistant and chloramphenicol sensitive. Successful integrants were screened by PCR using primers specific for the pIB307 backbone, the *sac*/Kan cassette and the region of genetic material substituted (Fig.4, A).

The successful integration event creates an intermediate strain that can be used to create clean deletions or genetic modifications of the sequence substituted. For this the pIB307 plasmid containing the flanking regions is used with either no genetic sequence between the two flanking regions (to create a clean deletion) or genetic modifications of the sequence between them. This plasmid is electro-transformed into the intermediate strain and grown at 42°C in LB broth containing chloramphenicol, followed by incubation at 28°C in LB broth containing no antibiotics, to promote integration and excision of the plasmid. This creates a proportion of bacteria that have the *sac*/Kan cassette on the chromosome replaced with the sequence between the flanking regions of the plasmid. The removal of the *sac*/Kan cassette can be screened for as its presence in the intermediate strain makes the strain sensitive to growth on agar plates containing 6% sucrose (and no NaCl). This is due to the *sacB* gene, which produces levansucrase that polymerizes sucrose to create levans. These levans build up in the bacterial cell causing an osmotic imbalance, leading to bacterial cell death (Emmerson, J., *et al* 2006, Blomfield, I., *et al* 1991). Successful integrations are sucrose tolerant and chloramphenicol and kanamycin sensitive. Any positive clones are then screened by PCR using primers specific for the pIB307 backbone, the *sac*/Kan cassette and the sequence inserted/deleted in the strain (Fig.4, B).

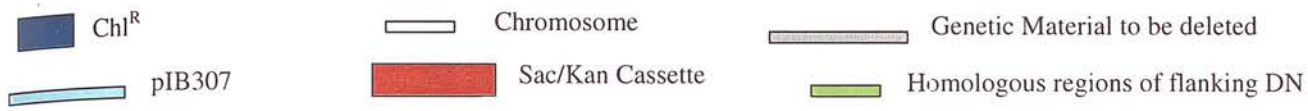

Step 1: Plasmid Integration: Inserting the *sacB*-Kan Cassette:

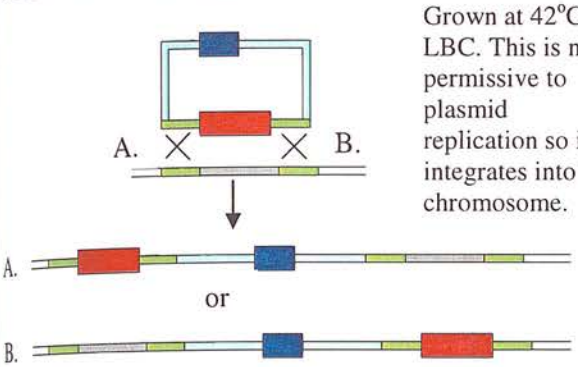

Grown at 42°C in LBC. This is not permissive to plasmid replication so it integrates into the chromosome.

Fig.4 Diagram of allelic exchange A) (Taken from Emmerson, J., *et al* 2006) The transfer of the *sacB*-Kan cassette into the chromosome requires two recombination events leading to plasmid integration followed by plasmid excision. Step 1: plasmid integrates into the wild-type strain at the non permissive temperature for plasmid replication (42°C). Steps 2 and 3: plasmid integrates are grown at 28°C in the presence of kanamycin to enrich for bacteria that have excised and cured the plasmid, leaving the cassette on the chromosome. Step 4: Growth on media containing LBC or LBK. Bacteria that can only grow on LBK are successful constructs of the intermediate strain.

Step 2: Plasmid Excision:
(Shown from integration B. from step 1)

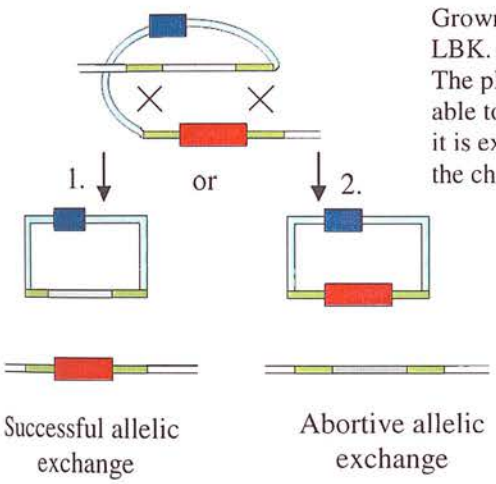

Grown at 28°C in LBK.
The plasmid is able to replicate so it is excised from the chromosome.

Step 3 & 4: Plasmid Curing and selection of the mutant:

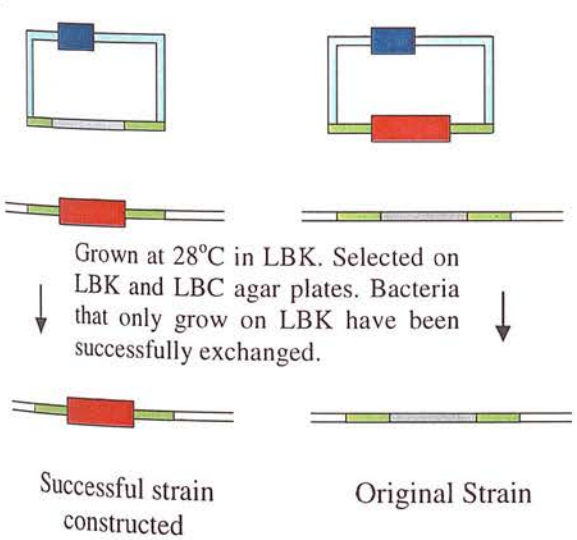

Grown at 28°C on LBK and LBC agar plates.
Positive clones are verified by PCR.

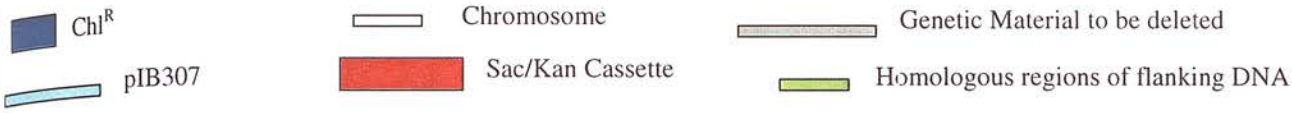

Step 1: Plasmid Integration: Removing the *sacB*-Kan Cassette:

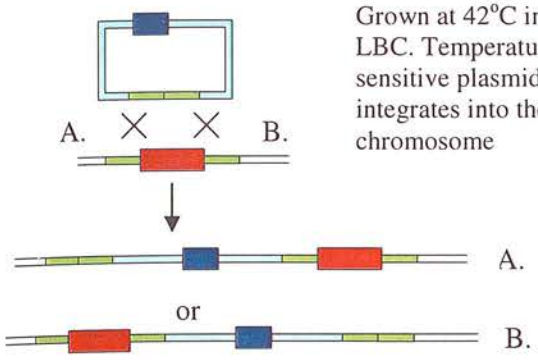

Grown at 42°C in LBC. Temperature sensitive plasmid integrates into the chromosome

Fig.5 Diagram of allelic exchange B) (Taken from Emmerson, J., *et al* 2006) Step 1: Plasmid integration in the intermediate strain is selected at the non permissive temperature for plasmid replication (42°C). Steps 2 and 3: Plasmid integrates are grown at 28°C in the absence of antibiotics to enrich for bacteria that have excised (Step 2) and later cured (Step3) the integrated plasmid. Step 4: Growth on media containing sucrose selects for successful strain constructs.

Step 2: Plasmid Excision:
(Shown from integration B. from step 1)

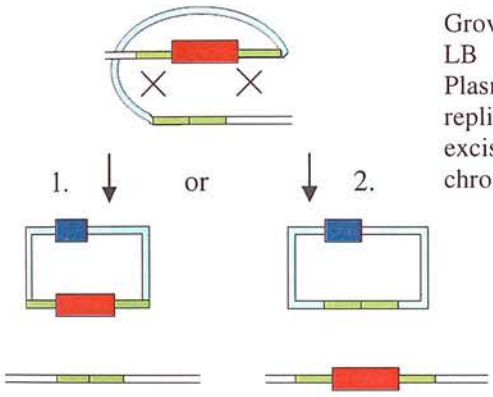

Grown at 28°C in LB
Plasmid is able to replicate so it is excised from the chromosome

Step 3 & 4: Plasmid Curing and selection of the mutant:

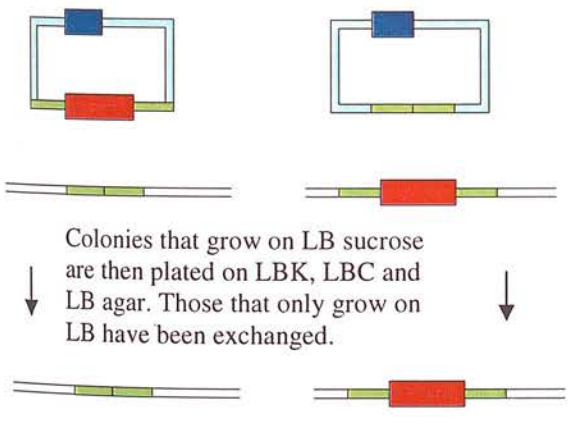

Grown at 28°C on LB sucrose agar plates. Then patch plated onto LBC,LBK and LB agar plates.

2.7 Methods for Protein Analysis

2.7.1 Whole Cell Protein Preparations

Bacteria were grown for 16hr in 5ml MEM-HEPES supplemented with 0.5% glucose, micronutrients and 0.26μM ferric nitrate at 37°C and 200rpm. This culture was used to inoculate 50ml supplemented MEM-HEPES to a starting OD_{600nm} of 0.01 and grown at 37°C for ~8hr until it had reached an OD_{600nm} of 0.8-0.9. Once this OD_{600nm} was reached the culture was transferred to ice-cold 50ml falcon tubes and centrifuged at 3220 *g* for 30min at 4°C and the pellet suspended in 0.5ml ice-cold sonication buffer. The suspension was then placed on ice and sonicated three times for 15sec at 5 microns amplitude using a Soniprep 150. After sonication cell debris was removed by two rounds of microcentrifugation at 13,400 *g* and 4°C for 10min. The final supernatant was used as a preparation of whole cell proteins and could be aliquoted and stored at -20°C until needed.

2.7.2 Supernatant Protein Preparations

For supernatant protein preparations the cultures were grown in an identical manner to the whole cell protein preparations. After they reached an OD_{600nm} of 0.8-0.9 the cultures were transferred to ice-cold 50ml falcon tubes and centrifuged at 3220 *g* for 30min at 4°C and the supernatant decanted and transferred to a sterile ice cold 50ml falcon tube. The supernatant was then filtered through a low protein binding 0.45μm PVDF filter (Millex-HV filter; Millipore, Watford, UK) and BSA was added to a final concentration of 4μg/ml. The supernatant was then made to 10% trichloroacetic acid (TCA acid) and incubated at 4°C for 16hr. After the incubation the solution was centrifuged at 3220 *g* for 30min at 4°C and the pellet suspended in a volume of sonication buffer that was adjusted according to the final OD_{600nm} reached by the culture; typically pellets for samples that reached an OD_{600nm} of 0.8 were suspended in 250μl of sonication buffer.

2.7.3 Cytoplasmic and Membrane Protein Preparations

The method for whole cell protein preparations was followed. When the final supernatant containing the whole cell samples had been obtain it was centrifuged in a Sorvall Discovery Ultra Centrifuge for 1hr at 4°C and 50,000 *g*. Following the ultra

centrifugation step the supernatant, containing the cytoplasmic proteins, was decanted into a chilled eppendorf and could be aliquoted and stored at -20°C. The pellet, containing the membrane proteins, was suspended in half the volume of the cytoplasmic samples (~250µl) in SDS gel loading buffer (not sonication buffer). This made the membrane samples twice as concentrated as the cytoplasmic samples and they did not need dilution with SDS gel loading buffer before running on SDS PAGE gels, so potentially more sample could be loaded.

2.7.4 Sodium Dodecyl Sulphate Polyacrylamide Gel Electrophoresis (SDS PAGE)

Samples for SDS PAGE were obtain by either whole cell, supernatant, cytoplasmic or membrane protein preparations. The whole cell, cytoplasmic and membrane protein preparations, which had not been adjusted for the OD_{600nm} of the original culture, had variable amounts loaded onto the gel. Typically 12µl was loaded of a protein preparation from a sample which had originated from a culture that had reached an OD_{600nm} of 0.8; this ratio was used to adjust all the samples that were loaded onto the gel. For membrane protein preparations 6µl was loaded for a culture that had grown to an OD_{600nm} of 0.8, as these samples were twice as concentrated as their corresponding cytoplasmic protein preparations. The supernatant protein preparations did not need adjusting for their OD_{600nm} so 12µl was loaded. 8µl SDS gel loading buffer was added to all the samples (except to the membrane protein preparations). All the samples for SDS PAGE mixed with the loading buffer were placed in 1.5 or 0.5ml eppendorfs, which had their lids pierced by a fine syringe needle, and were incubated in a water bath set to 100°C for 5min to denature the proteins. After the incubation the samples were centrifuged in a microcentrifuge at 13,000 *g* for 30sec and loaded onto the SDS PAGE gel.

The SDS PAGE BIO-RAD Mini-protean II gel apparatus (Bio-rad, Hertfordshire, UK) system was used to construct and run the SDS PAGE gels. Firstly the 12% resolving gel solution was prepared and applied to the vertical electrophoresis apparatus and allowed to polymerase (approx. 30min at room temperature). Once polymerised the 5% SDS PAGE stacking gel was prepared and the solution applied

on top of the polymerised resolving gel. Immediately after the stacking gel's application a 10 well comb was placed into the stacking gel. It was then allowed to polymerise. Once polymerised the BIO-RAD Mini-protean II gel apparatus for running the gel was assembled and the gel placed into the electrophoresis tank. SDS PAGE running buffer was added to the inner and outer compartments and the well comb removed. The boiled samples were loaded into the wells alongside 5µl of the molecular weight marker (Rainbow marker; Amersham Pharmacia Biotech, Buckinghamshire, UK). A constant voltage of 100V was used until the dye in the loading buffer had reached the bottom of the gel. Gradient gels of 10-20% (Bio-rad, Hertfordshire, UK) and gels of 18% (Bio-rad, Hertfordshire, UK) were used in an identical manner. However, these were purchased as pre-cast gels and so did not need any preparation before being placed in the BIO-RAD mini gel system.

2.7.5 Coomassie Blue Staining of SDS PAGE Gels

Polyacrylamide gels were stained with Coomassie blue (Colloidal blue; Invitrogen, Paisley, UK) according to manufacturer's instructions. Gels were then de-stained for 16hr in dH_2O and transferred onto two 3MM Whatman paper squares. Gel images were captured using a Flowgen MultiImage^{TM} Light cabinet after which gels were dried at 75°C for at least 180min in a vacuum and heated gel drier (Bio-rad, Hertfordshire, UK).

2.7.6 Tricine SDS PAGE

Tricine gels were purchased from Bio-rad (Hertfordshire, UK). They were placed into the BIO-RAD Mini-protean II gel apparatus and the outside chamber was filled with the cathode buffer and the inside chamber with the anode buffer. The samples were loaded in the same manner as for SDS PAGE protocol (section 2.7.4) and the gels run at a constant voltage of 30V until the samples had reached the bottom of the gel (~6hr).

2.7.7 Antibodies

All antibodies used, their application and incubation time are listed in Tables 4.

Table 4: Description of the primary antibodies used in this study

IgG Antibody Name	Poly/monoclonal	Western blotting: dilution factor and incubation time	Microscopy staining: dilution factor and incubation time
J-L8 (anti GFP; Clontech, Saint-Germain-En-Laye, France)	Monoclonal Mouse	1:2000, 1hr	-
GroEL (Sigma, Dorset, UK)	Monoclonal Mouse	1:4000, 1hr	-
OmpA (Dr. J. Leong, USA)	Polyclonal Rabbit	1:4000, 1hr	-
EspA	Polyclonal Rabbit	1:2000, 1hr	1:250, 1.5hr
EspD	Monoclonal Mouse	1:2000, 1hr	-
HA (Sigma, Dorset, UK)	Monoclonal Mouse	1:1000, 2hr	-
HA (Abcam, Cambridge, UK)	Monoclonal Mouse	1:1000, 2hr	-
EscJ (Prof. Abe, Japan)	Polyclonal Rabbit	1:2000, 1hr	1:250, 2hr
EscF (Prof. Abe, Japan)	Polyclonal Rabbit	1:1000, 1hr	1:250, 2hr

Table 5: Description of the secondary antibodies used in this study.

IgG Antibody Name	Poly/monoclonal	Western blotting: dilution factor and incubation time	Microscopy staining: dilution factor and incubation time
Anti mouse IgG HRP (Dako, Glostrup, Denmark)	Polyclonal goat, anti mouse IgG	1:4000, 1hr	-
Anti Rabbit IgG HRP (Dako, Glostrup, Denmark)	Polyclonal goat, anti rabbit IgG	1:4000, 1hr	-
Alexa Fluor 488 (Invitrogen, Paisley, UK)	Polyclonal goat, anti rabbit IgG	-	1:1000, 2hr

2.7.7.1 Absorbing Antibodies with a Mutant Strain

Two cultures of the relevant strain for absorption were grown in 50ml supplemented MEM-HEPES. At an OD_{600nm} of 0.8 both the cultures were centrifuged at 3220 *g* for 15min and 4°C. One of the bacterial pellets was suspended in 1ml of a 1:250 dilution of the relevant antibody in 1x phosphate buffer saline (PBS; Oxoid, Hampshire, UK). This was incubated for 2hr on a rocking platform at 4°C. After 2hr the mixture was centrifuged at 13,000 *g* for 5min at 4°C and the supernatant used to suspend the bacterial pellet from the second 50ml MEM-HEPES culture. This was incubated for 2hr on a rocking platform at 4°C and then centrifuged at 13,000 *g* for 5min at 4°C. The supernatant was filtered through a low protein binding 0.45μm PVDF filter (Millex-HV filter; Millipore, Watford, UK). The filtrate was used in Western blot analysis as primary antibody diluted 1:10.

2.7.8 Western Blotting

Proteins separated by SDS PAGE and Tricine SDS PAGE were transferred from the polyacrylamide gel onto a nitrocellulose membrane (Amersham Pharmacia Biotech, Buckinghamshire, UK) using the Bio-rad transfer apparatus (Bio-rad, Hertfordshire, UK). The nitrocellulose membrane and 4 pieces of 3MM Whatman paper were cut to the size of the gel and soaked in transfer buffer with two sponges. The wells on the polyacrylamide gel were removed and the transfer apparatus constructed with the gel and the membrane between the 4 pieces of Whatman paper (two either side) and the two sponges (one either side). These were held together in the plastic clamp and placed into the transfer tank with an ice pack (Bio-rad, Hertfordshire, UK) and filled with transfer buffer. The transfer was performed at a constant voltage of 60V for 100min. Upon completion of the transfer the nitrocellulose membrane was removed and blocked in blocking buffer at 4°C for 16hr. Excess blocking buffer was removed by three 10min washes with washing buffer and the membrane was immersed in primary antibody solution and incubated at room temperature on a rocking platform. After the incubation the excess primary antibody was removed by three 10min washes in washing buffer, following which the membrane was incubated in secondary antibody solution at room temperature on a rocking platform. Excess secondary antibody was then removed with a final set of three 10min washes in

washing buffer. The membrane was then incubated in 10ml ECL solution and left on the bench for 5min. The chemiluminescence from the ECL reaction was detected using Hyperfilm^{TM} ECL chemiluminescence film (Amersham Pharmacia Biotech, Buckinghamshire, UK) and developed in a Protec automatic film processor (Optimax, Nottingham, UK). After developing, the film and the membrane were lined up and the Rainbow marker bands were marked onto the film with a permanent marker pen.

2.7.8.1 Quantification of Western Blot bands using ImageJ software

The ImageJ software (National Institute of Health, USA) was used to quantify the amount of signal from Western blot X-ray films. The film, once developed, was scanned as a high resolution image file and loaded into the ImageJ software. The software tools were used to invert the image and draw a box around the band to be measured. The box was then copied and placed over an area of film containing no sample. The analysis function was used to measure the amount of pixilation in each box. The value for the background was subtracted from the value for the sample band giving an approximation of the signal from the sample. This was repeated for the number of bands to be measured, using the same drawn box and background reading.

2.8 Fluorescence Microscopy

2.8.1 Immunofluorescence Antibody Staining

Samples for antibody staining were grown in 5ml supplemented MEM-HEPES for 16hr. This was used to inoculate 10ml or 50ml supplemented MEM-HEPES to a starting OD_{600nm} of 0.01. At an OD_{600nm} of 0.8 the bacteria were placed on ice and aliquots of the culture were fixed for microscopy.

2.8.1.1 Paraformaldehyde (PFA) Fixation

A sample of the culture was mixed with 4% paraformaldehyde (PFA) in a ratio of 1:4. The suspension was inverted to gently mix the bacteria and incubated for 16hr at 4°C or for 15min at room temperature. 20µl of the sample was spotted into a well on a 10 well glass microscope slide and dried at 37°C.

2.8.1.2 Methanol Fixation

Methanol fixation was used to fix and permeabilise bacteria for antibody staining within the cell. A sample of the culture was mixed with 99% ice-cold methanol in a ratio of 1:1. After gentle mixing the suspension was immediately incubated at -20°C for at least 10min. Once incubated 20µl of the sample was spotted into a well on a 10 well glass microscope slide and dried at 37°C.

The dried slides were heat fixed with a Bunsen burner flame to ensure the bacteria were not dislodged from the slide during the antibody staining technique. Then the slides were washed with 1x PBS (Oxoid, Hampshire, UK) by pipetting 20µl of PBS into each well and removing it, this was repeated three times. After this the wells were incubated in 20µl of primary antibody solution and placed on a rocking platform at room temperature inside a sealed box containing wet tissue (to stop the slides from drying). The slides were then washed three times with 1x PBS to remove the primary antibody and the wells were incubated in 20µl of secondary antibody solution and placed on a rocking platform inside the sealed box. Following this incubation the slides were washed with 1x PBS for a final three times and mounted with fluorescence mounting medium (Dako; Glostrup, Denmark). Cover slips were placed on the slides and they were allowed to dry for 48hr in the dark before visualising them on a DM LB2 microscope (Leica, Milton Keynes, UK) using a 100x objective lens with image acquisition and analysis performed using OpenLab software (Improvision, Coventry, UK)

2.8.2 GFP Slide Preparation

Slides that were made with strains containing GFP fusions (i.e. strains that did not need antibody staining to be visualised by fluorescence microscopy) were fixed by the PFA fixation method. Once dry they were mounted with the fluorescence mounting medium (Dako; Glustrop, Denmark), left to dry for 48hr in the dark and visualised on the Leica DM LB2 microscope.

2.8.3 Improvision OpenLab Software

The Improvision (Coventry, UK) OpenLab software was used to control the exposure time of a captured image and to contrast enhance the image to the software's 'best guess' parameter. Both the exposure time and whether the image has been contrast enhanced is stated in the relevant results sections.

2.9 Whole Population Fluorescence Measurements using the FLUOstar OPTIMA Apparatus

To measure whole population fluorescence the bacteria were grown in an identical manner as for fluorescence microscopy. During their growth from an OD_{600nm} of 0.01 to 0.8, ~5 FLUOstar OPTIMA readings were taken. For each reading three 200µl aliquots were taken and placed in three wells of a black 96 well plate. This was assayed in a Flurostar fluorimeter (FLUOstar OPTIMA, Bath, UK), using 485nm absorbance and 520nm emission, at a gain of 1750. The results were expressed in relative fluorescence units (rfu) and plotted against the OD_{600nm} measured at the time the samples were taken.

2.10 DNA Sequencing

All DNA sequencing for this study was performed by MWG-Biotech, London, UK (single read DNA sequencing services), with forward and reverse sequencing primers designed and sent to MWG-Biotech according to the company's guidelines.

All the recombinant vectors constructed from the ligation of a PCR product to a plasmid were sequenced. Clones into the pCR4®-TOPO® vector were sequenced using the T3 and T7 primers, which flank the TOPO® cloning site.

A double-stranded DNA sequence for each plasmid was assembled by aligning contigs obtained from MWG-Biotech using ContigExpress, a component of Vector NTI Suite 8.0 (Invitrogen, Paisley, UK). Sequence chromatograms were viewed with CodonCode Aligner v.1.3.4 when any variations between the sequence and the reference strain were observed to ensure the variation was genuine.

2.11 Solutions

All chemicals are from Sigma Aldrich (Dorset, UK) unless otherwise stated.

2.11.1 Media

2.11.1.1 LB Broth:

For 1L: 10g Tryptone

5g Yeast extract

5g NaCl

Dissolved in distilled water (dH_2O) to make 1L and autoclaved.

2.11.1.2 LB Agar:

For 1L:10g Tryptone

5g Yeast extract

5g NaCl

15g Bacto agar

Dissolved in dH_2O to make 1L and autoclaved.

2.11.1.3 MEM-HEPES Supplements

2.11.1.3.1 MEM-HEPES - Ferric Nitrate:

0.4g dissolved in 100ml dH_2O and filter sterilised to make a stock solution of 10mM.

Store at 4°C and add 13µl to 500ml MEM-HEPES.

2.11.1.3.2 MEM-HEPES – Micronutrients:

100ml of 1000x Micronutrients:

30µl 1mM Ammonium molybdate

400µl 1mM Boric acid

300µl 1mM Cobolt chloride

100µl 1mM Copper sulphate

800µl 1mM Manganese chloride

100µl 1mM Zinc sulphate

Make to 100ml with dH_2O and store at -20°C protected from light.

2.11.1.4 Antibiotics (1000x stocks)

50mg/ml Ampicillin: 1g dissolved in 20ml dH_2O, aliquoted and stored at -20°C.

25mg/ml Chloramphenicol: 0.5g dissolved in 20ml 100% ethanol, aliquoted and stored at -20°C.

25mg/ml Kanamycin: 0.5g dissolved in 20ml dH_2O, aliquoted and stored at -20°C.

10mg/ml Tetracyclin: 0.2g dissolved in 20ml 1:1 ethanol:dH_2O, aliquoted and stored at -20°C.

2.11.2 CTAB DNA Extraction

2.11.2.1 TE buffer:

10mM	Tris-HCl (pH 8.0)
1mM	Ethylinediamine tetraacetic acid (EDTA)

1ml 1M Tris-HCL (pH8.0) added to 200µl 0.5M EDTA and made up to 100ml with MQ water.

2.11.2.2 5M NaCl:

292.2g NaCl dissolved in 1L dH_2O and autoclaved.

2.11.2.3 CTAB/NaCl – 10% CTAB in 0.7M NaCl:

4.1g NaCl dissolved in 80ml dH_2O and 10g CTAB slowly added whilst heating and stirring (if necessary heat to 65°C to dissolve). dH_2O added to 100ml.

2.11.3 PCR

2.11.3.1 dNTP mix:

0.4µM of dATP, dCTP, dTTP, and dGTP (Roche, Burgess Hill, UK) in MQ water (4µl of 100mM dNTP solutions dissolved in 984µl MQ water, aliquoted and stored at -20°C).

2.11.3.2 10 × PCR Reaction Buffer (Roche, Burgess Hill, UK):

100mM	Tris-HCl (pH8.3 @ 20°C)
15mM	Magnesium chloride ($MgCl_2$)
500mM	Potassium chloride (KCl)

Supplied with *Taq* DNA polymerase enzyme (Roche, Burgess Hill, UK).

2.11.3.3 Expand Long Template PCR System (Roche, Burgess Hill, UK)

2.11.3.3.1 10x Expand Long Template PCR System Buffer:

100mM Tris-HCl (pH8.3 @ 20°C)

17.5mM $MgCl_2$

500mM KCl

Supplied with Expand Long Template PCR System (Roche, Burgess Hill, UK).

2.11.4 DNA Agarose Electrophoresis

2.11.4.1 TBE Buffer:

89mM Tris (hydroxymethyl) aminomethane (Fisher, Leicestershire, UK)

89mM Boric acid

2mM EDTA

10x TBE buffer was purchased from Fisher (Leicestershire, UK).

2.11.5 NEB Buffers (Supplied with NEB Enzymes)

2.11.5.1 10x NEB Buffer 1:

10mM Bis Tris Propane-HCl, 10mM MgCl, 1mM dithiothreitol (pH7.0 at 25°C).

2.11.5.2 10x NEB Buffer 2:

50mM NaCl, 10mM Tris-HCl, 1mM dithiothreitol (pH7.0 at 25°C).

2.11.5.3 10x NEB Buffer 3:

100mM NaCl, 50mM Tris-HCl, 10mM $MgCl_2$, 1mM dithiothreitol (pH7.9 at 25°C).

2.11.5.4 10x NEB Buffer 4:

50mM potassium acetate, 20mM Tris-acetate, 10mM magnesium acetate, 1mM dithiothreitol (pH7.9 at 25°C).

2.11.6 Transformations

2.11.6.1 Transformation Buffer I (TFB I):

For 1L: 30mM (2.94g) Potassium acetate

10mM (1.47g) Calcium chloride

100mM (7.45g) Potassium chloride

15% (150ml) Glycerol

Dissolved in 900ml dH_2O, autoclaved and added to 100ml of autoclaved 500mM manganese chloride (9.9g/100ml). Aliquoted and stored at -20°C.

2.11.6.2 Transformation Buffer II (TFB II):

For 1L: 75mM (11.03g) Calcium chloride

10mM (0.75g) Potassium chloride

15% (150ml) Glycerol

100mM (2.09g) MOPs

Made to pH7.0 with 10M sodium hydroxide and autoclaved. Aliquoted and stored at -20°C.

2.11.7 6% Sucrose Plates:

For 1L: 14g Bacto agar

10g Tryptone

5g Yeast extract

Dissolved in 850ml dH_2O and autoclaved. Add 150ml of 40% sucrose stock solution (filter sterilised), plates poured and stored at 4°C.

2.11.8 Sonication/Protein Buffer:

For 10mls: 10mM (20µl) Sodium chloride

50mM (500µl) Tris-HCl pH7.6

1mM (20µl) EDTA

0.1mM (1µl) Dithiothreitol (DTT)

0.001mM (1µl) Phenylmethylsulphonyl fluoride (PMSF)

Made to 10ml with dH_2O, filter sterilized and stored at 4°C

2.11.9 SDS PAGE

2.11.9.1 12% SDS PAGE Resolving Gel:

3ml Acrylamide / N,N'-methylenebisacrylamide (bisacrylamide) (37.5:1)

4.3ml dH_2O

2.5ml 1.5M Tris-HCl pH8.8

0.1ml 10% SDS

0.1ml 10% Ammonium persulphate

10µl N,N,N',N'-Tetramethylethylenediamine (TEMED)

2.11.9.2 5% SDS PAGE Stacking Gel:

0.625ml Acrylamide / N,N'-methylenebisacrylamide (bisacrylamide) (37.5:1)

3ml dH_2O

1.26ml 0.5M Tris-HCl pH6.8

50µl 10% SDS

50µl 10% APS

5µl TEMED

2.11.9.3 10x SDS PAGE Running Buffer:

For 1L: 30g Tris

144g Glycine

Dissolved in dH_2O to make 1L, should have pH8.8, heat and stir to dissolve.

2.11.9.4 SDS PAGE Loading Buffer:

For 20ml: 8ml 10% SDS

2.4ml Glycerol

0.4ml β-mercaptoethanol

1ml 1M Tris-HCl pH6.8

Small spatula of brilliant blue granules to colour

6.5ml dH_2O

Aliquoted and stored at -20°C.

2.11.10 Tricine SDS PAGE

2.11.10.1 5x Anode Buffer:

For 1L: 121.1g Tris

Dissolved in 1L dH_2O (adjusted pH to 8.9).

2.11.10.2 Cathode Buffer:

For 1L: 12.11g Tris

17.92g Tricine

1g SDS

Dissolved in 1L dH_2O (adjusted pH to 8.2 if necessary).

2.11.11 Western Blotting

2.11.11.1 Transfer Buffer:

2.42g Tris

11.54g Glycine

200ml Methanol

dH_2O added to 1L.

2.11.11.2 Blocking buffer:

1x PBS (Oxoid, Hampshire, UK): 2 tablets dissolved in 200ml dH_2O and autoclaved.

8% Dried semi-skimmed milk (Marvel): 16g dissolved in 200ml 1x PBS.

2.11.11.3 Washing Buffer:

2.11.11.3.1 Low Stringency Blots:

For 1L: 1x PBS (10 Oxoid PBS tablets in 1L dH_2O)

0.05% Tween 20 (0.5ml in 1L).

2.11.11.3.2 High Stringency Blots:

Same as low stringency but with 1% dried semi-skimmed milk (Marvel) added.

2.11.11.4 Enhanced Chemiluminescence ECL Reagent

2.11.11.4.1 ECL Solution 1:

1ml Stock luminol

0.44ml Stock p-courmaric acid

10ml 1M Tris-HCl pH8.5

Added dH_2O to 100ml.

2.11.11.4.2 ECL Solution 2:

64µl 30% Hydrogen peroxide

10ml 1M Tris-HCL pH8.5

Added dH_2O to 100ml

Store both ECL 1 and 2 at 4°C for up to one month. One Western blot from an SDS PAGE mini gel required 5ml of solution 1 added to 5ml of solution 2 immediately before use, mixed and applied to blot.

2.11.11.4.3 Stock Luminol:

Luminol (Fluka; Sigma, Dorset UK) dissolved in 250mM dimethyl sulfoxide DMSO (0.886g/20ml), stored at -20°C.

2.11.11.4.4 Stock p-Coumaric Acid:

p-Coumaric acid (Sigma, Dorset, UK) dissolved in 90mM DMSO (0.296g/20ml), stored at -20°C.

Chapter 3
Strategy and Cloning

3 Strategy and Cloning

This chapter describes the strategy employed to create tagged proteins in the basal apparatus of the T3SS. The initial description is generic, describing a method devised to create the tagged proteins which, in theory, could be transferred to any genes in *E. coli* requiring genetic manipulation to add a tag with minimal changes to the wild type sequence. The chapter goes on to describe specific details relating to the strategy surrounding the *esc* genes that have been chosen for this project, followed by the proof of constructs and strains made and the problems and solutions encountered when manipulating these genes.

The T3SS basal apparatus proteins that are predicted to be in the inner membrane are Esc D, V, R, S, T, U, and the associated cytoplasmic ATPase EscN (Fig.2, B). In the EHEC O157:H7 LEE pathogenicity island the genes *escV* and *escN* are situated next to each other on the LEE3 operon and the genes *escR, S, T,* and *U* are next to each other on the LEE1 operon (Fig.2, A). These two sets of genes are two distinct targets. *EscD* is upstream from the LEE4 operon, isolated from the genes for the other predicted inner membrane basal apparatus proteins. This project will not focus on *escD* as the two sets of genes on LEE1 and LEE3 offer the opportunity to manipulate six *esc* genes with related intermediate steps. The strategies for LEE3 were devised but not implemented, and can be seen in Appendix 1.

For the strategy and cloning sections all the primers have been given a number, which is referred to throughout the results chapters. Table 3 contains the sequence of all the primers and a description of their use. All the strains and plasmids created are listed in Table 1 and Table 2.

3.1 Strategy

3.1.1 Site Directed Mutagenesis

3.1.1.2 Principle

A cloning strategy was created for the addition of REase recognition sites at the 3' end of the genes *escN, V, R, S, T,* and *U*. Only the strategies for *escR* and *escU* will be taken forward, the rationale for this will be explained under the relevant results section. *EscR* and *escU* will have the genes for fluorescent proteins or antigenic peptides cloned into the sites to create C terminal protein fusions detectable by immunochemistry techniques or by direct visualisation with fluorescence microscopy. Fundamental to the strategy is using allelic exchange to create Walla3 strains where the genes *escRSTU* are substituted with the *sac/*Kan cassette. The intermediate strain created allows for a second round of allelic exchange in which the *sac/*Kan cassette is replaced by an *esc* gene fused to the gene for the fluorescent protein or the antigenic peptide. The EHEC O157:H7 strain will now have a single copy of the *escR* or *escU* fusion gene on the chromosome in its original genetic context, being expressed under its natural promoter.

3.1.1.2.1 Creating an *escRSTU*<>*sac/*Kan Strain

Creating a *sac/*Kan substitution for groups of genes (*escRSTU)* means the cloning strategy can be designed to manipulate more than one gene at a time, for example: creating a Walla3 strain where both the genes *escR* and *escU* have a tag at their 3' end, allowing detection of both proteins in the same strain.

In the strategy the allelic exchange method will be used to create the initial deletions of the LEE1 genes. Instead of amplifying 1Kb flanking regions from either side of the chosen gene cluster and cloning them into an exchange vector (as described in Roe, A., *et al* 2007), the whole of the sequence for *escRSTU* will be amplified with ~1Kb of homologous sequence either side and cloned into the exchange vector. The two sequences to be amplified will be chosen to contain unique REase sites that, following digestion, removes the genes of interest, leaving the 1Kb of flanking sequence needed to create the substitution to form the intermediate strain (Fig.6). The *sac/*Kan cassette will

be ligated into the restricted plasmid replacing the *esc* genes. This creates the plasmid for the first round of allelic exchange. In this round the *esc* genes that are removed from the plasmid after restriction digestion (esc*RSTU*) will be substituted on the Walla3 chromosome by the *sac*/Kan cassette. This will create an intermediate strain which is sucrose sensitive, kanamyacin resistant and lacks the *esc* genes *R, S, T, U* or *N, V* (Fig.7). The next stage of the strategy is to use the original plasmid containing the *esc* genes to add unique REase sites at the 3' end of the gene(s) of interest, then to use these REase recognition sites to add the genes for the fluorescent protein or antigenic peptide, creating the gene fusions. This plasmid can then be used in the second round of allelic exchange in the intermediate strain to replace the *sac*/Kan cassette with the tagged *esc* gene.

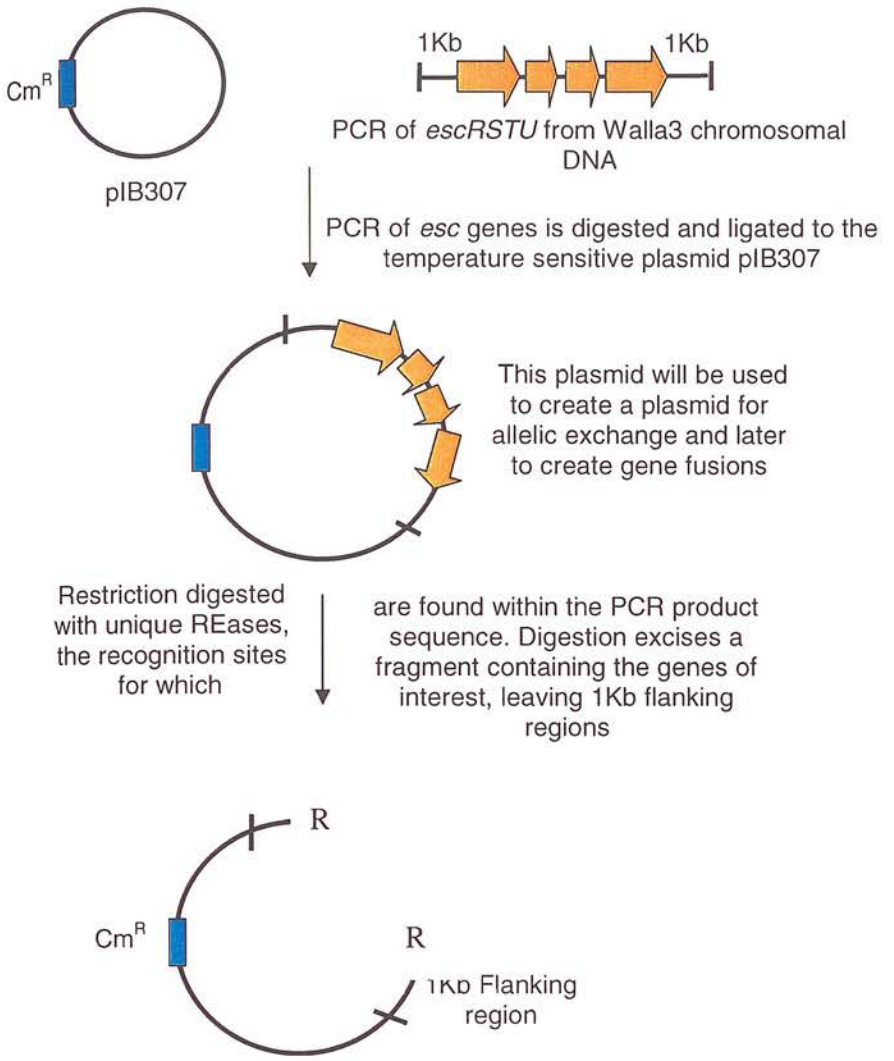

Fig.6 Schematic diagram showing the creation of a plasmid containing the *esc* genes and its restriction with unique REases (R) to leave 1Kb of flanking DNA. The plasmid is now ready to have the *sac*/Kan cassette ligated into it on the digested restriction sites.

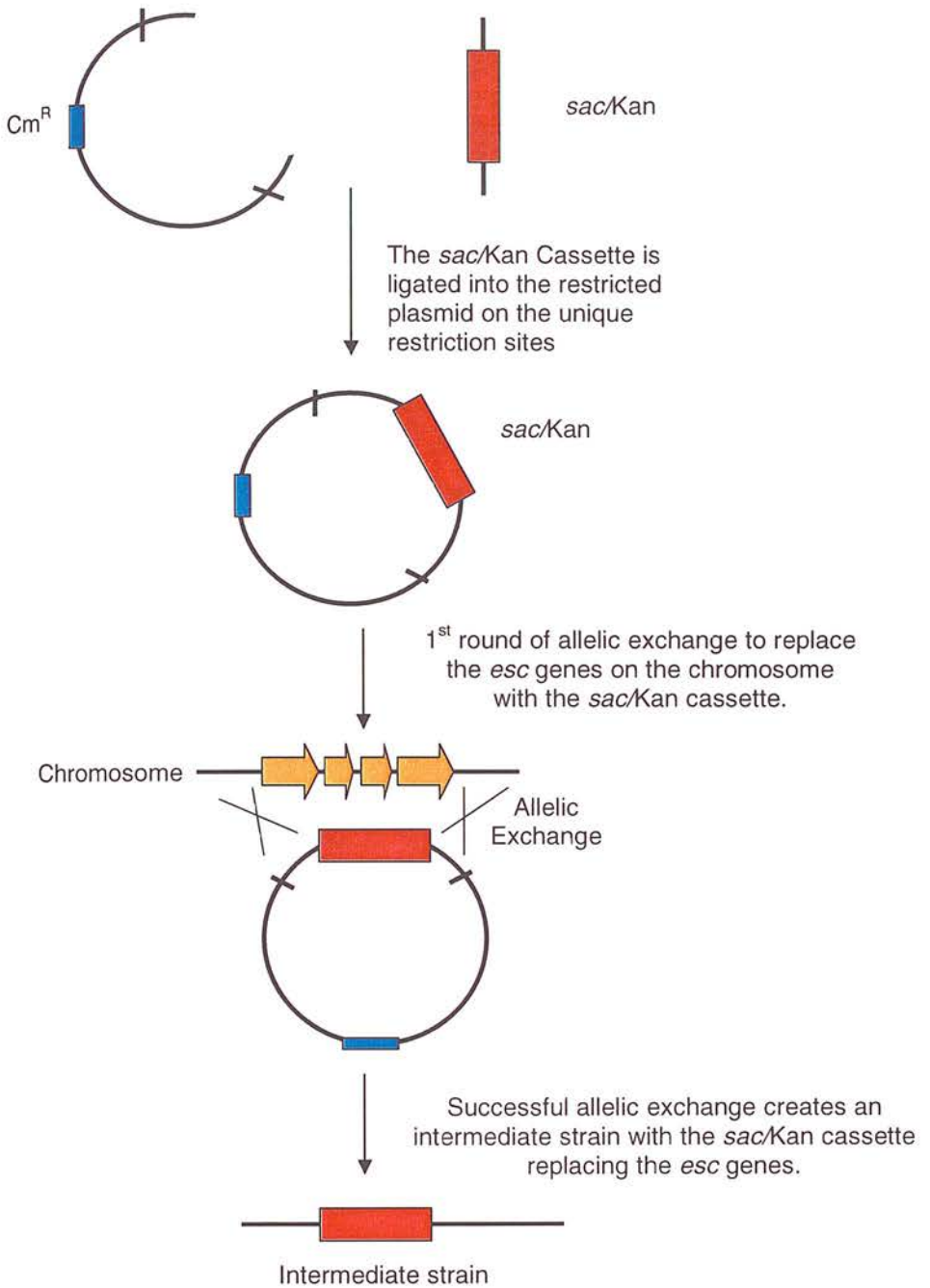

Fig.7 Schematic diagram showing the creation of the exchange plasmid used in the first round of allelic exchange to create the intermediate strain.

3.1.1.2.2 Addition of 3' REase Recognition Sites

After the PCR products for the *esc* genes are cloned into the pIB307 vector two unique restriction sites will be chosen that are situated ~1Kb either side of the 3' end of *escR* and *escU* gene. A 5' and 3' primer will be designed over these sites (creating a 2Kb product when they are used in a PCR). Over the 3' end of the gene two more primers will be designed. These two primers will overlap one another but are not identical to the wild type sequence, using overlapping site directed mutagenesis to add a new REase recognition site (see Chapter 2 for overlapping site directed mutagenesis method and diagram). The overlapping primers are paired with either the 3' or 5' primers designed over the unique restriction sites ~1Kb up or down stream. PCR with these two sets of primers creates two 1Kb products with the 5' end of one product identical to the 3' end of the other. These two products, after PCR purification, will be used as the DNA template in a third PCR reaction, using the two outside primers (sitting over the wild type unique restriction sites) to create one product of ~2Kb. This product is identical to the wild type sequence apart from the introduced unique REase recognition site (Fig.8).

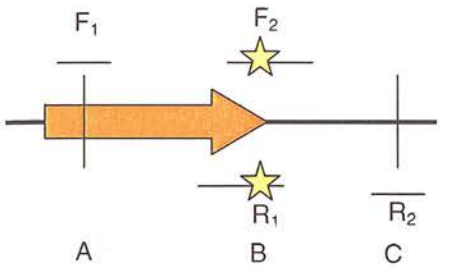

Primers are numbered F_1, F_2, R_1 and R_2. REase recognition sites labelled A, B and C

Primers F_1 and R_2 are designed over unique REase recognition sites (A and C) on the chromosome. Primers F_2 and R_1 are overlapping and paired with R_2 and F_1 respectively. The overlapping primers contain base changes that introduce a novel REase recognition site (B) at the 3' end of the gene (marked with a star)

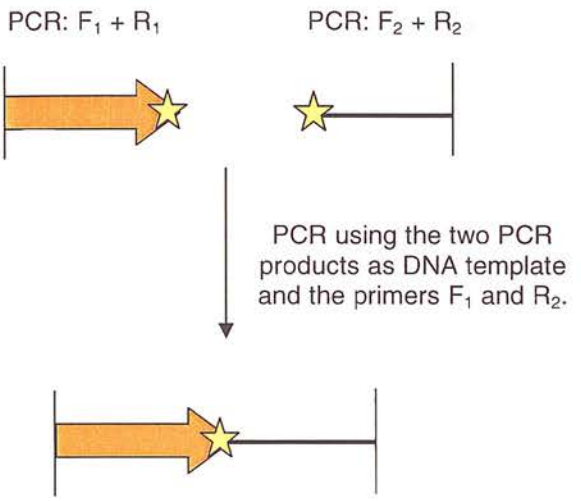

Fig.8 Diagram showing the creation of two PCR products that overlap at their 3' and 5' ends. The overlapping region contains sequence changes added to the primers which introduce a unique REase recognition site (B). These two products are used in a PCR reaction as the DNA template with the primers F_1 and R_2. This PCR creates a 2Kb PCR product that is identical to the wild type sequence except for the added restriction site.

The 2Kb product will then be restricted by the unique REases whose recognition sites are present in the wild type sequence. The plasmid containing the *escR* or *escU* gene PCR

product is restricted with the same REases and the 2Kb fragment removed is replaced by the 2Kb PCR product containing the added REase recognition site. The resulting plasmid is identical to the parent plasmid apart from a unique restriction site added to the 3' end of the *esc* gene. This site is then used in non-directional cloning to add the gene for either a fluorescent protein or an antigenic peptide. A second round of allelic exchange is performed in the intermediate strain with this plasmid, now containing a tagged gene, to replace the *sac*/Kan cassette (Fig.9).

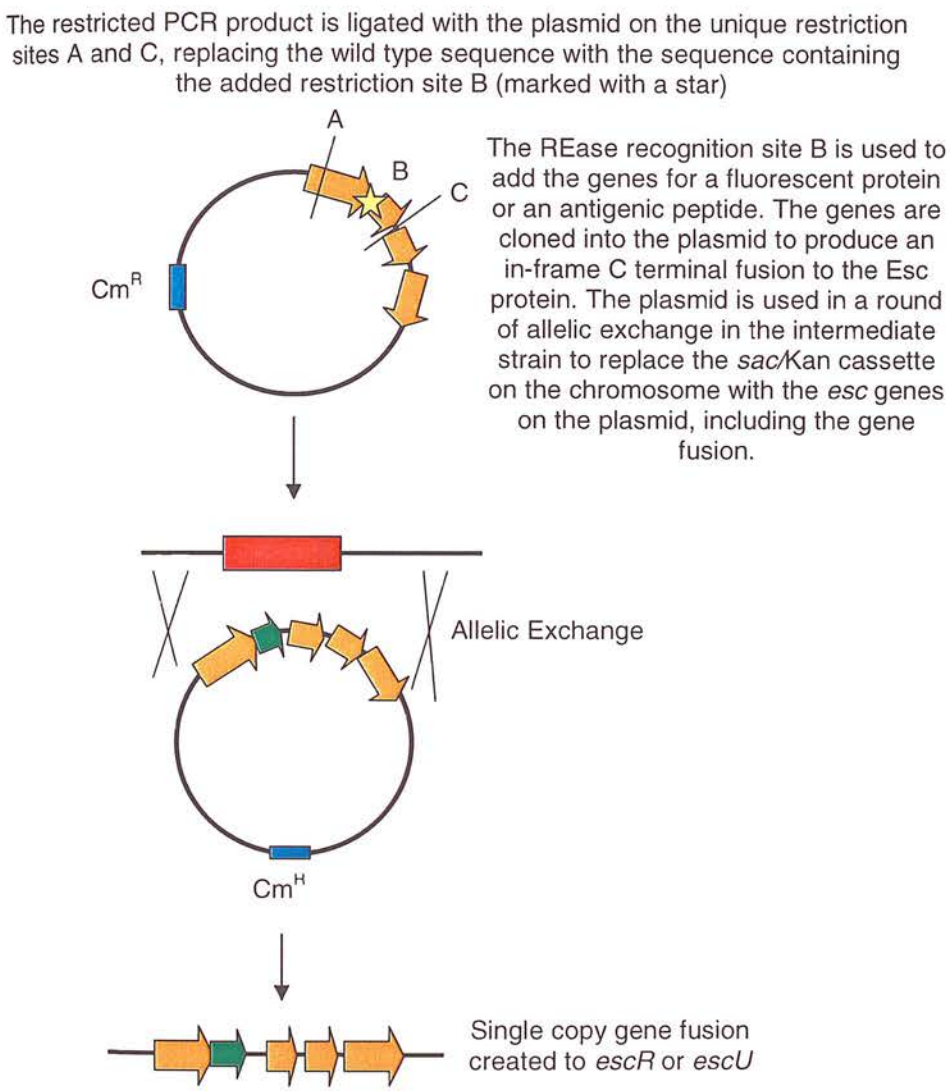

Fig.9 The addition of a unique REase recognition site allows for the non-directional cloning of a chosen tag at the 3' end of the *esc* gene. This plasmid can be used in a round of allelic exchange to replace the *sac*/Kan cassette from the intermediate strain with the *esc* genes on the plasmid.

To enable the tagging of more than one *esc* gene at a time the added REase recognition site has to be unique and only used for one *esc* gene. Bearing this in mind, whilst trying to create minimal changes in the wild type sequence, strategies to add a 3' endonuclease recognition site were designed for all six *esc* genes in LEE1 and LEE3. Only the strategies for *escR* and *escU* are shown, but strategies for *escS, T, V, N* can be seen in Appendix 1.

3.1.4 Strategy for *escR*

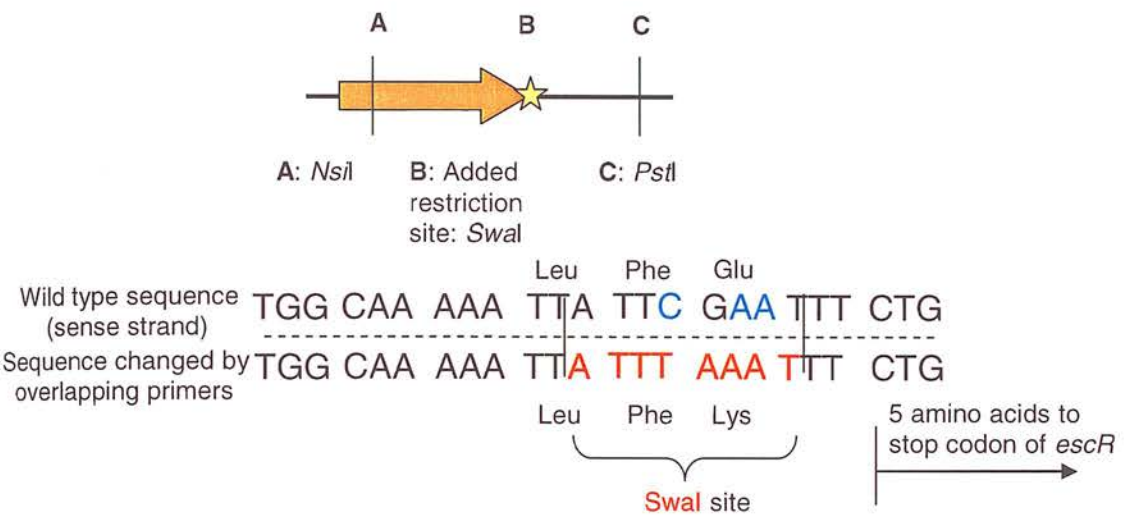

Fig.10 Diagram showing the REases to be used in the strategy for *escR* to add a *Swa*I recognition site. The nucleotides in blue will be changed in the wild type sequence to form the recognition sequence for *Swa*I (shown in red).

For *escR*, primer 9 (primer F_1) sits over the unique REase recognition site for *Nsi*I and primer 10 (primer R_2) is designed over the recognition site for *Pst*I. A *Pst*I recognition site is also present in the pIB307 plasmid, meaning that either a partial digest is required for successful cloning or the *Pst*I site in the pIB307 backbone has to be removed. The site added by the overlapping primers 11, 12 at the 3' end of *escR* is *Swa*I (Fig.10). Although this site has been used for *escV* it can be used for *escR* as the two genes will not be cloned together on the same allelic exchange plasmid. The start codon for *escS* is 19bp beyond the added *Swa*I site. Again this is designed to minimise interference with the transcription and translation of *escS*. However, it means the sequence for the last 6 amino acids of *escR* will be added in the tail of the 5' primer used in the PCR for the tag.

3.1.7 Strategy for *escU*

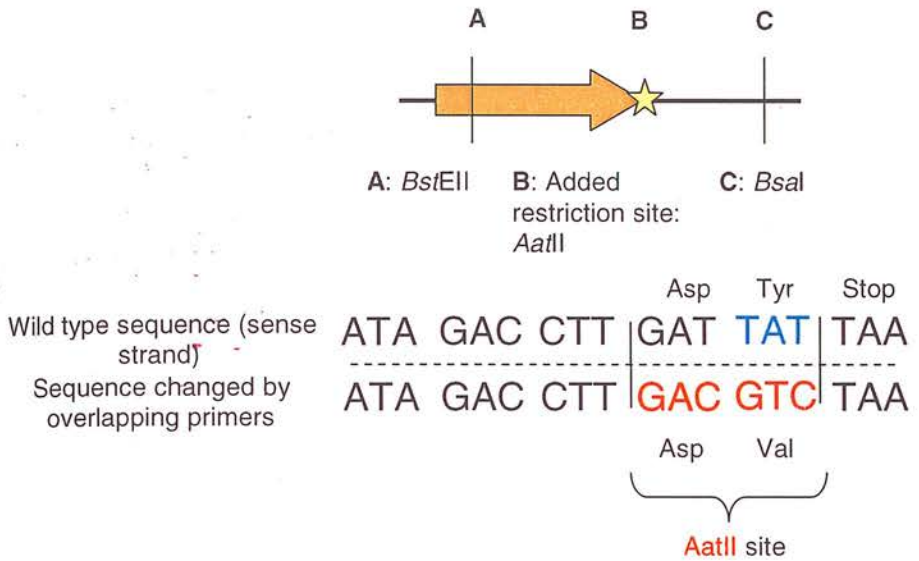

Fig.11 Diagram showing the REases to be used in the strategy for *escU* to add an *Aat*II recognition site. The nucleotides in blue will be changed in the wild type sequence to form the recognition sequence for *Aat*II (shown in red).

Primer 19 sits over the REase recognition site *Bst*EII and primer 20 over *Bsa*I. Primers 21, 22 overlap and contain the changes to add the REase recognition site for *Aat*II (Fig.11). The strategy for *escU* is the only strategy that changes the last six nucleotides of the gene into the added REase recognition site. It is designed this way because the downstream gene (*rorf3*) is transcribed in the opposite direction. The stop codon for *rorf3* is UAA comprised of the last T from the tyrosine (the last amino acid in EscU, Fig.12) and the first two nucleotides of the *escU* stop codon TA, making TTA; this transcribed on the antisense strand is the stop codon UAA. The AatII restriction site was chosen as it changes the EscU amino acid sequence from a tyrosine to a valine. This changes the stop codon of the downstream gene from UAA to the stop codon UAG. Therefore, the addition of the *Aat*II site has a minimal effect on both genes and requires no added nucleotides to either end of the primers used to PCR amplify the tags.

3.2 Cloning

Although strategies for LEE1 genes *escRSTU* and LEE3 genes *escNV* were designed only the LEE1 clone was created. The decision was made because the LEE1 clone offered the opportunity to manipulate four basal apparatus proteins, while there are only two on the LEE3 clone. As the strategies for tagging *escN* and *escV* have been designed it can be revisited at a later date if required.

Every strain made throughout the project was stored in 20% glycerol at -70°C. The plasmids constructed were also stored in this way, either in the strain TOP10 or the strain AAEC185, the plasmids were also extracted using the QIAprep™ spin plasmid miniprep kit (QIAGEN, West Sussex, UK) and stored at -20°C.

3.2.1 Creating the Strain Walla3 *escRSTU*<>*sac*/Kan (ZAP1140)

3.2.1.1 Constructing the pJRE01 Plasmid

The section of the LEE1 operon containing the genes *escRSTU* and ~1Kb of left and right flanking sequence was amplified using expand long template PCR system (Roche, Burgess Hill, UK) and the primer pair 23, 24 (Fig.12).

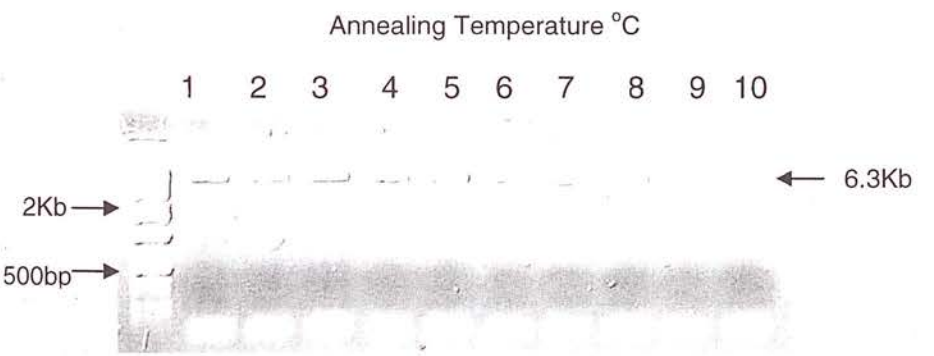

Fig.12 Expand long range template *escRSTU* product. The annealing temperature was a gradient from 60°C to 70°C with approximately one-degree increments. The DNA template for the reaction was 1µl of a 1:150 dilution of Walla3 DNA extracted by the CTAB method.
Lane1: 1Kb DNA ladder
Lane2-11: PCR product for *escRSTU* on temperature gradient 60-10°C

The *escRSTU* PCR product was cloned into the pCR4®-TOPO® vector creating the plasmid pJRE02. The pCR4®-TOPO® cloning step was added to facilitate the final cloning step into pIB307 as it generates high quantities of the digested *escRSTU* fragment, following restriction digestion with *Xma*I (primer 23) and *Xba*I (primer 24) and gel extraction.

The creation of pJRE02 was confirmed by restriction analysis with the REase *Eco*RI. The QIAprep™ spin plasmid miniprep kit (QIAGEN, West Sussex, UK) was used to extract plasmid DNA from recovered TOP10 colonies (Fig.13, A). The pJRE02 plasmid was then digested with the REases *Xba*I and *Xma*I to remove the 6.3Kb *escRSTU* fragment.

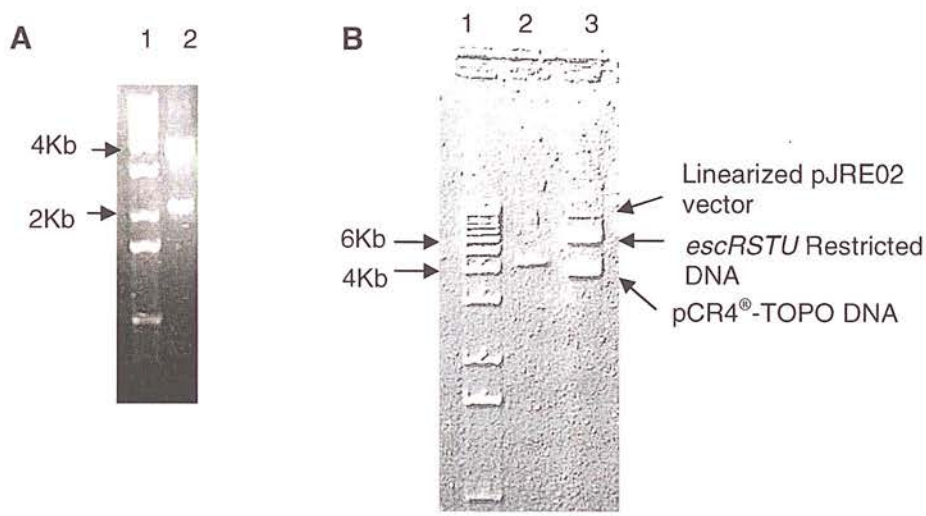

Fig.13, A) *Eco*RI digest of pJRE02 - expected band sizes for pJRE02 are 4.1Kb, 3.9Kb, and 2.2Kb
Lane1: 1Kb DNA ladder
Lane2: pJRE02 clone digested with *Eco*RI
(expected size of bands: 4118bp, 3936bp, 2192bp)
B) pJRE02 digested with *Xma*I and *Xba*I – removal of the 6.3Kb *escRSTU* fragment
Lane1: 1Kb ladder
Lane2: pIB307 vector digested with *Xba*I and *Xma*I
Lane3: pJRE02 clone digested with *Xba*I and *Xma*I

This fragment was purified from an agarose gel and ligated to *Xma*I and *Xba*I digested pIB307 vector (Fig.13, B. Lane2). The ligation mixture was transformed into chemically competent AAEC185 cells. The colonies were screened for successful ligations by *Kpn*I digestion of plasmid DNA (Fig.14) extracted by the QIAprep™ spin plasmid miniprep kit (QIAGEN, West Sussex, UK).

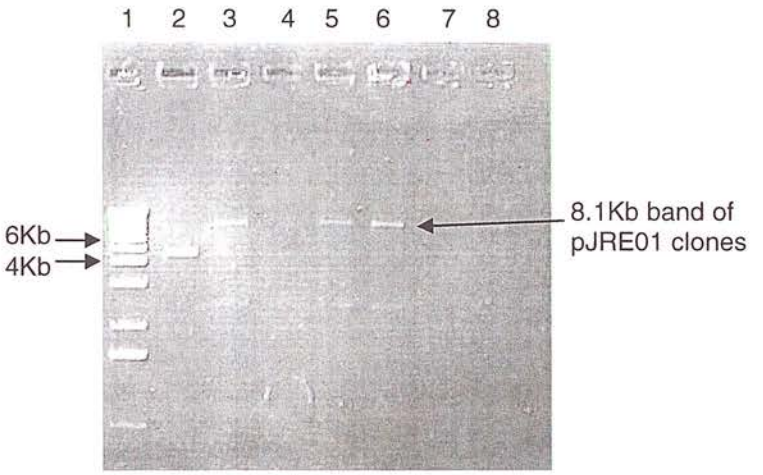

Fig.14 *Kpn*I digest of positive clones for pJRE01.
Lane1: 1Kb DNA ladder
Lane2: pIB307 vector (control). Expected band size: 4.2Kb
Lane3-8: pJRE01 clones. Expected band size: 8.1 Kb and 2.3Kb

3.2.1.2 Constructing the pJRE03 Plasmid

The PCR of the genes *escRSTU* was designed to include the REase recognition sites for HpaI (Fig.17). This enzyme digests the plasmid at two sites to remove the *esc* genes and leave 1-1.8Kb of flanking DNA necessary for allelic exchange.

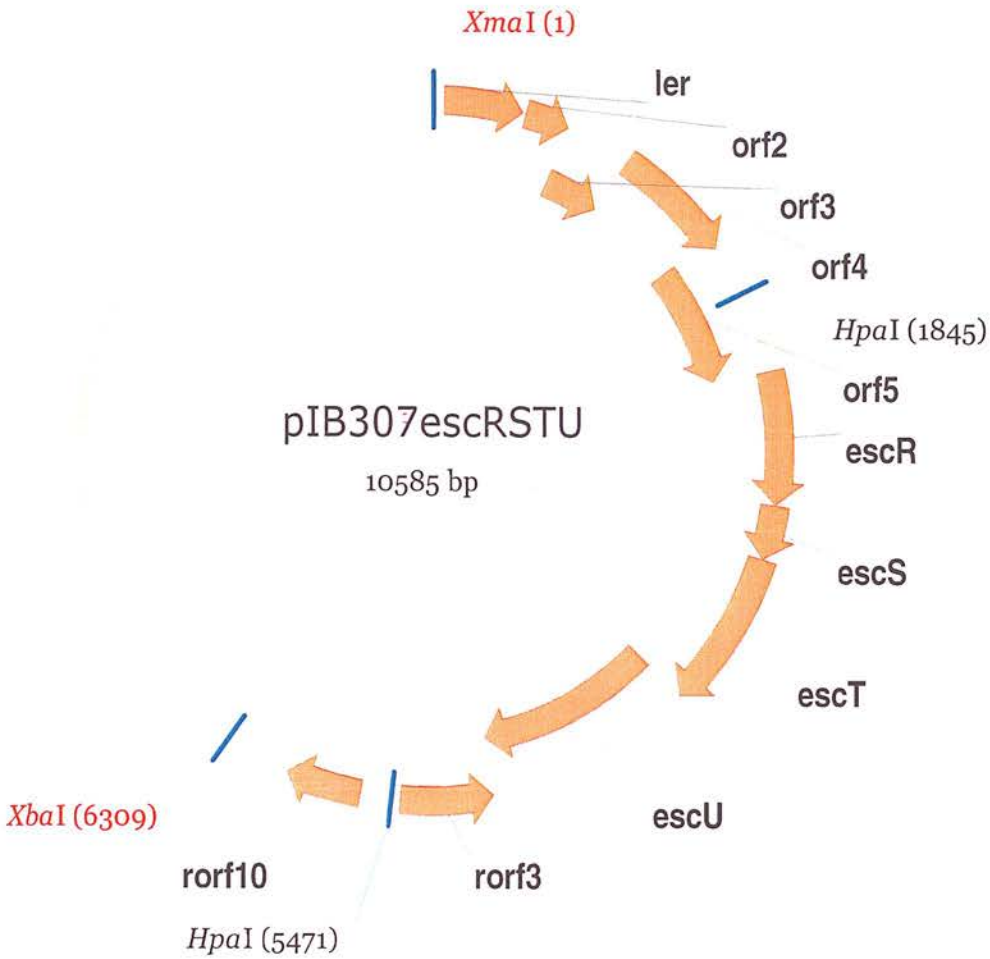

Fig.15 Vector NTI map of pJRE01 plasmid showing Hpal sites and *Xma*l and X*ba*l site.

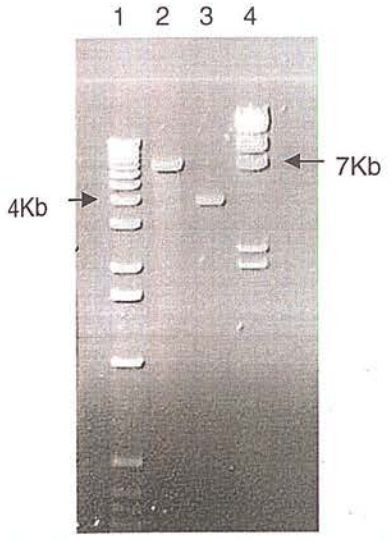

Fig.16 pJRE01 digested with *Hpa*I and the *sac*/Kan cassette after Klenow treatment and extracted from a 0.8% agarose gel - To be ligated together at 4°C for 16hr. The ligation mixture was then transformed into chemically competent AAEC185 cells, recovered for 40hrs at 28°C and plated on LBC plates.
Lane1: 1Kb DNA ladder.
Lane2: pJRE01 plasmid *Hpa*I digested, gel extracted and religated. Then *Hpa*I digested again. Expected band size 6.9Kb
Lane3: *sac*/Kan cassette BamHI digested, Klenow treated. Expected band size 3.8Kb
Lane4: *Hind*III DNA ladder

The *sac*/Kan cassette was restricted with *Bam*HI, treated with DNA polymerase, large fragment (Klenow) and gel extracted. The cassette was ligated to pJRE01 which had been restricted by the REase *Hpa*I, the *esc* genes removed and the 7.2Kb backbone gel extracted (Fig.16). The fragments were ligated together and recovered colonies were patched on LBK plates to screen for the insertion of the *sac*/Kan cassette, which confers kanamyacin resistance. The resulting plasmid (pJRE03) contains the flanking regions (for creating the *escRSTU* substitution) and the *sac*/Kan cassette.

Kanamycin resistant clones were screened by restriction digest analysis with the REase *Rsa*I, the digest shows which plasmids are positive for insertion of the *sac*/Kan cassette and the orientation the *sac*/Kan cassette is in. Either orientation can be used in the allelic exchange process (Fig.17).

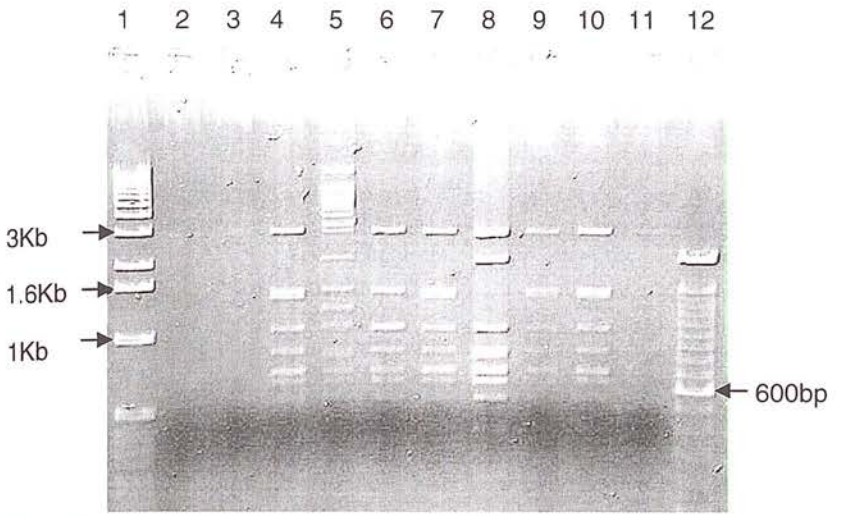

Fig.17 *Rsa*I digest of possible pJRE03 clones for allelic exchange process. Orientation one has the band pattern 2.8Kb, 1.4Kb, 1.4Kb, 1Kb, 859bp, 713bp, 706bp, 635bp, 538bp, 377bp, and 187bp and orientation two has the band pattern 2.8Kb, 2Kb, 1Kb, 859bp, 827bp, 713bp, 706bp, 635bp, 538bp, 377bp, 187bp
Lane1: 1Kb DNA ladder.
Lane4,7,9,10: pJRE03 plasmids containing the *sac*/Kan cassette in orientation one.
Lane8: pJRE03 plasmid with the *sac*/Kan cassette in orientation two.
Lane12: 100bp DNA ladder

A pJRE03 plasmid with the *sac*/Kan cassette in orientation one was used in allelic exchange to replace the genes *escRSTU* with the *sac*/Kan cassette in the EHEC O157:H7 Walla3 strain to create the strain ZAP1140. A schematic diagram for creating the *escRSTU*<>*sac*/Kan strain by allelic exchange is detailed in Fig.18.

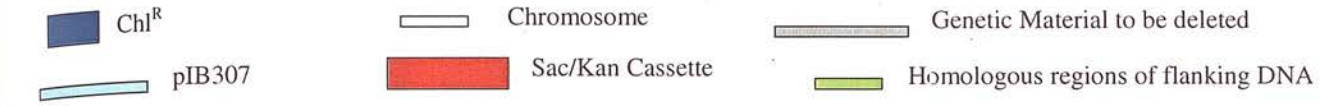

Step 1: Plasmid Integration: Inserting the *sacB*-Kan Cassette:

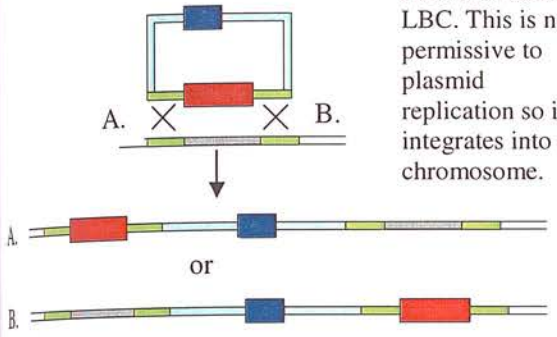

Grown at 42°C in LBC. This is not permissive to plasmid replication so it integrates into the chromosome.

Step 2: Plasmid Excision:
(Shown from integration B. from step 1)

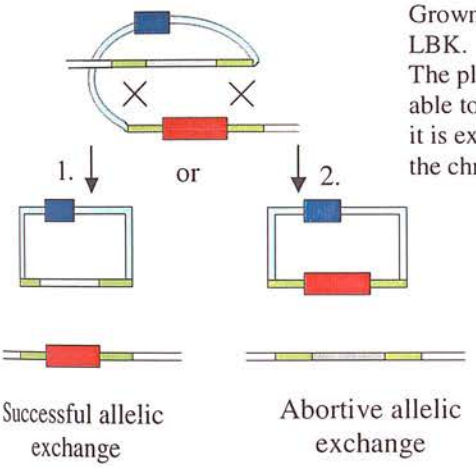

Grown at 28°C in LBK.
The plasmid is able to replicate so it is excised from the chromosome.

Step 3 & 4: Plasmid Curing and selection of the mutant:

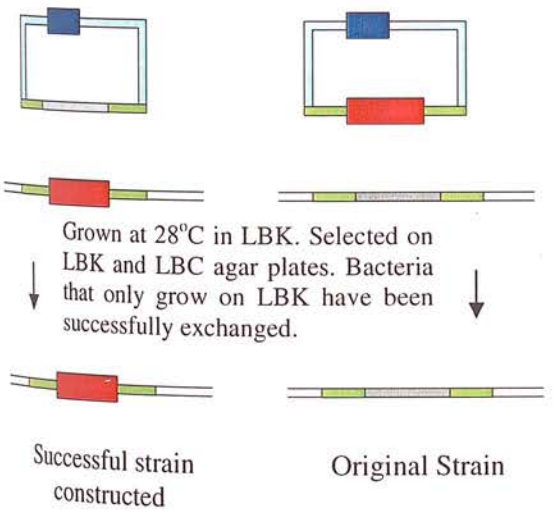

Grown at 28°C on LBK and LBC agar plates.
Positive clones are verified by PCR.

Fig.18 Diagram of allelic exchange method – creating an intermediate strain (Taken from Emmerson, J., *et al* 2006) The transfer of the *sac*/Kan cassette into the chromosome requires two recombination events leading to plasmid integration followed by plasmid excision. Step 1: plasmid integrates into the wild-type strain at the non permissive temperature for plasmid replication (42°C). Steps 2 and 3: plasmid integrates are grown at 28°C in the presence of kanamycin to enrich for bacteria that have excised and cured the plasmid, leaving the cassette on the chromosome. Step 4: Growth on media containing LBC or LBK. Bacteria that can only grow on LBK are successful constructs of the intermediate strain.

3.2.2 Screening the Strain Walla3 *escRSTU<>sac*/Kan (ZAP1140)

Walla3 colonies with the correct resistance profiles for the successful chromosomal insertion of the *sac*/Kan cassette and excision of the pIB307 plasmid were screened by PCR (Fig.19). A PCR was also designed with the 5' primer (primer 25) sitting outside the left flanking region on the bacterial chromosome paired with a 3' primer (primer 27) specific for the *sacB* gene. This PCR will only work, giving a product of 3.4Kb, if the *sac*/Kan cassette has been inserted into the correct place on the chromosome. Fig.19, Lane9 contains the correct PCR product from this reaction in the ZAP1140 strain.

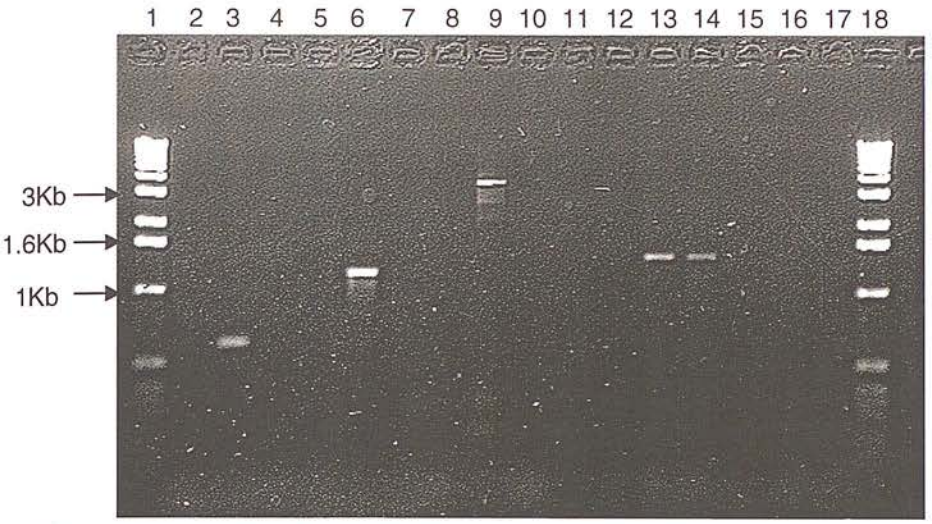

Fig.19 PCR screening of Walla3 *escRSTU<>sac*/Kan (ZAP1140). strain Primer pairs 10, 11 and 20, 21 for *escR* (1.4Kb product) and *escU* (572bp product) were used with a blank DNA negative control, 1µl of a CTAB Walla3 DNA extraction (diluted 1:150) as a DNA template for a positive control and crude DNA lysate from the ZAP1140 strain being screened
Lane1: 1Kb DNA ladder
Lane2: *escU* PCR 2 DNA blank negative
Lane3: *escU* PCR 2 Walla3 DNA template positive
Lane4: *escU* PCR 2 ZAP1140 strain
Lane5: *escR* PCR 2 DNA blank negative
Lane6: *escR* PCR 2 Walla3 DNA template positive
Lane7: *escR* PCR 2 ZAP1140 strain
Lane8: Outside left flanking region PCR DNA blank negative (55°C)
Lane9: Outside left flanking region PCR ZAP1140 strain (55°C)
Lane10: Outside left flanking region PCR DNA blank negative (56°C)
Lane11: Outside left flanking region PCR ZAP1140 strain (56°C)
Lane12: Inside left flanking region PCR DNA blank negative (55°C)
Lane13: Inside left flanking region PCR pJRE01 DNA positive (55°C)
Lane14: Inside left flanking region PCR ZAP1140 strain (55°C)
Lane15: Inside left flanking region PCR DNA blank negative (56°C)

A PCR with a 5' primer situated in the left flanking region and a 3' primer specific for *sacB* was also used to screen the Walla3 *escRSTU<>sac*/Kan (ZAP1140) strain (primers 28, 27) giving a 1.4Kb product (Fig.19, Lane12-17).

The Walla3 *escRSTU<>sac*/Kan strain was screened for the absence of the *esc* genes *escR, escS, escT,* and *escU* (Fig.20).

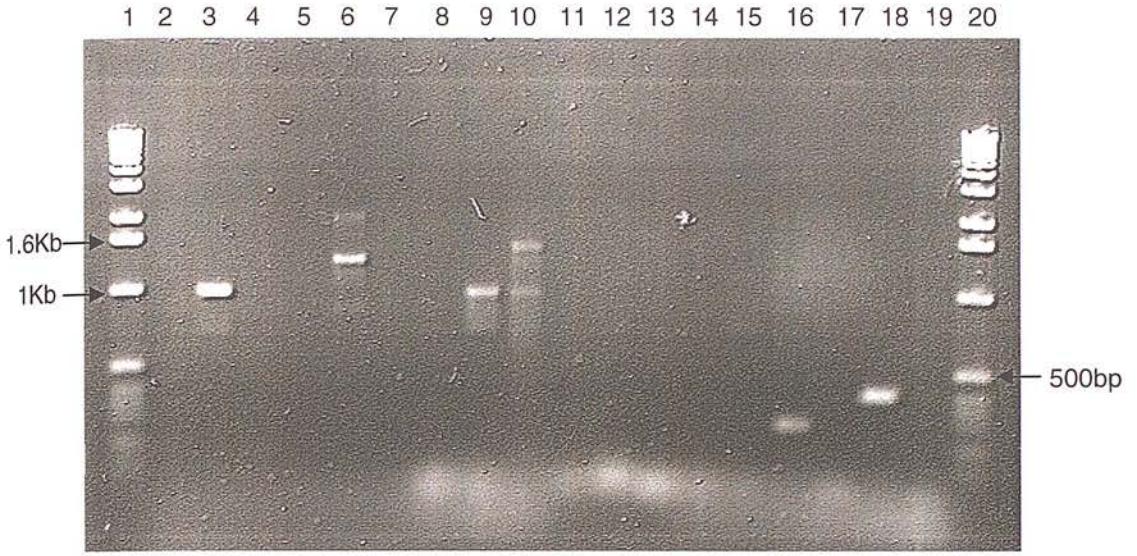

Fig.20 PCR screening of Walla3 *escRSTU<>sacI*/Kan (ZAP1140) strain (cont.). Screening for the absence of the *esc* genes *escR* (primers 9, 12 giving a 957bp product), *escS* (primers 13, 10 giving a 1.2Kb product and primers 14, 9 giving a 1Kb product), *escT* (primers 15, 18 giving a 1Kb product and primers 16, 17 giving a 670bp product) and *escU* (primers 19, 22 giving a 346bp product)
Lane1: 1Kb DNA ladder
Lane2: *escR* PCR DNA blank negative
Lane3: *escR* PCR Walla3 DNA template positive
Lane4: *escR* PCR ZAP1140 strain
Lane5: *escS* PCR DNA blank negative
Lane6: *escS* PCR Walla3 DNA template positive
Lane7: *escS* PCR ZAP1140 strain
Lane8: *escS* PCR 2 DNA blank negative
Lane9: *escS* PCR 2 Walla3 DNA template positive
Lane10: *escS* PCR 2 ZAP1140 strain
Lane11: *escT* PCR DNA blank negative
Lane12: *escT* PCR Walla3 DNA template positive
Lane13: *escT* PCR ZAP1140 strain
Lane14: *escT* PCR 2 DNA blank negative
Lane15: *escT* PCR 2 Walla3 DNA template positive
Lane16: *escT* PCR 2 ZAP1140 strain
Lane17: *escU* PCR DNA blank negative
Lane18: *escU* PCR Walla3 DNA template positive
Lane19: *escU* PCR ZAP1140 strain
Lane20: 1Kb DNA ladder

The Walla3 *escRSTU<>sacI*/Kan strain was also screened with primers specific for the *sacB* gene and primers specific for the pIB307 plasmid backbone (Fig.21, Lane5-10). These PCR products confirmed the observed resistance profile for the strain ZAP1140

(kanamycin resistant and chloramphenicol sensitive). Another PCR screening for the absence of the *escR* gene was also carried (Fig.21, Lane2-4).

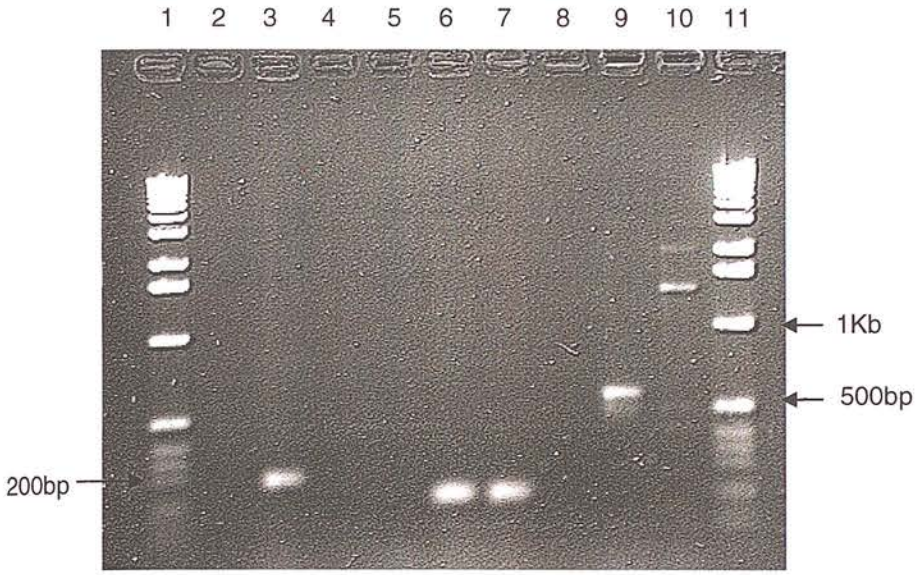

Fig.21 PCR screening of Walla3 *escRSTU<>sac*/Kan (ZAP1140) strain (cont. II). Screening with primers specific for the *sacB* gene (primers 26, 27 to give a 230bp PCR product) and primers specific for the pIB307 plasmid backbone (primers 29, 30 to give a 520bp PCR product) and *escR* gene using primers 31, 32 to give a product of 270bp
Lane1: 1Kb DNA ladder
Lane2: *escR* PCR 3 DNA blank negative
Lane3: *escR* PCR 3 Walla3 DNA template positive
Lane4: *escR* PCR 3 ZAP1140 strain
Lane5: *sacB* gene PCR DNA blank negative
Lane6: *sacB* gene PCR pJRE03 DNA template positive
Lane7: *sacB* gene PCR ZAP1140 strain
Lane8: pIB307 specific PCR DNA blank negative control
Lane9: pIB307 specific PCR pJRE03 DNA template positive
Lane10: pIB307 specific PCR ZAP1140 strain

The resistance profile of the strain and the PCR results confirm that the ZAP1140 stain is a successful substitution of the *escRSTU* genes for the *sac*/Kan cassette.

3.2.3 Creating the Walla3 *escRSTU<>sac*/Kan Restored Strain (ZAP632)

The next stage was to manipulate the pJRE01 plasmid to add REase recognition sites at the 3' end of the *esc* genes. First the pJRE01 plasmid was sent to MWG for sequencing to check that the expand long template PCR system (Roche, Burgess Hill, UK) did not introduce any errors into the *escRSTU* sequence. The sequencing results showed that,

when compared to the available sequence for the EHEC O157:H7 strain EDL933, there were three base changes. One was a silent mutation in ORF5, another changed a valine into an alanine in ORF3, and the third change was in EscU changing a phenylalanine to a serine. At this stage it was impossible to tell, without repeating the PCR and sending it for sequencing again, whether these were errors or true base changes in the Walla3 strain when compared to the EDL933.

The pJRE01 plasmid was used in the allelic exchange process with the intermediate strain Walla3 *escRSTU<>sac*/Kan (ZAP1140) to replace the *sac*/Kan cassette with the *esc* genes on the plasmid to create the restored Walla3 strain – with a restored T3SS. This was an important check for the pJRE01 plasmid; if it was able to restore T3S in the ZAP1140 strain by producing a functioning basal apparatus then the plasmid could be used to manipulate the LEE1 sequence to add the tags. It also meant the pJRE01 plasmid could be verified despite the two amino acid substitutions in the amplified sequence.

3.2.4 PCR Screen of the T3SS Restored Strain (ZAP632)

The Walla3 *escRSTU<>sac*/Kan restored strain (ZAP632) was screened in a similar way to the Walla3 *escRSTU<>sac*/Kan strain. Colonies with the correct resistance profiles were patched and crude DNA extracts made. They were screened using the PCR primers used to detect the absence of the *esc* genes in the strain Walla3 *escRSTU<>sac*/Kan and the primers specific for the pIB307 and *sacB* gene (Fig.22, A, B, C). All the PCR products confirmed that the restored T3SS strain contained the *esc* genes and had excised and cured the pIB307 plasmid with the *sac*/Kan cassette.

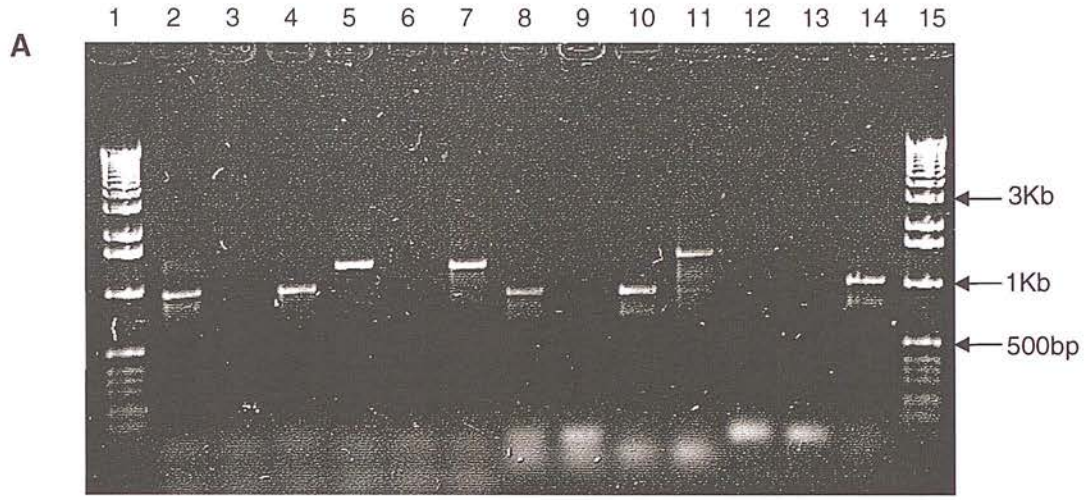

Fig.22 For each set of PCR primers there was a positive control of 1µl of a 1:150 dilution of CTAB extracted Walla3 DNA or a positive control of pJRE03 plasmid DNA, a negative control containing no template DNA and crude DNA extracted from the ZAP632 strain being screened. For PCR products *escS* PCR 1 and 2, *escR* PCR 2 and *escT* PCR 2 the ZAP1140 strain was also used as a negative control.
A) PCR screen of restored T3SS ZAP632 strain.
Lane1: 1Kb DNA ladder
Lane2: *escR* PCR Walla3 template DNA positive control
Lane3: *escR* PCR DNA blank negative control
Lane4: *escR* PCR ZAP632 strain DNA template
Lane5: *escS* PCR Walla3 template DNA positive control
Lane6: *escS* PCR DNA blank negative control
Lane7: *escS* PCR ZAP632 strain DNA template
Lane8: *escS* PCR 2 Walla3 template DNA positive control
Lane9: *escS* PCR 2 DNA blank negative control
Lane10: *escS* PCR 2 ZAP632 strain DNA template
Lane11: *escS* PCR 2 ZAP1140 strain DNA template
Lane12: *escT* PCR Walla3 template DNA positive control
Lane13: *escT* PCR DNA blank negative control
Lane14: *escT* PCR ZAP632 strain DNA template.
Lane15: 1Kb DNA ladder

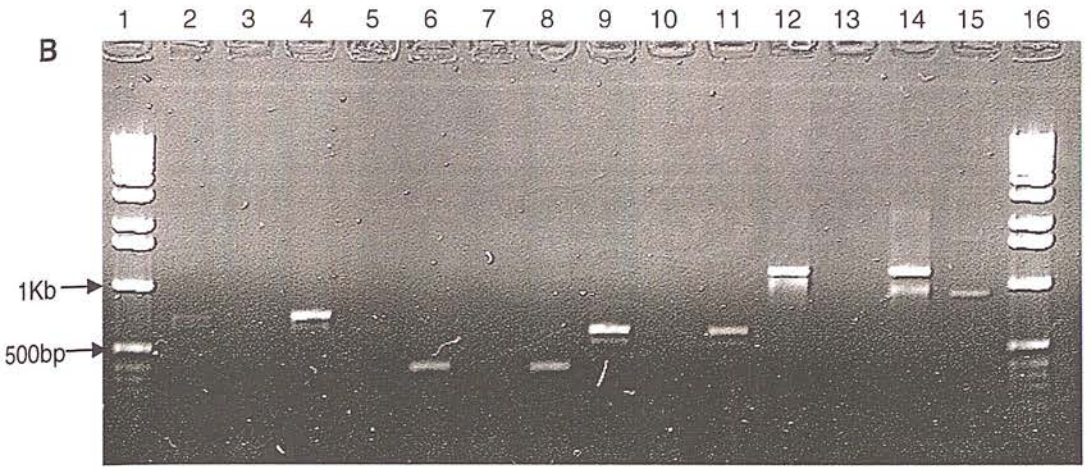

Fig.22 B) PCR screen of ZAP632 strain with a restored T3SS (cont.).
Lane1: 1Kb DNA ladder
Lane2: *escT* PCR 2 Walla3 template DNA positive control
Lane3: *escT* PCR 2 DNA blank negative control
Lane4: *escT* PCR 2 ZAP632 strain DNA template
Lane5: *escT* PCR 2 ZAP1140 strain DNA template
Lane6: *escU* PCR Walla3 template DNA positive control
Lane7: *escU* PCR DNA blank negative control
Lane8: *escU* PCR ZAP632 strain DNA template
Lane9: *escU* PCR 2 Walla3 DNA positive control
Lane10: *escU* PCR 2 DNA blank negative control
Lane11: *escU* PCR 2 ZAP632 strain DNA template
Lane12: *escR* PCR 2 Walla3 template DNA positive control
Lane13: *escR* PCR 2 DNA blank negative control
Lane14: *escR* PCR 2 ZAP632 strain DNA template.
Lane15: *escR* PCR 2 ZAP1140 strain DNA template
Lane16: 1Kb DNA ladder

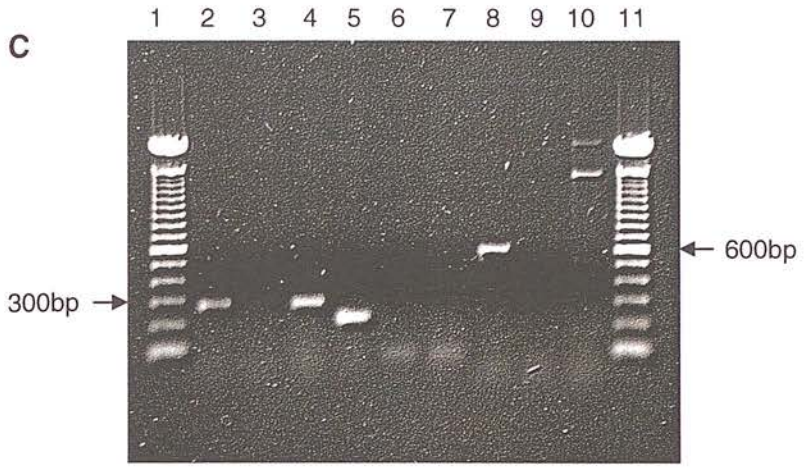

Fig.22 C) PCR screen of *ZAP632* strain with a restored T3SS (cont. II).
Lane1: 100bp DNA ladder
Lane2: *escR* PCR 3 Walla3 template DNA positive control
Lane3: *escR* PCR 3 DNA blank negative control
Lane4: *escR* PCR 3 ZAP632 strain DNA template
Lane5: *sacB* gene pJRE03 DNA template positive control
Lane6: *sacB* gene PCR DNA blank negative control
Lane7: *sacB* gene PCR ZAP632 strain DNA template
Lane8: pIB307 specific PCR pJRE03 DNA template positive control
Lane9: pIB307 specific PCR DNA blank negative control
Lane10: pIB307 specific PCR ZAP632 strain DNA template
Lane11: 100bp DNA ladder

3.3 Western Blot Detection of EspD from the Strains Walla3, Walla3 *escRSTU*<>*sac*/Kan (ZAP1140) and the T3SS Restored Strain (ZAP632)

After the creation and PCR verification of the ZAP632 strain it was checked for its ability to secrete EspD. Walla3, Walla3 *escRSTU*<>*sac*/Kan and T3SS Restored Strain supernatants and whole cell proteins were run on a SDS PAGE gel. After transfer to a nitrocellulose membrane the blot was incubated with in EspD antibody. Western blot analysis demonstrated that when the *sac*/Kan cassette was substituted for the *escRSTU* genes (strain ZAP1140) EspD secretion does not occur, while the wild type phenotype is restored in the ZAP632 strain (Fig.23). Interestingly the whole cell fraction for the ZAP1140 strain contains EspD at wild type levels, indicating that having no EscR, S, T, U proteins in the basal apparatus does not feedback on the production of EspD inside the cell. The Western blot demonstrates that the *escRSTU* genes on pJRE01, when exchanged back into the LEE1 locus, can restore EspD secretion, an indication that the strain is now

producing a functional T3SS. This plasmid can now be used to engineer REase recognition sites into the *escRSTU* genes.

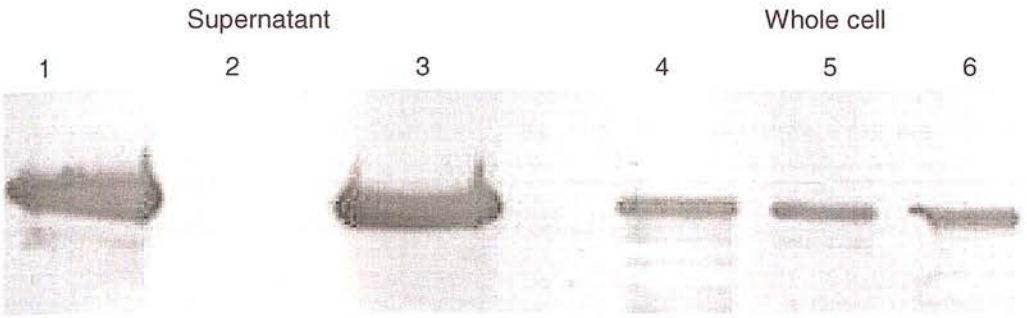

Fig.23 Western blot analysis with a 1:2000 dilution of EspD primary antibody on supernatant and whole cell proteins from Walla3, Walla3 *escRSTU<>sac*/Kan and the restored T3SS ZAP632 strain (12% SDS PAGE gel)
Lane1: Walla3 supernatant
Lane2: ZAP1140 supernatant
Lane3: ZAP632 supernatant
Lane4: Walla3 whole cell
Lane5: Zap1140 whole cell
Lane6: ZAP632 whole cell

3.4 Addition of 3' REase Recognition Sites

Due to time restraints *escR* and *escU* were chosen as the genes to manipulate by adding the REase site at their 3' end. EscU was chosen as its homologous proteins in the flagellar system (FlhB) and the *Yersinia* TTSS (YscU) have large cytoplasmic domains. *EscU* also has a unique restriction site (*Bst*EII) upstream from the 3' end of the gene. This restriction site was also used to add tags to create EscU fusion proteins. These tags were embedded in the cytoplasmic domain rather than inserted into the C terminal amino acids. *EscU* is also the only gene which was planned to have the added REase recognition site in its last six nucleotides of the gene. This meant the primers used to PCR amplify the tags did not need to include any *escU* sequence in their non complementary tails, as was the case for the other *esc* genes.

EscR is a smaller protein than EscU and is predicted to have its C terminus in the periplasm. Although this limits the tags that are able to be added to its restriction site, due

to the different environment in the periplasm compared to the cytoplasm, it did offer the opportunity to tag a periplasmic tail.

3.4.1 Overlapping Site Directed Mutagenesis

For *escR*, the PCR products *escR* PCR 1 and *escR* PCR 2 were used as the DNA template for the overlapping PCR with primers 9, 10. Five PCR mixtures were set up as seen in Fig.24:

Lane1: 1Kb DNA ladder
Lane2: 2µl of *escR* PCR 1 and 2µl of *escR* PCR 2 as DNA template
Lane3: 5µl of each *escR* PCR product as template.
Lane4: 2µl of *escR* PCR 1 for DNA template as a negative control
Lane5: 2µl of *escR* PCR 2 for DNA template as a negative control
And Lane6: A positive control containing 1µl pJRE01 DNA for template.

Fig.24 shows that the PCR needed a lot of optimisation; the predominant band is a 1Kb non specific product, the main product when only using *escR* PCR 1 as DNA template. The positive control (containing pJRE01) also worked poorly. The need for optimisation of the overlapping PCR meant a second technique to add the REase sites to the 3' end of *escR* and *escU* was required. This technique involved cloning the PCR 1 and PCR 2 products into pCR4®-TOPO® vectors, then combining both PCR products into a single pCR4®-TOPO® vector. The tag was then added to this plasmid and the whole section removed and cloned into the pJRE01 plasmid replacing *esc* gene sequence.

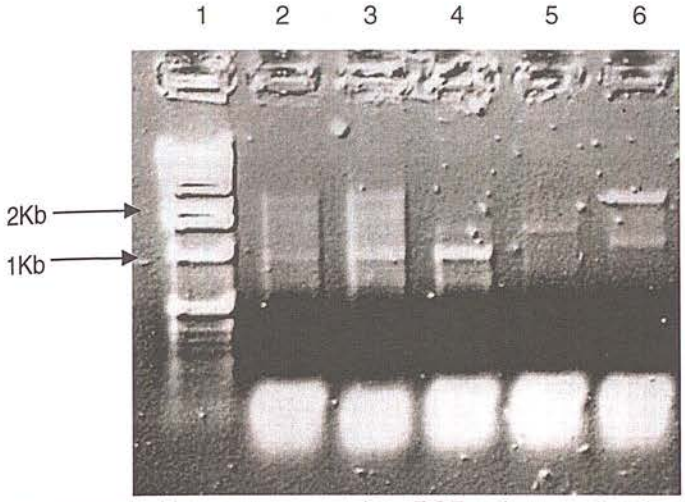

Fig.24 Expand long range template PCR using overlapping PCR products 1 and 2 for *escR* (obtained using the primer pairs 9, 12 and 10, 11 with 1µl of CTAB extracted Walla3 DNA [1:150 diluted]).
Lane1: 1Kb DNA ladder
Lane2: Over lapping PCR containing 2µl of each PCR 1 and 2 products as DNA template
Lane3: Over lapping PCR containing 5µl of each PCR 1 and 2 products as DNA template
Lane4: Over lapping PCR containing 5µl of *escR* PCR 1 product as DNA template as negative control
Lane5: Over lapping PCR containing 5µl of *escR* PCR 2 product as DNA template as negative control
Lane6: Over lapping PCR containing 1µl pJRE01 DNA template as positive control

3.4.2 pCR4®-TOPO® Cloning

The PCR product can be ligated into the pCR4®-TOPO® in either orientation. The orientation of the pCR4®-TOPO® cloned PCR products was deduced by digesting the clones with the REase *Pst*I and the endonuclease for the added restriction site. This either linearized the pCR4®-TOPO® clone or removed the PCR product that was added. To combine the two PCR products into one pCR4®-TOPO® plasmid, one pCR4®-TOPO® clone was digested with either the restriction endonuclease *Pme*I or *Sna*BI (depending on the orientation) and the added restriction site in the PCR product to linearise the plasmid. The second pCR4®-TOPO® clone was digested with *Pme*I or *Sna*BI (depending on orientation) and the added restriction site to remove the PCR product (Fig.25). The two

fragments were ligated together on the overhangs left after digestion with the added REase site and the blunt ends left by restriction with *Pme*I or *Sna*BI. The resulting clone contained both PCR products for the *esc* gene with the added restriction site. This REase recognition site was then used to add the tag, before the entire *esc* section and the tag were cloned into the pJRE01 plasmid replacing the native sequence.

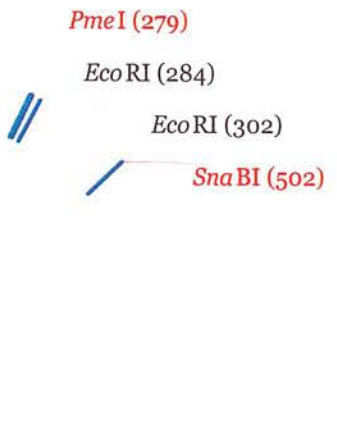

Fig.25 Vector NTI map of pCR4®-TOPO® plasmid. The map shows the *Eco*RI recognition sites, in between which the poly-A tailed PCR product is inserted. It also shows the position of the recognition sites for the blunt-cutting REases *Pme*I and *Sna*BI.

3.4.2.1 Constructing the Plasmid pJRE06

pJRE04 (pCR4®-TOPO® with *escU* PCR product 1) was digested with *Aat*II and S*na*BI to linearise the plasmid (4.2Kb) and pJRE05 (pCR4®-TOPO® with *escU* PCR 2) was digested with *Aat*II and *Sna*BI to remove the PCR fragment (700bp) (Fig.26). The digested pJRE05 plasmid was gel extracted. This fragment was ligated to the digested pJRE04 plasmid and the ligation mixture transformed. The plasmid DNA was removed

from the recovered colonies by the QIAprep™ spin plasmid miniprep kit (QIAGEN, West Sussex, U.K). The clones were screened by restriction digestion with *Eco*RI to excise the whole fragment (giving two bands at 4Kb and 933bp) and a double restriction digestion with *Nde*I, a REase that has a recognition site in the cloned fragment, and *Pst*I which digests the DNA in the pCR4®-TOPO® backbone (to give 4Kb and a 843bp fragment) (Fig.27). A positive clone for pJRE06 was selected and sent for sequencing before adding the tag into the *Aat*II restriction REase site. The clone had three sequence changes introduced by PCR. One created a silent mutation in rORF3 changing the codon for an alanine, another in rORF3 changed a threonine to an alanine and in EscU a glycine was mutated to a glutamic acid.

Fig.26 pJRE04 digested with AatII and *Sna*BI and the *escU* PCR product 2 removed from pJRE05 by restriction digestion with the enzymes *Aat*II and *Sna*BI – viewed by negative exposure . The fragments were ligated together and the ligation mixture transformed into TOP10 chemically competent cells and recovered on LBA plates at 37°C
Lane1: 1Kb DNA ladder
Lane2: pJRE04 containing escU PCR 1
Lane3: *escU* PCR 2
Lane4: *Hind*III DNA ladder

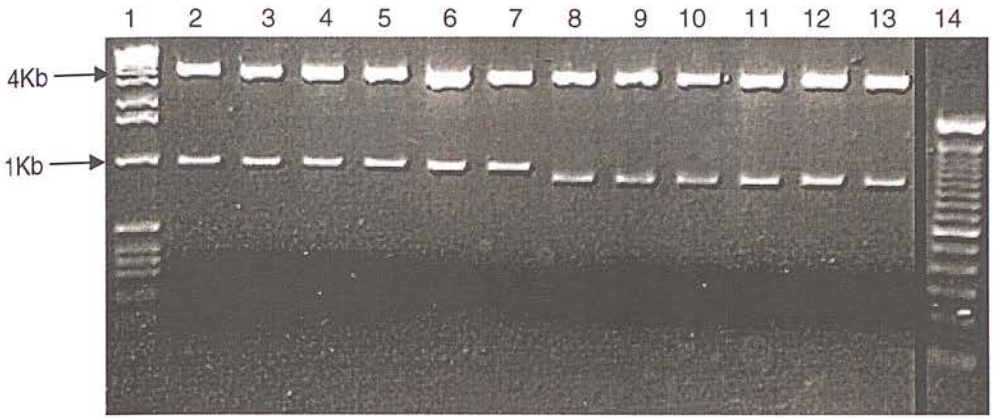

Fig.27 Diagnostic restriction digest for screening successful construction of pJRE06.
Digested with *Eco*RI and *Pst*I and *Nde*I
Lane1: 1Kb DNA ladder
Lane2-7: Positive clones digested with *Eco*RI (expect 4Kb and 933bp bands)
Lane8-13: Positive clones digested with *Pst*I and *Nde*I (expect 4Kb and 847bp bands)
Lane14: 100bp DNA ladder

None of the sequence changes matched those in the sequenced pJRE01 plasmid, and all the remaining sequence matched that of the EDL933 sequence.

3.5 $EscU_{CC::eGFP}$

pJRE06 was digested with the REase *Aat*II. A PCR for the *egfp* gene was carried out and the PCR product digested with the REase *Aat*II (Fig.28) and ligated with the digested pJRE06, transformed into chemically competent TOP10 cells and recovered on LBA plates at 37°C, to create pJRE07.

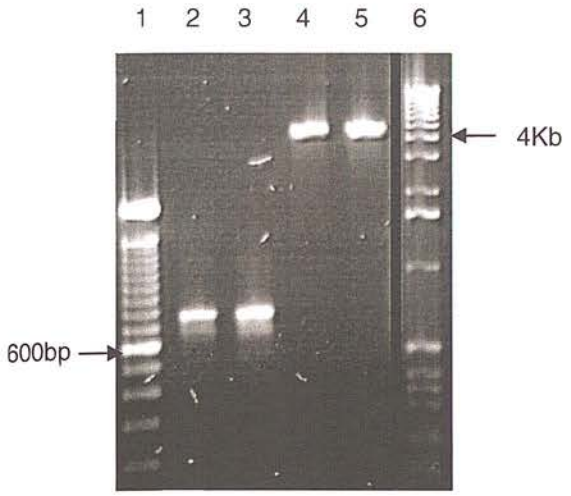

Fig.28 Agarose gel showing *Aat*II digested PCR product for *egfp* (using the primers 33, 34 [both containing the *Aat*II site in their non complementary tails], with 1µl of pMT01 plasmid DNA as template) and pJRE06. to be ligated overnight at 16°C
Lane1: 100bp DNA ladder
Lane2-3: *egfp* PCR restricted with *Aat*II
Lane4-5: pJRE06 restricted with *Aat*II
Lane6: 1Kb DNA ladder

Potential clones of pJRE07 were screened by restriction analysis with the REase *Rsa*I. The *egfp* PCR product could be ligated into the plasmid in one of two orientations. Only one orientation gave the translational fusion, in the other orientation *egfp* would not be transcribed (Fig.29).

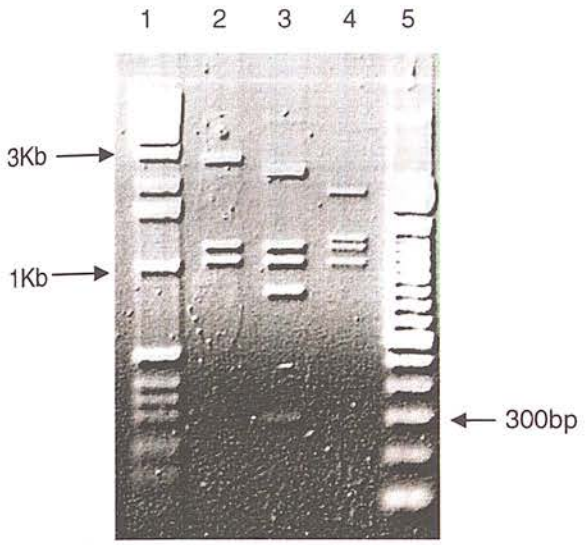

Fig.29 Agarose gel showing *Rsa*I digestion analysis of clones for pJRE07. The band pattern for the restriction fragments of the pJRE06 plasmid is 3.2Kb, 1.1Kb, 1Kb and 60bp (Lane2), for pJRE07 (containing *egfp* in the correct orientation) the bands are 2.7Kb, 1.1Kb, 1Kb 957bp, 282bp and 60bp (Lane3), and for pJRE06 with *egfp* in the incorrect orientation the bands are 2.2Kb, 1.3Kb, 1.1Kb, 1Kb, 282bp, and 60bp
Lane1: 1Kb DNA ladder
Lane2: pJRE06
Lane3: pJRE07 *egfp* in correct orientation
Lane4:pJRE08 *egfp* in wrong orientation
Lane5: 100bp DNA ladder

The plasmid pJRE07 was then used to replace the wild type sequence on the pJRE01 plasmid between the REase recognition sites *Bst*EII and *Bsa*I. pJRE01 was restriction digested with *Bst*EII and *Bsa*I, removing a 1.6Kb fragment. This fragment was discarded and the pJRE01 backbone gel extracted. The pJRE07 plasmid was digested with *Bst*EII and *Bsa*I, which excises two fragments of 1.6Kb, one fragment is *escU::egfp*, and the other is made entirely of pCR4®-TOPO® plasmid DNA. The pCR4®-TOPO® 1.6Kb fragment contains an *Eag*I REase recognition site, so further digestion with *Eag*I is necessary. The 1.6Kb fragment that remains, after *Eag*I digestion, is the *escU::egfp* fragment and was gel extracted and ligated (Fig.30).

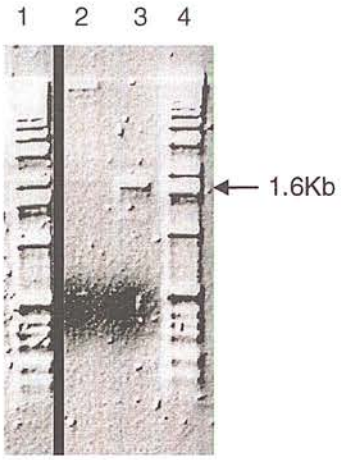

Fig.30 pJRE01 digested with *Bsa*I and *Bst*EII and pJRE07 digested with *Bst*EII, *Bsa*I and *Eag*I. Both were gel extracted and ran on an agarose gel then ligated at 16°C and transformed into TOP10 cells.
Lane1: 1Kb marker
Lane2: pJRE01 *Bst*EII and *Bsa*I digested
Lane3: Fragment of pJRE07 after restriction with the REases *Bst*EII, *Bsa*I and *Eag*I after gel extraction
Lane4: 1Kb marker.

The colonies obtained after 40hrs growth at 28°C had their plasmid DNA extracted using the QIAprep™ spin plasmid miniprep kit (QIAGEN, West Sussex, UK) and the clones screened for the creation of pJRE08 by *Aat*II restriction digestion and *Rsa*I restriction digestion (Fig31). In pJRE08 the *Aat*II digest should remove the *egfp* gene from the plasmid (Fig.31, Lane3 contains the 723bp *egfp* band).

After the creation of pJRE08 (Fig.32) was confirmed with restriction analysis the plasmid was used in allelic exchange in the intermediate strain ZAP1140.

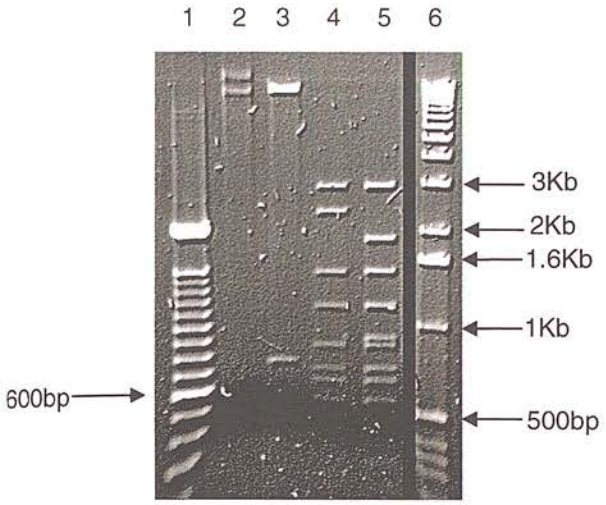

Fig.31 Restriction analysis of pJRE08 - After *Rsa*I digestion the pJRE01 plasmid gave the banding pattern 2.8Kb, 2.3Kb, 1.5Kb, 1.1Kb, 859bp, 713bp, 635bp, 538bp, 39bp and 26bp (Lane4) and the pJRE08 plasmid the pattern 2.8Kb, 1.8Kb, 1.5Kb, 1.1Kb, 906bp, 859bp, 713bp, 635bp, 538bp, 282bp, 39bp and 26bp (Lane 5)
Lane1: 100bp DNA ladder
Lane2: pJRE07 AatII restriction digest
Lane3: pJRE08 AatII restriction digest
Lane4: pJRE07 RsaI restriction digest
Lane5: pJRE08 RsaI restriction digest
Lane6: 1KB DNA ladder

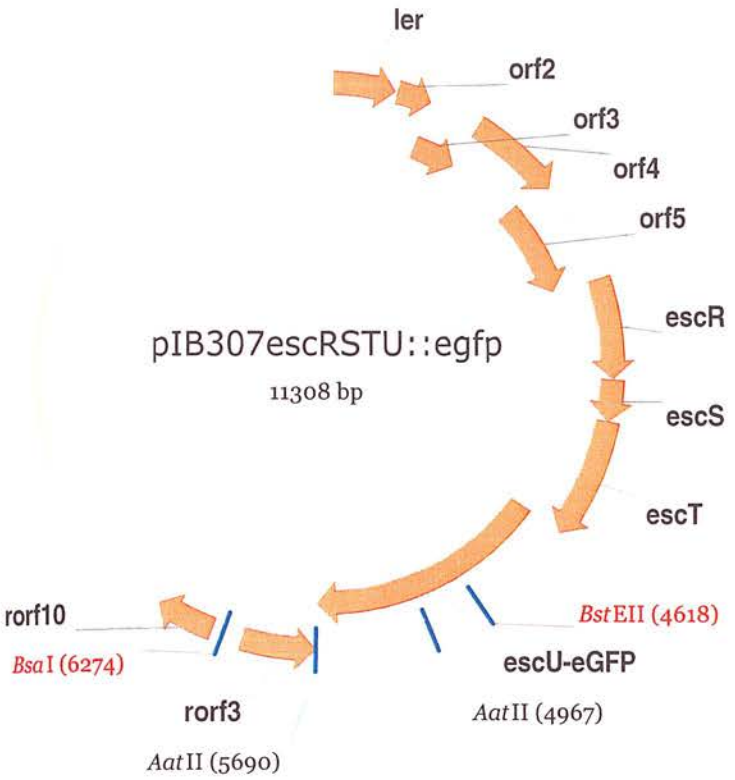

Fig.32 Vector NTI map of pJRE08

The resulting strain is Walla3 *escU*<>*escU*$_{cc::egfp}$ (ZAP1141) and now contains all the *esc* genes on the chromosome, replacing the *sac*/Kan cassette, with the *escU* gene fused to *egfp*. Walla3 *escU*<>*escU*$_{cc::egfp}$ was screened using the primers for the PCR products *escR* PCR 1 and 2, *escS* PCR 1 and 2, and *escT* PCR 2 (Fig.33, A, B, C). A PCR screen using primers 35, 36 was used to confirm the presence of the *egfp* gene (Fig.33, D). Also the PCR using primers specific for the *sacB* gene and the pIB307 plasmid was carried out to confirm the resistance profile (Fig.33, E).

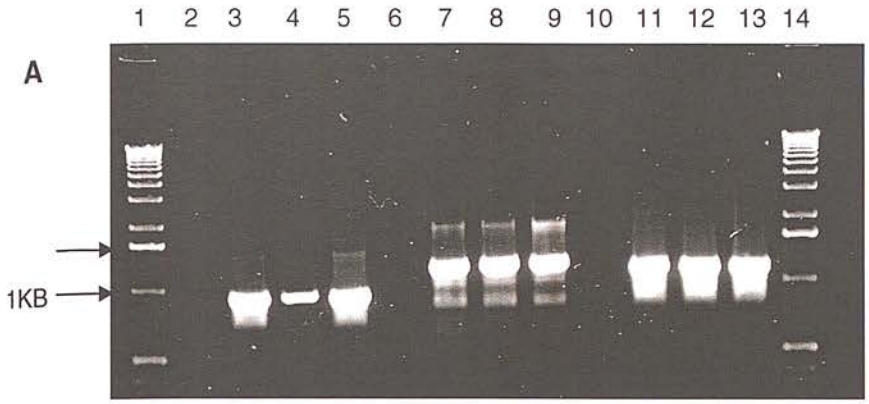

Fig.33 In each PCR a DNA blank was used as a negative control, 1µl of CTAB extracted Walla3 DNA (1: 150 dilution) was the template for the positive control as was the pJRE08 plasmid
A) PCR screen of Walla3 *escU*<>*escU*$_{cc::egfp}$ (ZAP1141) strain
Lane1: 1Kb DNA ladder
Lane2: *escR* PCR DNA blank negative control
Lane3: *escR* PCR Walla3 DNA template positive control
Lane4: *escR* PCR pJRE08 DNA template positive control
Lane5: *escR* PCR ZAP1141 strain DNA template
Lane6: *escS* PCR DNA blank negative control
Lane7: *escS* PCR Walla3 DNA template positive control
Lane8: *escS* PCR pJRE08 DNA template positive control
Lane9: *escS* PCR ZAP1141 strain DNA template
Lane10: *escR* PCR 2 DNA blank negative control
Lane11: *escR* PCR 2 Walla3 DNA template positive control

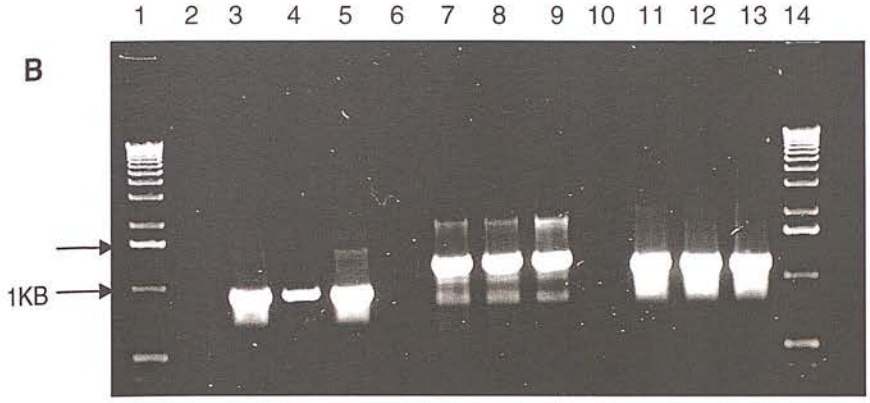

Fig.33 B) PCR screen of Walla3 *escU*<>*escU*$_{cc::egfp}$ (ZAP1141) strain
Lane1: 1Kb DNA ladder
Lane2: *escR* PCR DNA blank negative control
Lane3: *escR* PCR Walla3 DNA template positive control
Lane4: *escR* PCR pJRE08 DNA template positive control
Lane5: *escR* PCR ZAP1141 strain DNA template
Lane6: *escS* PCR DNA blank negative control
Lane7: *escS* PCR Walla3 DNA template positive control
Lane8: *escS* PCR pJRE08 DNA template positive control
Lane9: *escS* PCR ZAP1141 strain DNA template
Lane10: *escR* PCR 2 DNA blank negative control
Lane11: *escR* PCR 2 Walla3 DNA template positive control
Lane12: *escR* PCR 2 pJRE08 DNA template positive control
Lane13: *escR* PCR 2 ZAP1141 strain DNA template
Lane14: 1Kb DNA ladder

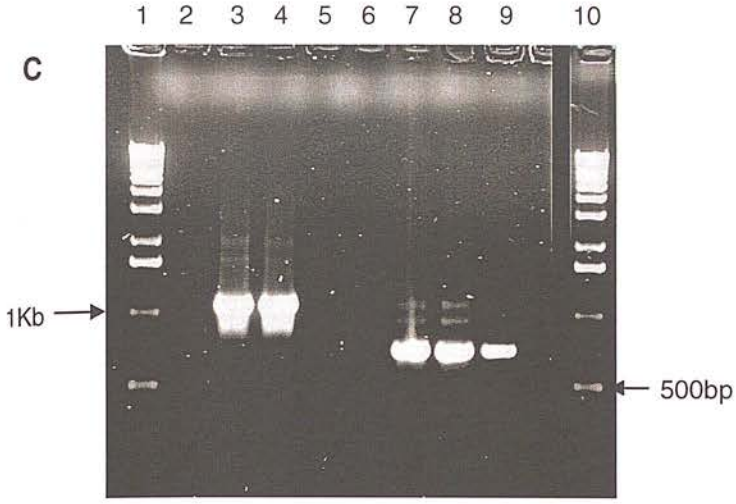

Fig.33 C) PCR screen of Walla3 *escU*<>*escU*$_{cc::egfp}$ (ZAP1141) strain (cont.)
Lane1: 1Kb DNA ladder
Lane2: *escS* PCR 2 DNA blank negative control
Lane3: *escS* PCR 2 Walla3 DNA template positive control
Lane4: *escS* PCR 2 pJRE08 DNA template positive control
Lane5: *escS* PCR 2 ZAP1141 strain DNA template
Lane6: *escT* PCR 2 DNA blank negative control
Lane7: *escT* PCR 2 Walla3 DNA template positive control
Lane8: *escT* PCR 2 pJRE08 DNA template positive control
Lane9: *escT* PCR 2 ZAP1141 strain DNA template
Lane10: Lane14: 1Kb DNA ladder

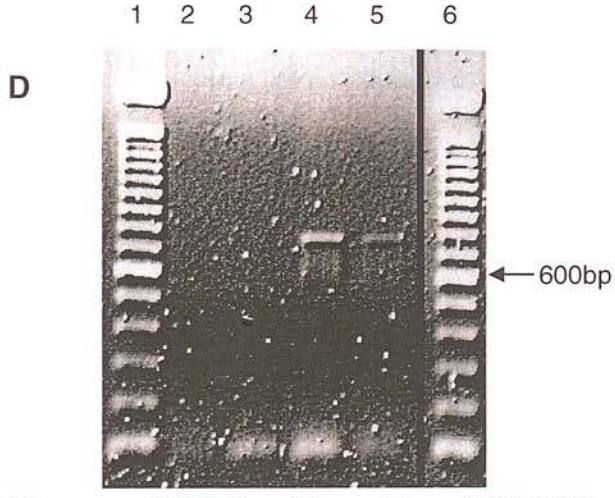

Fig.33 D) PCR screen of Walla3 *escU*<>*escU*$_{cc::egfp}$ (ZAP1141) strain (cont. II)
Lane1: 100bp DNA ladder
Lane2: *egfp* PCR DNA blank negative control
Lane3: *egfp* PCR Walla3 DNA template negative control
Lane4: *egfp* PCR pJRE08 DNA template positive control
Lane5: *egfp* PCR ZAP1141 strain DNA template

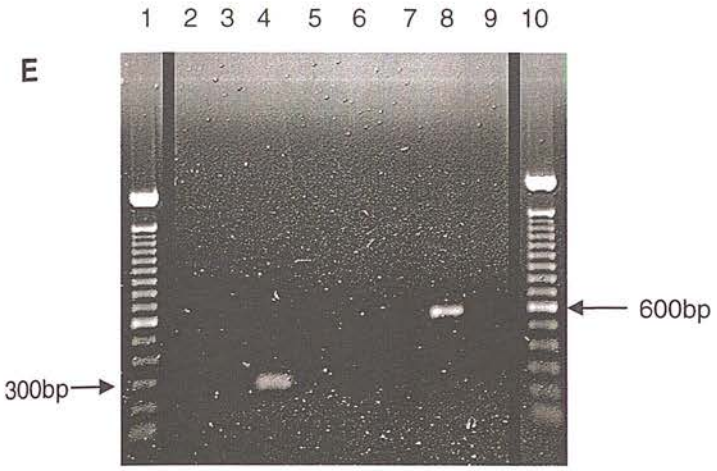

Fig.33 E) PCR screen of Walla3 *escU*<>*escU*$_{cc::egfp}$ (ZAP1141) strain (cont. III)
Lane1: 100bp DNA ladder
Lane2: *sacB* specific PCR DNA blank negative control
Lane3: *sacB* specific PCR Walla3 DNA template negative control
Lane4: *sacB* specific PCR pJRE03 DNA template positive control
Lane5: *sacB* specific PCR ZAP1141 strain DNA template
Lane6: pIB307 specific PCR DNA blank negative control
Lane7: pIB307 specific PCR Walla3 DNA template negative control
Lane8: pIB307 specific PCR pJRE03 DNA template positive control
Lane9: pIB307 specific PCR ZAP1141 strain DNA template
Lane10: 100bp DNA ladder

3.6 EscU$_{CC::GFP+}$

The pJRE06 plasmid was used to create a *gfp*+ fusion in the same way the *egfp* fusion was created; using primers 37, 38 to PCR amplify *gfp*+ from 1µl of pARJ145 purified plasmid as DNA template. The *gfp*+ PCR product was cloned into the pJRE06 plasmid to create pJRE09. pJRE09 was digested with the REases *Bsa*I, *Bst*EII and *Eag*I and the 1.6Kb fragment gel extracted and ligated to the large fragment of pJRE01 after digestion with *Bsa*I and *Bst*EII. This was carried out with identical steps to the creation of pJRE08. When ligated together the two fragments created the plasmid pJRE10, which was screened by restriction analysis with the REase *Rsa*I (Fig.34).

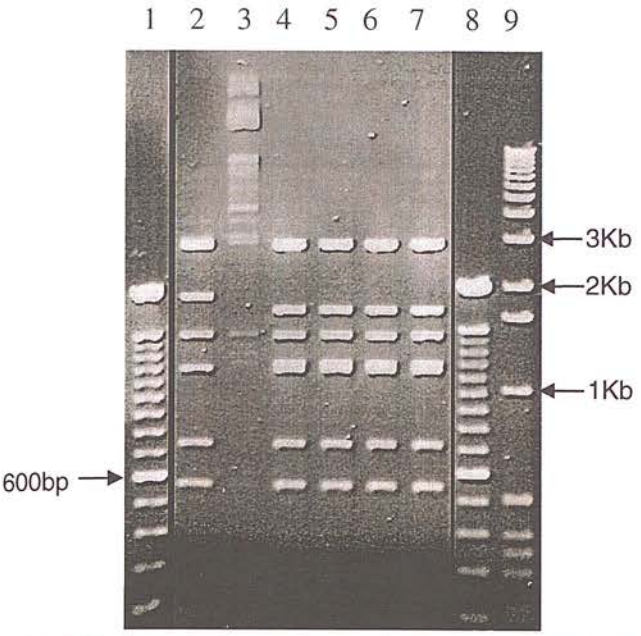

Fig.34 *Rsa*I restriction analysis of pJRE10 clones. The *Rsa*I restriction banding pattern for the pJRE10 plasmid is 2.8Kb, 1.7Kb, 1.4Kb, 1.2Kb, 1.1Kb, 713bp, 538bp, 249bp, 39bp and 26bp
Lane1: 100bp DNA ladder
Lane2-3: Negative clones for pJRE10
Lane4-7: Positive clones for pJRE10
Lane8: 100bp DNA ladder
Lane9: 1Kb DNA ladder

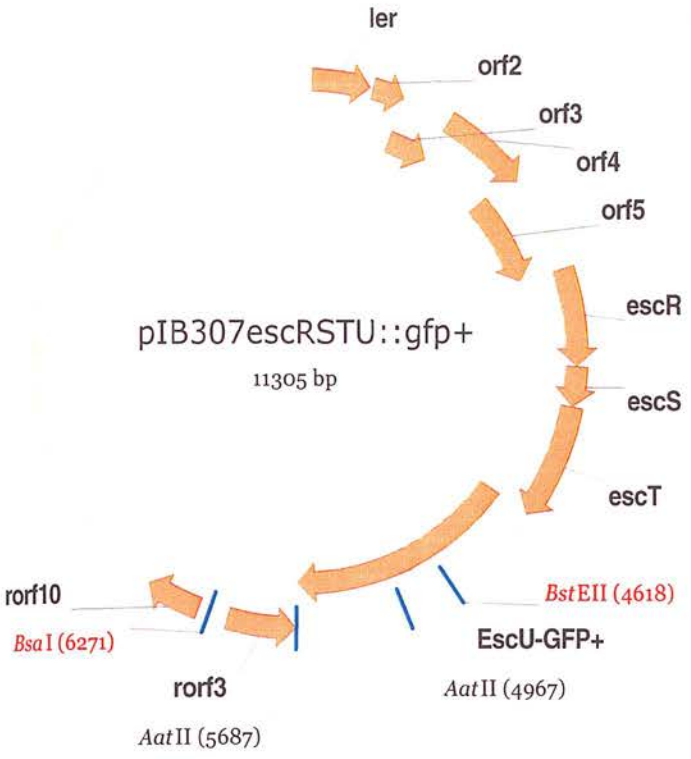

Fig.35 Vector NTI map of pJRE10

The pJRE10 plasmid (Fig.35) was used in the allelic exchange process in the intermediate strain to replace the *sac*/Kan cassette. The resulting strain Walla3 *escU*<>$escU_{cc::gfp+}$ was screened using the same PCR screens used to screen the Walla3 *escU*<>$escU_{cc::egfp}$ strain. The PCR screening primers used to screen for the presence of *egfp* were used as they sit in the *escU* sequence so are not specific for *egfp* but for addition of DNA in the AatII site (primers 35, 36). The gels are not shown.

3.7 *Age*I *ler* Deletion

Despite the construction of two mutant strains the plasmid pJRE01 proved difficult to work with. The pIB307 plasmid is a low copy number plasmid, but the plasmid yield decreased significantly when the PCR product containing the genes *escRSTU* was cloned into the plasmid. The colony morphology also changed with the TOP10 cells growing to a smaller colony size when carrying the plasmid. One possibility for the poor growth of the bacteria was expression of the *esc* genes from the pIB307 plasmid. This could be due to the expression of *ler* from the LEE1 promoter; pJRE01 contains *ler* and the LEE1

promoter up to the sequence for the -10 region. To solve this problem the pJRE01 plasmid was digested with the REase *Age*I. This restriction reaction removes 1.5Kb of sequence; 1Kb of flanking region sequence and 500bp of pIB307 sequence. This leaves 700bp as the left hand side flanking region, enough for the allelic exchange protocol, but removes all the LEE1 promoter sequence, *ler* and the first three and a half genes on the LEE1 operon.

After digestion with *Age*I the large 9Kb fragment was gel extracted and ligated on the *Age*I site, while the 1.5Kb fragment was discarded. The ligation mixture was transformed into TOP10 chemically competent cells and recovered on LBC plates. Colonies recovered had their plasmid DNA extracted and were screened with an *Rsa*I REase digest to confirm the removal of the LEE1 sequence (Fig. 36) and the creation of pJRE11 (Fig.37).

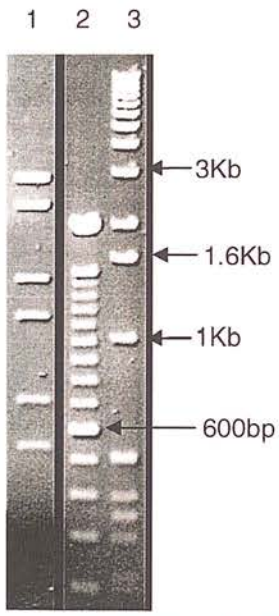

Fig.36 *Rsa*I digest of pJRE11 has the banding pattern of 2.8Kb, 2.3Kb, 1.4Kb, 1.1Kb, 713bp, 538bp, 39bp and 26bp on an agarose gel (Lane1).
Lane1: pJRE11.
Lane2: 100bp DNA ladder
Lane3: 1Kb DNA ladder

The pJRE11 plasmid was grown in TOP10 cells, which are more robust than the K12 AAEC185 strain. It was then used to create all the remaining clones.

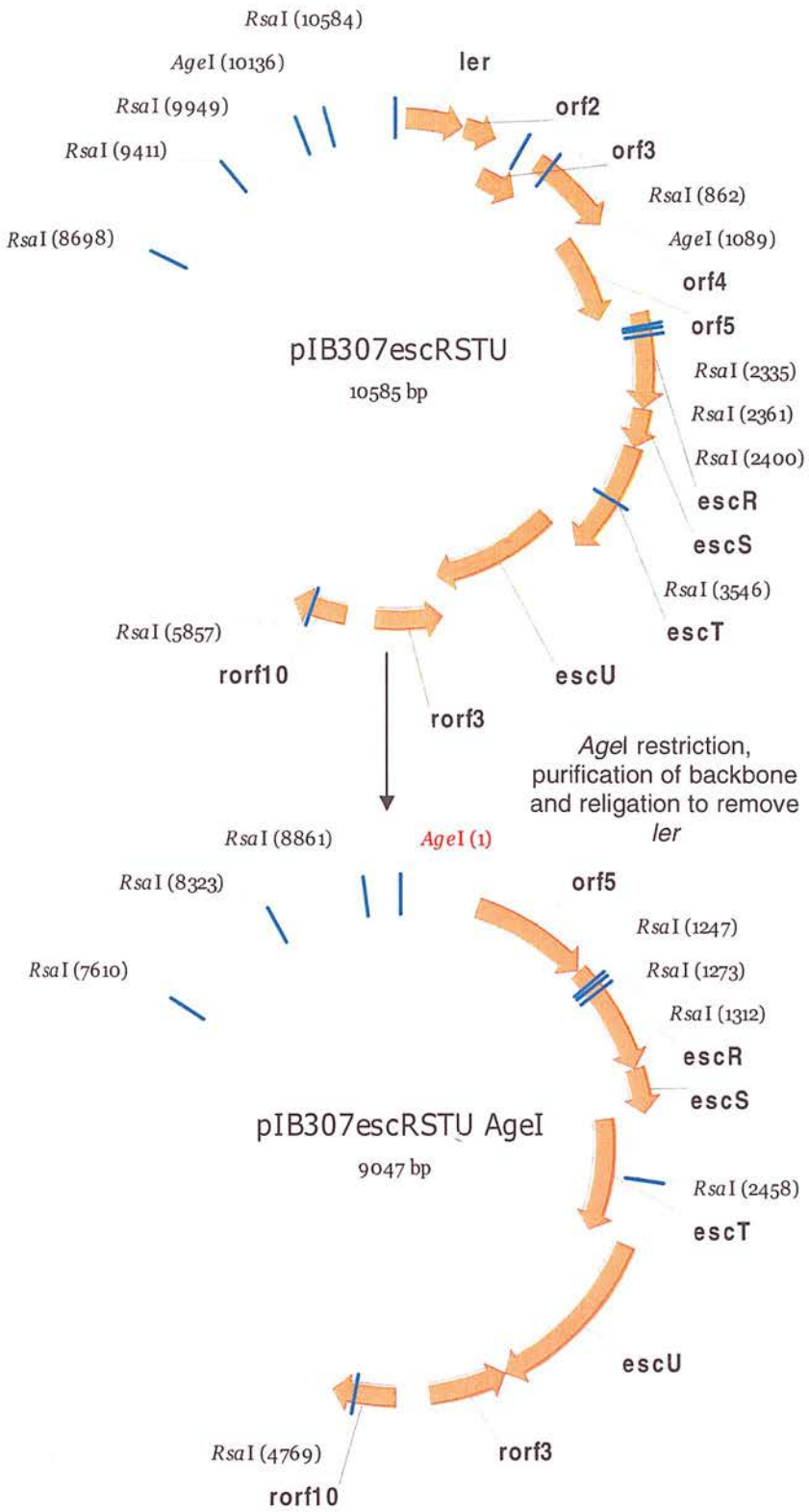

Fig.37 Vector NTI map of the removal of LEE1 sequence by digestion of the pJRE01 plasmid with *Age*I, showing the RsaI sites. The plasmid is religated after the sequence is removed to create pJRE11.

3.8 $EscU_{CN::GFP+}$

In the *escU* sequence there is a natural recognition site for the REase *Bst*EII, 685bp from the ATG start of the gene and 344bp from the stop codon. The *Bst*EII recognition site sits in the cytoplasmic domain of EscU, 117 amino acids from the C terminus were the *Aat*II site was added. The *gfp*+ gene will be cloned into the BstEII recognition site, as will the sequence for the HA tag.

The primers 39, 40 were used to PCR amplify the *gfp*+ gene (with 1µl of the pMT01 plasmid DNA as template). The PCR product and the pJRE11 plasmid were both digested with *Bst*EII. They were purified using the QIAquick PCR purification kit (QIAGEN, West Sussex, UK), ligated together and transformed into the AAEC185 strain which had been made chemically competent. The colonies had their plasmid DNA removed by the QIAquick PCR purification kit (QIAGEN, West Sussex, UK) and were screened for the successful creation of pJRE12 by restriction analysis with the REases *Hind*III, *Eco*RV and *Sac*I, *Eco*RV (Fig.38).

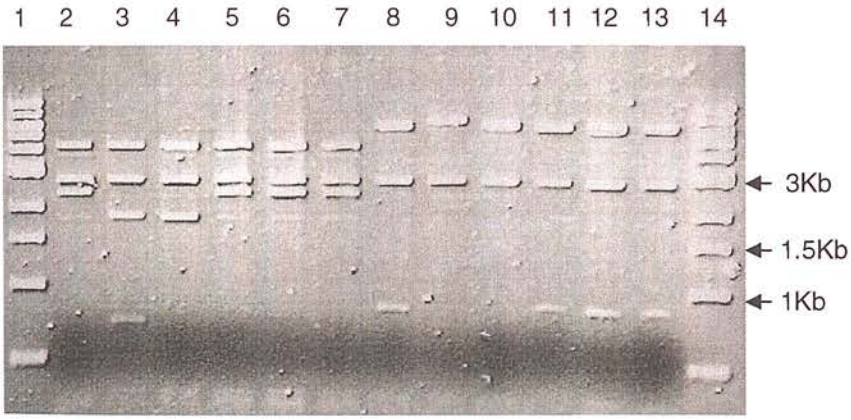

Fig.38 *Hind*III, *Eco*RV and *Sac*I, *Eco*RV restriction analysis of possible clones for pJRE12. After restriction digestion with *Hind*III and *Eco*RV the pJRE12 plasmid has a banding pattern of 4.2Kb, 2.6KB, 2.1Kb, 291bp and two bands at 234bp (Lane2,5,6,7) and after SacI and EcoRV digestion the banding pattern is 6Kb, 2.6Kb, 820bp, 291bp 234bp (Lane8,11,12,13)
Lane1: 1Kb DNA ladder
Lane2,5,6,7: Positive *Hind*III, *Eco*RV REase digests on pJRE12
Lane3,4: Negative *Hind*III, *Eco*RV REase digests
Lane8,11,12,13 Positive *Sac*I, *Eco*RV REase digests on pJRE12
Lane9,10: Negative *Sac*I, *Eco*RV REase digests
Lane14: 1Kb DNA Ladder

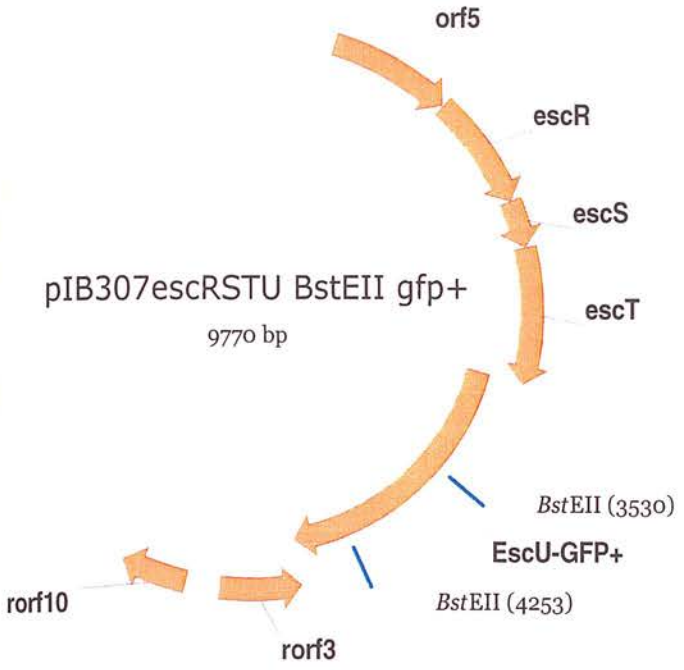

Fig.39 Vector NTI map of pJRE12

pJRE12 (Fig.39) was used in the allelic exchange process in the intermediate strain Walla3 *escRSTU<>sac*/Kan to replace the *sac*/Kan cassette with the *esc* genes on the plasmid, including $escU_{cn::gfp+}$. The resulting Walla3 $escU<>escU_{cn::gfp+}$ (ZAP635) strain was screened using the same PCR primers used to screen the strains Walla3 $escU<>escU_{cc::egfp}$ and Walla3 $escU<>escU_{cc::gfp+}$ plus a PCR with the primers 41, 42 to screen for insertion in the *Bst*EII site. The PCR products confirmed the *esc* genes were present, with *gfp+*, and the *sacB* gene and the pIB307 backbone had been lost (gels not shown).

3.9 $EscU_{CN::HA}$

The HA tag was inserted into pJRE11 at the *Bst*EII REase recognition site. Two oligonucleotides were ordered from Sigma Genosys (Cambridge, UK) (oligonucleotides 43 and 44 in Table 3), these contained the sequence for the HA tag, flanked by the *Bst*EII recognition sequence. The oligonucleotides were ~35bp in length and complementary to one another. 5µl of each oligonucleotide were mixed together and heated to 95°C, the mixture was allowed to cool to room temperature and then digested by the REase *Bst*EII. The HA tag was PCR purified and ligated with *Bst*EII restricted pJRE11 plasmid. The ligation mixture was transformed and recovered. The recovered colonies had their plasmid DNA removed by the QIAprep™ spin plasmid miniprep kit (QIAGEN, West Sussex, UK) and PCR screened for the presence of the HA tag (Fig.40).

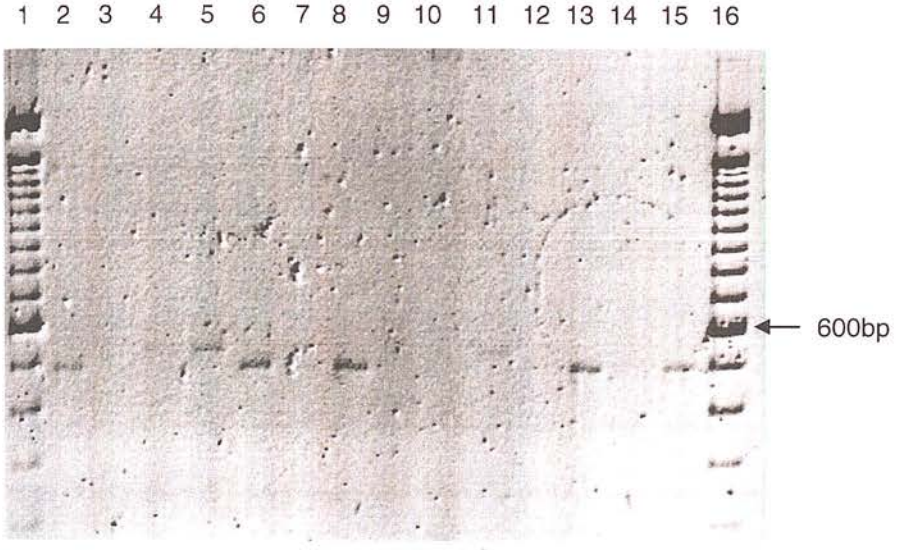

Fig.40 PCR screen for positive pJRE13 clones - primers 41, 42 with crude DNA extract from the possible clones of pJRE13
Lane1: 100bp DNA ladder
Lane5,11: Positive clones
Lane2-4,6-10,12-15: Negative clones
Lane16: 100bp ladder

The clone in Fig.40, Lane5 was positive for the HA tag by PCR, and sent to MWG for sequencing.

The pJRE13 plasmid (Fig.41) was used in allelic exchange in the intermediate strain Walla3 *escRSTU<>sac*/Kan to replace the *sac*/Kan cassette from the chromosome. The resulting strain Walla3 *escU<>escU*$_{cn::HA}$ (ZAP634) was checked by PCR to confirm the presence of the *esc* genes, the HA tag (primers 41, 42) and the absence of the *sacB* gene and the pIB307 plasmid (gels not shown).

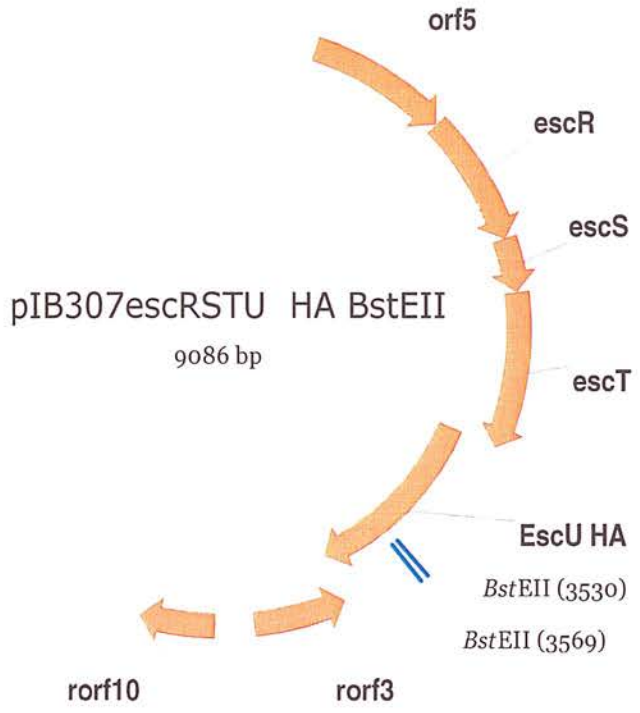

Fig.41 Vector NTI map of pJRE13

3.10 Removing the REase Recognition Site *Pst*I

The cloning strategy for *escR* uses the REase *Pst*I, which has a recognition site in the *escU* sequence that will be used to transfer tagged versions of *escR* into the pJRE11 plasmid. The enzyme *Pst*I also has a recognition site in the pIB307 plasmid backbone. Instead of carrying out a partial digest, to digest only one of the *Pst*I recognition sites, the *Pst*I site in the pIB307 backbone was removed. The site in the pIB307 sequence is flanked by *Hind*III and *Xba*I. After restriction digestion with these enzymes and treatment with the Klenow

fragment, the pJRE11 plasmid lost the sequence containing the *Pst*I recognition site and was ligated with itself to form pJRE14. Fig.42 shows the screening for successful clones of pJRE14. The pJRE14 plasmid can now be used in the *escR* cloning strategy.

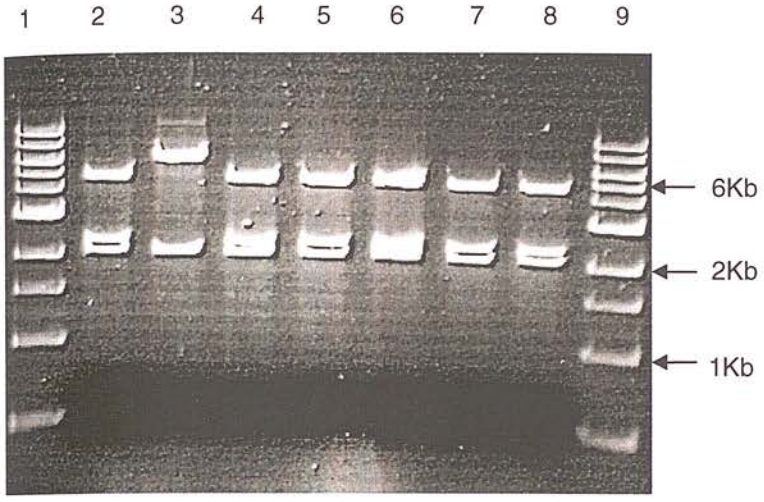

Fig.42 Restriction analysis of possible clones for the removal of a *Pst*I site in the pJRE14 plasmid digested with PstI and *Nsi*I. Lane3 contains a positive clone that, after restriction digestion with *Pst*I and *Nsi*I, a 2Kb fragment is removed instead of a 2Kb fragment and a 2.2Kb fragment (Lane1,4,-8).
Lane1: 1Kb DNA marker
Lane2,4-8: Negative clones for pJRE14
Lane3: Positive clone pJRE14
Lane9: 1Kb DNA marker

3.11 EscR::HA

The recognition site for the REase *Swa*I was added to the 3' end of *escR* by the pCR4®-TOPO® cloning technique used for *escU*. *EscR* PCR 1 and *escR* PCR 2 products were pCR4®-TOPO® cloned creating the two plasmids pJRE15 (containing *escR* PCR 1) and pJRE16 (containing *escR* PCR 2). The pJRE15 plasmid was linearized by digestion with the REases *Swa*I and *Pme*I and the pJRE16 plasmid was restriction digested with *Swa*I and *Pme*I to excise the fragment containing the *escR* sequence. This fragment was gel extracted and ligated to the linearized pJRE15. The ligation reaction mixture was transformed into chemically competent TOP10 cells. Successful ligations created the plasmid pJRE17 and the HA tag was cloned into the added *Swa*I recognition site. Instead

of adding the HA tag as a small oligonucleotide (as was the case for *escU*) the HA tag was added in a PCR reaction. Primer 45 was designed to incorporate the HA tag in its 3' tail. This was used in a PCR reaction with primer 10 to remake the *escR* PCR 2 product, containing the HA tag. The PCR product was digested with the REases *Swa*I and *Pst*I and used to replace the *escR* PCR 2 portion of the pJRE17 plasmid. The new pCR4®-TOPO® plasmid (pJRE18) was sent for sequencing. The pJRE18 plasmid was digested with the REases *Pst*I and *Nsi*I, the 2.1Kb fragment was gel extracted and ligated with the pJRE14 plasmid that had also been restriction digested with *Nsi*I and *Pst*I and the 6.9Kb backbone gel extracted. The ligation was carried out and the mixture transformed and cells recovered. Successful ligations created pJRE19; the pJRE14 plasmid containing *escR* labelled with the HA tag. A PCR screen was used to screen for pJRE19 (Fig.43)

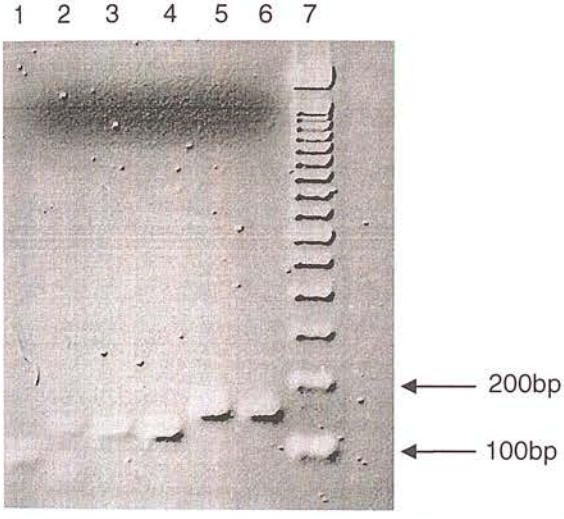

Fig.43 PCR screen of pJRE19 using the primers 46, 47
Lane1: HA screen PCR DNA blank negative control
Lane2: HA screen PCR Walla3 DNA template negative control
Lane3: HA screen PCR pJRE17 DNA template negative control
Lane4: HA screen PCR pJRE01 DNA template negative control
Lane5: pJRE18 DNA template positive control
Lane6: pJRE19 clone
Lane7: 100bp DNA ladder

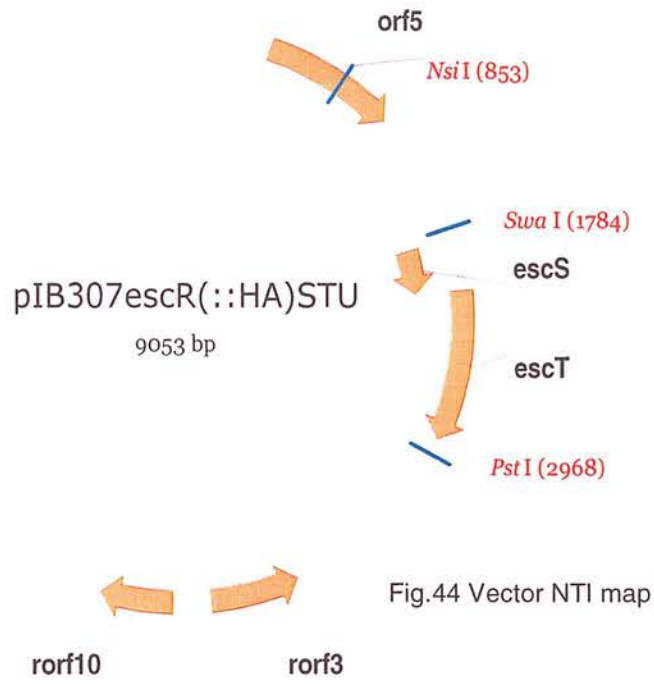

Fig.44 Vector NTI map of pJRE19

pJRE19 (Fig.44) was used in the allelic exchange process to replace the *sac*/Kan cassette in the intermediate strain Walla3 *escRSTU*<>*sac*/Kan. The resulting strain contains EscR with a C terminal HA tag (ZAP637). PCR was used to verify the strain with the primers for the *esc* genes and the HA tag (primers 46, 47) and the *sacB* and pIB307 specific primers (gels not shown).

3.12 Discussion

This chapter describes the creation of five strains of EHEC O157:H7 (Walla3), in which one of the predicted inner membrane proteins of the T3SS basal apparatus has been tagged. The fusion gene, encoding the tagged basal apparatus protein, is single copy on the chromosome, replacing the wild type gene. This means the fusion is expressed in the correct genetic background, under its natural promoter and in its original genetic context.

Four of the strains created contain a tagged version of EscU. In each of these strains either the tag used is different or its location within the protein has changed. The fifth stain contains a tagged version of EscR (see Table 6)

Table 6. Table showing the fusion proteins created in the Walla3 strain.

Protein Tagged	Tag Used and Position of Tag
EscU	C Terminal Fusion to eGFP
EscU	C Terminal Fusion to GFP+
EscU	HA tag Inserted into the Cytoplasmic Domain
EscU	GFP+ Inserted into the Cytoplasmic Domain
EscR	C Terminal Fusion to HA tag

To create these five strains an intermediate strain had to be made. This strain (ZAP1140) has the genes *escRSTU* replaced with the *sac*/Kan cassette. The plasmid pJRE01 was used to complement this strain by replacing the *sac*/Kan cassette with the cloned *escRSTU* genes. The resulting strain (ZAP632) provided evidence that the genes on the pJRE01 plasmid were capable of restoring T3SS function to the ZAP1140 strain. The pJRE01 plasmid could then be manipulated to add the tags to *escR* and *escU*.

The experiment was designed to add restriction sites at the 3' end of the *esc* genes by an overlapping PCR technique. This technique failed to be successful, requiring optimisation. The failure of the overlapping PCR required a second method involving the commercial cloning vector pCR4®-TOPO®. This technique added the restriction site by combining the two PCR products for each gene in a cloning step. This enabled the tag to be added in the 3' REase recognition site and the whole section used to replace the wild type sequence in the pJRE01 plasmid. All the tags were created in this way, except two strains labelled with GFP+ and HA tags in the cytoplasmic domain of EscU at the BstEII REase recognition site.

During construction of the strains it became apparent that plasmid purification of pJRE01 was not giving the expected yield. The plasmid pJRE01 contains the gene for

the LEE1 regulator Ler and some of the sequence for the LEE1 promoter. If Ler was being produced, causing the expression of the *esc* genes from the plasmid, this could prove toxic for the AAEC185 or TOP10 strains used to harvest the plasmid. To overcome this problem 1.5Kb of sequence was removed from this plasmid, which included the regulator Ler and any LEE1 promoter sequence. After its removal the yield of the plasmid increased, determined by gel electrophoresis of plasmid DNA after plasmid purification and digestion with a restriction enzyme, and the plasmid was used for the creation of three of the five strains.

To allow successful cloning of the *escR* tagged fragment into the pJRE11 plasmid, the PstI REase recognition site had to be removed from the pIB307 sequence. This was done by restriction digestion with enzymes that flanked the PstI recognition site. Upon digestion with these flanking enzymes the PstI recognition site was removed and the plasmid ligated with itself to create the plasmid pJRE14.

Although EscR and EscU are the two proteins that have been tagged, strategies for another four predicted inner membrane have been devised, these strategies can be revisited at a later date if required.

With EscR and EscU successfully tagged the next stage of the project was to localise the tagged proteins by Western blot analysis and directly with fluorescence microscopy.

Chapter 4

Microscopy and Western Blot Analysis of Strains Containing Tagged Proteins

4 Microscopy and Western Blot Analysis of Strains Containing Tagged Proteins

4.1 FLUOstar OPTIMA with Strains Walla3, Walla3 *escU*<>*escU*$_{cc::egfp}$ (ZAP1141), Walla3 *escU*<>*escU*$_{cc::gfp+}$ (ZAP1142) and Walla3 *escU*<>*escU*$_{cn::gfp+}$ (ZAP635)

FLUOstar OPTIMA was carried out on 10ml cultures of the strains Walla3, Walla3 *escU*<>*escU*$_{cc::egfp}$ (ZAP1141), Walla3 *escU*<>*escU*$_{cc::gfp+}$ (ZAP1142) and Walla3 *escU*<>*escU*$_{cn::gfp+}$ (ZAP635) grown in supplemented MEM-HEPES (as described in section 2.9). Approximately five FLUOstar OPTIMA readings were taken between an OD_{600nm} of 0.1 and 1 for each strain and the fluorescence readings plotted against the OD_{600nm} of the culture (Fig.45).

The graph (Fig.45) shows that the wild type Walla3 strain (containing no fluorescent tag) has a population fluorescence that is consistently lower than the strains containing a GFP variant. The fluorescence of the tagged strains remains similar to one another until an OD_{600nm} of 0.6. At this OD_{600nm} the strain ZAP1142 (Walla3 *escU*<>*escU*$_{cc::gfp+}$) starts to fluoresce at a higher intensity than the other two GFP tagged strains, with a fluorescence that peaks at 4,500rfu; over 500rfu more than strains Walla3 *escU*<>*escU*$_{cc::egfp}$ (ZAP1141) and Walla3 *escU*<>*escU*$_{cn::gfp+}$ (ZAP635) and 1,000rfu more than the Walla3 strain.

4.2 Microscopy with Strains Walla3 *escU*<>*escU*$_{cc::egfp}$ (ZAP1141), Walla3 *escU*<>*escU*$_{cc::gfp+}$ (ZAP1142) and Walla3 *escU*<>*escU*$_{cn::gfp+}$ (ZAP635)

Microscopy slides were made from the cultures after the final FLUOstar OPTIMA reading was taken. Five of the 10 wells on the glass microscope slides contained culture from Walla3 *escU*<>*escU*$_{cc::egfp}$ (ZAP1141), Walla3 *escU*<>*escU*$_{cc::gfp+}$ (ZAP1142) and Walla3 *escU*<>*escU*$_{cn::gfp+}$ (ZAP635) with the remaining five wells containing Walla3 (as a negative control). For the positive control a pACYC184 based plasmid with the gene *sepL* fused to *egfp* under the LEE4 promoter (pDW6) was electrotransformed into the Walla3 strain. A colony from the successful transformations was grown in 5ml of supplemented MEM-HEPES and chloramphenicol and used to create microscope slides in an identical manner to the mutant strains. This was used as a positive control for the

expression and visualization of eGFP when attached to a T3SS protein in the Walla3 strain.

Fig.46 depicts five selected microscope images that summarize the microscopy results. The image of the Walla3 strain containing the SepL-eGFP fusion was captured after 500ms exposure and needed no contrast enhancement to visualize the fluorescence from the eGFP fusion. The strains Walla3 *escU*<>*escU*$_{cc::egfp}$, Walla3 *escU*<>*escU*$_{cc::gfp+}$ and Walla3 *escU*<>*escU*$_{cn::gfp+}$ had images captured after 1000ms (1sec) and needed contrast enhancement to visualize the bacteria. Discrete foci of fluorescence were seen in the strains Walla3 *escU*<>*escU*$_{cn::gfp+}$ and Walla3 *escU*<>*escU*$_{cc::gfp+}$ but not the eGFP EscU tagged strain Walla3 *escU*<>*escU*$_{cc::egfp}$. However, when the same microscopy parameters were used on the wild type Walla3 strain (which contains no GFP) the fluorescent foci were also seen. Because of their presence in the Walla3 strain, the fluorescent foci were attributed to auto fluorescence of unknown protein(s) and not from fluorescence of the GFP fusions to EscU in the tagged strains. The detection of the foci is likely to be due to the long exposure time and the use of the contrast enhancement as they are not detectable without employing these techniques.

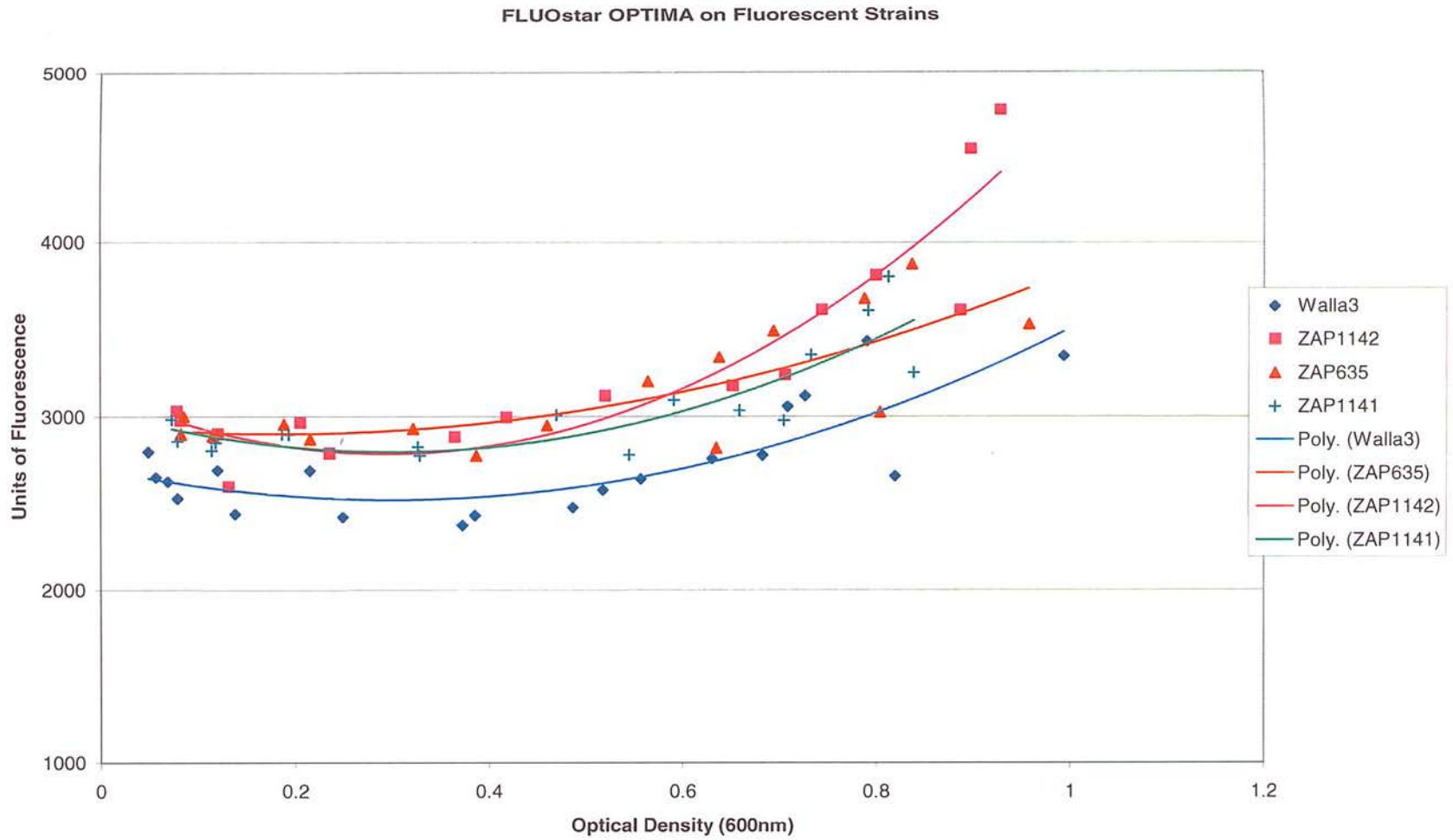

Fig.45 FLUOstar OPTIMA data for strains Walla3 *escU*<>*escU*$_{cc::egfp}$ (ZAP1141), Walla3 *escU*<>*escU*$_{cc::gfp+}$ (ZAP1142), Walla3 *escU*<>*escU*$_{cn::gfp+}$ (ZAP635) and Walla3. Relative fluorescence units are plotted against optical density at 600nm and a polynomial trend line added.

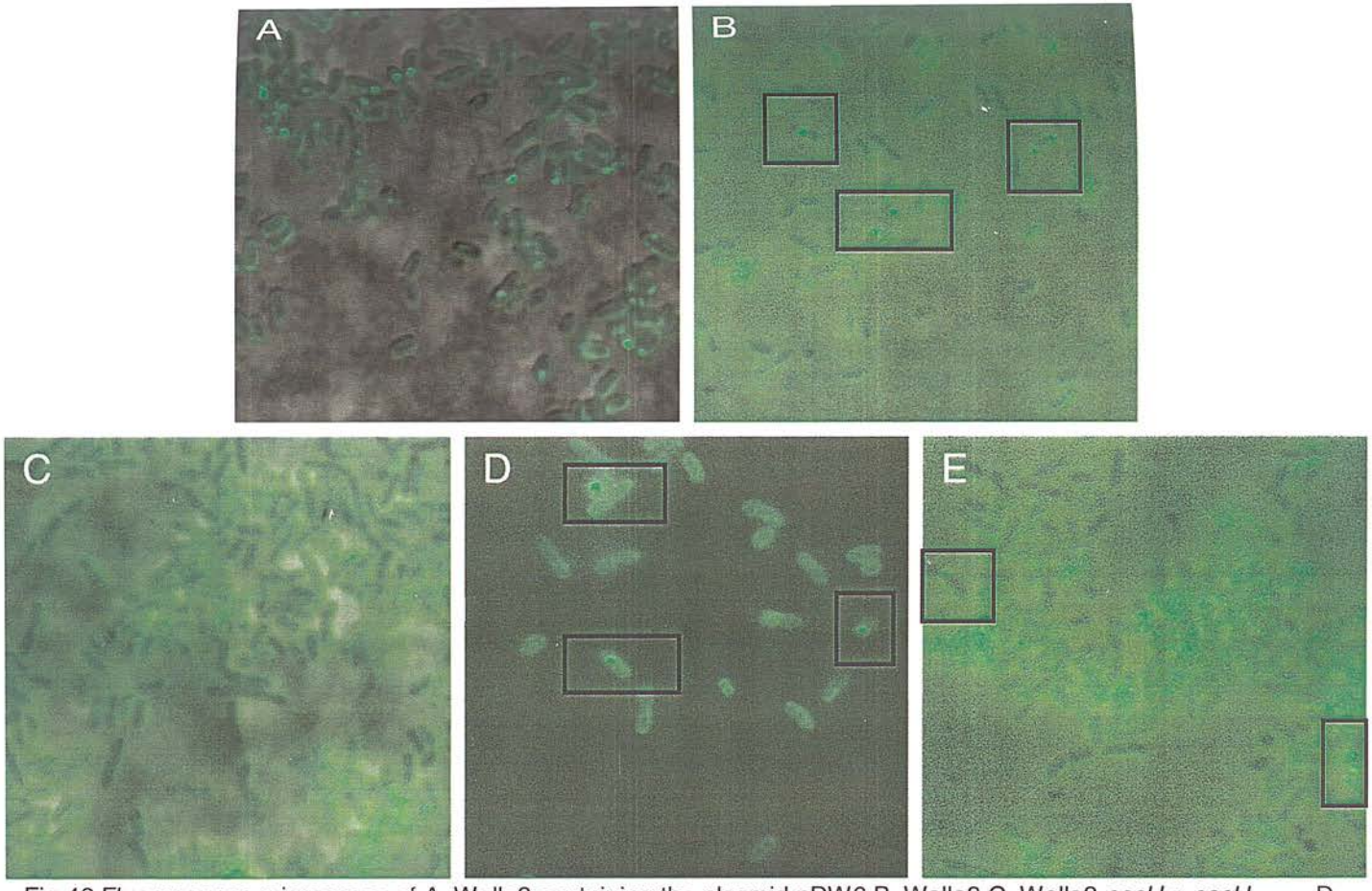

Fig.46 Fluorescence microscopy of A. Walla3 containing the plasmid pDW6 B. Walla3 C. Walla3 *escU<>escU*$_{cc::egfp}$ D. Walla3 *escU<>escU*$_{cc::gfp+}$ E. Walla3 *escU<>escU*$_{cn::gfp+}$. Examples of the fluorescent foci (without the pDW6 plasmid) are highlighted within the black boxes.

4.3 Increasing the Expression of *escU* with Ler

An attempt to increase the fluorescence of the tagged strains was made by increasing the expression of the genes on the LEE pathogenicity island. Although artificially increasing expression does not give an accurate measure of the level of wild type expression from the basal apparatus genes, it would allow localization of tagged basal apparatus proteins with other fusion proteins. It would also allow the production of the tag protein from the single copy gene fusion to be verified by microscopy. To increase the expression from genes on the LEE pathogenicity island (including the EscU::GFP fusions) pASL10, a pACYC184 based plasmid containing the LEE regulator *ler* under the regulation of an isopropyl β-D-I-thiogalactopyranoside (IPTG) inducible promoter (pTac), was electrotransformed into the strains Walla3 *escU*<>*escU*$_{cc::egfp}$ (ZAP1141), Walla3 *escU*<>*escU*$_{cc::gfp+}$ (ZAP1142), Walla3 *escU*<>*escU*$_{cn::gfp+}$ (ZAP635) and Walla3.

A colony from each strain containing pASL10 was grown for FLUOstar OPTIMA measurements. To induce expression from the pASL10 plasmid IPTG was added to the cultures during their final growth stage when they reached an OD_{600nm} of 0.1. The IPTG was added to a final concentration of 1mM. During their growth five FLUOstar OPTIMA readings were taken at regular intervals. The four strains Walla3 *escU*<>*escU*$_{cc::egfp}$, Walla3 *escU*<>*escU*$_{cc::gfp+}$, Walla3 *escU*<>*escU*$_{cn::gfp+}$ and Walla3 not containing the plasmid pASL10 were also grown in an identical manner (with IPTG added at an OD_{600nm} of 0.1) as negative controls for the experiment.

The polynomial trend lines added to the FLUOstar OPTIMA data for the four strains with and without the pASL10 plasmid (Fig.47 and Fig.48) showed little difference in the level of fluorescence after the expression of *ler*. The Walla3 strain had the least amount of detectable fluorescence, with the GFP+ fusion to the EscU C terminus having the most detectable fluorescence from an OD_{600nm} of 0.5 – 0.6. The initial high values of fluorescence from the Walla3 strain in both Fig.47 and Fig.48 is fluorescence carried over from the 5ml culture used to inoculate the 10ml culture and dissipates rapidly.

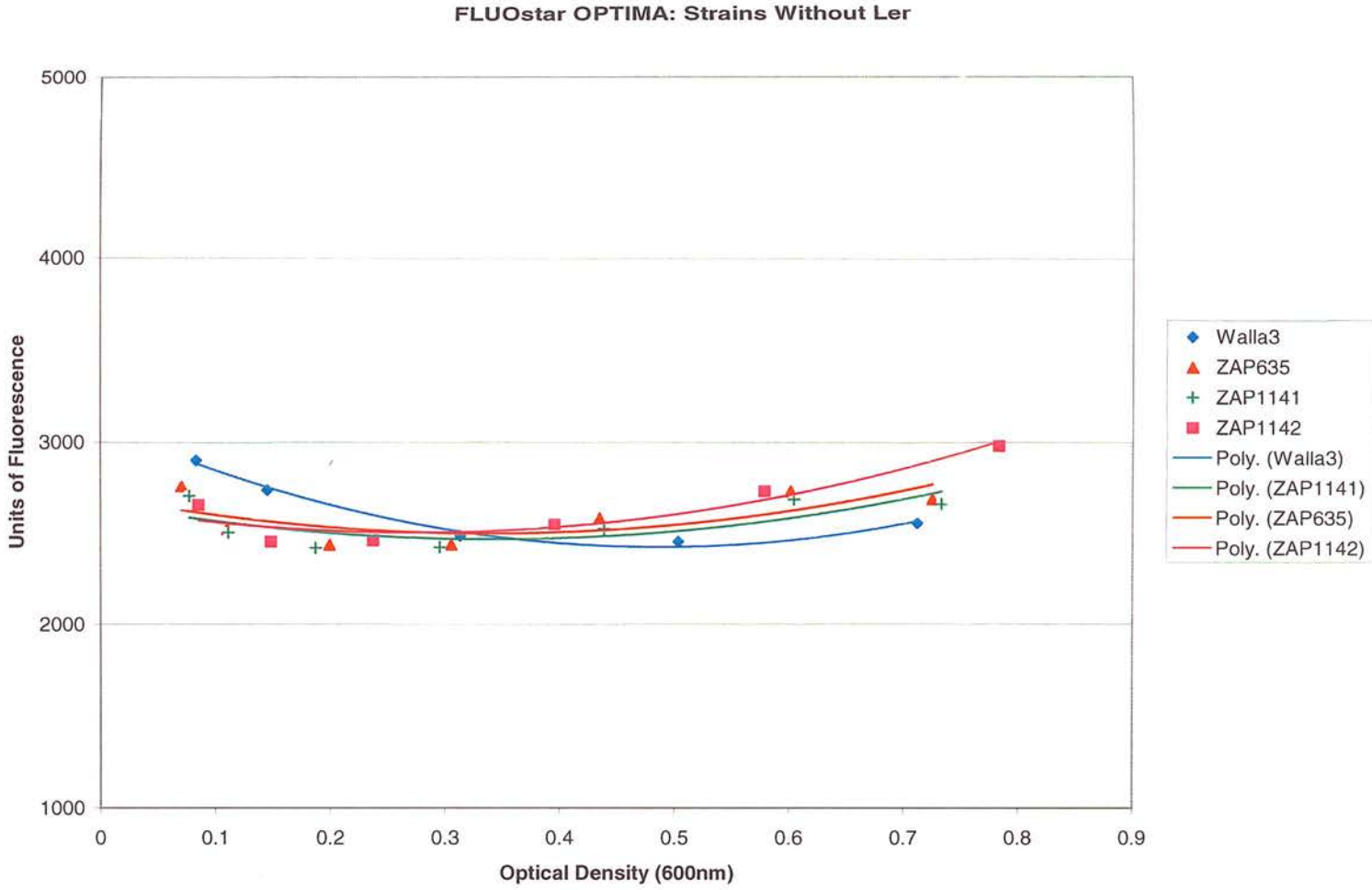

Fig.47 FLUOstar OPTIMA data for strains Walla3 *escU<>escU*$_{cc::egfp}$ (ZAP1141), Walla3 *escU<>escU*$_{cc::gfp+}$ (ZAP1142), Walla3 *escU<>escU*$_{cn::gfp+}$ (ZAP635) and Walla3 without the pASL10 plasmid. Relative fluorescence units are plotted against optical density at 600nm and polynomial trend lines added.

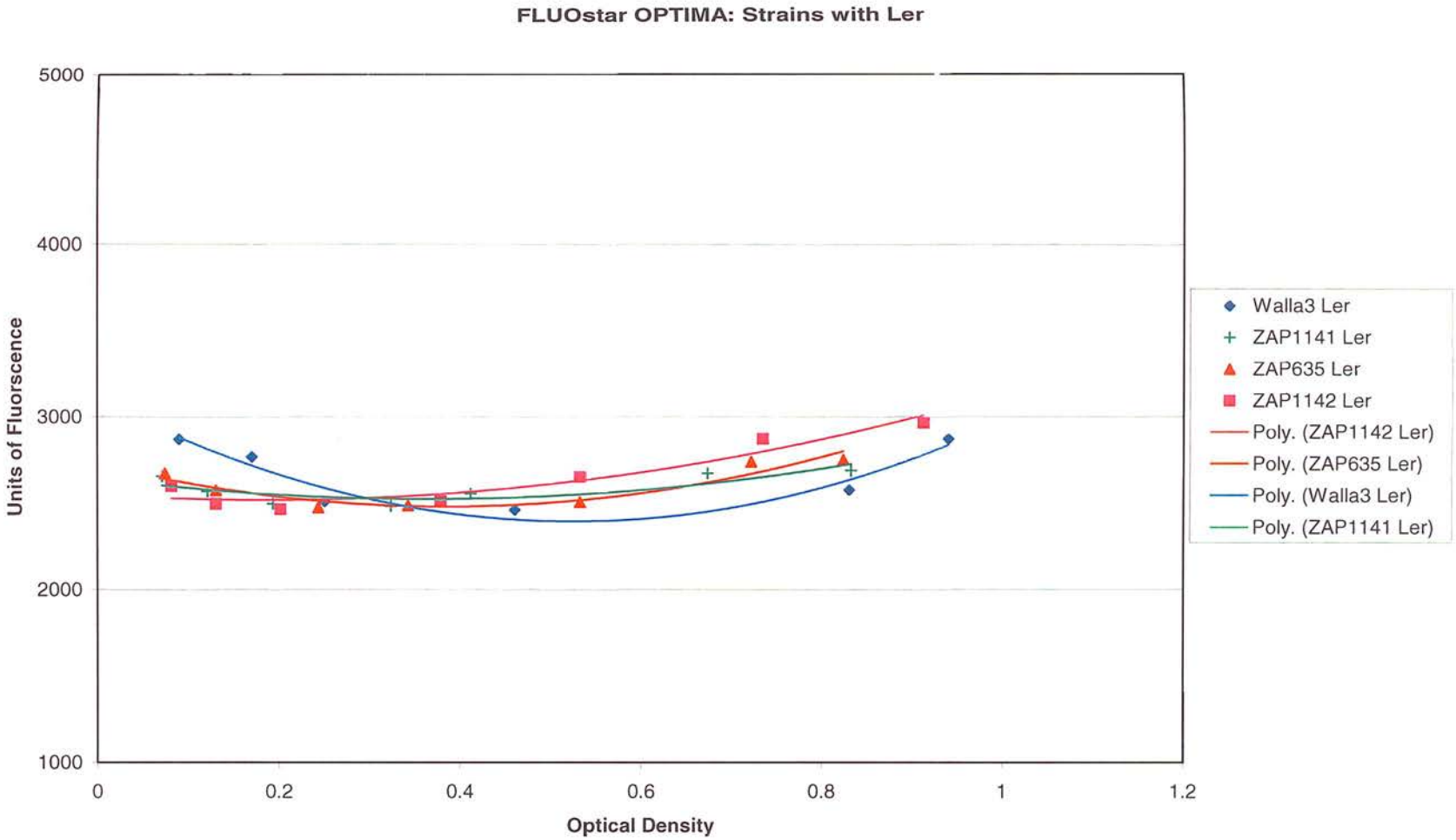

Fig.48 FLUOstar OPTIMA data for strains Walla3 *escU<>escU*$_{cc::egfp}$ (ZAP1141), Walla3 *escU<>escU*$_{cc::gfp+}$ (ZAP1142), Walla3 *escU<>escU*$_{cn::gfp+}$ (ZAP635) and Walla3 containing the pASL10 plasmid. Relative fluorescence units are plotted against optical density at 600nm and polynomial trend lines added.

4.4 Increasing EscU Expression with GrlA: FLUOstar OPTIMA

The pASL10 plasmid had not been previously used in the laboratory to increase the expression of genes on the LEE1 operon. The paper published by Ando, H., *et al* 2007 describes the successful use of a plasmid containing the gene for the positive regulator GrlA to increase the expression of T3SS basal apparatus genes in the EHEC O157:H7 strain EDL933, which were grown in LB broth.

The GrlA plasmid (pGEM-*grlA*) was kindly supplied by Hiroki Ando and transformed into the strains Walla3 *escU*<>$escU_{cc::egfp}$ (ZAP1141), Walla3 *escU*<>$escU_{cc::gfp+}$ (ZAP1142), Walla3 *escU*<>$escU_{cn::gfp+}$ (ZAP635) and Walla3. The transformants were grown in supplemented MEM-HEPES (with ampicillin for strains with pGEM-*grlA*) and IPTG (to a final concentration of 1mM) for FLUOstar OPTIMA measurements. After the final FLUOstar OPTIMA reading was taken microscopy slides were made as before. The general trend is repeated, as in all the FLUOstar OPTIMA results: The Walla3 strain has the lowest detectable fluorescence levels, followed by the strain ZAP1141 (Walla3 *escU*<>$escU_{cc::egfp}$), then the strain ZAP635 (Walla3 *escU*<>$escU_{cn::gfp+}$) and finally the highest detectable fluorescence in the strain ZAP1142 (Walla3 *escU*<>$escU_{cc::gfp+}$). When the FLUOstar OPTIMA data is plotted and compared (Fig.49 and Fig.50) there is little difference in the population levels of fluorescence between strains with and strains without the pGEM-*grlA* plasmid. Microscopy slides were visualized by fluorescence microscopy (pictures not shown) and showed no difference between strains with or strains without the plasmid.

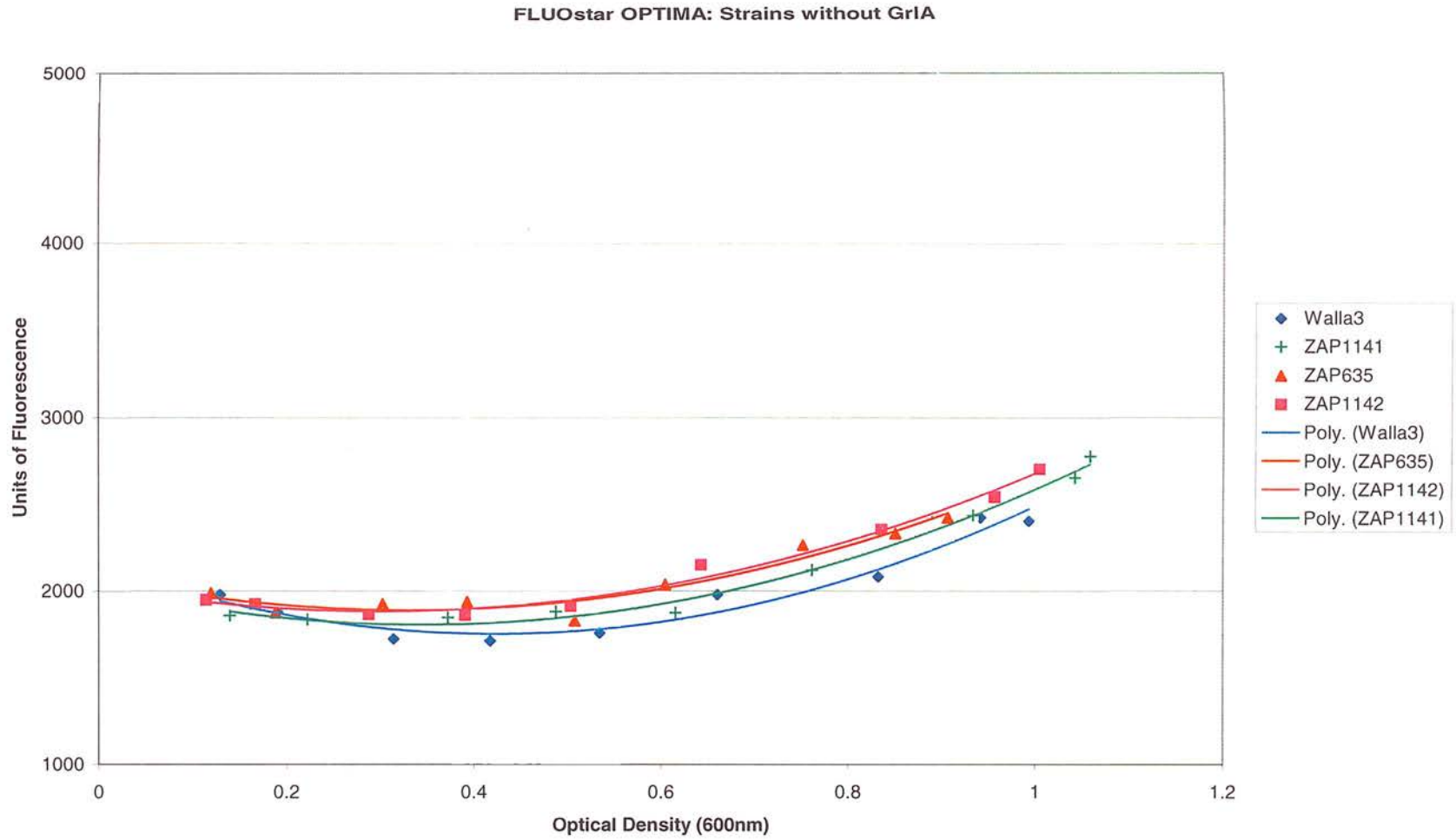

Fig.49 FLUOstar OPTIMA data for strains Walla3 *escU<>escU*$_{cc::egfp}$ (ZAP1141), Walla3 *escU<>escU*$_{cc::gfp+}$ (ZAP1142), Walla3 *escU<>escU*$_{cn::gfp+}$ (ZAP635)and Walla3 without the pGEM-*grlA* plasmid. Relative fluorescence units are plotted against optical density at 600nm and polynomial trend lines added.

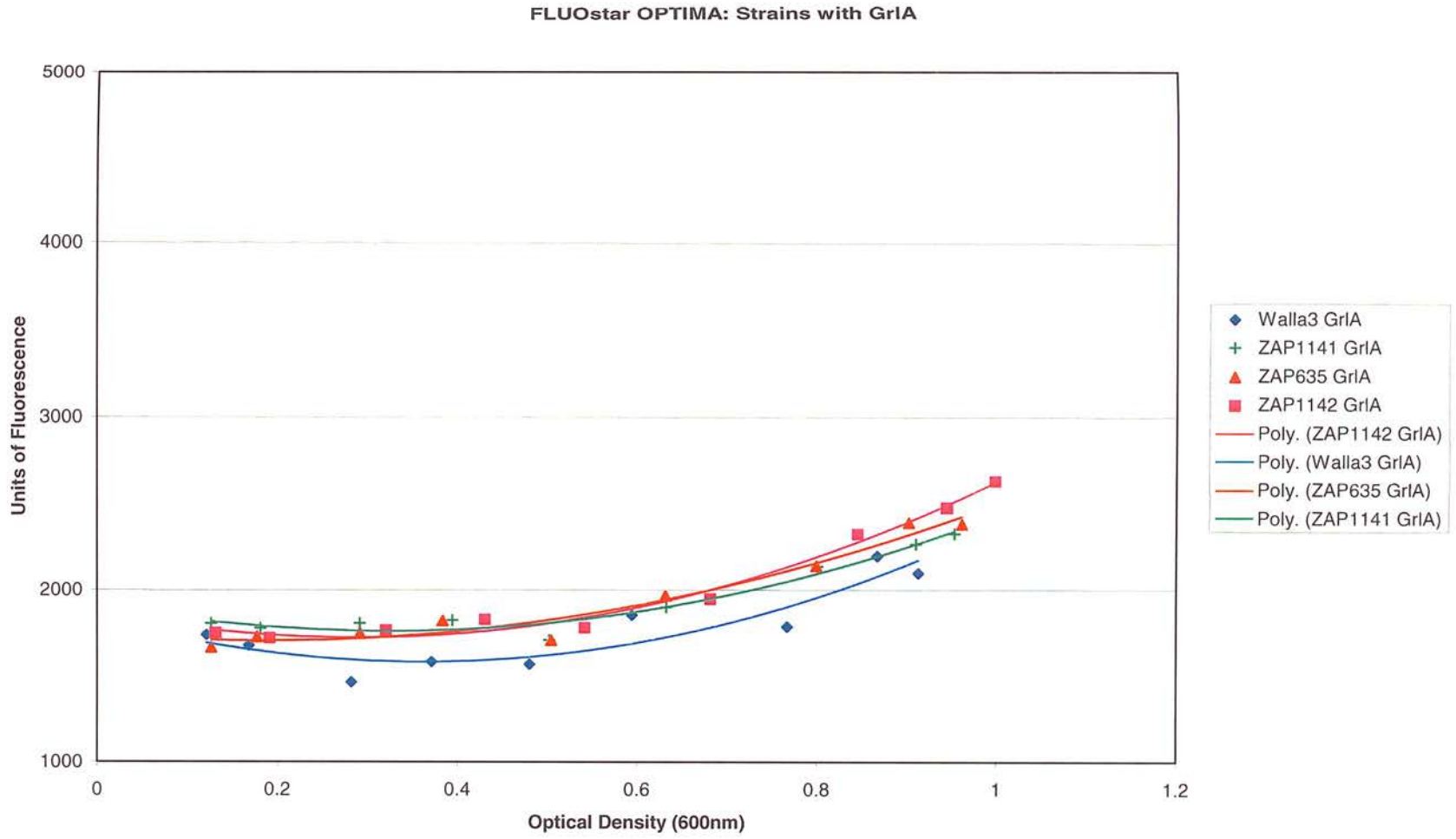

Fig.50 FLUOstar OPTIMA data for strains Walla3 *escU<>escU*$_{cc::egfp}$ (ZAP1141), Walla3 *escU<>escU*$_{cc::gfp+}$ (ZAP1142), Walla3 *escU<>escU*$_{cn::gfp+}$ (ZAP635)and Walla3 containing the pGEM-*grlA* plasmid. Relative fluorescence units are plotted against optical density at 600nm and polynomial trend lines added.

4.4.1 Increasing *escU* Expression with GrlA: SDS PAGE of Secreted Proteins

Secreted protein preparations were made from Walla3, Walla3 *escU*<>*escU*$_{cc::egfp}$ (ZAP1141), Walla3 *escU*<>*escU*$_{cc::gfp+}$ (ZAP1142) and Walla3 *escU*<>*escU*$_{cn::gfp+}$ (ZAP635) with and without the *grlA* plasmid (grown in the presence of 1mM IPTG). Secreted protein pellets (after TCA precipitation) and Coomassie staining of secreted proteins on an SDS PAGE gel showed a promising increase in the amount of protein secreted by the strains containing the plasmid. Western blot analysis with the anti GFP antibody was then used to determine whether the level of detectable GFP (fused to EscU) had increased.

4.4.2 Increasing *escU* Expression with GrlA: Western Blot Analysis with Anti GFP Antibodies

To determine whether artificially increasing the levels of GrlA increased the expression of the EscU GFP fusions, Western blot analysis was carried out. This analysis used anti GFP antibodies (J-L8; Table 4) on whole cell fractions of the strains Walla3 *escU*<>*escU*$_{cc::egfp}$ (ZAP1141), Walla3 *escU*<>*escU*$_{cc::gfp+}$ (ZAP1142), Walla3 *escU*<>*escU*$_{cn::gfp+}$ (ZAP635) and Walla3, with and without the *grlA* plasmid. Although FLUOstar OPTIMA results and microscopy did not show a difference when the strains carried the plasmid, Western blot analysis is more sensitive and can be quantified to highlight any increase.

The whole cell preparations of the strains with and without the *grlA* plasmid were run on a SDS PAGE gel and Western blott analysis carried out with anti GFP monoclonal antibody – in high stringency conditions. Western blot analysis showed the strains with and the strains without the pGEM-*glrA* plasmid had little difference in the amount of GFP being expressed (Fig.51). The intensities of the bands show a 1.5 times increase in eGFP detected in the strain ZAP1141 (with eGFP at the C terminus of EscU) with pGEM-*grlA* compared to without. For GFP+ fused to the EscU C terminus (ZAP1142) the intensities are almost identical, with a 0.03 times decrease when the GrlA plasmid is expressed. Interestingly the GFP+ at the C terminus gives a 1.8 times stronger band than

eGFP without the *grlA* plasmid. This increase in the amount GFP+ detected by Western blot analysis and its brighter fluorescence properties could explain the increase in fluorescence measured by the FLUOstar OPTIMA apparatus for this GFP+ strain.

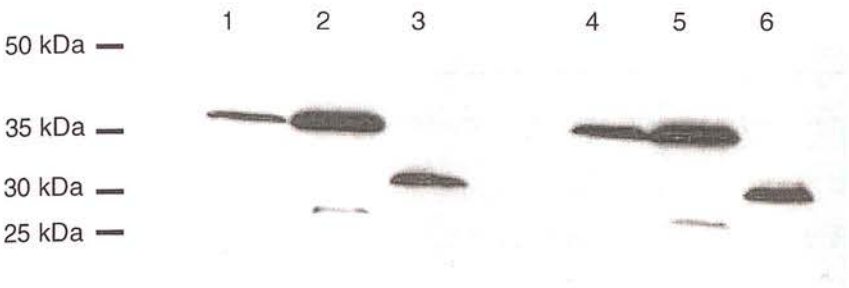

Fig.51 Western blot analysis to determine the effect of increased amount of GrlA on the expression of *escU::gfp* fusions (Walla3 *escU*<>*escU*$_{cc::egfp}$ [ZAP1141], Walla3 *escU*<>*escU*$_{cc::gfp+}$ [ZAP1142] and Walla3 *escU*<>*escU*$_{cn::gfp+}$ [ZAP635]). Run on a 12% SDS PAGE gel and detected using a 1:2000 dilution of anti GFP antibody on whole cell samples.
Lane1: ZAP1141 without pGEM-*grlA*
Lane2: ZAP1142 without pGEM-*grlA*
Lane3: ZAP635 without pGEM-*grlA*
Lane4: ZAP1141 with pGEM-*grlA*
Lane5: ZAP1142 with pGEM-*grlA*
Lane6: ZAP635 with pGEM-*grlA*

4.4.3 Increasing *escU* Expression with GrlA in non TTSS Promoting Conditions

The paper by Ando, H., *et al* 2007 detailed the plasmids use in LB broth to increase the expression of the T3SS apparatus proteins. A possible explanation for the higher levels of GrlA not increasing the amount of the EscU GFP fusion could be due to the fact that the Walla3 strain is a high secretor and the experiment is performed under conditions that promote secretion. This may mean that the TTSS will not be affected by the presence of extra GrlA because it is already expressing the LEE genes at maximal efficiency. The growth of Walla3 in LB media leads to a significant decrease in the expression of T3SS genes, which is thought to be due to a lack of the correct environmental signals. If increased GrlA is produced in the Walla3 strain grown in LB media then the need for the environmental signals may be by-passed and the genes on the LEE expressed at a higher level leading to a detectable increase (measured by EspD

secretion). This would validate the pGEM-*grlA* construct's ability to increase the expression of T3SS genes situated in the LEE.

Secreted protein preparations were made from the Walla3 strain grown in 1) 50ml supplemented MEM-HEPES 2) 50ml LB broth and 3) TheWalla3 strain with the *grlA* plasmid grown in 50ml LBA broth (with IPTG added to a final concentration of 1mM when the culture reached an OD_{600nm} of 0.1). The secreted protein preparations under went Western blot analysis with anti EspD antibody (Fig.52). When Walla3 is grown in supplemented MEM-HEPES EspD is secreted into the supernatant at high levels. When grown in LB broth the secretion of EspD decreases dramatically (Fig.52, Lane2). When the *grlA* plasmid is added the levels do not increase to that observed in the MEM media, but secretion is increased 1.4 times. This is not a large increase, especially when comparing the amount of EspD produced in favourable conditions (Fig.52, Lane1). The *grlA* plasmid appears to be having little effect on the expression of the LEE genes *espD* and *escU*.

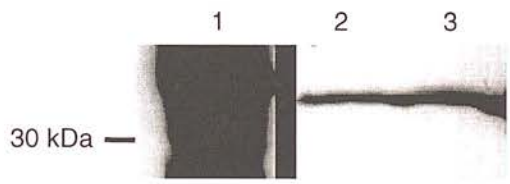

Fig.52 Western blot analysis showing the effect of increased levels of GrlA on Walla3 secretion of EspD after growth in LB broth - run on a 12% SDS PAGE gel and Western blot analysis carried out with a 1:2000 dilution of anti EspD antibody
Lane1: Walla3 EspD secreted after growth in supplemented MEM-HEPES
Lane2: Walla3 EspD secreted after growth in LB broth
Lane3: Walla3 with pGEM-*grlA* EspD secreted after growth in LB broth

4.5 EscU Cleavage

The GFP detected in the Western blots in Fig.60 showed that the GFP fusions were resolving on a 12% SDS PAGE gel at a much lower molecular mass than 66kDa, as would be expected from a fusion to the whole of EscU (39kDa of EscU and 27kDa of GFP, Fig.54 and 55). Fig.53 shows that in Lane2 there is some cleaved GFP+ detected

between the 25kDa and 30kDa marker bands. However, the main product in Lane2 and the only product in Lane1 are detected at ~37kDa. This is most likely 27kDa of the GFP protein and 10kDa of EscU, with the protein fusion being cleaved inside the EscU sequence.

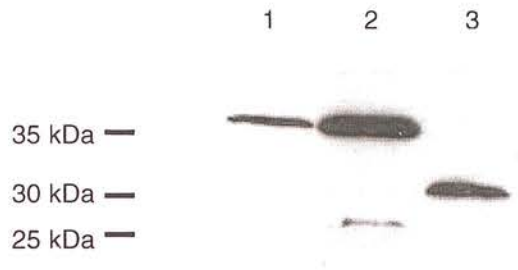

Fig.53 Western blot showing the cleavage of EscU GFP fusions (Walla3 *escU<>escU*$_{cc::egfp}$ [ZAP1141], Walla3 *escU<>escU*$_{cc::gfp+}$ [ZAP1142] and Walla3 *escU<>escU*$_{cn::gfp+}$ [ZAP635]), detected by anti GFP antibodies on whole cell samples.
Lane1: ZAP1141 whole cell sample
Lane2: ZAP1142 whole cell sample

The EscU Homologous proteins FlhB (from the flagellar system in *Salmonella* Typhimurium) and YscU (from the *Yersinia pseudotuberculosis* T3SS) have been shown to cleave a 10kDa fragment from their C terminus during the process of switching from making the needle to making the filament (Minamino, T., *et al* 2000, Lavander, M., *et al* 2002). This cleavage has not been observed in EscU from EHEC, but an alignment of the protein sequence from these three proteins (Fig.54) shows that the cleavage sequence NPTH is conserved. Cleavage of the homologous proteins, which is thought to be autocatalytic, can be stopped by mutating the NPTH cleavage site (Minamino, T., *et al* 2000, Lavander, M., *et al* 2002). The tagging of the C terminus in strains Walla3 *escU<>escU*$_{cc::egfp}$ and Walla3 *escU<>escU*$_{cn::gfp+}$ is after this conserved cleavage site. It is reasonable to conclude that the 37kDa protein detected in Lane1 and Lane2 of the Western blot in Fig.53 is the 10kDa of the EscU cleaved C terminus attached to the 27kDa of the GFP variant.

The Vector NTI (Invitrogen, Paisley, UK) program was used to demonstrate this point as it was possible to create hypothetical proteins that have cleaved at different sites and calculate their molecular weight (Fig.55 and Fig.56). Fig.55 shows how cleavage at the NPTH site leads to the bands observed on the Western blot in Fig.53, Lane1 and 2. Fig.56 illustrates that the band detected in the Western blot in Fig.53, Lane3, when GFP+ was fused before the NPTH cleavage site, is most likely GFP+ cleaved from EscU but attached to the 34 amino acids from the GFP+ to the cleaved NPTH sequence (31kDa). The eGFP protein has the same molecular mass as GFP+ (27kDa) so the expected band sizes were the same. N-terminal protein sequencing could have been used to confirm the cleavage of EscU was happening at the NPTH cleavage site, however, time restraints did not allow for this experiment.

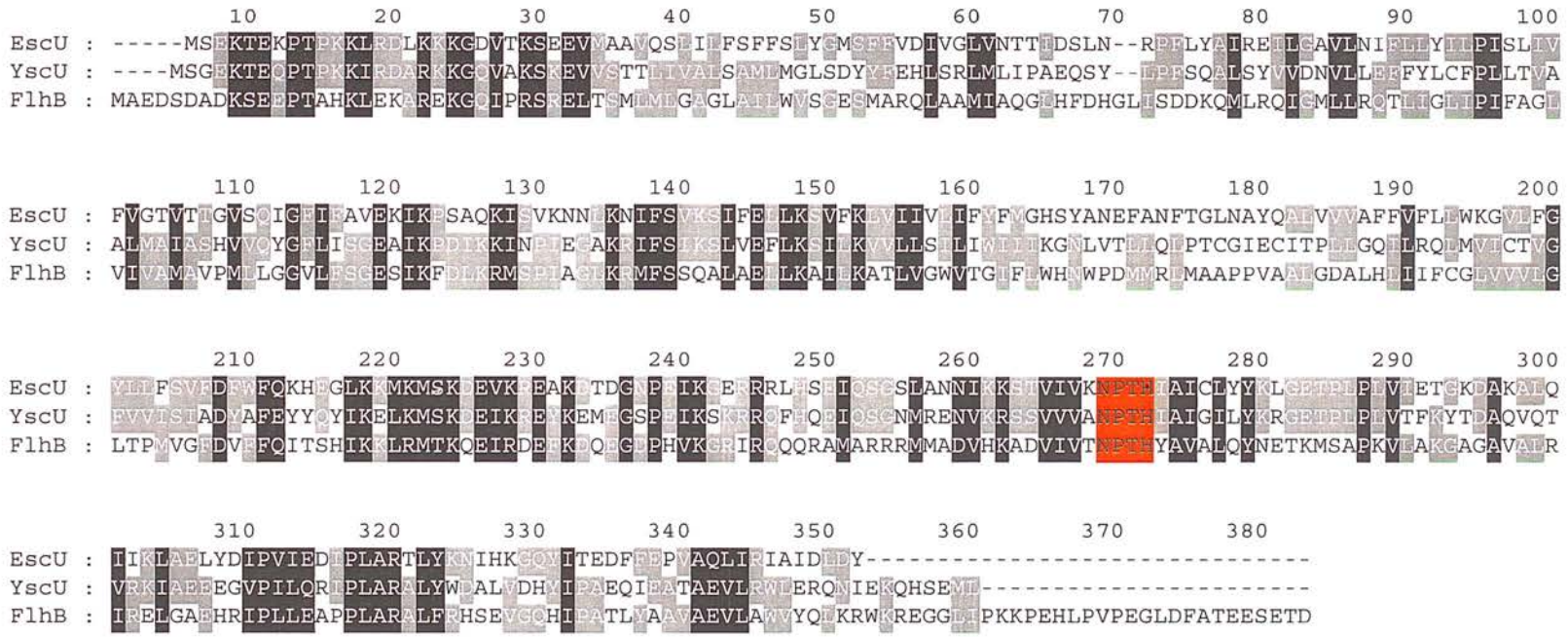

Fig.54 Sequence alignment of EscU (from EHEC O157:H7), YscU (from *Yersinia pseudotuberculosis*) and FlhB (from *Salmonella* Typhimurium) showing the conserved cleavage site NPTH (highlighted in red).

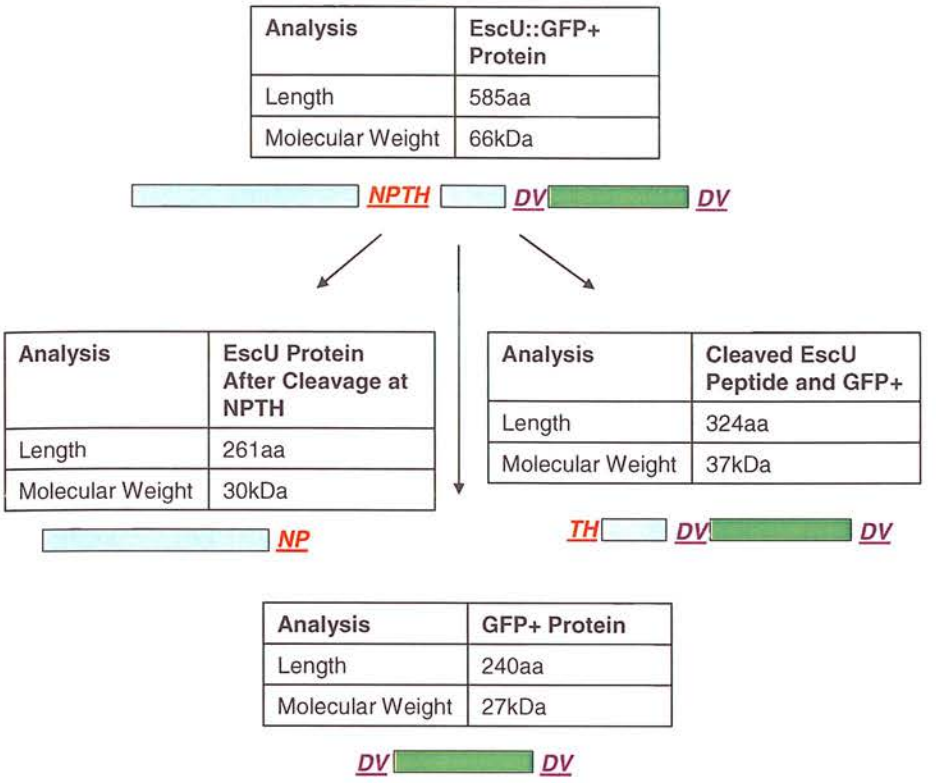

Fig.55 A schematic diagram showing some possible proteins created by the cleavage of the EscU fusion protein to GFP+ at the *Aat*II site. EscU is shown in blue, GFP+ is shown in green and the NPTH cleavage site is shown in red with the *Aat*II sites shown in purple (translated amino acids). The mass in kDa is estimated by the Vector NTI program (Invitrogen, Paisley, UK) and rounded up to the nearest kDa. The diagram shows that if cleavage only happens at NPTH then the detected protein would be 37kDa in mass and that GFP+ has a mass of approximately 27kDa.

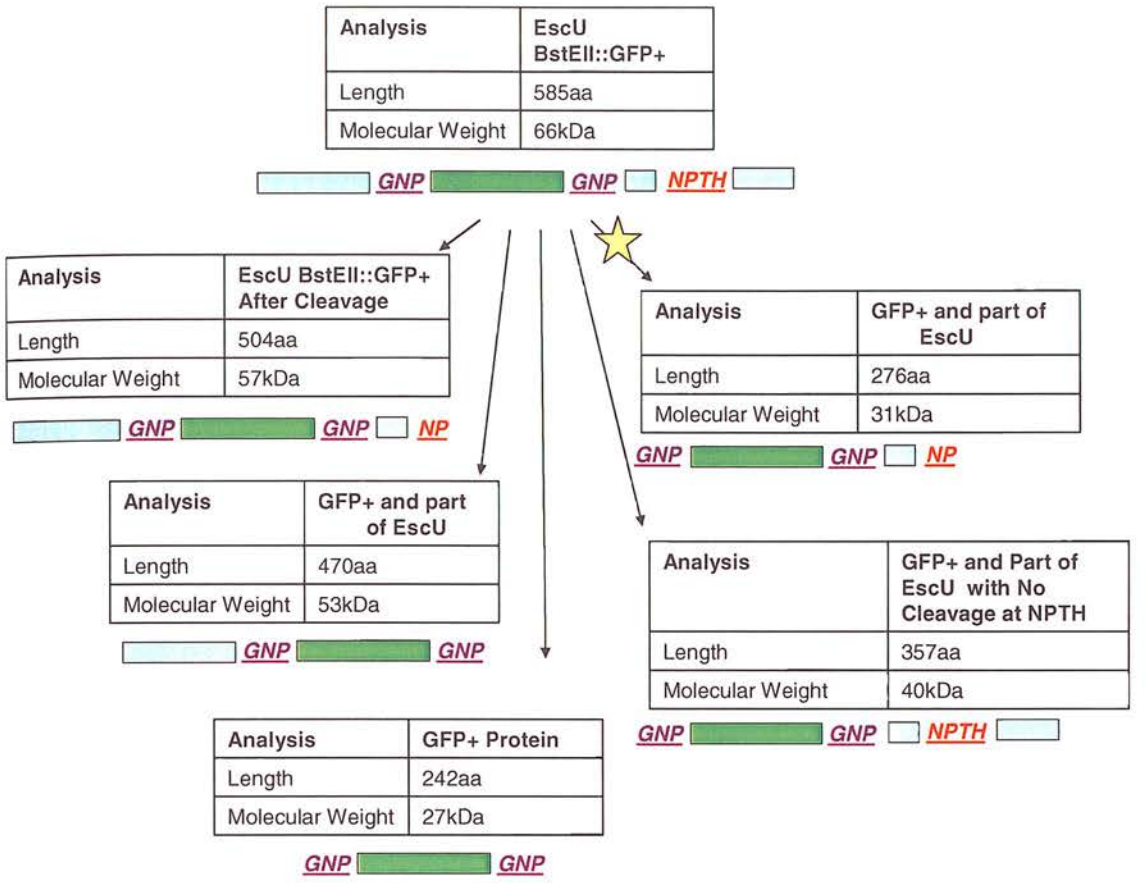

Fig.56 A schematic diagram showing some possible proteins created by the cleavage of the EscU fusion protein to GFP+ at the *Bst*EII site. EscU is shown in blue, GFP+ is shown in green and the NPTH cleavage site is shown in red with the *Bst*EII sites shown in purple (translated amino acids). The mass in kDa is estimated by the Vector NTI program (Invitrogen, Paisley, UK) and rounded up to the nearest kDa. The diagram shows that if cleavage only happens at the NPTH then the expected detectable protein would be 57kDa in mass. However, the fifth protein (marked with a yellow star) is most likely the one being detected.

The fusion of GFP+ in the *Bst*EII site of *escU* is before the cleavage sequence NPTH and gives an unexpected band on the Western blot. If the cleavage of EscU is happening at the NPTH site then the fusion in strain Walla3 *escU*<>*escU*$_{cn::gfp+}$ should give a band at 57kDa (30kDa of the large fragment of EscU after cleavage and 27kDa of GFP+). It is likely that this is not seen because the cleavage of EscU is not happening properly. Previous studies have shown that when the cleavage site is removed from YscU the protein cleaves randomly due to an altered conformation (Lavander, M., *et al* 2002). It is

likely that the addition of the large GFP+ protein in the cytoplasmic tail of EscU before the cleavage site distorts the proteins conformation and leaves EscU vulnerable to cleavage at alternative sites. This may not have been seen with the EscU C terminal fusions because the addition of the tags at the C terminus or N terminus are generally considered to interfere less with the protein they are labelling (Margolin, W., *et al* 2000).

4.6 EscU Localization

Because fluorescence microscopy could not localise the GFP fusions Western blot analysis was carried out using the anti GFP monoclonal antibody on bacterial cell preparations, which separate cytoplasmic, membrane and supernatant proteins. It was expected that the EscU protein localised to the membrane fraction, however, after cleavage the EscU C terminal peptide may leave the T3SS and be released into the cytoplasm to be degraded or carry out another function.

Western blot analysis carried out with the J-L8 anti GFP antibody. The samples run on the gel were cytoplasmic, membrane and supernatant preparations of the bacterial strain Walla3 *escU<>escU*$_{cc::egfp}$. The gel (Fig.57) also contained a positive control, which was a cytoplasmic fraction of the Walla3 strain expressing the pDW6 plasmid (Fig.57, Lane7). The highest band on the Western blot in the positive control is the GFP fusion to SepL, the middle band is degraded SepL fusion protein, and the lowest band is that of eGFP cleaved from the SepL fusion. Membrane, cytoplasmic and secreted protein preparations were also made from the Walla3 strain to act as a negative control. The Western blot (Fig.57) shows that eGFP can only be detected in the strain Walla3 *escU<>escU*$_{cc::egfp}$ and only in Lane2 and Lane4. Lane2 is the cytoplasmic fraction of the strain Walla3 *escU<>escU*$_{cc::egfp}$ and Lane4 is the membrane fraction. There is 3.6 times more eGFP detected in the membrane fraction of the Walla3 *escU<>escU*$_{cc::egfp}$ strain. This indicates that the cleaved fragment is localised to the membrane, either directly anchored to it or via a protein that is.

The membrane preparations were validated by a Western blot on the same samples using the GroEL antibody. The Western blot (not shown) has 1.6 times more GroEL present in the cytoplasmic protein fraction compared to the membrane fraction, as GroEL is a cytoplasmic protein this result validates that the cytoplasmic fraction is biased to cytoplasmic proteins.

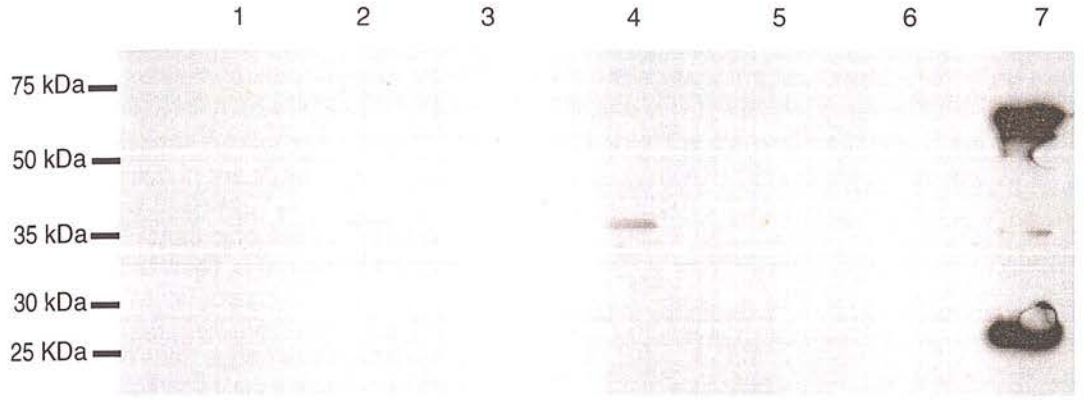

Fig.57 A 12% SDS PAGE gel was run and Western blot analysis showed the localisation of the cleaved fragment of the EscU eGFP fusion in the strain Walla3 *escU*<>*escU*$_{cc::egfp}$, (ZAP1141) detected by anti GFP antibody
Lane1: Walla3 cytoplasmic fraction
Lane2: ZAP1141 cytoplasmic fraction
Lane3: Walla3 membrane fraction
Lane4: ZAP1141 membrane fraction
Lane5: Walla3 supernatant proteins
Lane6: ZAP1141 supernatant proteins
Lane7: Walla3 containing pDW6 as a positive control.

The Western blot was repeated with new protein fractions prepared in an identical manner to confirm the result (Fig.58). This Western blot showed 3.3 times more eGFP detected in the membrane preparation of the Walla3 *escU*<>*escU*$_{cc::egfp}$ (ZAP1141) strain compared to the cytoplasmic protein preparation.

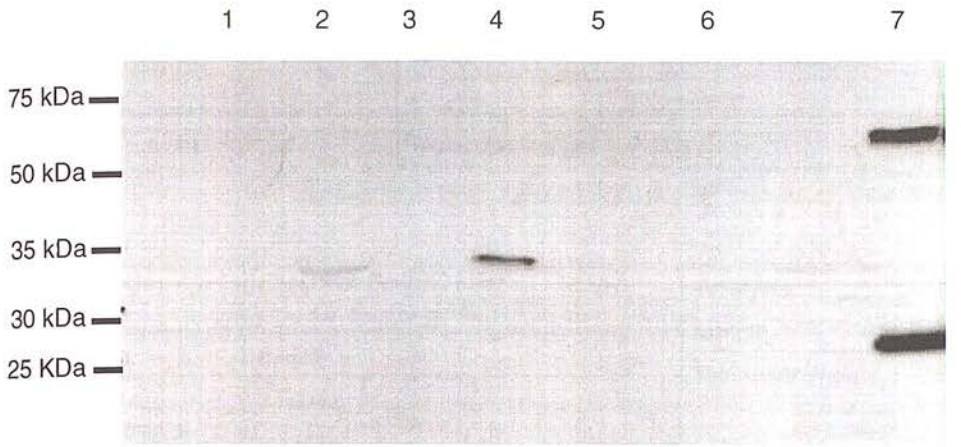

Fig.58 Repeat Western blot showing the localization of the cleaved fragment of the EscU eGFP fusion in the strain Walla3 *escU<>escU*$_{cc::egfp}$ (ZAP1141), detected by anti GFP antibodies.
Lane1: Walla3 cytoplasmic fraction
Lane2: ZAP1141 cytoplasmic fraction
Lane3: Walla3 membrane fraction
Lane4: ZAP1141 membrane fraction
Lane5: Walla3 supernatant proteins
Lane6: ZAP1141 supernatant proteins
Lane7: Walla3 containing pDW6 as a positive control.

4.7 HA Tag Detection in Strains Walla3 *escU<>escU*$_{cn::HA}$ (ZAP634) and Walla3 *escR<>escR::HA* (ZAP637)

The strains Walla3 *escU<>escU*$_{cn::HA}$ and Walla3 *escR<>escR::HA* contain the fusions EscU::HA and EscR::HA, respectively. The HA tag is an antigenic peptide that does not have intrinsic fluorescence properties, like GFP, so its detection requires conjugated antibodies. Before attempts were made to visualise the proteins via fluorescence microscopy the ability for the HA tag to be detected by antibodies was tested by Western blot analysis and EscR and EscU's localisation within the bacterial cell determined.

The Vector NTI (Invitrogen, Paisley, UK) program was used to predict the expected molecular weight (kDa) of the EscU::HA fusion protein, before and after cleavage at the NPTH site (Fig.59) and the EscR::HA fusion protein (Fig.60).

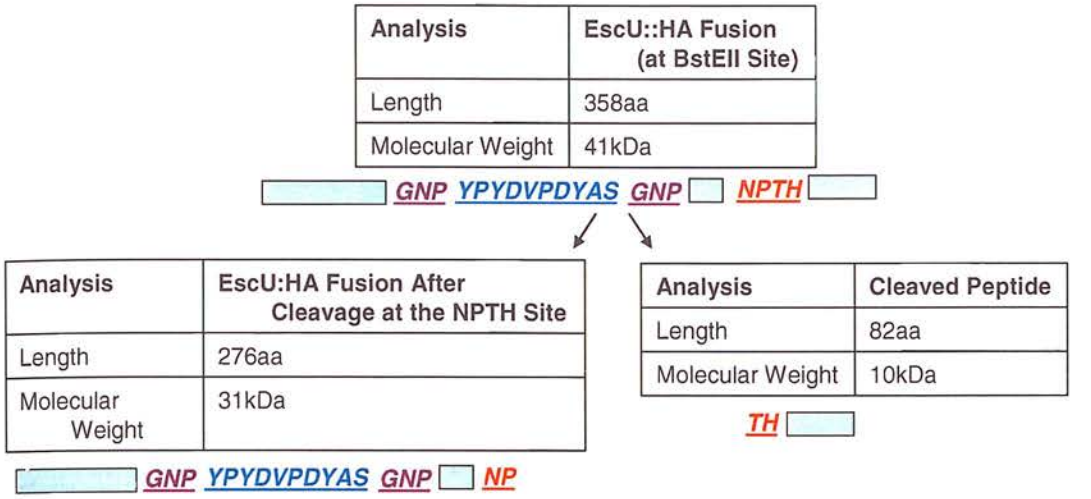

Fig.59 A schematic diagram showing the proteins created by the cleavage of the EscU::HA fusion at the NPTH cleavage site. EscU is shown as blue rectangles, the HA tag is shown as amino acids (dark blue letters), the NPTH cleavage sequence is shown in red and the *Bst*EII restriction sites shown in purple (translated amino acids). The mass in kDa is estimated by the Vector NTI program (Invitrogen, Paisley, UK) and rounded up to the nearest kDa. The diagram shows that if cleavage happens at the NPTH then the expected detectable protein would be 31kDa in mass and that the cleaved peptide has a mass of approximately 10kDa.

Analysis	EscR::HA Fusion
Length	227aa
Molecular Weight	26kDa

LFK YPYDVPDYAS FLLVVN

Fig.60 A schematic diagram showing the construction of the EscR::HA fusion protein. EscR is depicted as a blue rectangle, the HA tag is shown as amino acids (dark blue letters) and the SwaI restriction site is in purple (translated amino acids). The mass in kDa is estimated by the Vector NTI program (Invitrogen, Paisley, UK) and rounded up to the nearest kDa. There are no suspected cleavage sites in EscR so the detectable fusion protein should be approximately 26kDa.

Cytoplasmic, membrane and supernatant protein preparations were made of the strains Walla3 *escU<>escU*$_{cn::HA}$ and Walla3 *escR<>escR::HA*. Two Western blots were carried out – one with anti HA monoclonal antibody supplied by Sigma (Dorset, UK) and the other with anti HA monoclonal antibody supplied by Abcam (Cambridge, UK).

Both Western blots were carried out in high stringency conditions. This level of stringency was too high to see any bands that may have been present; after an hour exposure no bands were detected on the X ray film. The stringency was lowered and the amount of antibody used was raised. The Western blots then developed multiple non specific bands whilst still having no unique bands at the predicted size (Fig.61). When using the two different brands of anti HA antibodies the non specific bands were not the same (Fig.61, A and B).

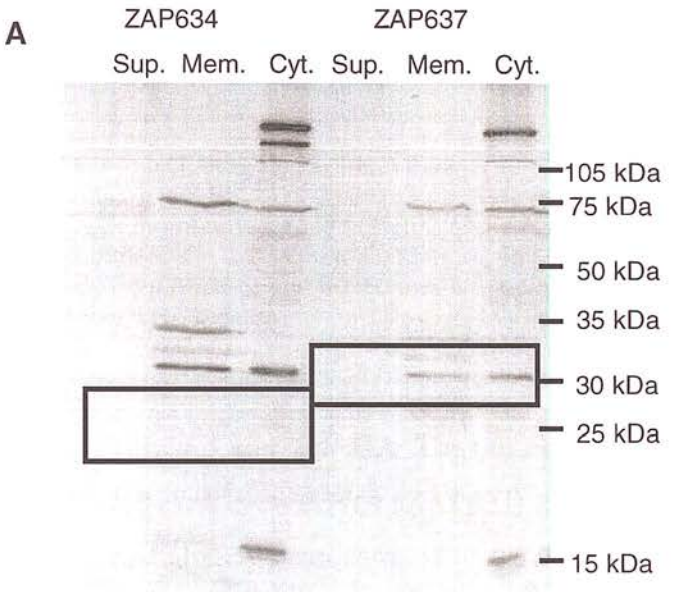

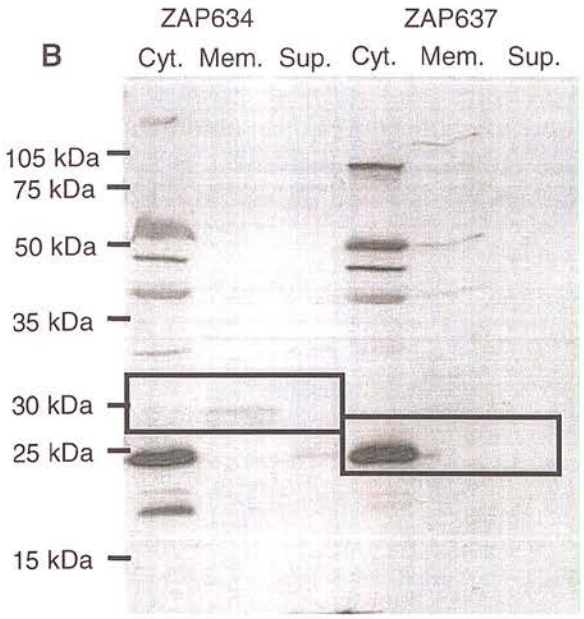

Fig.61 Western blot analysis to detect the HA tag in the strains Walla3 *escU<>escU*$_{cn::HA}$ (ZAP634) and Walla3 *escR<>escR::HA* (ZAP637) in cytoplasmic fraction (Cyt.), membrane fraction (Mem.) and supernatant fraction (Sup.) using two different commercially available antibodies A. Anti HA antibody from Sigma B. Anti HA antibody from Abcam. The boxed areas encompass the expected size for the EscU and EscR HA fusions.

4.7.1 Increasing Protein Load for HA Tagged Strains Walla3 *escU<>escU*$_{cn::HA}$ (ZAP634) and Walla3 *escR<>escR::HA* (ZAP637)

The previous work had already demonstrated that the GFP fusions were not present in high enough quantity to be detected by fluorescence microscopy and the GFP bands detected on the Western blots were faint. The lack of HA bands detected could, therefore, have been due to low levels of EscU translation. The growth conditions were changed to increase the quantity of EscU::HA or EscR::HA protein that was present in the strains Walla3 *escU<>escU*$_{cn::HA}$ and Walla3 *escR<>escR::HA*. Instead of preparing the protein preparations from 50ml supplemented MEM-HEPES the preparations were made from strains grown in 500ml. Although the bacterial pellet for the cytoplasmic and membrane fractions were resuspended in 1ml of sonication buffer, twice as much of the sample was loaded onto the 12% SDS PAGE gel. This equated to 10 times more protein loaded into the wells on the SDS PAGE gel. Both the Sigma (Dorset, UK) and the

Abcam (Cambridge, UK) antibodies were used to detect the HA tags and the presence of the Walla3 strain preparations on the blot enabled the non specific bands to be identified easier. Only the membrane and cytoplasmic fractions were used (Fig.62).

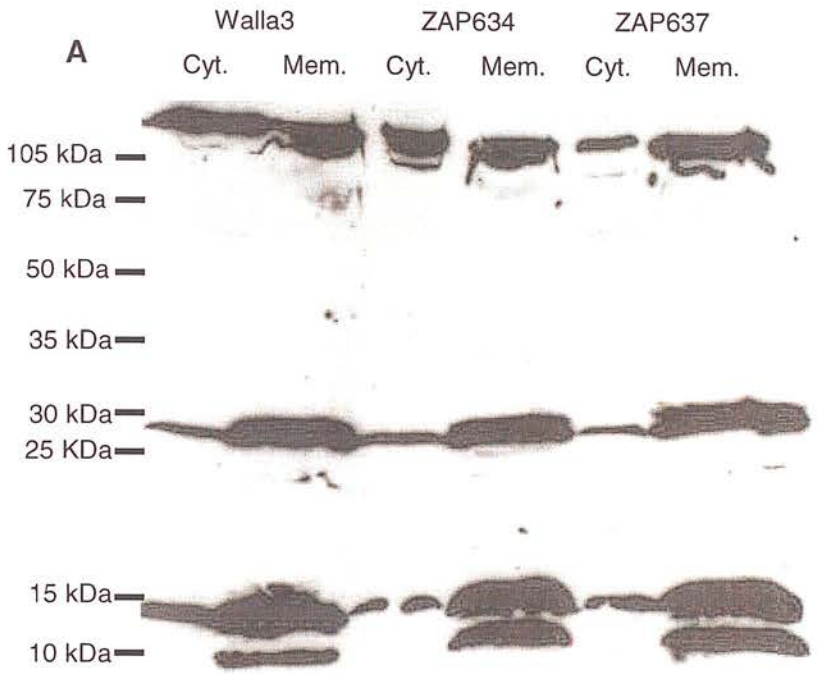

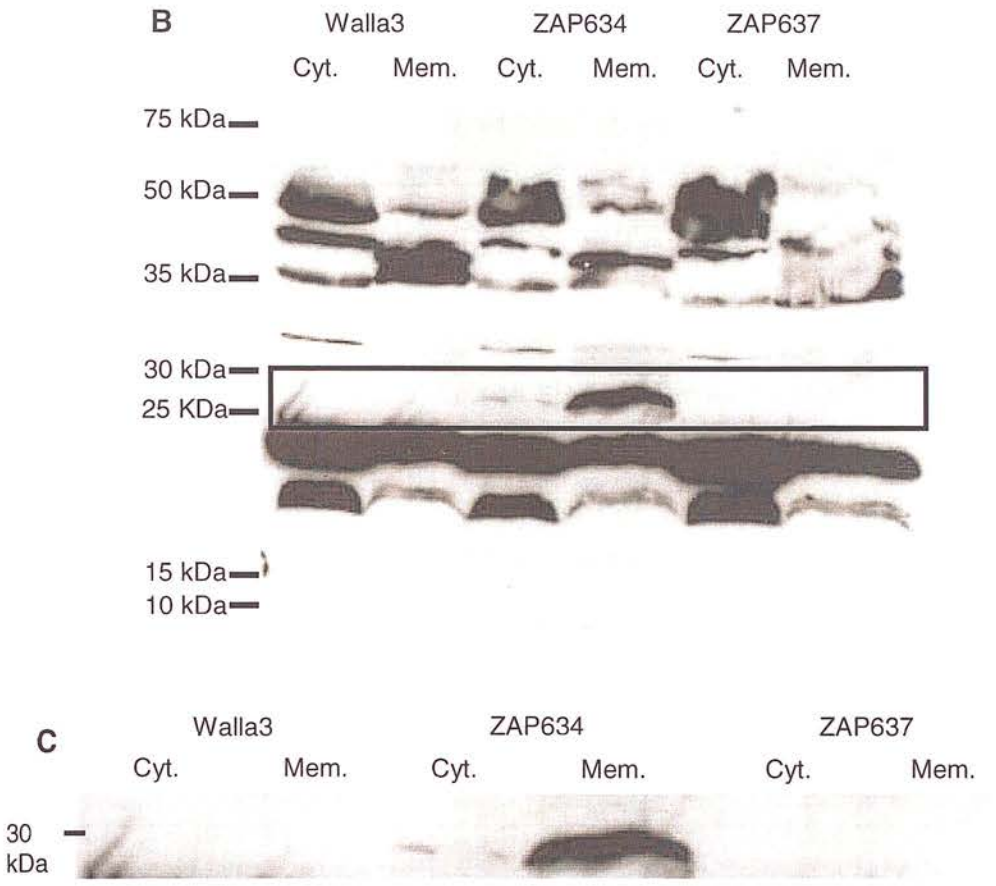

Fig.62 Western blot analysis of the strains Walla3 *escU<>escU*$_{cn::HA}$ (ZAP634), Walla3 *escR<>escR::HA* (ZAP637) and Walla3 grown in 500mls supplemented MEM-HEPES. Detection of HA fused proteins with two different commercially available antibodies in the cytoplasmic fraction (Cyt.) and the membrane fraction (Mem.). A. Anti HA antibody from Sigma B. Anti HA antibody from Abcam C.The boxed area in B is magnified and shown.

The Sigma (Dorset, UK) anti HA antibody did not show any bands unique to the Walla3 *escR<>escR::HA* strain compared to the Walla3 wild type strain. This antibody reacts to produce a non specific band at 30kDa that would mask the presence of the HA tag fused to the large fragment of EscU and there are no bands, at the correct size, in the EscR::HA membrane and cytoplasmic protein preparations (Fig.62, Lane3 and Lane4). The Abcam (Cambridge, UK) anti HA antibody gives a band of non-specific binding at the size for EscR::HA fusion protein making it impossible to judge whether it is detected. However, there is a band present at 30kDa in the lanes for the cytoplasmic and

membrane fractions of the EscU::HA tagged protein. Although present in both lanes it is disproportionately present in the membrane fraction being 5.33 times higher. This result indicates that the EscU protein is being detected by the Abcam (Cambridge, UK) anti HA antibody and that EscU is being cleaved into a ~30kDa protein and a ~10kDa peptide, both of which have been detected separately and localised to membrane protein preparations.

Western blot analysis was carried out on the membrane and cytoplasmic protein preparations using anti GroEL antibody and anti OmpA antibody. Although not shown, the cytoplasmic fractions of all the strains contained more GroEL protein than in the membrane fractions (1.3 times more) with the opposite being true for the detection of OmpA (1.4 times more in the membrane fraction). As GroEL is a cytoplasmic protein and OmpA is a membrane protein, these results confirm that the cytoplasmic fraction is biased towards cytoplasmic proteins and the membrane fraction biased to membrane proteins.

Due to the lack of sensitivity of the HA antibodies in detecting the HA fusion and the non specific bands, microscopy with the HA tagged strains was not carried.

4.8 EspA Filament Staining

The strains Walla3 *escRSTU<>sac*/Kan, Walla3 *escU<>escU*$_{cc::egfp}$, Walla3 *escU<>escU*$_{cc::gfp+}$, Walla3 *escU<>escU*$_{cn::HA}$, Walla3 *escU<>escU*$_{cn::gfp+}$, Walla3 *escR<>escR::HA* and Walla3 were used to create microscope slides that were fixed with PFA and incubated with anti EspA antibody for immunofluorescence antibody staining. This was to gauge the disruption the tags had on the secretion of EspA and the strains ability to form EspA filaments. Coomassie Blue stained SDS PAGE gels of the secreted proteins from the strains Walla3 *escU<>escU*$_{cc::egfp}$, Walla3 *escU<>escU*$_{cc::gfp+}$, and Walla3 *escU<>escU*$_{cn::gfp+}$, (gels not shown) indicated that there might be a disruption in the secretion of EspB, EspD and EspA. On each 10 well glass microscope slide five wells contained a mutant strain and the other five contained the strain Walla3. Four of

the five wells for each strain (including Walla3) were incubated with anti EspA primary antibody. Then, after washing, all five wells were incubated with the secondary antibody: goat Alexa Fluor 488 conjugate to anti-rabbit IgG. Fluorescence microscopy was carried out on the slides; representative frames were selected (Fig.63), which highlight the difference between the Walla3 strain and the mutant ZAP strains.

The Walla3 strain showed EspA filamentation in a heterogeneous population (as previously described Roe, A., *et al* 2003). When incubated with only the secondary antibody the Walla3 strain lost these fluorescent foci. All the other strains, including the strain ZAP1140 which has the genes *escRSTU* substituted for the *sac*/Kan cassette, did not show any EspA filamentation. This, along with the Coomassie Blue staining of the secreted proteins, indicates that the tags are having a serious effect on the T3SS's ability to secrete proteins that make the translocon.

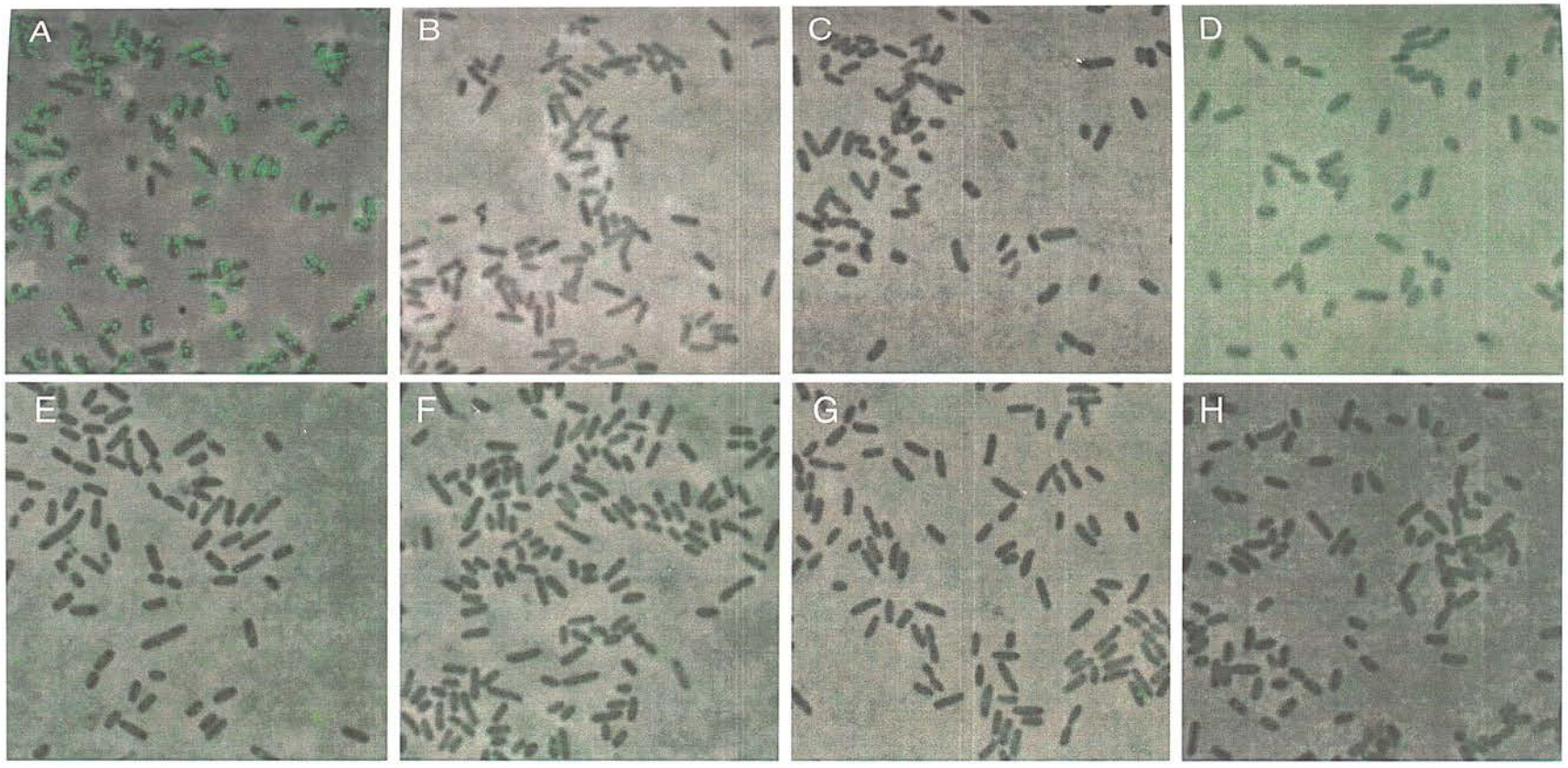

Fig.63 Microscopy images showing strains labelled for EspA filaments, each panel relates to the following strain (200ms exposure): A. Walla3 B. Walla3 *escRSTU<>sac*/Kan C. Walla3 *escU<>escU*$_{cc::gfp+}$ D. Walla3 *escU<>escU*$_{cn::gfp+}$ E. Walla3 *escU<>escU*$_{cc::egfp}$ F. Walla3 *escU<>escU*$_{cn::HA}$ G. Walla3 *escR<>escR::HA* H. Walla3 with secondary antibody only.

4.9 Discussion

The tagging of EscU and EscR created the opportunity to study the expression and localization of two TTSS proteins in the bacterial cell. The method used created a single copy gene fusion that replaces the native gene on the wild type Walla3 chromosome. Having the gene under its own promoter in its original genetic context means the genes expression should be similar to that of the wild type gene, allowing better understanding in the regulation and timing of these basal apparatus proteins.

The low level expression of GFP from the chromosome decreased the likelihood of artifacts and misleading results due to high levels of the fluorescent protein. However, for the fluorescence from the GFP to be detectable by fluorescence microscopy there needs to be a group of GFP molecules in close proximity to allow emitted photons to be detected. If too few molecules of GFP are present the number of photons emitted can be below the threshold of the camera used in fluorescence microscopy (Niswender, K., *et al* 1995). It was hoped that this would not be a problem during this project as the basal apparatus proteins chosen have been shown, by yeast two hybrid system, to interact with each and with themselves (Creasey, E., *et al* 2003) indicating that more than one of the each molecule is present in each basal apparatus.

The fluorescent constructs (those that contain GFP protein fusions) were grown in a T3SS promoting media and the fluorescence of the population measured using the FLUOstar OPTIMA apparatus and plotted against the OD_{600nm} of the culture. The fluorescence of the tagged strains did not increase far from the base line of fluorescence set by the wild type Walla3 strain. The GFP+ protein fusions did record marginally higher fluorescence values than the eGFP fusions. Although this small increase was encouraging, fluorescence microscopy was needed to deduce whether the constructs allowed visualization and localization of the EscU protein at a single cell level.

Microscopy with strains Walla3 *escU<>escU*$_{cc::egfp}$, Walla3 *escU<>escU*$_{cc::gfp+}$ and Walla3 *escU<>escU*$_{cn::gfp+}$, all containing EscU GFP protein fusions, showed that after

high levels of exposure and contrast enhancement fluorescent foci could be visualized. The observation of these fluorescent foci in the Walla3 strain, containing no fluorescent tag, demonstrated that it was an auto fluorescence phenomenon, but did not discount that it was auto fluorescence from the T3SS basal apparatus. To exclude this possibility the strain ZAP1140 (containing a substitution of *escRSTU* for the *sac*/Kan cassette) was imaged in the same way and the fluorescent foci were seen (data not shown). Panel A. in Fig.63 also supports that these observed foci are not due to auto fluorescence of the T3SS as the staining with the anti EspA antibody on the Walla3 strain reveals more filaments per bacterium and on a greater proportion of bacteria than the observed foci.

The FLUOstar OPTIMA data demonstrated that on a population basis there is a small increase in the level of fluorescence from strains containing a protein fusion to a GFP variant but this increase is not detectable at a single cell level by fluorescence microscopy, most likely due to the low levels of GFP in each bacterium.

To overcome the limitation of low levels of GFP an attempt to alter the amount of expression from the *escU* fusion was made using a plasmid containing the gene for the positive regulator Ler. FLUOstar OPTIMA data showed no increase in fluorescence in strains expressing Ler compared to those that did not. A second construct was then used, that contained an inducible copy of *grlA*, another positive regulator of the LEE. This plasmid had previously been published, where it was used to increase the expression of genes on the LEE pathogenicity island from the EHEC strain EDL933 (Ando, H., *et al* 2007). The expression of *grlA* did not increase the fluorescence of the strains when using the FLUOstar OPTIMA apparatus and microscopy revealed no difference in fluorescence at a single cell level. The secreted protein profiles of the strains with and without the pGEM-*grlA* plasmid were used to see whether the plasmid increased the amount of secreted proteins. The increased size of the protein pellets from the secreted protein preparations of the strains containing the *grlA* plasmid indicated that the strains were secreting at a higher level, however Coomassie Blue staining of the SDS PAGE gel of the resuspended secreted protein pellets was hard to interpret due to a lack of secreted

proteins from the tagged strains. A Western blot was carried out with the whole cell preparations of the strains with and without the *grlA* plasmid using a monoclonal anti GFP antibody (J-L8) to measure any increase in the amount of GFP being produced. The Western blot analysis showed that there was a small increase in the amount of eGFP in the strain Walla3 *escU*<>$escU_{cc::egfp}$ being produced when *grlA* was expressed.

The Walla3 strain was then grown in LB, a non T3SS promoting media, to see whether the pGEM-*grlA* plasmid could increase the levels of EspD secretion. The increase of EspD secretion with the *grlA* plasmid was minimal, measuring a 1.4 times increase in comparison to the Walla3 strain grown in LB without the plasmid.

The Western blot analysis using the anti GFP antibody showed the band detected was 37kDa and not 66kDa. An amino acid sequence alignment with studied homologues from the flagellar system of *Salmonella* Typhimurium and the T3SS of *Yersinia pseudotuberculosis* showed that a known cleavage site is preserved in the EscU protein. This cleavage site (NPTH) cleaves a small 10kDa cytoplasmic peptide from these EscU homologues, which is reported to be important in switching from making the needle of the T3SS/flagella to making the filament. The eGFP fusion had one band at 35kDa, the correct size for the cleaved portion of EscU fused to eGFP. The GFP+ fusion had two bands, a strong band at 37kDa and a smaller band at 27kDa, the smaller band being the correct size for the GFP+ cleaved from the EscU peptide. These C terminal fusions support the idea that EscU is cleaved in a similar way. This means the EscU C terminus can be given the same nomenclature as FlhB and YscU proteins. The C and N terminus are written as $EscU_C$ and $EscU_{TM}$ respectively, with $EscU_C$ consisting of $EscU_{CN}$ and $EscU_{CC}$ (Fig.64).

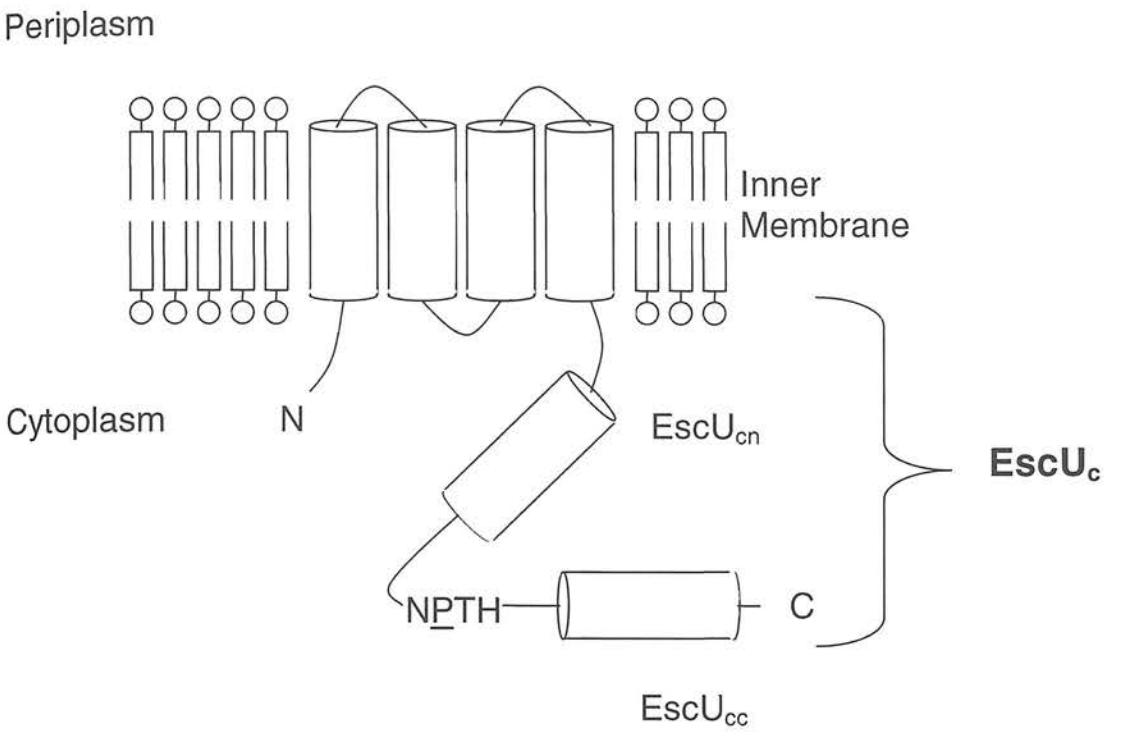

Fig.64 Schematic diagram showing the predicted structure of EscU (based on Lavender, M., *et al* 2002). The diagram is labelled with nomenclature for the C terminus of EscU (EscU$_C$) before and after cleavage at the conserved cleavage site NPTH (N=Asparagine P=Proline, T=Threonine, H=Histidine.)

The Western blot of the GFP+ fusion to the large fragment of EscU (at the *Bst*EII site, see Fig.65) does not show a band pattern that would be expected. The fusion should sit at 57kDa (30kDa for the large cleaved fragment of EscU and 27kDa for GFP+) but instead a band at ~31kDa is observed. This band is too small for the fusion and too large to be GFP+ by itself. It is most likely that the addition of the large GFP+ protein altered the conformation of EscU to such a degree that alternative cleavage happened. This can be confirmed by looking at the HA tag in the same position. This tag allows detection of the 31kDa EscU fragment (30kDa for the large cleaved fragment of EscU and 1kDa for the HA tag) due to its small size which does not cause such dramatic conformational changes.

Because microscopy was unsuccessful and attempts to increase the fluorescence levels failed, Western blot analysis was used to localize the EscU GFP fusions. The cleaved

10kDa fragment was localized to the membrane protein preparation. It could be possible that the cleavage in the EscU molecule causes a C terminal conformational change that alters its affinity for translocon proteins, as shown in the flagellar system and *Yersinia* T3SS. In both these systems the cleaved portion interacts with the remaining protein it was cleaved from and remains anchored to the membrane. The large fragment of EscU (labeled with the HA tag) was also localized to the membrane.

In the strain Walla3 *escR<>escR::HA* the EscR::HA fusion was not detected with Western blot analysis, non specific bands on the gel masked any bands at the correct size for the fusion and at higher stringencies no bands were detected.

EspA filament staining was carried out on all the mutant strains to determine the effect the tag had on the T3SS. All the strains showed no detectable EspA filaments (visualized by fluorescence microscopy). The presence of GFP and the small HA peptide must interfere with the formation of EspA filaments. This result was unexpected and further investigation into the extent of the disruption on the T3SS was carried out and is detailed in Chapter 5.

Chapter 5

The Effect of Tagging Basal Apparatus Proteins on the Type Three Secretion System and Analysis of EscU

5. The Effects of Tagging Basal Apparatus Proteins on the Type Three Secretion System and Analysis of EscU

In Chapter 4 the mutant strains that contain a tagged EscU basal apparatus protein were unable to be visualised by fluorescence microscopy but were localised to bacterial cell fractions by Western blot analysis. This analysis demonstrated that the EscU protein is most likely cleaved into a 10kDa peptide and 30kDa protein at a conserved cleavage site with the amino acid sequence NPTH. Both the 10kDa peptide and the 30kDa protein were independently localised to the membrane fraction of the bacterial cell. The cleavage of the homologous proteins in the flagellar system of *Salmonella* Typhimurium (FlhB) and in the *Yersinia pseudotuberculosis* T3SS (YscU) is thought to be involved in a switching mechanism that controls the timing of secreting needle proteins and secreting filament proteins (Minamino, T., *et al* 2000, Lavander, M., *et al* 2002). To investigate the role of this cleavage in the EscU protein a deletion of the $EscU_{CC}$ domain was made in the Walla3 strain. This strain was added to the repertoire of strains to be studied in order to determine whether a functioning T3SS could be formed. The $EscU_{CC}$ deletion strain allows the elucidation of the role of the $EscU_{CC}$ domain in the construction of a T3SS, the secretion of filament proteins and the secretion of effector proteins.

5.1 Strategy for Creating ZAP633 (Walla3 *escU*<>*escU*$_{\Delta cc}$)

To delete the $EscU_{CC}$ domain in the Walla3 strain the plasmid pJRE10 first had the *ler* gene and the partial LEE1 promoter removed in an identical manner to that of pJRE11, which created the plasmid pJRE20. This increased plasmid yield, making it easier to manipulate (Fig.66). pJRE20 was restriction digested with the REase *Bst*EII (upstream from the NPTH cleavage site) and the REase *Aat*II (the REase site added at the 3' end of the *escU* gene). The digestion removed a 1069bp fragment from the pJRE20 plasmid, between the *Bst*EII restriction site and the 3' end of the *escU* gene. The restricted plasmid was treated with the DNA polymerase I (Klenow) large fragment, and the blunt ends formed were ligated together, which reformed the *Bst*EII site (Fig.65), making the plasmid pJRE21 (Fig.66). The wild type sequence from the *Bst*EII site to the cleavage site was added to the pJRE21 plasmid to create the pJRE22 plasmid. The PCR product was digested with the REase *Bst*EII and the

reaction mixture purified using the QIAquick PCR purification kit (QIAGEN, West Sussex, UK). It was ligated with the pJRE21 plasmid, which had also been digested with *Bst*EII and purified by the QIAquick PCR purification kit (QIAGEN, West Sussex, UK). The pJRE22 plasmid was sent to MWG for sequencing showing that the $EscU_{CC}$ domain successfully deleted up to the NPTH cleavage site, which was replaced by the codons for NPVT-Stop (Fig.65).

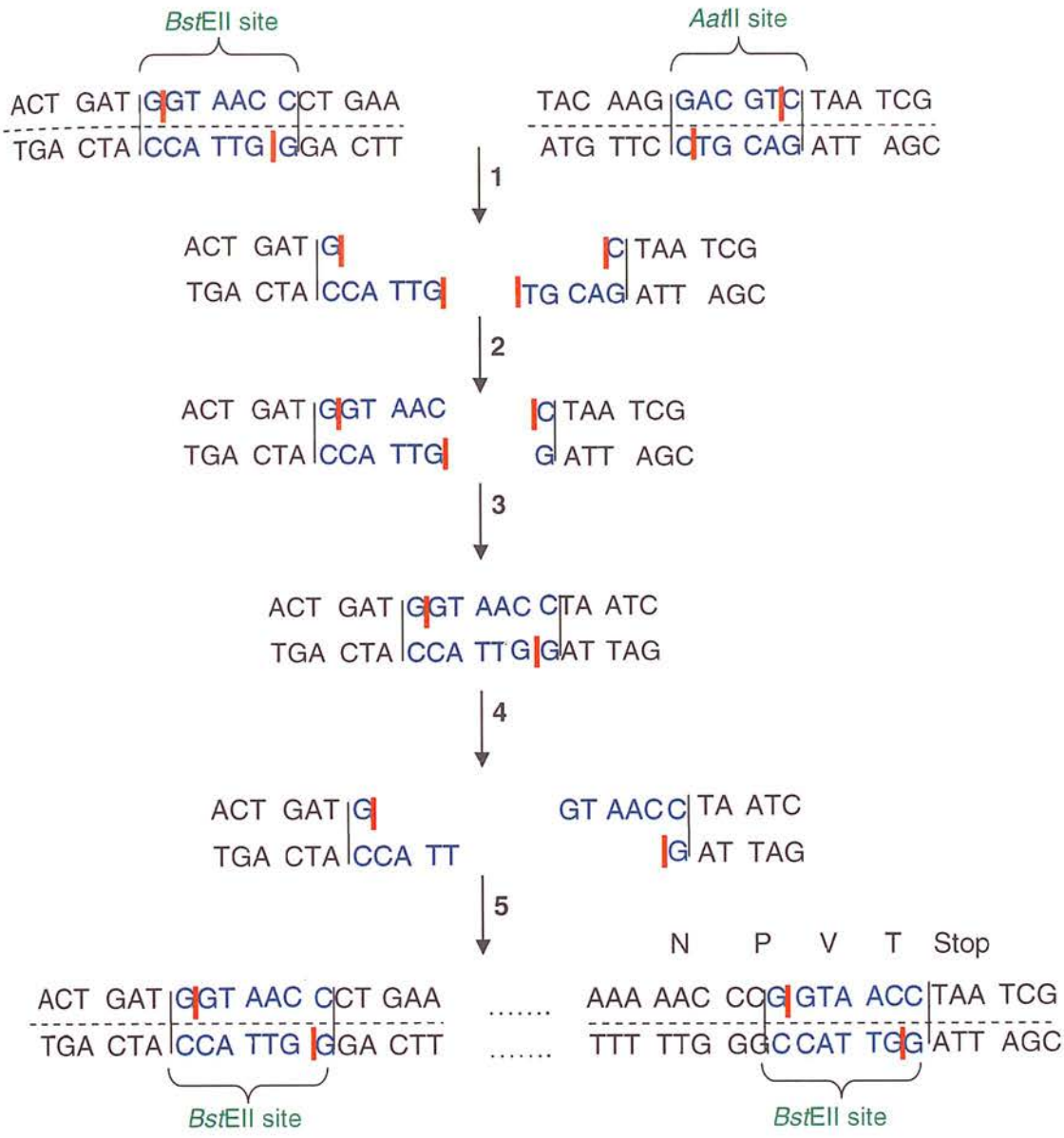

Fig.65 Creating the plasmid pJRE22. 1. pJRE20 was digested by the REase *Bst*EII and AatII. 2. The plasmid was treated with the klenow fragment to form blunt ends. 3. The plasmid was ligated with itself to reform the recognition site for the REase *Bst*EII and make the plasmid pJRE21. 4. The pJRE21 plasmid was digested with *Bst*EII and 5. ligated with the PCR product of the wild type sequence from the *Bst*EII recognition site to the cleavage sequence.

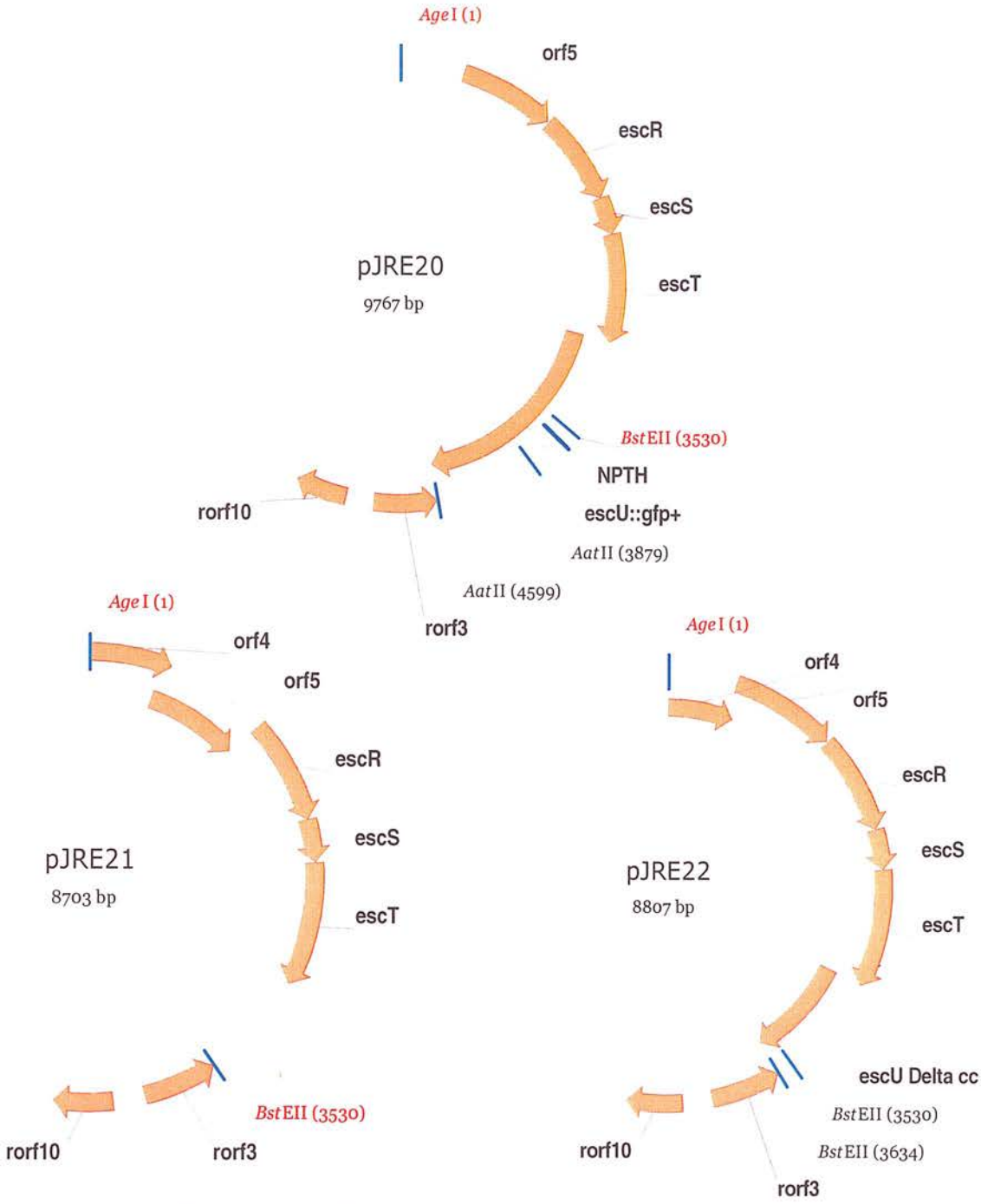

Fig.66 Vector NTI maps of the plasmid pJRE20, the intermediate plasmid pJRE21 and the pJRE22 plasmid containing the deletion *escU*$_{\Delta CC}$.

5.2 Construction of Plasmids pJRE20, pJRE21 and pJRE22

The creation of pJRE21 was confirmed by a diagnostic digestion with the REase *Rsa*I (Fig.67).

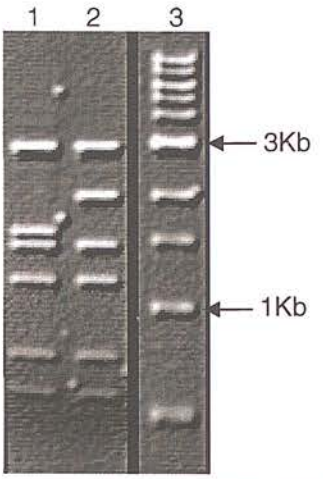

Fig.67 *Rsa*I digest of pJRE20 and pJRE21. The digestion mixture was run a 1% agarose gel with a positive clone for pJRE21 having bands at 2841bp, 1967bp, 1433bp, 1146bp, 713bp, and 538bp.
Lane1: *Rsa*I digest of pJRE20 expected band pattern (bp): 2841, 1700, 1433, 1182, 1146, 713, 538, 149, 39, 26
Lane2: *Rsa*I digest of pJRE21 expected band pattern (bp): 2841, 1967, 1433, 1146, 713, 538, 39, 26
Lane3: 1Kb DNA ladder (Invitrogen, Paisley, UK)

The PCR product from primers 48, 49 was run on an agarose gel (Fig.68).

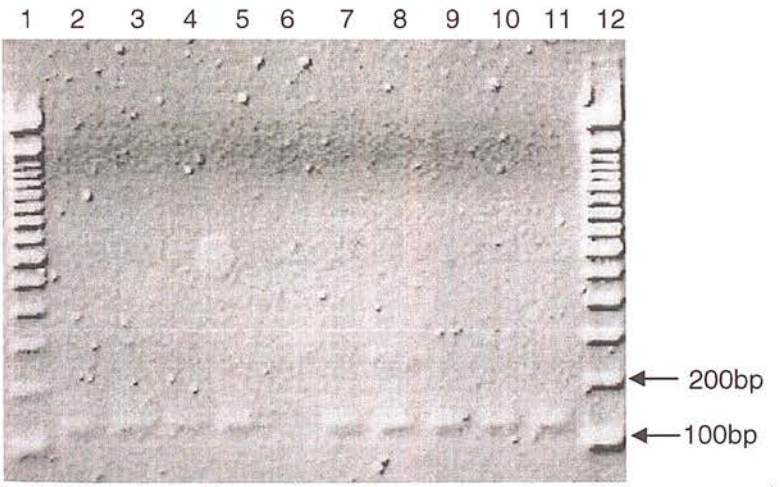

Fig.68 PCR product from primers 48, 49 run on a 1.2% agarose gel.
Lane1 and 12: 100bp DNA ladder
Lane2-11: T_a of PCR increases in one degree increments from 55-65°C

The PCR product from this reaction was purified and digested with the REase *Bst*EII, ligated with the pJRE21 plasmid and transformed into 185 chemically competent cells. Successful transformations had the plasmids extracted by the QIAprep™ spin plasmid miniprep kit (QIAGEN, West Sussex, UK) and were screened for the creation of pJRE22 by diagnostic digestion with the REase *Bst*EII, which removed the added PCR fragment (Fig.69). Four positive clones for the pJRE22 plasmid were sent for sequencing.

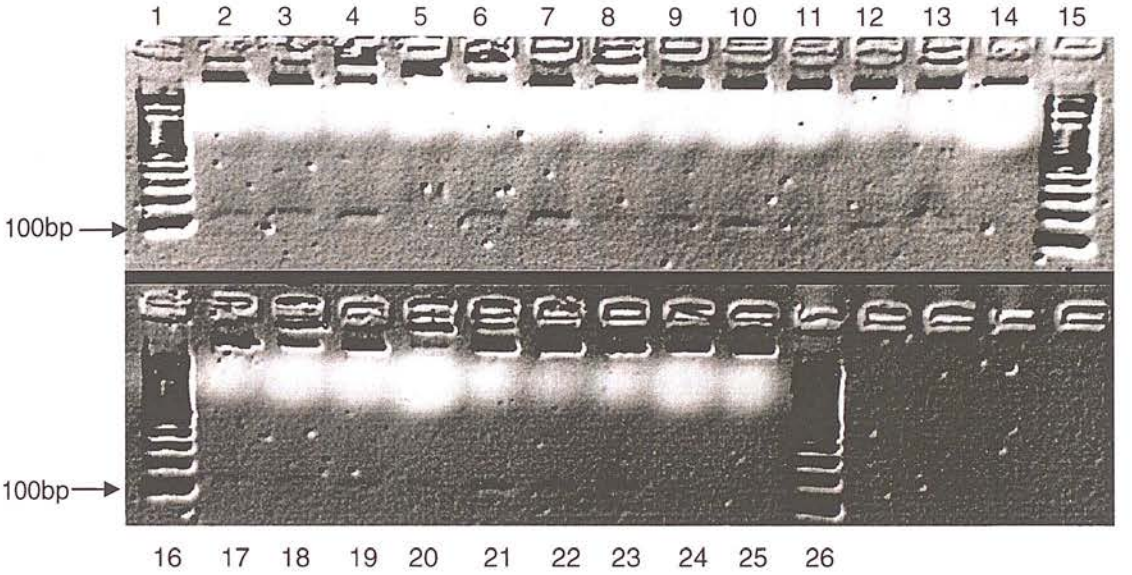

Fig.69 Diagnostic digestion screen with the REase *Bst*EII for positive clones of pJRE22 – run on a 1.2% agarose gel. Lanes3, 6, 18 and 21 were sent for sequencing.
Lane1: 1Kb DNA ladder
Lane2-11: Possible clones of pJRE22
Lane15-16: 1Kb DNA ladder
Lane17-25: Possible clones of pJRE22
Lane26: 1Kb DNA ladder

5.3 Allelic Exchange to Create the Strain Walla3 *escU*<>*escU*$_{\Delta cc}$ (ZAP633)

The pJRE22 plasmid was transformed into the strain Walla3 *escRSTU*<>*sac*/Kan and exchanged onto the chromosome to replace the *sac*/Kan cassette with the *esc* genes on the plasmid, including *escU*$_{\Delta cc}$. The colonies from the allelic exchange were PCR screened for the creation of the strain Walla3 *escU*<>*escU*$_{\Delta cc}$ using primers specific for the *sac*/Kan cassette, the pIB307 plasmid and for the genes *escR*, *escT*, *escS* and *escU*$_{\Delta cc}$ (gels not shown).

5.4 FLUOstar OPTIMA with the Strains Walla3, Walla3 *escRSTU*<>*sac*/Kan (ZAP1140) and Walla3 *escU*<>*escU*$_{\Delta cc}$ (ZAP633) Containing LEE1-5 Promoter Fusions to *egfp*

To determine whether deleting the $EscU_{CC}$ domain had an effect on the expression of LEE1, 2, 3, 4 and 5 and to further investigate the effect of deleting the genes *escRSTU*, plasmids containing promoter regions for the LEE1-5 operons fused to *egfp* (pAJR71-pAJR75) were transformed into the strains Walla3, Walla3 *escRSTU*<>*sac*/Kan and Walla3 *escU*<>*escU*$_{\Delta cc}$. The transformed colonies were grown in 10ml supplemented MEM-HEPES and regular FLUOstar OPTIMA readings taken. The relative fluorescence was plotted against the OD_{600nm} of the culture and the Walla3 strain containing no *egfp* plasmid was used as a negative control (Fig.70, 71, 72, 73, and 74).

The FLUOstar OPTIMA data showed that the expression of LEE2 and LEE3 was almost identical in the strains Walla3 *escRSTU*<>*sac*/Kan (ZAP1140) and Walla3 *escU*<>*escU*$_{\Delta cc}$ (ZAP633) and Walla3. The LEE1, LEE4 and LEE5 promoters fused to *egfp* show that the Walla3 strain has lower values of fluorescence than the two mutant strains. In these cases the relative units of fluorescence of the Walla3 strain had started at a lower value than the ZAP1140 and ZAP633 strain. If the values for the units of fluorescence for the Walla3 strain are increased by the difference measured from the starting fluorescence then the trend lines on the graph overlap one another. The level of fluorescence at the beginning of the experiment was variable and appeared to depend on the fluorescence and expression from the overnight culture. Although the experiments were repeated in a hope to eliminate this variation the initial fluorescence of the cultures could not be standardised. Even after taking this small variation into account it appeared that there was no feedback from either removing the genes *escRSTU* or the *escU*$_{cc}$ domain on the expression from the LEE promoters. It has previously been shown that there is no observed feedback to the LEE after deleting genes for the basal apparatus in *Citrobacter rodentium* TTSS when looking at whole cell detection of Tir and EspB (Deng, W., *et al* 2004).

It was observed earlier in this project that substituting the LEE1 genes *escRSTU* for the *sac*/Kan cassette (Walla3 *escRSTU*<>*sac*/Kan) had no effect on the detectable amount of EspD in the whole cell protein fraction of the mutant compared to the wild type (Fig.23) and no EspD was detected in the supernatant of Walla3 *escRSTU*<>*sac*/Kan. The high levels of EspD detected in the Walla3 supernatant were not observed in the whole cell protein fraction of the Walla3 *escRSTU*<>*sac*/Kan strain i.e. there is no build up of EspD inside the cells of Walla3 *escRSTU*<>*sac*/Kan bacteria due to its inability to be secreted. The promoter fusions show that this feedback is not at the transcriptional level. In the wild type strain it is proposed that the LEE4 mRNA is produced and transported to the TTSS where translation and translocation are coupled (Roe, A., *et al* 2003). When there is no functioning TTSS, as in Walla3 *escRSTU*<>*sac*/Kan, translation would not take place as translocation can not occur. This means the EspD levels inside the cell remain the same as the wild type strain.

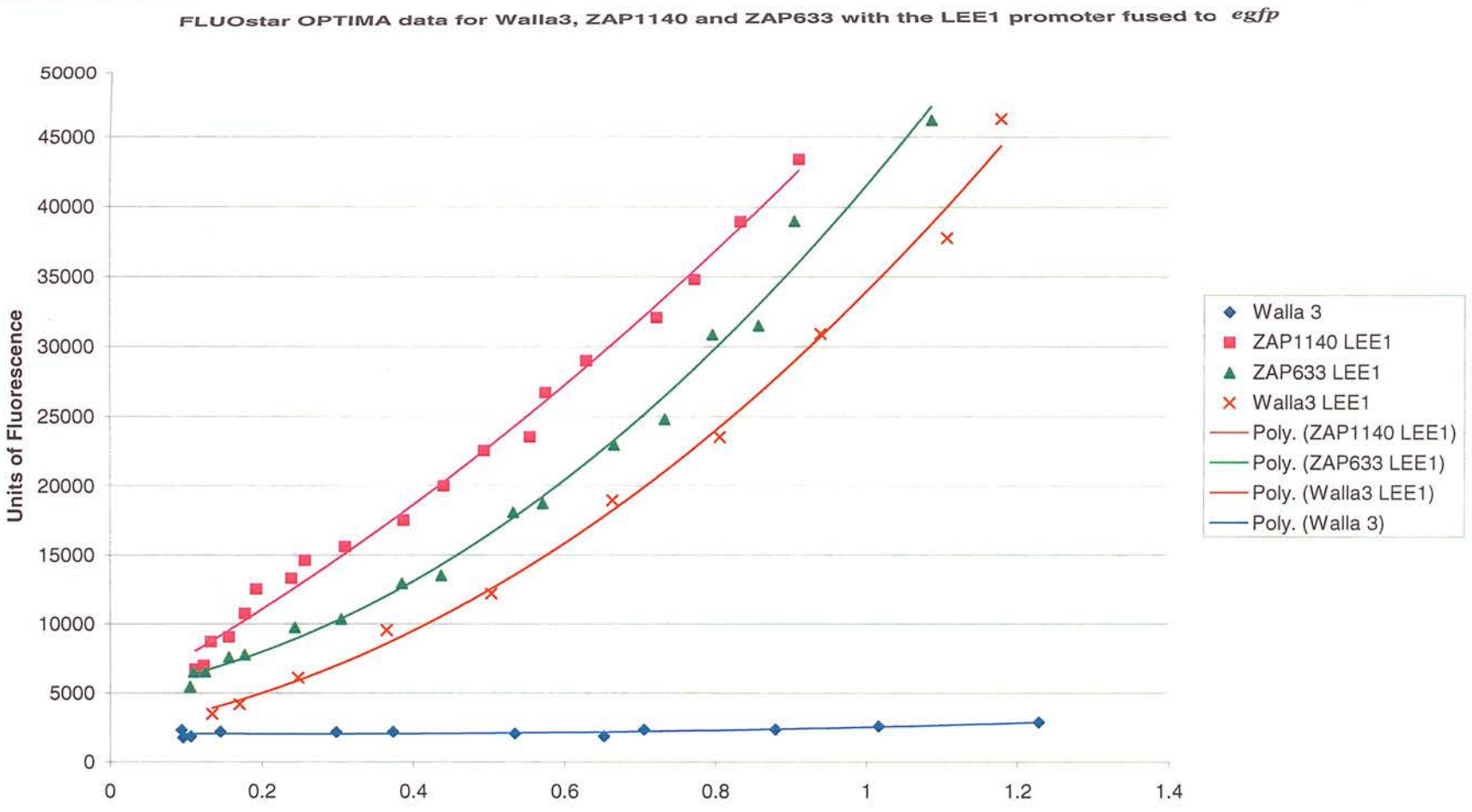

Fig.70 FLUOstar OPTIMA readings for the strains Walla3, Walla3 *escRSTU<>sac*/Kan (ZAP1140) and Walla3 *escU<>escU*$_{\Delta cc}$ (ZAP633) with a pACYC184 based plasmid containing the LEE1 promoter fused to *egfp* (pAJR71).

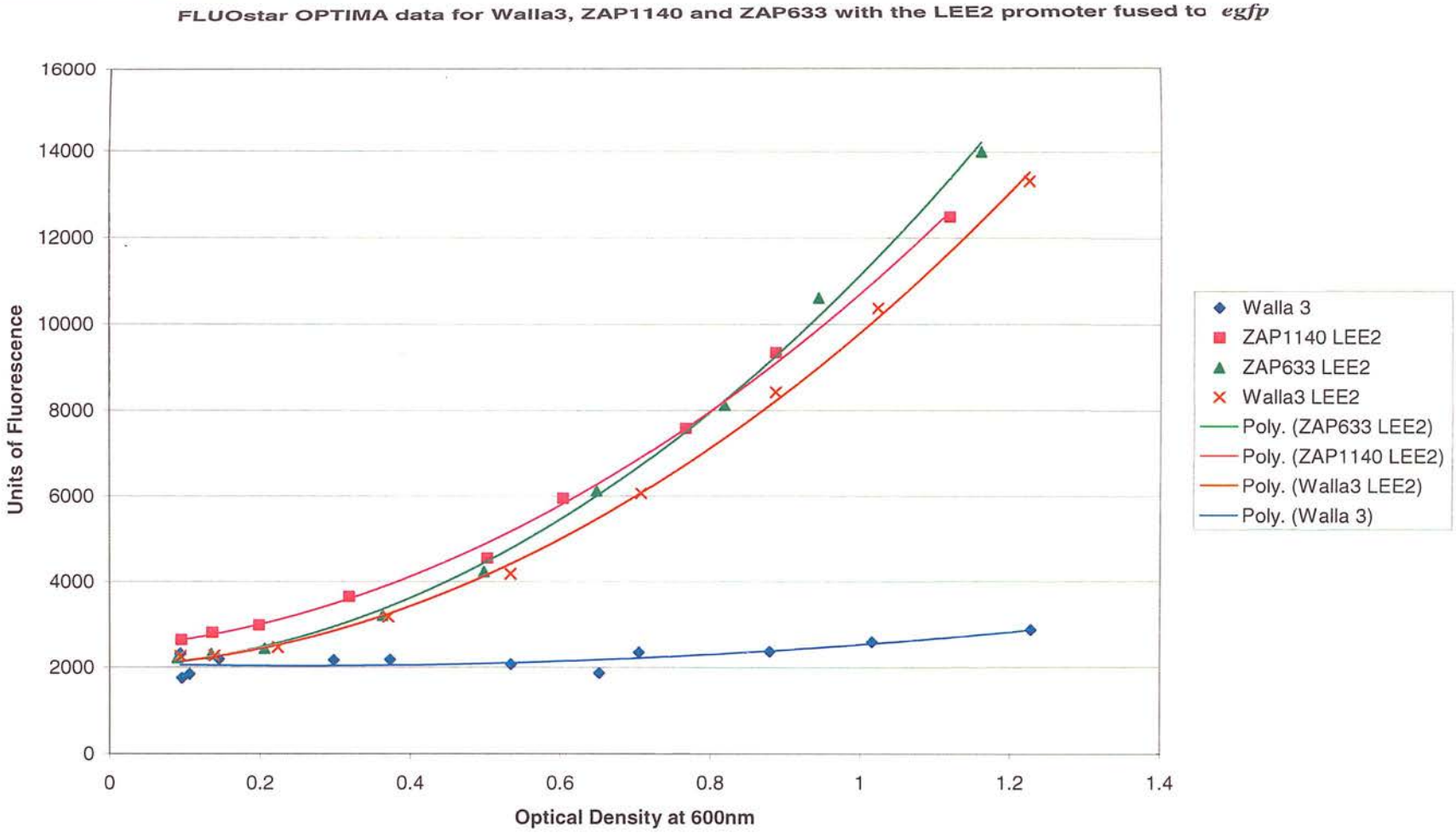

Fig.71 FLUOstar OPTIMA readings for the strains Walla3, Walla3 *escRSTU<>sac*/Kan (ZAP1140) and Walla3 *escU<>escU*$_{\Delta cc}$ (ZAP633) with a pACYC184 based plasmid containing the LEE2 promoter fused to *egfp* (pAJR72).

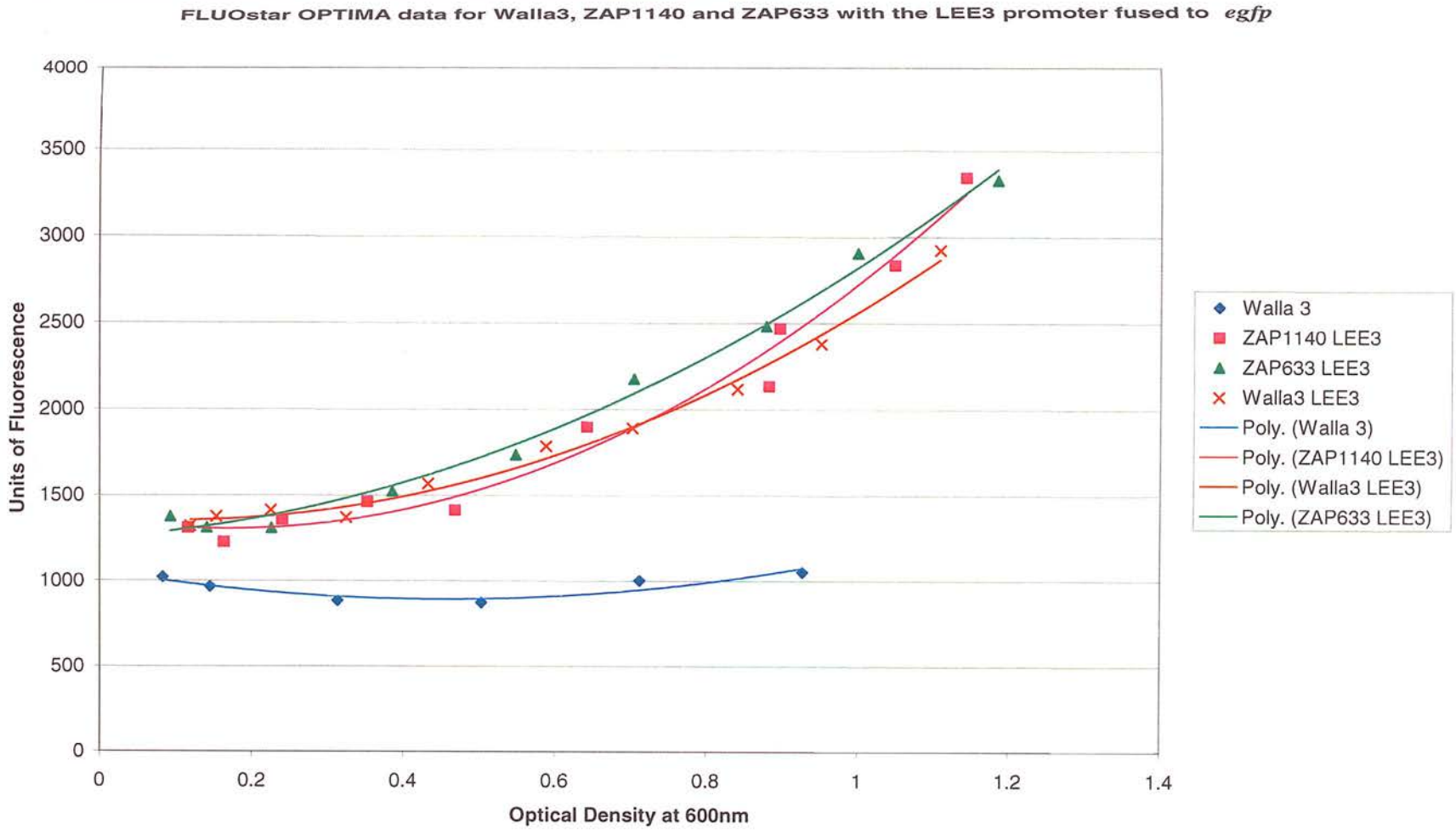

Fig.72 FLUOstar OPTIMA readings for the strains Walla3, Walla3 *escRSTU<>sac*/Kan (ZAP1140) and Walla3 *escU<>escU*$_{\Delta cc}$ (ZAP633) with a pACYC184 based plasmid containing the LEE3 promoter fused to *egfp* (pAJR73).

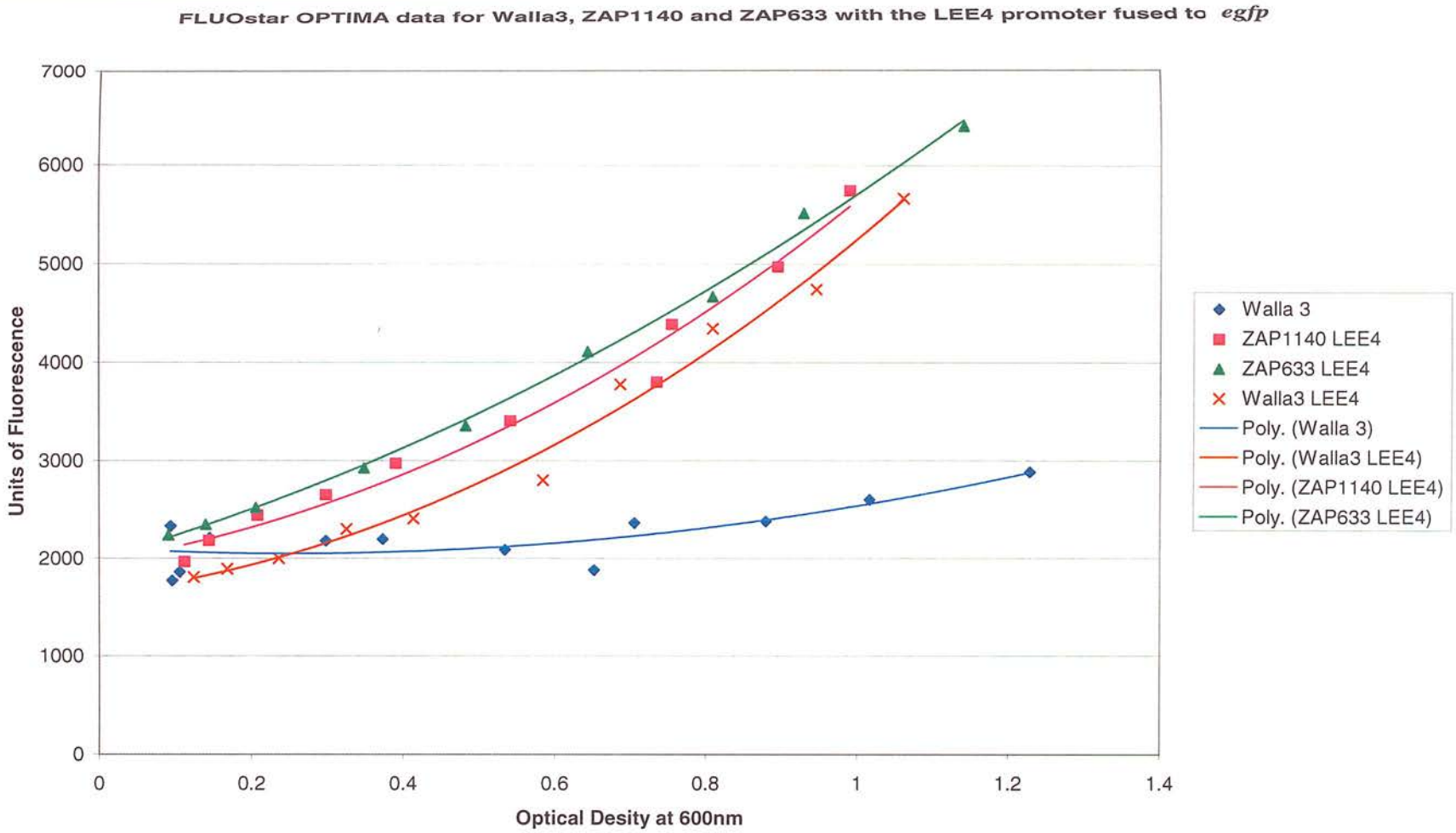

Fig.73 FLUOstar OPTIMA readings for the strains Walla3, Walla3 *escRSTU<>sac*/Kan (ZAP1140) and Walla3 *escU<>escU*$_{\Delta cc}$ (ZAP633) with a pACYC184 based plasmid containing the LEE4 promoter fused to *egfp* (pAJR74).

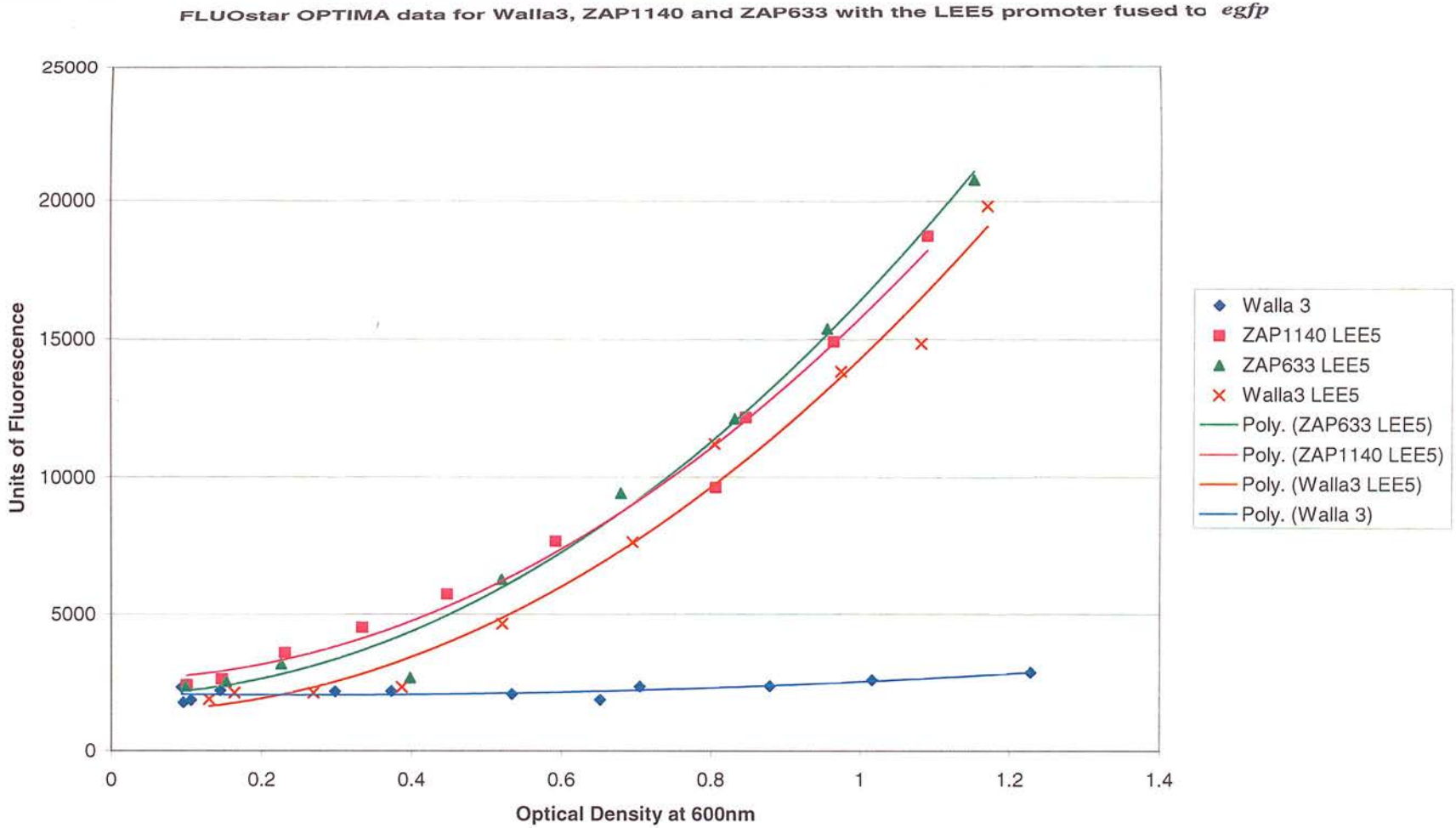

Fig.74 FLUOstar OPTIMA readings for the strains Walla3, Walla3 *escRSTU<>sac*/Kan (ZAP1140) and Walla3 *escU<>escU*$_{\Delta cc}$ (ZAP633) with a pACYC184 based plasmid containing the LEE5 promoter fused to *egfp* (pAJR75).

5.5 Secreted Protein Profiles of the Strains Walla3, Walla3 *escU<>escU*$_{\Delta cc}$ (ZAP633), Walla3 *escU<>escU*$_{cc::egfp}$ (ZAP1141), Walla3 *escU<>escU*$_{cc::gfp+}$ (ZAP1142), Walla3 *escU<>escU*$_{cn::HA}$ (ZAP634) and Walla3 *escR<>escR::HA* (ZAP637)

When looking at the effect of the expression of *grlA* in the strains Walla3, Walla3 *escU<>escU*$_{cc::egfp}$, Walla3 *escU<>escU*$_{cc::gfp+}$ and Walla3 *escU<>escU*$_{cn::gfp+}$ the supernatants were run on a SDS PAGE gel and Coomassie blue stained (gel not shown). This revealed that the strains secreted less protein into the supernatant when compared to the wild type Walla3 strain. To further elucidate the effect of tagging EscU or deleting the EscU$_{CC}$ domain the strains Walla3, Walla3 *escU<>escU*$_{\Delta cc}$, Walla3 *escU<>escU*$_{cc::egfp}$ and Walla3 *escU<>escU*$_{cc::gfp+}$ were screened for their ability to secrete Tir and EspD and their secreted protein profiles were observed by Coomassie blue staining (Fig.75, A). The strains Walla3 *escU<>escU*$_{cn::HA}$ and Walla3 *escR<>escR::HA* were also screened for their ability to secrete EspD and had their secreted proteins Coomassie blue stained (Fig.76, A). The mutant strains ability to secrete EspD or Tir were measured by Western blot analysis using anti EspD mouse monoclonal antibody and anti Tir mouse monoclonal antibody on supernatant protein preparations and compared to the supernatant of the wild type Walla3 strain (Fig.75, B, C and Fig.76, B, C).

The Coomassie blue stained SDS PAGE gels (Fig.75, A and Fig.76, A) show that the mutant strains secrete less proteins compared to the Walla3 strain. In the strains measured for Tir (Fig.75, B) only the wild type Walla3 strain had detectable levels in the supernatant. The secretion of EspD is also effected by the tagging of EscU or deletion of the EscU$_{CC}$ domain. Only the Walla3 strain and the Walla3 *escU<>escU*$_{cc::gfp+}$ strain have detectable amounts of EspD in the supernatant protein fractions. Interestingly the EspD detected in the Walla3 *escU<>escU*$_{cc::gfp+}$ strain is approximately 12 times less than that detected in the Walla3 strain (determined by the ImageJ software, section 2.7.8.1) and may be present due to the cleavage of GFP+ from the EscU$_{CC}$ domain (Fig.75, C). This cleavage may allow some of the EscU$_{CC}$ peptide to function unhindered and account for the small amount of EspD detected. The lack of secretion in the HA tagged strains (ZAP634 and ZAP637) was

interesting as the HA tag is only nine amino acids in length and was chosen as it should have caused the least interference with the function of the protein being tagged.

The strain Walla3 *escU*<>*escU*$_{\Delta cc}$ was also screened by fluorescence microscopy for the presence of EspA filaments and none were visualised (images not shown).

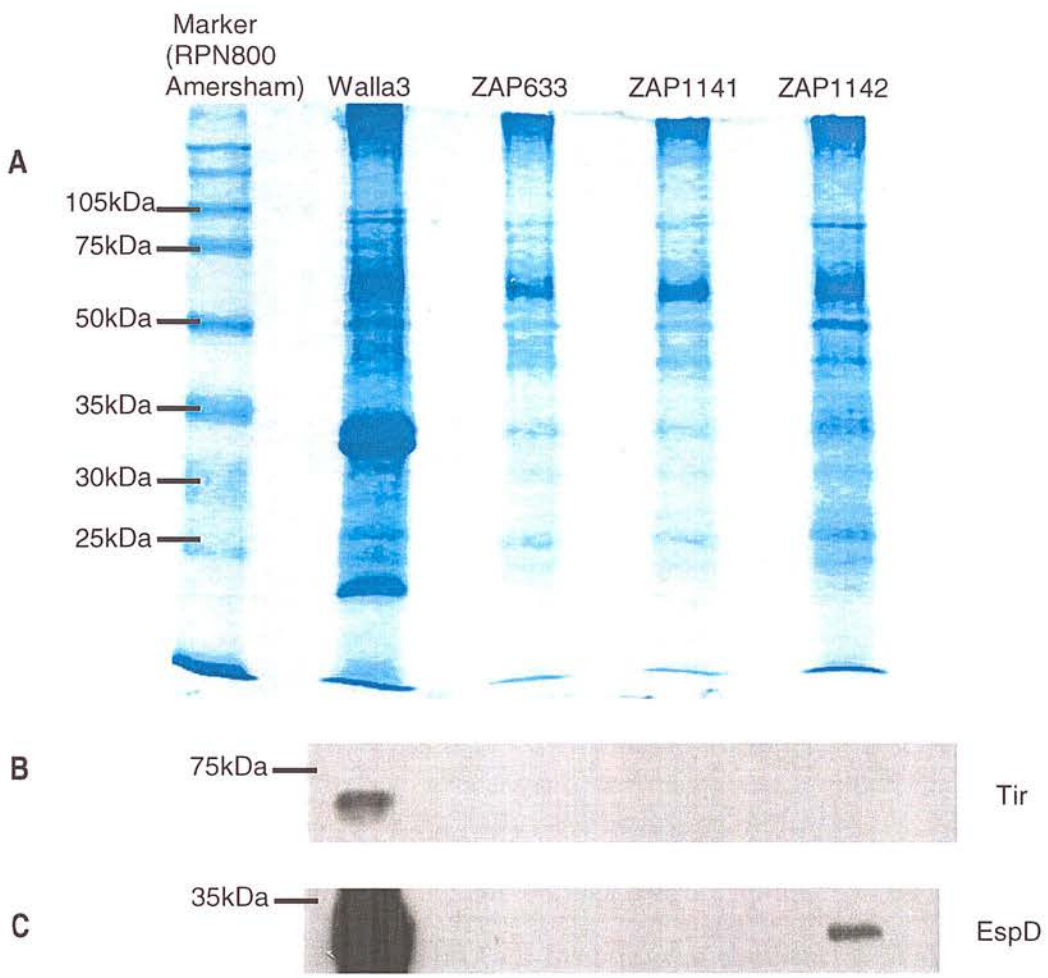

Fig.75 The secretion profiles of Walla3, Walla3 *escU*<>*escU*$_{\Delta cc}$ (ZAP633), Walla3 *escU*<>*escU*$_{cc::egfp}$ (ZAP1141) and Walla3 *escU*<>*escU*$_{cc::gfp+}$ (ZAP1142). A. 12% SDS PAGE gel of supernatants from Walla3, ZAP633, ZAP1141 and ZAP1142 was stained with Coomassie blue. B. Western blot analysis of the same supernatant protein samples with the anti Tir antibody. C. Western blot analysis with the secreted protein samples with the anti EspD antibody

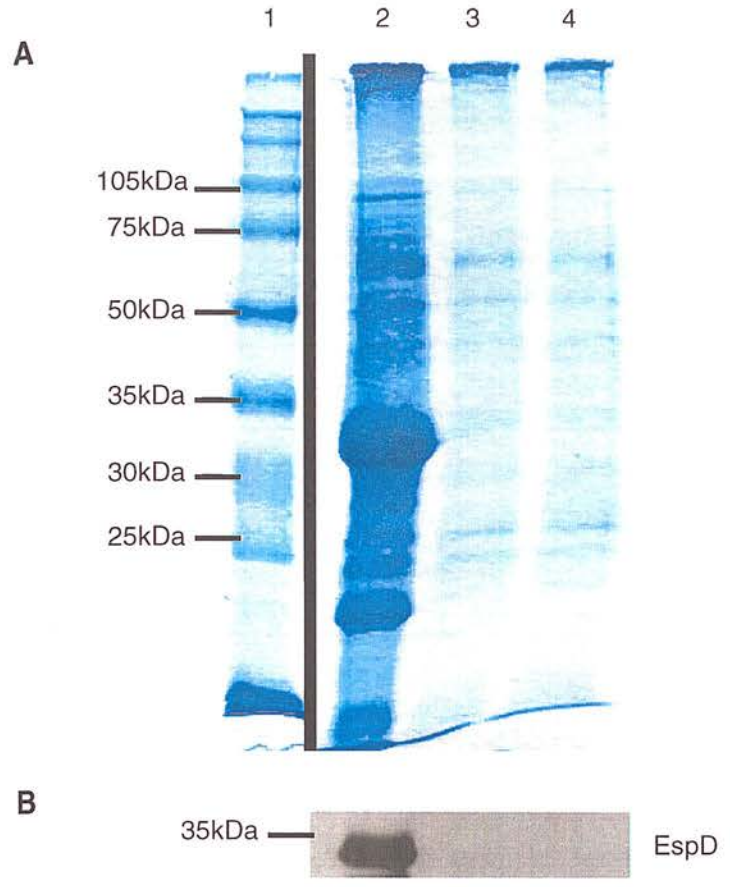

Fig.76 The secretion profiles of Walla3, Walla3 *escU<>escU*$_{cn::HA}$ (ZAP634) and Walla3 *escR<>escR::HA* (ZAP637). A. 12% SDS PAGE gel of secreted proteins from the strains Walla3, ZAP634 and ZAP637 stained with Coomassie blue. B. Western blot analysis of the same secreted protein samples with the anti EspD antibody.
Lane1: Full range rainbow marker RPN800 (Amersham)
Lane2: Walla3
Lane3: ZAP634
Lane4: ZAP637

5.6 Detection of EspD in Bacterial Cell Fractions of the Strains Walla3, Walla3 *escU<>escU*$_{\Delta cc}$ (ZAP633), Walla3 *escU<>escU*$_{cc::egfp}$ (ZAP1141), Walla3 *escU<>escU*$_{cc::gfp+}$ (ZAP1142), Walla3 *escU<>escU*$_{cn::HA}$ (ZAP634), Walla3 *escR<>escR::HA* (ZAP637), Walla3 *escRSTU<>sac*/Kan (ZAP1140) and Walla3 *escU<>escU*$_{cn::gfp+}$ (ZAP635)

Following this analysis the strains Walla3, Walla3 *escU<>escU*$_{\Delta cc}$, Walla3 *escU<>escU*$_{cc::egfp}$, Walla3 *escU<>escU*$_{cc::gfp+}$, Walla3 *escU<>escU*$_{cn::HA}$, Walla3 *escR<>escR::HA*, Walla3 *escRSTU<>sac*/Kan and Walla3 *escU<>escU*$_{cn::gfp+}$ were

screened for the presence of EspD in the supernatant protein fraction, cytoplasmic protein fraction and the membrane protein fraction. Western blot analysis was carried out with anti EspD antibody on the cell fractions (Fig.77). The Walla3 strain shows some EspD detected in the cytoplasmic fraction, 1.9 times more detected in the membrane fraction and at least 1.3 times more detected in the supernatant fraction. All the mutant strains have wild type levels of EspD in the cytoplasmic fraction. The mutant strains then have less EspD detected in the membrane fraction than the Walla3 membrane fraction (Walla3 *escRSTU<>sac*/Kan (ZAP1140) 3.1 times less, Walla3 *escU<>escU*$_{\Delta cc}$ (ZAP633) 15.1 times less, Walla3 *escU<>escU*$_{cc::egfp}$ (ZAP1141) 3.8 times less, Walla3 *escU<>escU*$_{cc::gfp+}$ (ZAP1142) 4.1 times less, Walla3 *escU<>escU*$_{cn::gfp+}$ (ZAP635).3 times less, Walla3 *escU<>escU*$_{cn::HA}$ (ZAP634) 2.4 times less and Walla3 *escR<>escR::HA* (ZAP637) ZAP637 2.4 times less). The amount detected in the membrane of the mutant strains is also an average of 5.1 times less than the amount detected in the mutant strains cytoplasmic fraction. Only two strains have any EspD detected in the supernatant, ZAP1142 and ZAP634. The EspD detected in ZAP634 is most likely signal detected from the cytoplasmic and membrane fractions in the neighbouring SDS PAGE gel wells as the band is faint and undefined. The strain Walla3 *escU<>escU*$_{cc::gfp+}$ (ZAP1142);, however, has already been shown to secrete EspD, although the level of EspD detected is at least 4 times less than that of the wild type strain.

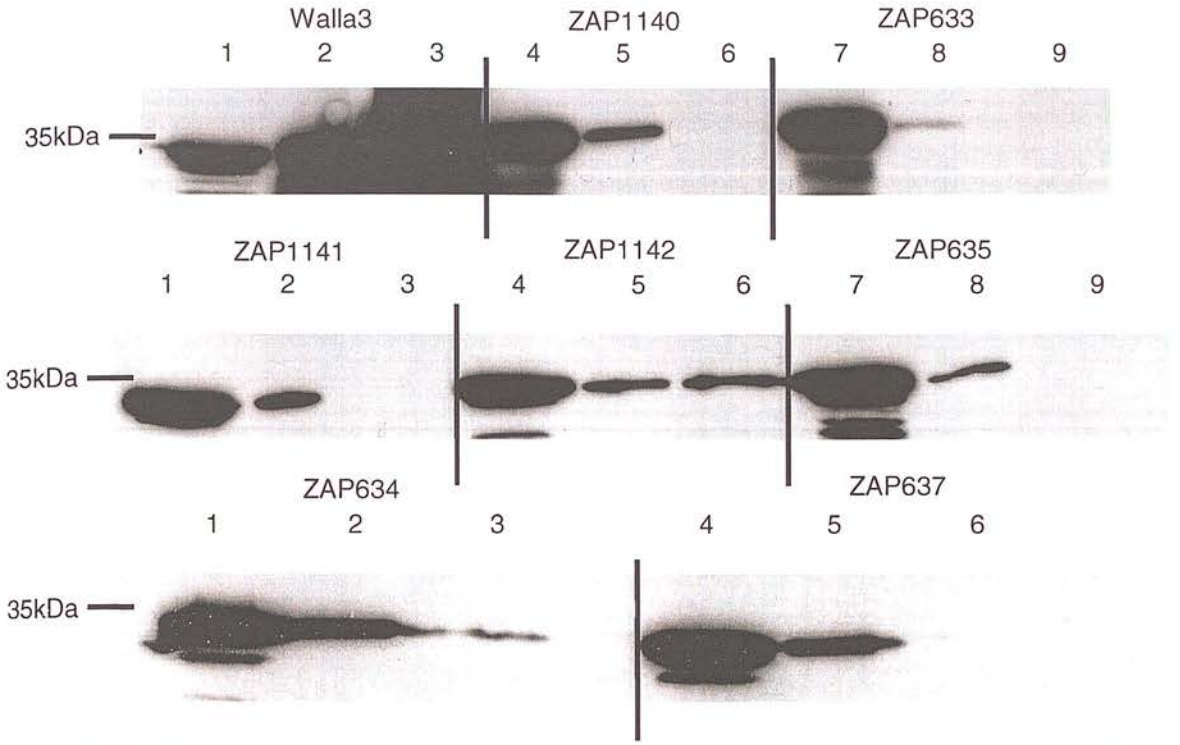

Fig.77 EspD secretion detected by Western blot analysis using 1:2000 dilution of anti EspD antibody after running 12% SDS PAGE gel of cell fractions from the strains Walla3, Walla3 *escU<>escU*$_{\Delta cc}$ (ZAP633), Walla3 *escU<>escU*$_{cc::egfp}$ (ZAP1141), Walla3 *escU<>escU*$_{cc::gfp+}$ (ZAP1142), Walla3 *escU<>escU*$_{cn::HA}$ (ZAP634), Walla3 *escR<>escR::HA* (ZAP637), Walla3 *escRSTU<>sac*/Kan (ZAP1140) and Walla3 *escU<>escU*$_{cn::gfp+}$ (ZAP635). Lane1,4,7: Cytoplasmic fraction. Lane2,5,8: Membrane fractions. Lane3,6,9,: Supernatant fractions.

5.7 Complementation of Strains Walla3 *escU<>escU*$_{\Delta cc}$ (ZAP633), Walla3 *escU<>escU*$_{cc::egfp}$ (ZAP1141), Walla3 *escU<>escU*$_{cc::gfp+}$ (ZAP1142), Walla3 *escU<>escU*$_{cn::HA}$ (ZAP634) and Walla3 *escRSTU<>sac*/Kan (ZAP1140) with the pJRE02 Plasmid

To see whether the reduction of EspD secretion observed with the mutant strains can be attributed to the modifications made in the LEE1 sequence the strains Walla3 *escU<>escU*$_{\Delta cc}$, Walla3 *escU<>escU*$_{cc::egfp}$, Walla3 *escU<>escU*$_{cc::gfp+}$, Walla3 *escU<>escU*$_{cn::HA}$ and Walla3 *escRSTU<>sac*/Kan had the pJRE02 plasmid transformed into them. This was to determine whether this plasmid could complement the mutants and restore EspD secretion. The pJRE02 plasmid contains 6.3Kb of the LEE1 sequence, which includes the LEE1 promoter up to the -10 region. Although expression from this plasmid was not demonstrated colonies of TOP10 cells carrying pJRE02 grew to a smaller colony size and yielded less plasmid

than expected, a phenotype that was reversed when the sequence encoding the *ler* gene and the partial LEE1 promoter was removed (to form pJRE11).

pJRE02 was transformed into the strains and colonies from each transformation were grown in 50ml supplemented MEM-HEPES with ampicillin and secreted protein preparations were made. Western blot analysis was carried out on the samples with anti EspD antibody.

Western blot analysis showed that with the pJRE02 plasmid there was partial complementation in all the strains tested (Fig.78). The Walla3 *escU*<>*escU*$_{cc::gfp+}$ strain did secrete less EspD than previously observed (14.6 times less than the Walla3 strain), however the strains Walla3 *escRSTU*<>*sac*/Kan, Walla3 *escU*<>*escU*$_{\Delta cc}$, Walla3 *escU*<>*escU*$_{cc::egfp}$ and Walla3 *escU*<>*escU*$_{cn::HA}$ all secreted a detectable amount of EspD (1.9, 5.7, 3.1 and 2.7 times less than Walla3 respectively), which had not been detected in previous EspD Western blots. The ability of the strain Walla3 *escRSTU*<>*sac*/Kan to secrete EspD when the pJRE02 plasmid was introduced was encouraging as the strain contains no *escRSTU* and has been fully complemented by allelic exchange with the sequence present on the pJRE02 plasmid. Having only a partial LEE1 promoter on pJRE02 may be the reason the complementation was not to wild type levels. Also strains containing tagged versions of the EscU protein have had the tagged protein localised to the membrane where it may be competing with the EscU produced from the pJRE02 plasmid, causing a decrease in the level of complementation.

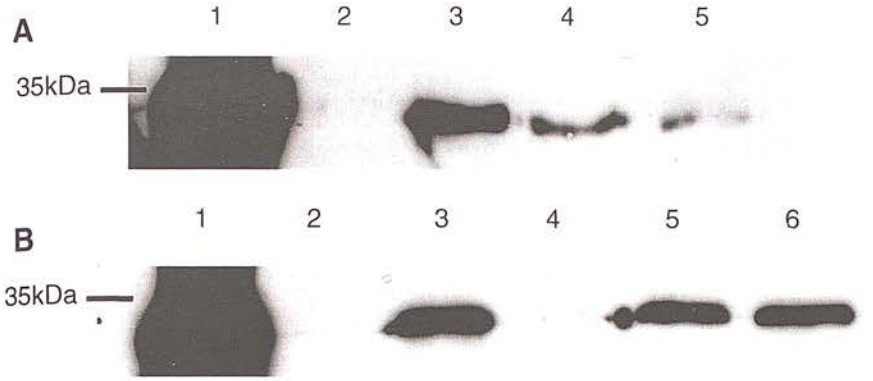

Fig.78 Complementation of strains Walla3 *escU*<>*escU*$_{\Delta cc}$ (ZAP633), Walla3 *escU*<>*escU*$_{cc::egfp}$ (ZAP1141), Walla3 *escU*<>*escU*$_{cc::gfp+}$ (ZAP1142), Walla3 *escU*<>*escU*$_{cn::HA}$ (ZAP634) and Walla3 *escRSTU*<>*sac*/Kan (ZAP1140),, with the pJRE02 plasmid. Western blot analysis carried out with 1:2000 dilution of anti EspD antibody after running the samples on a 12% SDS PAGE gel.
A ·
Lane1: Walla3 supernatant proteins
Lane2: Empty well
Lane3: ZAP1140 supernatant proteins
Lane4: ZAP633 supernatant proteins
Lane5: ZAP1142 supernatant proteins
B:
Lane1: Walla3 supernatant proteins
Lane2: Empty well
Lane3: ZAP1140 supernatant proteins
Lane4: Empty well
Lane5: ZAP634 supernatant proteins
Lane6: ZAP1141 supernatant proteins

5.8 Complementation of Walla3 *escU*<>*escU*$_{\Delta cc}$ (ZAP633) with the EscU$_{CC}$ Peptide

In order to further understand the deletion of the EscU$_{CC}$ domain in the strain Walla3 *escU*<>*escU*$_{\Delta cc}$ a plasmid copy of the domain was used to complement the ability of the strain to secrete EspD. PCR primers were designed to amplify the *escU*$_{cc}$ sequence from the Walla3 strain. One set of primers (50, 51) contained the sequence for the HA tag in the 5' primers non complementary tail which was preceded by the codon for a methionine as the start codon for transcription. The second set of primers (52, 51) contained no HA tag and started with the codon for a methionine (Fig.79). Both pairs of primers were designed to allow the PCR product to be cloned into the plasmid pKC21 using the REases KpnI and HindIII. pKC21 is a pACYC184 based plasmid that contains the pTac promoter, inserting a gene between the KpnI REase recognition site and the HindIII recognition site places the gene in front of the pTac

promoter. Upon the addition of IPTG the pTac promoter is induced and the gene is expressed.

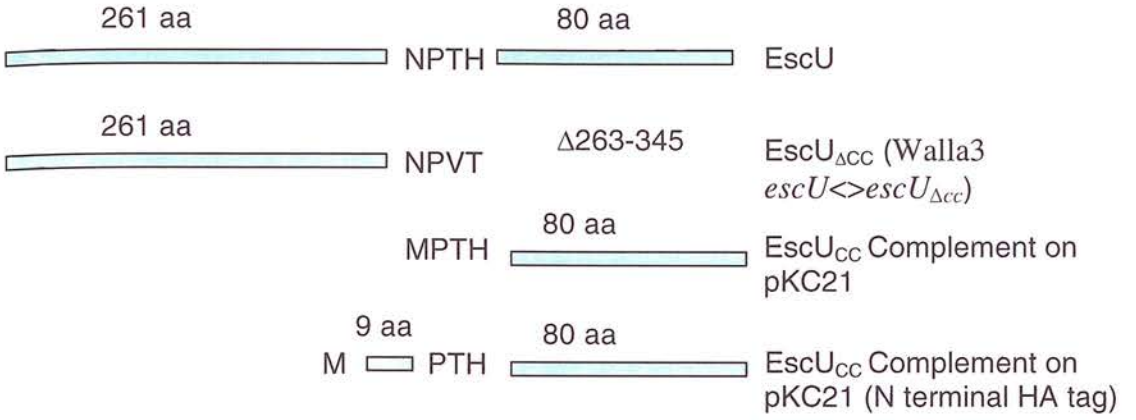

Fig.79 Diagram of the deleted amino acids in the strain Walla3 *escU*<>*escU*$_{\Delta cc}$ (ZAP633) and the two peptides used to complement the strain (M = Methionine, N=Asparagine P=Proline, T=Threonine, H=Histidine, V=Valine).

5.8.1 Creating the Plasmids pJRE23 and pJRE24

The PCR reactions using the primer pairs 50, 51 and 52, 51 were carried out (Fig.80, A and B).

The two PCR products were purified using the QIAquick PCR purification kit (QIAGEN, West Sussex, UK) and restriction digested with the REases *Kpn*I and *Hind*III. The plasmid pKC21 was extracted from the AAEC185 strain by the QIAprep™ spin plasmid miniprep kit (QIAGEN, West Sussex, UK) and also digested by the REases *Kpn*I and *Hind*III. After the restricted plasmid and the digested PCR products were purified from the digestion mixture with the QIAquick PCR purification kit (QIAGEN, West Sussex, UK) the plasmid was ligated separately with each PCR product. The ligation mixtures were transformed into chemically competent AAEC185 cells.

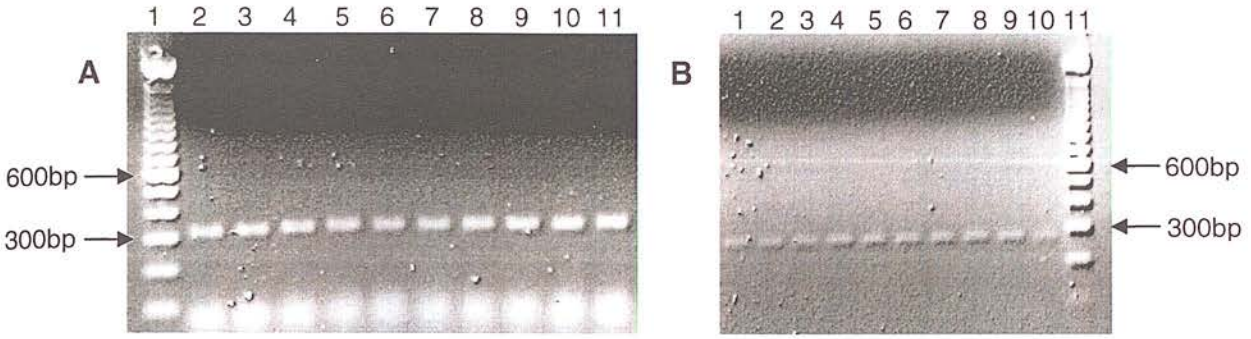

Fig.80 PCR reactions using primer pairs 50, 51 and 52, 51 for cloning into the pKC21 plasmid. Using 1µl of a 1:150 dilution of Walla3 CTAB extracted genomic DNA for template. Both sets of primers annealed at each 1°C temperature increment between 55°C and 65°C to produce a small ~300bp product
A Lane1: 1Kb DNA ladder
Lane2-11: One degree increments in T_a (55-65°C) for PCR with primers 50 and 51 (containing no HA tag sequence)
B Lane1-10: One degree increments in T_a (55-65°C) for PCR with primers 52 and 51 (containing the HA tag sequence in the 5' primer tail)
Lane11: 1Kb DNA ladder

The transformants were screened by removing plasmid DNA with the QIAprep™ spin plasmid miniprep kit (QIAGEN, West Sussex, UK) and diagnostic restriction analysis was carried out with the REases *Kpn*I and *Hind*III. This removed the PCR fragment from successful clones and linearized the pKC21 plasmid (Fig.81).

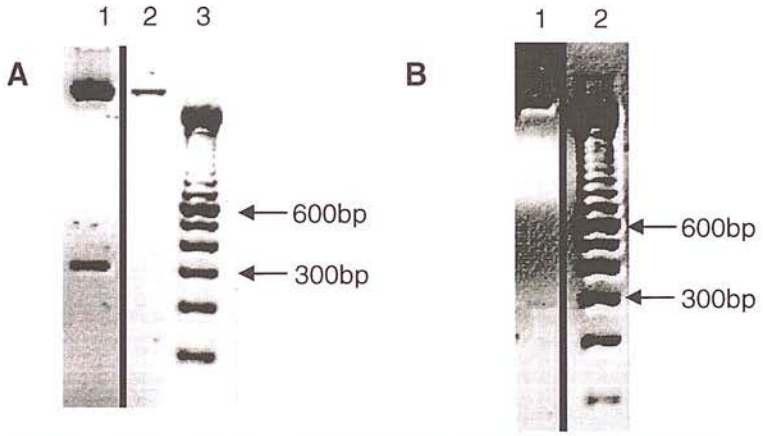

Fig.81 *Kpn*I and *Hind*III REase digestion of pJRE23 and pJRE24 to excise the PCR product - a successful clone for the complement plasmid with the HA tag (A) and for the complement plasmid without the HA tag (B), also included is the parent plasmid pKC21 digested with the same REases (A Lane2)..
A Lane1: pJRE23 digestion
Lane2: pKC21
Lane3: 100bp DNA ladder
B Lane1: pJRE24 digestion
Lane2: 100bp DNA ladder.

Both the clones were sent to MWG for sequencing. Vector NTI maps for each construct are shown in Fig.82.

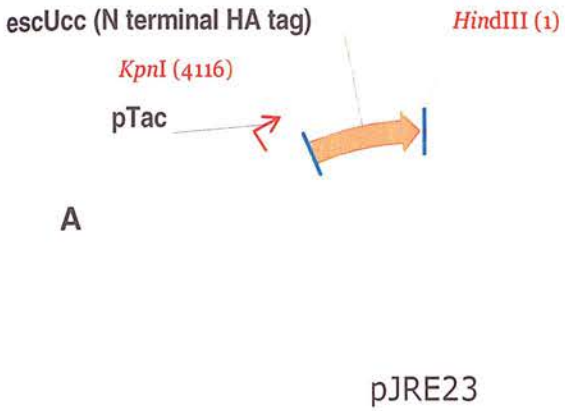

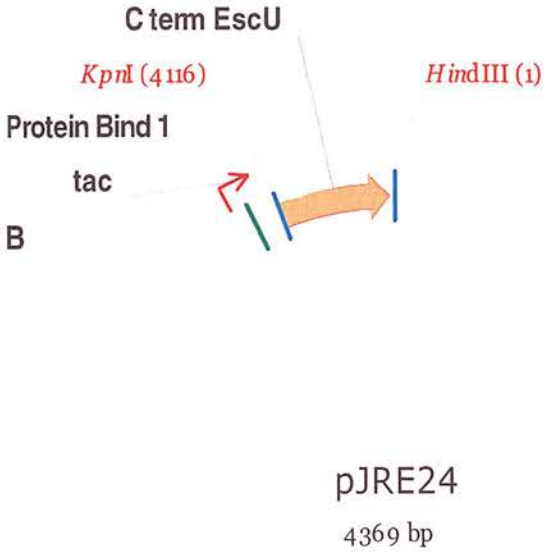

Fig.82, A) Vector NTI map of pJRE23: *escU*$_{cc}$ with a 5' HA tag expressed from the pTac promoter.
B) Vector NTI map of pJRE24: *escU*$_{cc}$ expressed from the pTac promoter.

5.8.2 Western Blot Analysis Detecting $EscU_{CC::HA}$ in the Strain Walla3 *escU<>escU*$_{\Delta cc}$ (ZAP633)

Both pJRE23 and pJRE24 were transformed into the Walla3 *escU<>escU*$_{\Delta cc}$ strain. Initially three 50ml cultures in supplemented MEM-HEPES (with chloramphenicol where appropriate) were set up; one containing Walla3 *escU<>escU*$_{\Delta cc}$ with no plasmid and the remaining two cultures containing ZAP633 with pJRE23. At an OD_{600nm} of 0.1 one of the Walla3 *escU<>escU*$_{\Delta cc}$ cultures with pJRE23 had IPTG added to a final concentration of 1mM to induce expression from the pTac promoter. Whole cell preparations were made from all the cultures and Western blot analysis carried out with anti HA mouse monoclonal antibody (Sigma, Dorset, UK). The Western blot analysis demonstrated that the small $EscU_{CC}$ 10kDa fragment was being produced and detected in the Walla3 *escU<>escU*$_{\Delta c}$ strain (Fig.83).

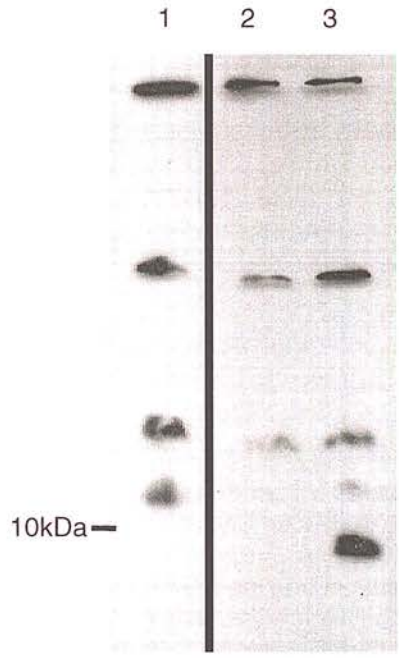

Fig.83 Western blot analysis of the HA peptide fused to the N terminus of $EscU_{CC}$ (from the pJRE23 plasmid). Using 1:1000 dilution of anti HA antibody after using a 18% SDS PAGE gel
Lane1: Walla3 *escU<>escU*$_{\Delta}$ (ZAP633)
Lane2: ZAP633 with pJRE23 (uninduced)
Lane3: ZAP633 with pJRE23 (induced).

5.8.3 Western Blot Analysis Detecting $EscU_{cc::HA}$ in Walla3 *escU<>escU*$_{\Delta cc}$ (ZAP633), Walla3 *escU<>escU*$_{cc::egfp}$ (ZAP1141), Walla3 *escU<>escU*$_{cc::gfp+}$ (ZAP1142), Walla3 *escU<>escU*$_{cn::HA}$ (ZAP634), Walla3 *escRSTU<>sac*/Kan (ZAP1140) and Walla3

The strains Walla3, Walla3 *escU<>escU*$_{\Delta cc}$, Walla3 *escU<>escU*$_{cc::egfp}$, Walla3 *escU<>escU*$_{cc::gfp+}$, Walla3 *escU<>escU*$_{cn::HA}$ and Walla3 *escRSTU<>sac*/Kan were transformed with the pJRE23 plasmid in an identical manner as the Walla3 *escU<>escU*$_{\Delta cc}$ strain. All the strains containing the plasmid and the Walla3 strain without the plasmid were used to prepare cytoplasmic, membrane and supernatant fractions. The fractions were used in Western blot analysis with the anti HA mouse monoclonal antibody (Sigma, Dorset, UK). Fig.84 shows the results for Walla3 with and with out the plasmid and the two strains, Walla3 *escU<>escU*$_{\Delta cc}$ and Walla3 *escRSTU<>sac*/Kan, which produced detectable amounts of the $EscU_{CC::HA}$ peptide.

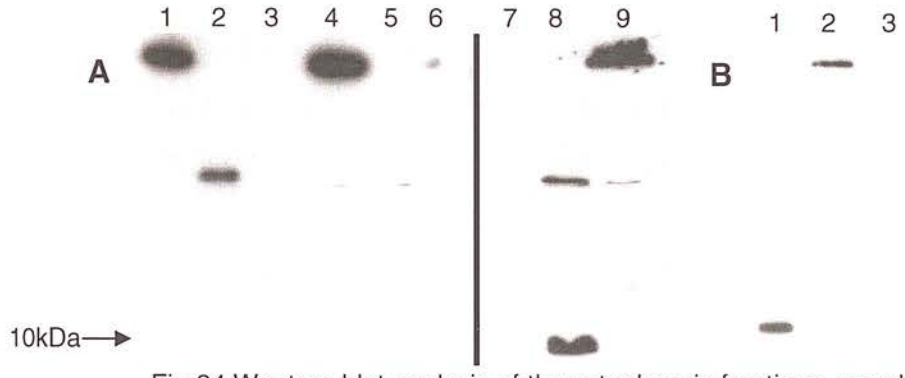

Fig.84 Western blot analysis of the cytoplasmic fractions, membrane fractions and supernatant fractions of the strains Walla3 without pJRE23 and Walla3, Walla3 *escU<>escU*$_{\Delta cc}$ (ZAP633) and Walla3 *escRSTU<>sac*/Kan (ZAP1140) with pJRE23. Samples were run on an 18% SDS PAGE gel and incubated with 1:1000 dilution of anti HA antibody
A Lane1: Walla3 without pJRE23 cytoplasmic fraction
Lane2: Walla3 without pJRE23 membrane fraction
Lane3: Walla3 without pJRE23 supernatant fraction
Lane4: Walla3 with pJRE23 cytoplasmic fraction
Lane5: Walla3 with pJRE23 membrane fraction
Lane6: Walla3 with pJRE23 supernatant fraction
Lane 7: ZAP633 with pJRE23 cytoplasmic fraction
Lane8: ZAP633 with pJRE23 membrane fraction
Lane9: ZAP633 with pJRE23 supernatant fraction
B Lane1: ZAP1140 with pJRE23 membrane fraction
Lane2: ZAP1140 with pJRE23 cytoplasmic fraction
Lane3: ZAP1140 with pJRE23 supernatant fraction.

The results in Fig.84 show the $EscU_{CC}$ peptide was only detected in the strains Walla3 *escRSTU<>sac*/Kan and Walla3 *escU<>escU*$_{\Delta cc}$. Interestingly, in both strains the peptide is localised to the membrane fraction of the bacteria. This is intriguing as the Walla3 *escRSTU<>sac*/Kan strain does not contain the genes *escRSTU* so the $EscU_{CC}$ peptide is not being anchored to the membrane by interacting with the $EscU_{CN}$ domain in this strain.

5.8.4 Western Blot Analysis Detecting EspD Secretion with pJRE23 and pJRE24 Complement Plasmids in the Walla3 *escU<>escU*$_{\Delta cc}$ (ZAP633) Strain

The ZAP633 strain was used to see if the EspD secretion was restored by the presence of $EscU_{CC}$. The supernatant fractions from the preparations when $EscU_{CC::HA}$ was detected in the membrane of ZAP633 had Western blot analysis carried out using anti EspD mouse monoclonal antibody (Fig.85). A supernatant fraction from the strain Walla3 *escU<>escU*$_{\Delta cc}$ (ZAP633) transformed with the pJRE24 plasmid, grown and prepared at the same time and in an identical manner to the induced pJRE23 plasmid was also used (Fig.85). The samples from Walla3 *escU<>escU*$_{\Delta cc}$ with pJRE24 were screened for their ability to restore EspD secretion in case the HA tag disrupted the function of the $EscU_{CC}$ peptide.

Fig.85 shows that the production of the HA tagged $EscU_{CC}$ peptide does not restore secretion of EspD to wild type levels and if the $EscU_{CC}$ untagged protein is being produced, this also does not restore secretion. Empty wells in this Western blot (Fig.85, Lane2 and Lane4) contain signal from the detection of EspD from the Walla3 strain. Upon repeating the Western blot this artefact was observed again and is most likely due to the wells on the SDS PAGE gel leaking. In each repeat of this Western the final lane, containing the secreted proteins of the Walla3 *escU<>escU*$_{\Delta cc}$ strain with the induced pJRE24 plasmid, did have a small amount of detectable EspD that was not from the well containing the Walla3 sample. The presence of the $EscU_{CC}$ domain by itself is not enough to restore EspD secretion to a wild type level.

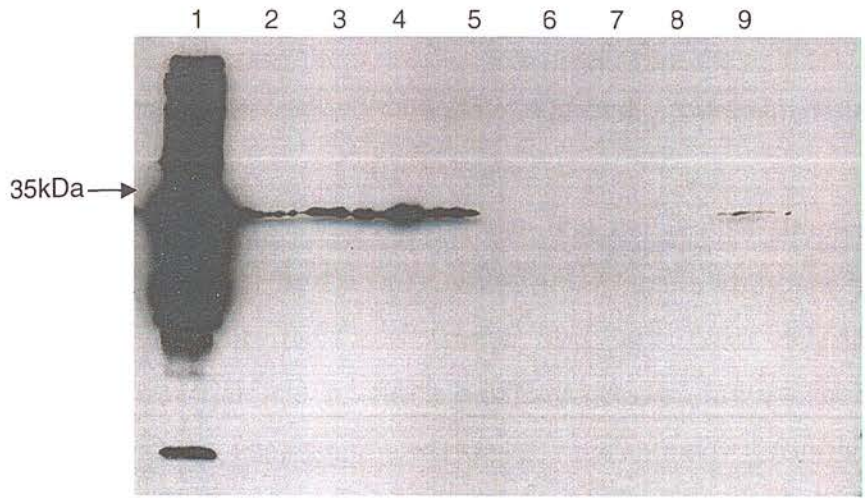

Fig.85 EspD secretion from the Walla3 and Walla3 *escU<>escU*$_{\Delta cc}$ (ZAP633), strains with and without pJRE23 and pJRE24 (induced and uninduced). 12% SDS PAGE gel used, with 1:2000 dilution of anti EspD antibody
Lane1: Walla3 supernatant protein
Lane2: Empty well
Lane3: ZAP633 supernatant protein
Lane4: Empty well
Lane5: ZAP633 with pJRE24 (uninduced) supernatant protein
Lane6: ZAP633 with pJRE23 (uninduced) supernatant protein
Lane7: Empty well
Lane8: ZAP633 with pJRE24 (induced) supernatant protein
Lane9: ZAP633 with pJRE23 (induced) supernatant protein

Attempts to clone the whole of *escU* into the pKC21 plasmid, the pWSK29 plasmid (Wang, R. *et al* 1991) or into the tetracycline gene of the pBR322 plasmid (NEB, Hertfordshire, UK) failed. This may have been due to toxicity problems.

5.9 Anti EscJ Antibody: Western Blot Analysis

Anti EscJ and anti EscF antibodies were kindly supplied by Professor Akio Abe from Kitasato University, Tokyo, Japan. The antibodies were used on strains containing EscU mutants to determine whether EscJ and EscF were located in the correct location (i.e. the membrane fraction of the cell). The location of EscF and EscJ in the mutant strains indicates whether the mutants are capable of forming a T3SS basal apparatus, as EscF and EscJ insertion into the membrane requires other basal apparatus proteins to be present (Gauthier, A., *et al* 2003b). In essence, they provide evidence that the formation of the basal apparatus is not being hindered due to the mutations in EscU. The anti EscJ antibody was checked for specificity using membrane preparations from the strains Walla3, ZAP193Δ*escN*, 148a and Walla3

escRSTU<>sac/Kan (ZAP1140). The strains were grown in supplemented MEM-HEPES and membrane preparations were made from the cultures. The samples were used in Western blot analysis with anti EscJ rabbit polyclonal antibody (Fig.86).

The EscJ Western blot (Fig.86) showed that the Walla3 strain had a band at the correct size for EscJ as did the ZAP193Δ*escN* strain whilst the 148a strain (which does not contain the *escJ* gene) had no EscJ detected. The Walla3 *escRSTU<>sac*/Kan had 1.6 times less EscJ detected in the membrane compared to the Walla3 strain. The results seem to verify the antibody is for EscJ and indicate that the ATPase EscN might be required for wild type levels of EscJ, whilst the basal apparatus proteins EscR, S, T and U do not need to be present for EscJ to be localised to the membrane

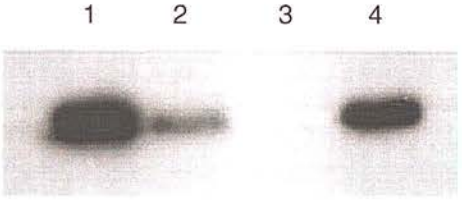

Fig.86 1:1000 dilution of anti EscJ antibody used in Western blot analysis of membrane preparations from the strains Walla3, ZAP193Δ*escN*, 148a and Walla3 *escRSTU<>sac*/Kan (ZAP1140) run on a 12% SDS PAGE gel.
Lane1: Walla3 membrane preparation
Lane2: ZAP193Δ*escN* membrane preparation
Lane3: 148a membrane preparation
Lane4: ZAP1140 membrane preparation

The anti EscJ antibody was used with cytoplasmic, membrane and secreted protein fractions of all the strains to see whether EscJ can be detected. All the strains were grown in 50ml supplemented MEM-HEPES. Membrane, cytoplasmic and secreted protein fractions were prepared and Western blot analysis carried out with anti EscJ antibody (Fig.87)

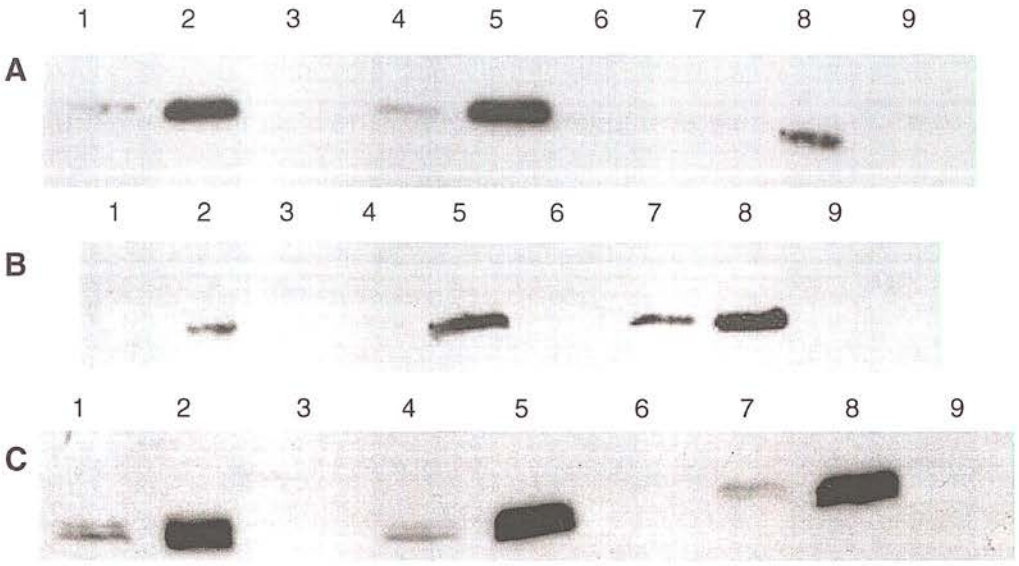

Fig.87 Western blot analysis on the cytoplasmic, membrane and secreted protein fractions of Walla3, Walla3 *escU<>escU*$_{\Delta cc}$ (ZAP633), Walla3 *escU<>escU*$_{cc::egfp}$ (ZAP1141), Walla3 *escU<>escU*$_{cc::gfp+}$ (ZAP1142), Walla3 *escU<>escU*$_{cn::HA}$ (ZAP634), Walla3 *escRSTU<>sac*/Kan (ZAP1140), Walla3 escU<>escU$_{cn::gfp+}$ (ZAP635) and Walla3 escR<>escR::HA (ZAP637) using 1:1000 dilution of the anti EscJ antibody. Lanes1, 4 and 7 are cytoplasmic fractions, Lanes2, 5 and 8 are membrane fractions and Lanes3, 6 and 9 are supernatant fractions.
A Lanes1-3: Walla3
Lanes4-6: ZAP633
Lanes7-9: Zap1140
B Lanes1-3: ZAP1142
Lanes4-6: ZAP1141
Lanes7-9: ZAP635
C Lanes1-3: Walla3
Lanes4-6: ZAP634
Lanes7-9: ZAP637

Western blot analysis (Fig.87) showed that EscJ was detected in the membrane fraction of all eight strains, and detected in the cytoplasmic fractions of six strains. The amount of EscJ detected in the membrane fractions was variable, with less being detected in the strains Walla3 *escRSTU<>sac*/Kan (2.1 times), Walla3 *escU<>escU*$_{cc::gfp+}$ (3.5 times) and Walla3 *escU<>escU*$_{cc::egfp}$ (1.2 times) when compared to the Walla3 strain. In the Walla3 strain there is at least 10 times more EscJ detected in the membrane preparation than the cytoplasmic preparation, this ratio of the amount of EscJ detected in the membrane fraction compared to the cytoplasmic fraction remains fairly constant in all the strains.

All the Western blots containing membrane and cytoplasmic fractions were verified by Western blot analysis with both anti GroEL and anti OmpA antibodies. The results for all the gels (not shown) show a bias of OmpA in the membrane fraction and a bias of GroEL to the cytoplasmic fraction.

5.9.1 Anti EscJ Antibody: Fluorescence Microscopy

The antibody was used for fluorescence microscopy to detect EscJ in the bacterial membrane/periplasm. The Walla3 strain (positive control) was used alongside the 148a strain (negative control) to test whether the antibody was effective at labelling bacteria for fluorescence microscopy. Microscopy slides were made using the methanol fixation/permeabilistaion method. The slides were incubated with a 1:25 dilution of the anti EscJ antibody then incubated with the secondary antibody goat Alexa Fluor 488 conjugate to anti-rabbit IgG. Examples of the microscopy are shown in Fig.88 and Fig.89.

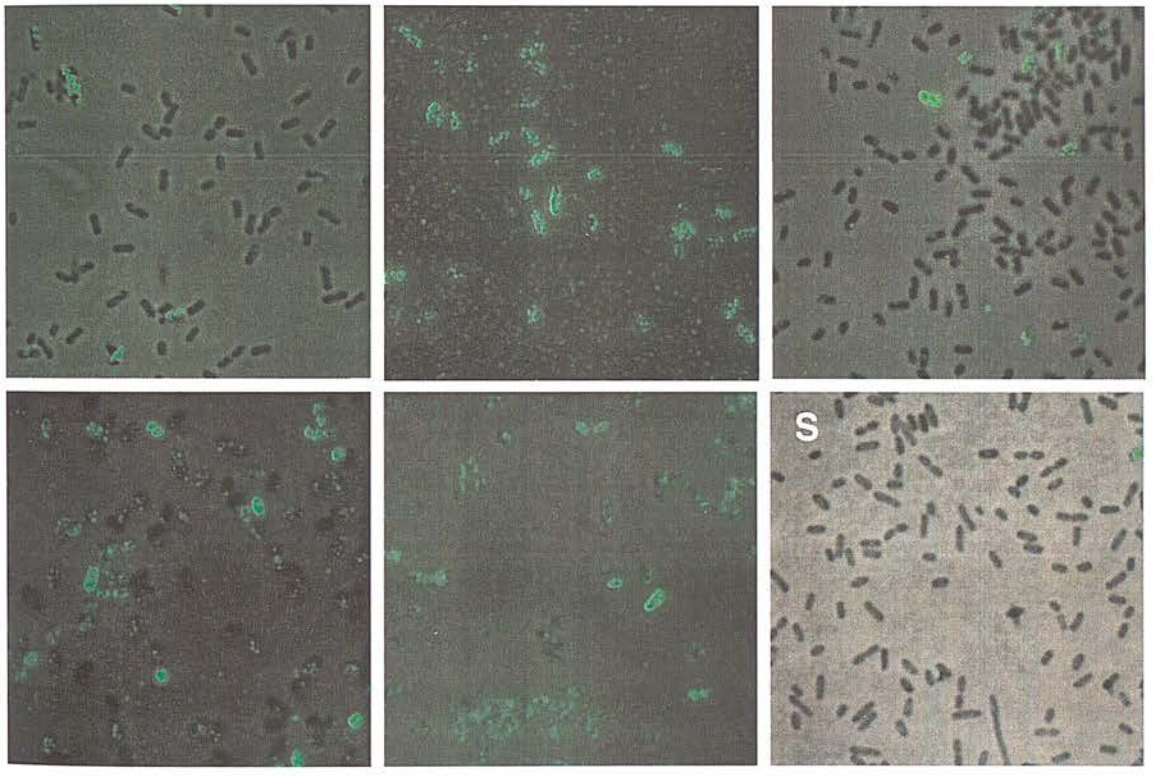

Fig.88 Microscopy with the anti EscJ antibody labelling the Walla3 strain. The slides were visualised using a DM LB2 microscope (Leica, Milton Keynes, UK) with a 100X objective lens and an exposure time of 500ms. The panel 'S' contains bacteria visualised after incubation with only the secondary antibody.

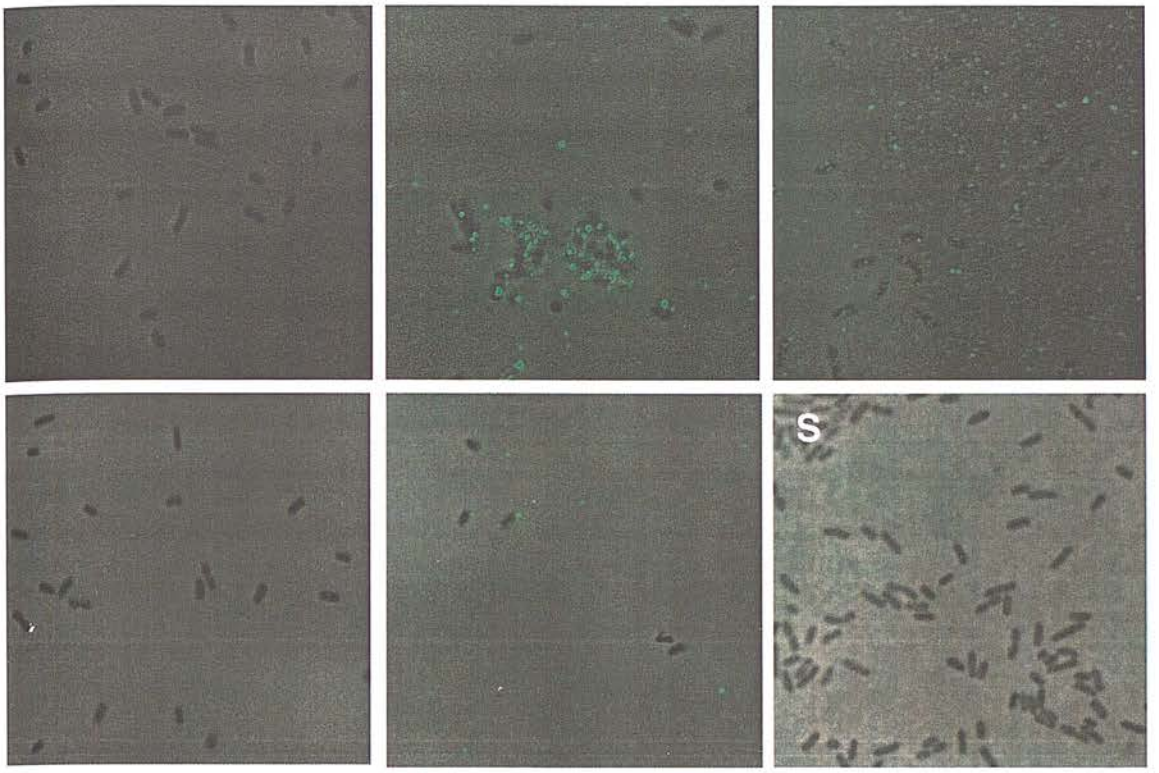

Fig.89 Microscopy with the anti EscJ antibody labelling the 148a strain. The slides were visualised using a DM LB2 microscope (Leica, Milton Keynes, UK) with a 100X objective lens and an exposure time of 500ms. The panel 'S' contains bacteria visualised after incubation with only the secondary antibody.

Microscopy with the anti EscJ antibody gave varying images. Although grown in an identical manner the images for the Walla3 strain did not repeat. The number of fluorescent bacteria and the nature of the fluorescence were not constant; occasionally the fluorescence was in fine focused spots and other times it appeared more dispersed. In the 148a the majority of the repeats showed images with no staining, but some microscopy slides showed fluorescence with groups of bacteria having fluorescent foci.

The results led to the conclusion that the antibody, although good for Western blot analysis, was not suited for labelling strains for fluorescence microscopy.

5.10 Anti EscF Antibody: Western Blot Analysis

The anti EscF antibody was first screened using membrane preparations of Walla3, ZAP193Δ*escN* and Walla3 *escRSTU<>sac*/Kan (ZAP1140). These preparations were used for Western blots where they were incubated with anti EscF antibody (Fig.90).

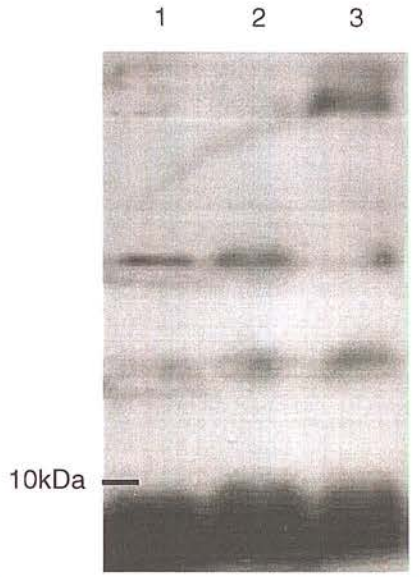

Fig.90 Western blot analysis using 1:1000 dilution of the anti EscF antibody on membrane preparations from the strains Walla3, ZAP198Δ*escN* Walla3 *escRSTU<>sac*/Kan (ZAP1140), after samples were run on an 18% SDS PAGE gel.
Lane1: Walla3 membrane preparation
Lane2: ZAP198Δ*escN* membrane preparation
Lane3: ZAP1140 membrane preparation

Western blot analysis detected three main bands when using the anti EscF antibody on membrane preparations. The most intense band was between the 10kDa marker and the dye front of the SDS PAGE gel, a promising candidate for the 8kDa EscF monomer. The other two bands may have been dimers and trimers of the EscF protein. This result indicated that EscF could be detected in large amounts in the membrane fraction of the three strains screened. Due to filament shearing EscF may have been detectable in the supernatants of the strains. Supernatant protein preparations were easier to prepare and contain fewer proteins for cross reactivity, so supernatant proteins of the *escU* mutant strains and the Walla3 strain were screened by Western blot analysis for EscF. The strains Walla3, Walla3 *escU<>escU*$_{\Delta cc}$, Walla3 *escU<>escU*$_{cc::egfp}$, Walla3 *escU<>escU*$_{cc::gfp+}$, Walla3 *escU<>escU*$_{cn::HA}$, Walla3 *escRSTU<>sac*/Kan and Walla3 escU<>escU$_{cn::gfp+}$, were grown in 50ml supplemented MEM-HEPES and supernatant preparations were made and run on a 10-20% gradient gel (Bio-rad, Hertfordshire, UK). These gels were used in the Western blot procedure with the anti EscF antibody in high stringency conditions (Fig.91)

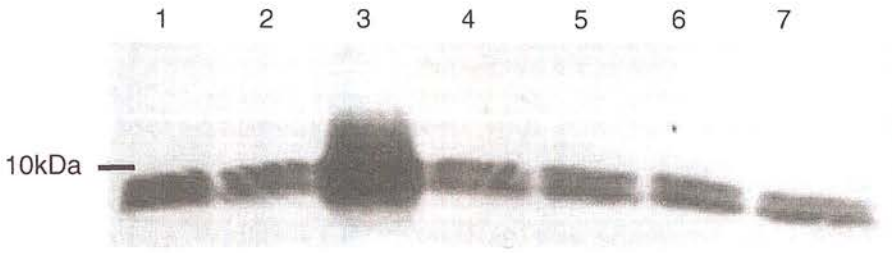

Fig.91 Western blot analysis with the anti EscF antibody on supernatant proteins from Walla3, Walla3 *escU<>escU*$_{\Delta cc}$ (ZAP633), Walla3 *escU<>escU*$_{cc::egfp}$ (ZAP1141), Walla3 *escU<>escU*$_{cc::gfp+}$ (ZAP1142), Walla3 *escU<>escU*$_{cn::HA}$ (ZAP634), Walla3 *escRSTU<>sac*/Kan (ZAP1140) and Walla3 escU<>escU$_{cn::gfp+}$ (ZAP635)
Lane1: Walla3 supernatant proteins
Lane2: ZAP1141 supernatant proteins
Lane3: ZAP1142 supernatant proteins
Lane4: ZAP635 supernatant proteins
Lane5: ZAP634 supernatant proteins
Lane6: ZAP633 supernatant proteins
Lane7: ZAP1140 supernatant proteins

Western blot analysis of the supernatant proteins showed that the anti EscF antibody was detecting a double band below the 10kDa marker. This could be two forms of EscF, one form modified to increase the molecular mass or one form cleaved to decrease it. The Western blot also shows a large increase in the amount of EscF detected in the Walla3 *escU<>escU*$_{cc::gfp+}$ strain. If the antibody is specific for EscF then fusing GFP+ to the C terminus of EscU has a dramatic effect in the amount of EscF being secreted.

5.10.1 Creating a Walla3 LEE4 Deletion Strain (ZAP636)

Before any conclusion could be reached about the effect of modifying EscU on the amount of EscF being secreted the anti EscF antibody was verified. To confirm the antibody was detecting the EscF protein a LEE4 deletion in the Walla3 strain was created (deleting the entire LEE4, including *escF*). The plasmid pHY10 was transformed and used to replace the LEE4 sequence for the *sac*/Kan cassette by allelic exchange. Colonies from the allelic exchange were screened by PCR for the presence of *escF*. PCR screening was also used to verify the pIB307 plasmid had been cured and the *sac*/Kan cassette was present in the strain (gels not shown). Successful allelic exchange created the Walla3 LEE4<>*sac*/Kan strain, which

contained no *escF* and acted as a negative control for the Western blots with the anti EscF antibody.

5.10.2 Anti EscF Antibody: Western Blot Analysis with the Walla3, Walla3 LEE4<>*sac*/Kan (ZAP636) and Walla3 *escU*<>*escU*$_{cc::gfp+}$ (ZAP1142) Strains

Initially the strain Walla3 LEE4<>*sac*/Kan was compared with the Walla3 strain. Both strains were grown supplemented MEM-HEPES and cytoplasmic, membrane and supernatant protein fractions made. Western blot analysis was carried out on these samples using the anti EscF antibody (Fig.92).

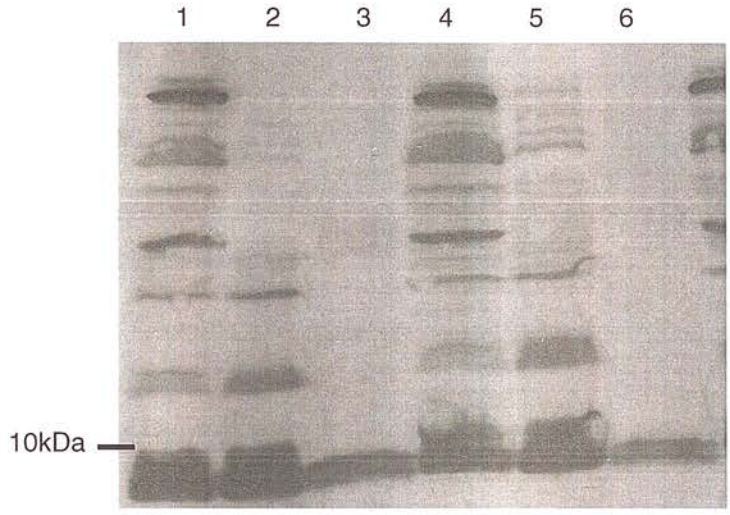

Fig.92 Western blot analysis of membrane, cytoplasmic and supernatant protein fractions of Walla3 and Walla3 LEE4<>*sac*/Kan (ZAP636) with 1:1000 dilution anti EscF antibody. Samples were initially run on a 10-20% SDS PAGE gel (Bio-rad, Hertfordshire, UK). Western blot analysis was carried out in low stringency condiditons
Lane1: Walla3 cytoplasmic fraction
Lane2: Walla3 membrane fraction
Lane3: Walla3 supernatant fraction
Lane4: ZAP636 cytoplasmic fraction
Lane5: ZAP636 membrane fraction
Lane6: ZAP636 supernatant fraction.

Fig.92 shows that the Walla3 LEE4<>*sac*/Kan mutant strain, which contains no *escF*, has the double band below the 10kDa marker. This indicates that the previously detected band was not EscF. EscF may still be detected on the Western blots but masked by the cross reactivity with another small peptide. To minimise cross reactivity the anti EscF antibody was absorbed using the Walla3 LEE4<>*sac*/Kan strain. The strains Walla3, Walla3 LEE4<>*sac*/Kan and Walla3

escU<>*escU*$_{cc::gfp+}$ were grown in supplemented MEM-HEPES and cytoplasmic, membrane and supernatant protein fractions made. The strain Walla3 *escU*<>*escU*$_{cc::gfp+}$ was used as it showed an increase in the protein detected by the anti EscF antibody. If this is indeed an increase in EscF then the Walla3 *escU*<>*escU*$_{cc::gfp+}$ strain may produce enough EscF to be seen after the cross reactivity has been removed. The samples were run on a 10-20% SDS PAGE gel (Bio-Rad, Hertfordshire, UK) and a 1:10 dilution of the absorbed antibody used in a low stringency Western blot to detect EscF (Fig.93)

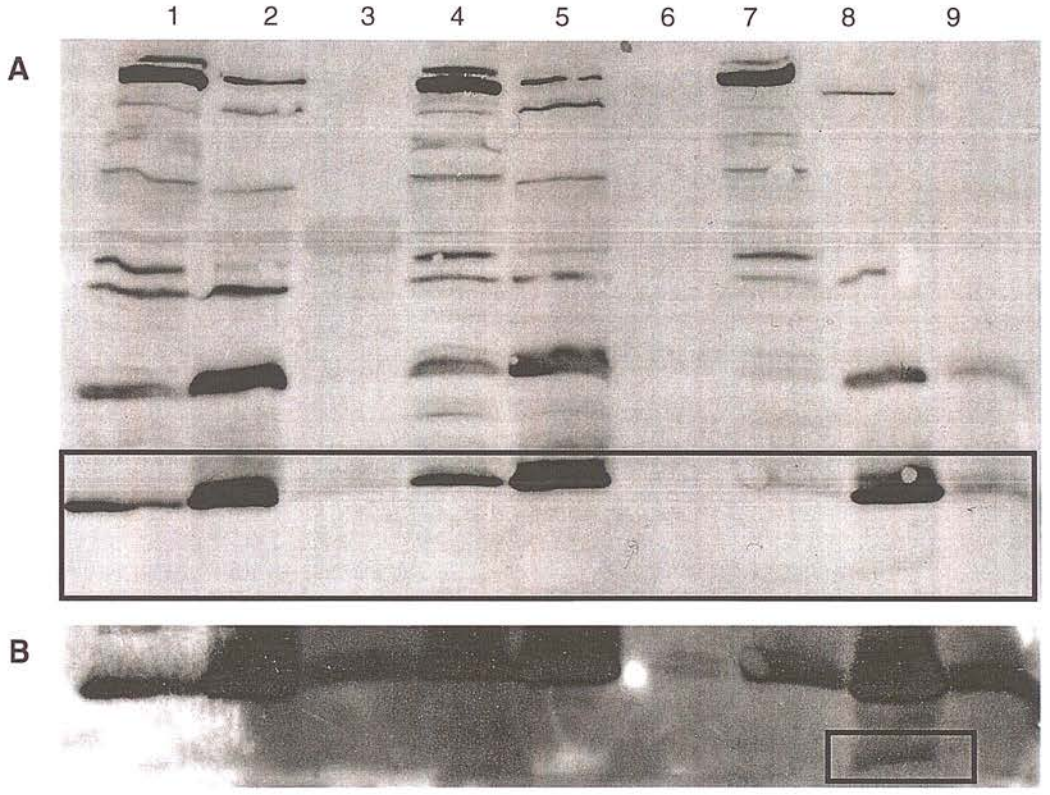

Fig.93 Western blot analysis of membrane, cytoplasm and supernatant protein preparations of Walla3, Walla3 LEE4<>*sac*/Kan (ZAP636) and Walla3 *escU*<>*escU*$_{cc::gfp+}$ (ZAP1142) using a 1:10 dilution of absorbed anti EscF antibody. The boxed area in A. is shown from a longer exposed X-ray film in B. The box in B. highlights a small and faint band which may be EscF.
Lane1: Walla3 cytoplasmic protein fraction
Lane2: Walla3 membrane protein fraction
Lane3: Walla3 supernatant protein fraction
Lane4: ZAP636 cytoplasmic protein fraction
Lane5: ZAP636 membrane protein fraction
Lane6: ZAP636 supernatant protein fraction
Lane7: ZAP1142 cytoplasmic protein fraction
Lane8: ZAP1142 membrane protein fraction
Lane9: ZAP1142supernatant protein fraction

5.10.3 Anti EscF antibody: Antibody Absorption and Tricine Gels

The absorbed antibody did reduce the intensity of the two bands detected below the 10kDa marker in the supernatant protein fractions, however, the bands were still observed in the Walla3 LEE4<>*sac*/Kan strain (Fig.93, B Lane6). Below these bands but before the dye front for the SDS PAGE gel, was another band detected only in the Walla3 *escU*<>*escU*$_{cc::gfp+}$ strain; which could be the EscF monomer detected by the antibody.

To determine whether the absorbed anti EscF antibody is detecting EscF tricine gels (Bio-Rad, Hertfordshire, UK) were run with the Walla3 and Walla3 LEE4<>*sac*/Kan membrane, cytoplasm and supernatant protein samples and purified EscF. The purified EscF was supplied by Sean McAteer from the ZAP lab, CID, the University of Edinburgh. The EscF was purified using a 6 His tag expression system and had been detected by Western blot analysis in the final elution using anti His antibody. The Walla3 and Walla3 LEE4<>*sac*/Kan samples were run on the tricine gel with a whole cell sample from the expression strain with the EscF-His tag plasmid which had not been induced, a whole cell sample of the strain when the plasmid had been induced and 5µl of the final column elute (Fig.94).

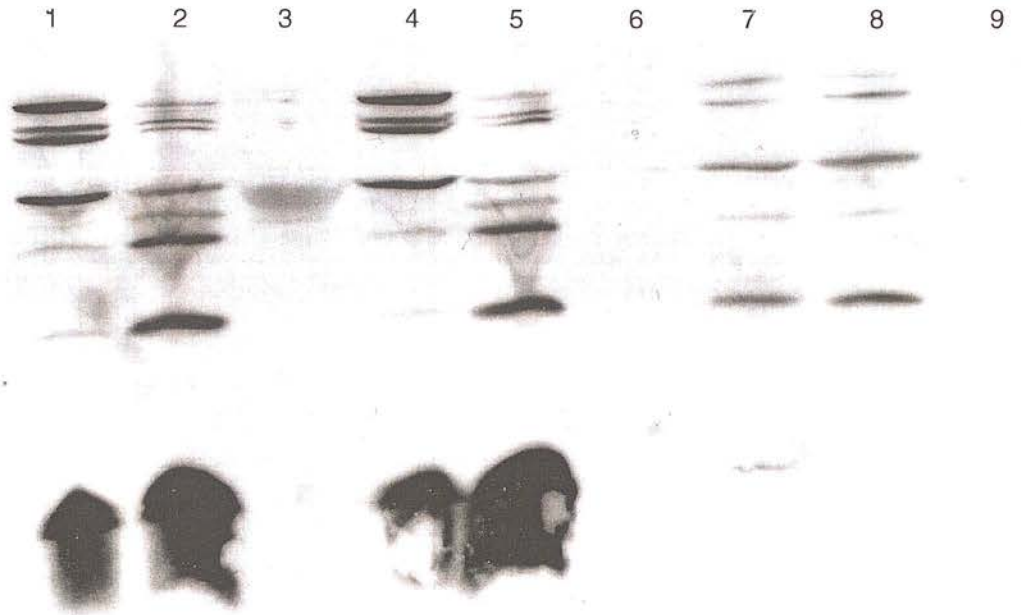

Fig.94 Western blot analysis of the cytoplasmic, membrane and supernatant proteins of Walla3 and Walla3 LEE4<>*sac*/Kan (ZAP636) and whole cell fractions from the expression strain with the EscF-His tagged expression vector induced and not induced and the final elution of purified EscF. The Western blot was carried out in low stringency conditions with a 1:10 dilution of the absorbed antibody.
Lane1: Walla3 cytoplasmic protein fraction
Lane2: Walla3 membrane protein fraction
Lane3: Walla3 supernatant protein fraction
Lane4: ZAP636 cytoplasmic protein fraction
Lane5: ZAP636 membrane protein fraction
Lane6: ZAP636 supernatant protein fraction
Lane7: Uninduced expression vector (whole cell)
Lane8: Induced expression vector (whole cell)
Lane9: Final column elute, purified EscF.

The tricine gel never detected the purified EscF using the anti EscF antibody and there were no differences observed between the Walla3 strain and the LEE4 deletion strain Walla3 LEE4<>*sac*/Kan.

5.10.4 Anti EscF Antibody: Fluorescence Microscopy

The anti EscF antibody was used in fluorescence microscopy to determine whether it could directly label EscF on bacterial cells. Fluorescence microscopy was carried out on the strains Walla3, Walla3 *escU*<>*escU*$_{\Delta cc}$, Walla3 *escU*<>*escU*$_{cc::egfp}$, Walla3 *escU*<>*escU*$_{cc::gfp+}$, Walla3 *escRSTU*<>*sac*/Kan Walla3 LEE4<>*sac*/Kan and Walla3 *escRSTU*<>*sac*/Kan and using the PFA fixation technique. The anti EscF antibody

was the primary antibody with the Alexa Fluor 488 conjugate to anti-rabbit IgG the secondary. Eexamples of the images obtained are presented in Fig.95-Fig.98.

Although the quality of the antibody staining varied, fluorescence microscopy using the anti EscF antibody on the Walla3 strain did produced discrete fluorescent foci on a subset of bacteria. When the antibody was used to stain the Walla3 LEE4<>*sac*/Kan strain the discrete foci were replaced with a more diffuse fluorescence that did not consistently repeat (Fig.95 panel D and F). The Walla3 *escRSTU*<>*sac*/Kan strain appeared to have less staining with the anti EscF antibody, which occasionally produced faint foci and the Walla3 *escU*<>*escU*$_{\Delta cc}$ strain had foci similar to Walla3 (Fig.96). Panels A-C (Fig.97) show the strain Walla3 *escU*<>*escU*$_{cc::egfp}$ had brighter fluorescent foci than the wild type strain and rings of fluorescence (particularly noticeable in panel A). Finally in the strain Walla3 *escU*<>*escU*$_{cc::gfp+}$ (Fig.97, Panels D-F) there was an average increase of over 6 times in the amount of fluorescence detected from individual bacterium when compared to the Walla3 strain. Only in Fig.97 panel F can foci be distinguished, the other panels contain bacteria where the level of fluorescence is too high to visualise individual foci. This is interesting as the strain Walla3 *escU*<>*escU*$_{cc::gfp+}$ had 3.2 times more signal detected when using the anti EscF antibody in Western blot analysis when compared to the wild type strain (Fig.91). Fig.108 is the secondary antibody only, used as a negative control for the staining method.

Although the microscopy images were variable it would appear that the antibody did bind to bacteria which had an *escF* deletion. The wild type strain produces fluorescent foci in a subset of bacteria. Although deleting the EscU$_{CC}$ peptide had little effect on staining with the anti EscF antibody the addition of eGFP to the EscU$_{CC}$ domain increases the amount of fluorescence detected, and the addition of GFP+ increases it further. This is unlikely to be due to the fluorescence from these GFP variants as no direct fluorescence can be detected from either the eGFP or the GFP+ constructs.

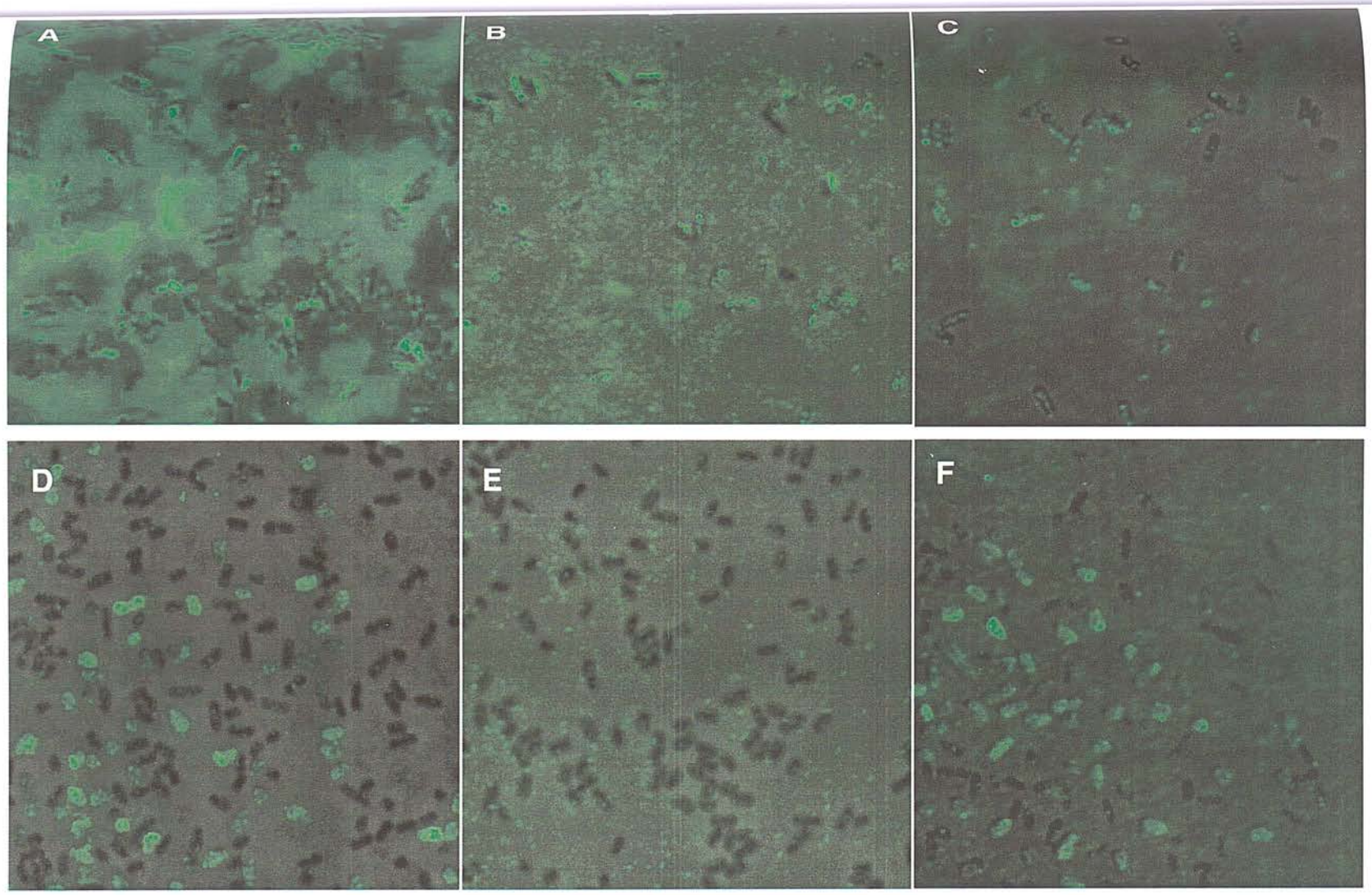

Fig.95 Fluorescence microscopy using the anti EscF antibody on Walla3 strain (panels A, B and C) and the Walla3 LEE4<>*sac*/Kan (ZP636) strain (panels D, E and F). The strains were grown in 10ml of supplemented MEM-HEPES. The microscope slides were incubated with 1:25 dilution of the anti EscF antibody for two hours and for 1hr with a 1:1000 dilution of the secondary antibody.

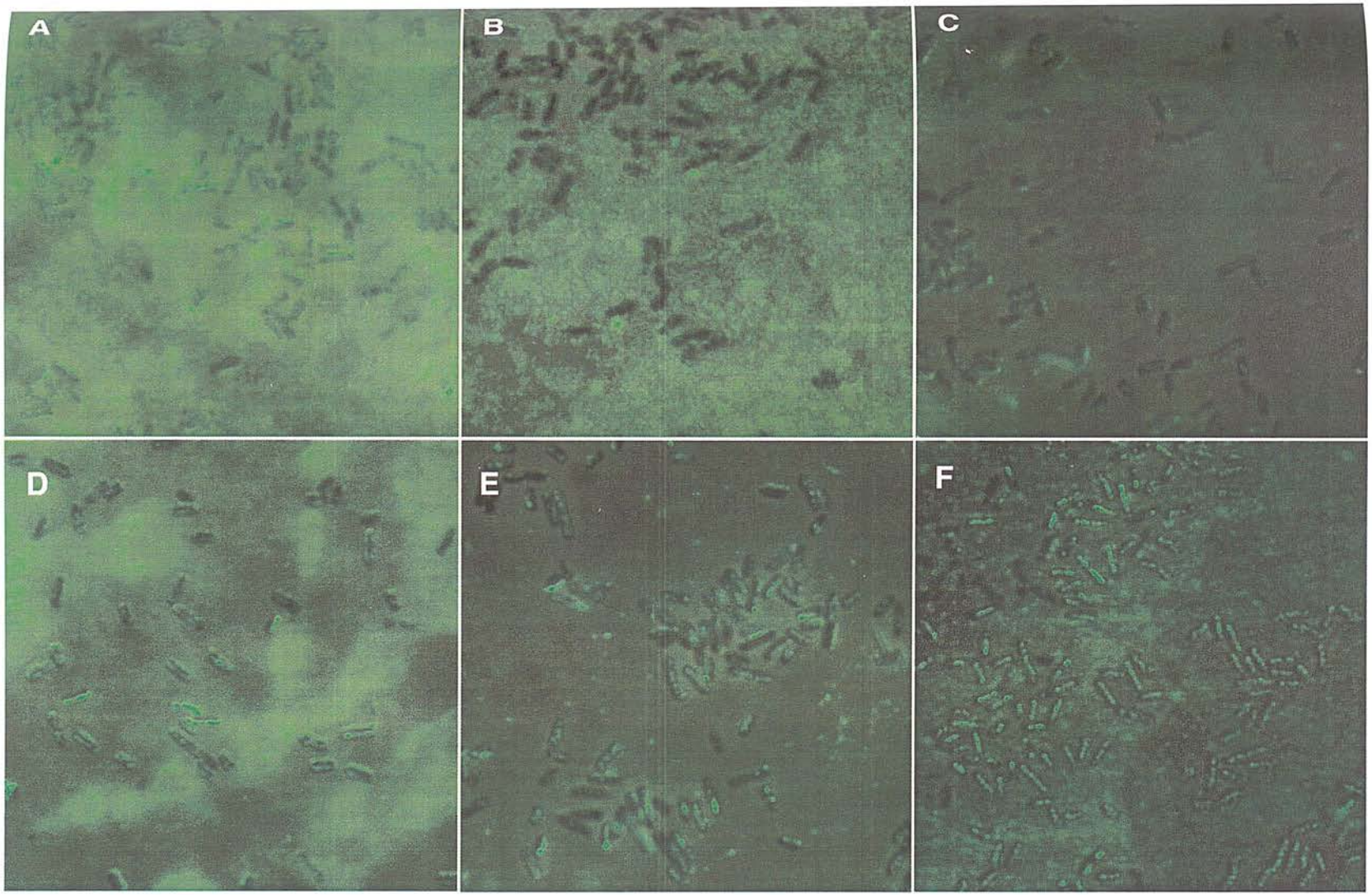

Fig.96 Fluorescence microscopy using the anti EscF antibody on the strain Walla3 *escRSTU<>sac*/Kan (ZAP1140) (panels A, B and C) and the Walla3 *escU<>escU*$_{\Delta cc}$ (ZAP633) strain (panels D, E and F). strains were grown in 10ml of supplemented MEM-HEPES. The microscope slides were incubated with 1:25 dilution of the anti EscF antibody for two hours and for 1hr with a 1:1000 dilution of the secondary antibody

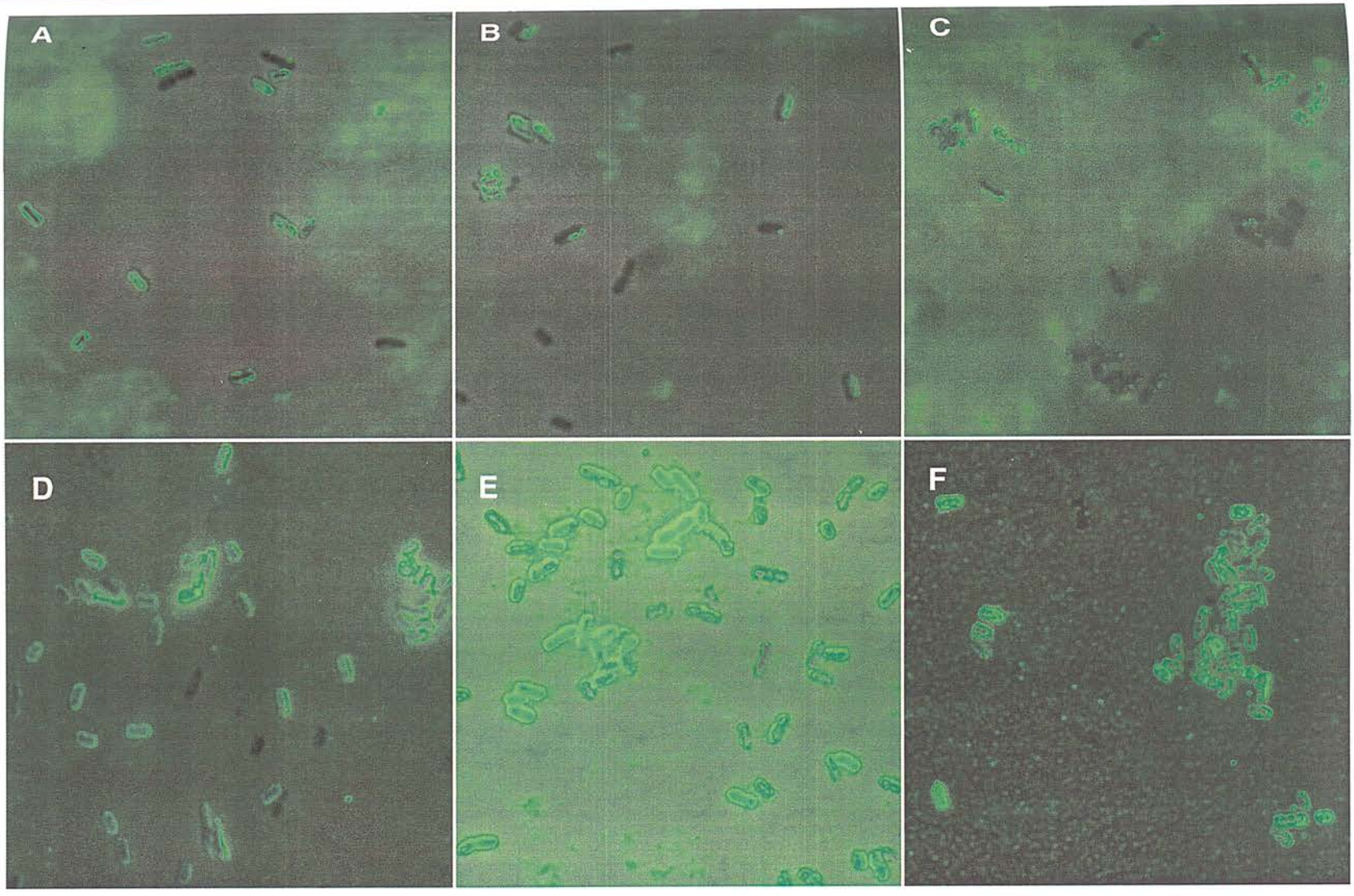

Fig.97 Fluorescence microscopy using the anti EscF antibody on the strain Walla3 *escU*<>*escU*$_{cc::egfp}$ (ZAP1141) (panels A, B and C) and the Walla3 *escU*<>*escU*$_{cc::gfp+}$ (ZAP1142) strain (panels D, E and F). strains were grown in 10ml of supplemented MEM-HEPES. The microscope slides were incubated with 1:25 dilution of the anti EscF antibody for two hours and for 1hr with a 1:1000 dilution of the secondary antibody.

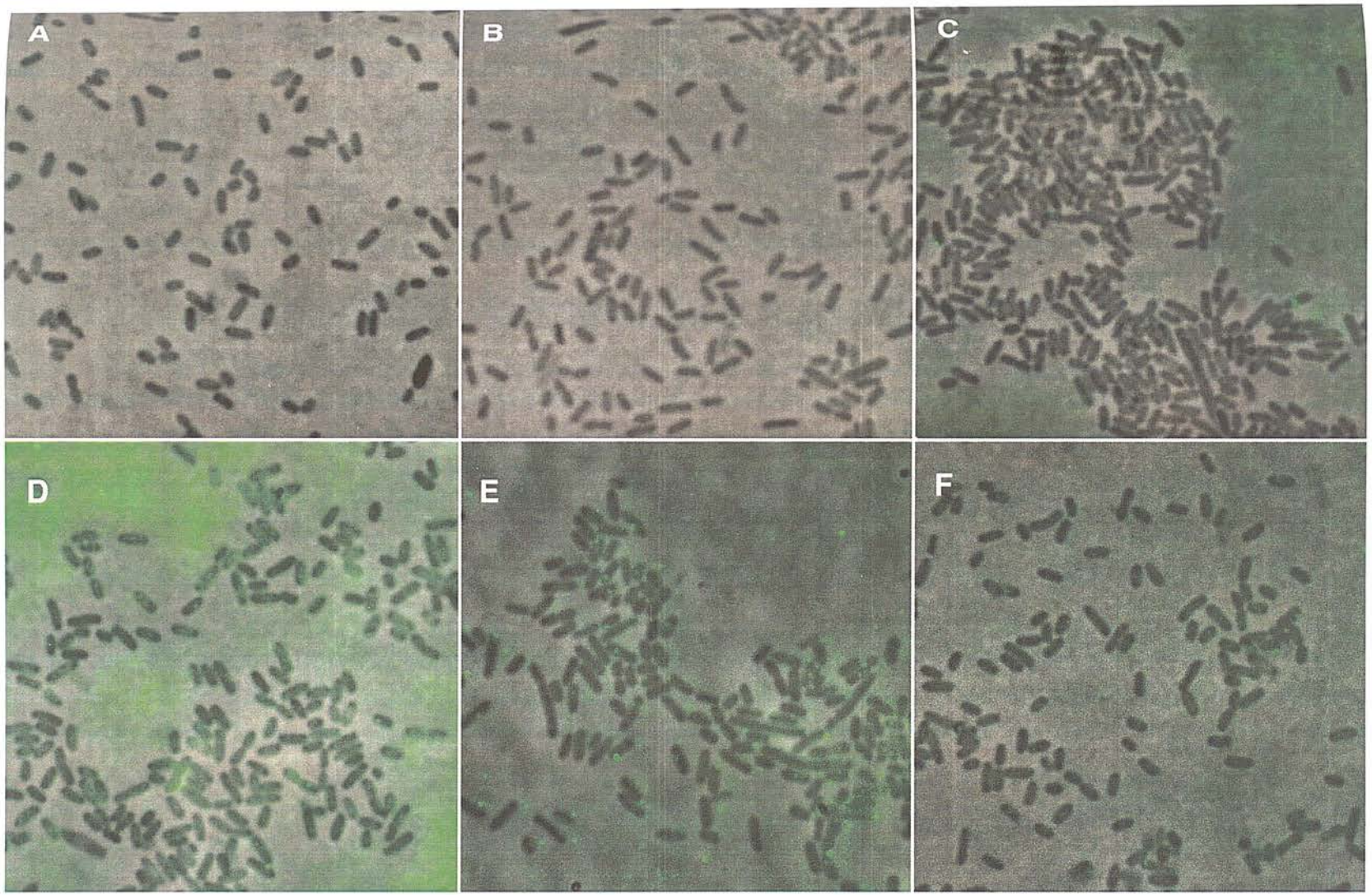

Fig.98 Fluorescence microscopy using the secondary antibody only (Alexa Fluor 488 conjugate) on the strains Walla3 (panel A), Walla3 LEE4<>*sac*/Kan (ZP636) (panel B), Walla3 *escRSTU*<>*sac*/Kan (ZAP1140) (panel C), Walla3, Walla3 *escU*<>*escU*$_{\Delta cc}$ (ZAP633) (panel D), Walla3 *escU*<>*escU*$_{cc::egfp}$ (ZAP1141) (panel E), and Walla3 *escU*<>*escU*$_{cc::gfp+}$ (ZAP1142) (panel F). strains were grown in 10ml of supplemented MEM-HEPES. The microscope slides were incubated with 1:25 dilution of the anti EscF antibody for two hours and for 1hr with a 1:1000 dilution of the secondary antibody

5.11 Discussion

The tagged strains provided the tools to investigate the function of the EscU protein in more detail. The work demonstrated that like its homologues in the *Yersinia pseudotuberculosis* T3SS and *Salmonella* Typhimurium flagellar system (Minamino, T., *et al* 2000, Lavander, M., *et al* 2002), the EscU protein in EHEC T3SS is most likely cleaved into a 10kDa and a 30kDa protein at the conserved cleavage site NPTH. For EscU it was unclear whether this cleavage played a role in the switching from secreting needle protein (EscF) to secreting filament protein (EspA).

The REase recognition site added to the *escU* sequence was used in a cloning strategy that removed the C terminal region of EscU from the cleavage site NPTH. This was used to generate a strain that produced only a truncated EscU protein (ZAP633). Analysis of this strain and the previously created mutants demonstrated that all (apart from the strain Walla3 *escU*<>$escU_{cc::gfp+}$ [ZAP1142]) did not secrete EspD into the supernatant at detectable levels with Western blot analysis and the EspD secreted by Walla3 *escU*<>$escU_{cc::gfp+}$ was more than 4 times less when compared to the wild type level. The strains Walla3 *escU*<>$escU_{\Delta cc}$, Walla3 *escU*<>$escU_{cc::egfp}$ and Walla3 *escU*<>$escU_{cc::gfp+}$ also secreted no detectable Tir into their supernatant protein fractions. It was seen whether the substitution in the strain ZAP1140 of *escRSTU* for the *sac*/Kan cassette and the deletion of $EscU_{CC}$ domain in the ZAP633 strain effected the transcription from the LEE1-5 promoters. A negative feedback mechanism may have existed that stopped the transcription of the TTSS genes when the basal apparatus could not be formed. However, this was not the case as both the ZAP1140 and ZAP633 strains had LEE promoter expressions that matched that of the Walla3 strain.

The strains Walla3 *escU*<>$escU_{\Delta cc}$, Walla3 *escU*<>$escU_{cc::egfp}$, Walla3 *escU*<>$escU_{cc::gfp+}$, Walla3 *escRSTU*<>*sac*/Kan and Walla3 escU<>$escU_{cn::HA}$ had their secretion of EspD partially complemented after transformation with the pJRE02 plasmid. Although it contains the sequence that was substituted for the *sac*/Kan cassette in the Walla3 *escRSTU*<>*sac*/Kan strain it does not carry a full LEE1 promoter, which may explain the partial complementation. However, this result did

confirm that the strains were not secreting EspD due to the modifications made to this LEE1 sequence.

The $EscU_{CC}$ peptide was artificially expressed from plasmids in the Walla3 *escU*<>$escU_{\Delta cc}$ strain to determine whether EspD secretion could be restored. Two versions of the plasmid were constructed, one containing the $EscU_{CC}$ peptide N terminally labelled with the HA tag, enabling detection to confirm it was being translated. The other version was without the HA tag, in case the tag interfered with the function of the peptide. $EscU_{CC::HA}$ from the pJRE23 plasmid was expressed in all the strains but only detected in Walla3 *escU*<>$escU_{\Delta cc}$ and Walla3 *escRSTU*<>*sac*/Kan, where it was localised to the membrane fraction of the cell. This was interesting as it was assumed that the $EscU_{CC}$ peptide localised to the membrane via an interaction with the $EscU_{CN}$ domain after cleavage but the Walla3 *escRSTU*<>*sac*/Kan strain contains no EscR, S, T or U. The peptide may still localise to the membrane via $EscU_{CN}$, but in the absence of EscU it may be free to bind to another molecule which is also anchored to the membrane. The $EscU_{CC::HA}$ may have only been detected in strains not containing a chromosomal copy of the peptide because the peptide produced by this chromosomal EscU gene may interact at the membrane leaving $EscU_{CC::HA}$ to be denatured in the cytoplasm.

The detection of $EscU_{CC::HA}$ in the Walla3 *escU*<>$escU_{\Delta cc}$ strain enabled the secreted proteins from these samples to be tested for EspD secretion. The EspD Western blots showed that the peptide could not fully complement the Walla3 *escU*<>$escU_{\Delta cc}$ strain. The complementation may have failed because the whole EscU protein is needed for the secretion of EspD. In the EscU homologues cleavage is a timing mechanism and a switch to stop secreting hook proteins and start secreting filament proteins. If the cleavage of EscU has a similar function then not having the whole EscU protein present could lead to no EscF being secreted. It could be the case that without EscF then no EspD or EspA can be secreted through the T3SS as its assembly is not complete.

An anti EscJ antibody was used to detect EscJ in preparations of protein fractions from the mutant strains. It showed that EscJ was present in the mutant strains and localised to the membrane fraction. This means that EscJ is present in the right bacterial cell compartment for its TTSS function, which is not surprising as it is thought to be transported to the periplasm in a Sec-dependent manner (Gauthier, A., et al 2003b). It was known that all the strains, except Walla3 *escU<>escU*$_{cc::gfp+}$, do not secrete EspD or EspA, but it was not known at what stage the TTSS process stops functioning. The presence of EscJ in the membrane fraction of the mutants could mean that the TTSS basal apparatus can form but the mechanism for secretion of EspD and EspA has been affected by the addition of the tags. If the Sec-dependent secreted proteins are present in the membrane then EscV, EscC and EscJ (Gauthier, A., et al 2003b) would be localised there as well as tagged EscU, which was shown to be present in the membrane fraction. The EscJ antibody was used with the Walla3 strain to try and visualise the TTSS by fluorescence microscopy. The strain 148a containing no *escJ* was used as a negative control. Although the antibody yielded clean Western blots the fluorescence microscopy had non specific binding in the 148a mutant, which appeared as discrete fluorescent foci. This meant it was not able to be used for fluorescence microscopy with the mutant strains.

The anti EscF antibody was used to see whether the EscU mutants were effecting the secretion of EscF, the needle component of the TTSS. The initial Western blots were promising, showing an intense band at ~10kDa that was resolved further in the supernatants of the strains to two bands, possibly a modified and unmodified EscF. The strain Walla3 *escU<>escU*$_{cc::gfp+}$ showed a large increase in the secreted protein that was being detected. The Walla3 *escU<>escU*$_{cc::gfp+}$ strain is also the only strain that has a detectable amount of EspD in the supernatant and has been shown to cleave the GFP+ from the C-terminus. This cleavage could produce a small number of functioning TTSS apparatus which are altered in their timing of switching between secreting EscF and secreting filament proteins, secreting EscF for longer. However, when a LEE4 substitution was made, replacing the LEE4 genes (including *escF*) for the *sac*/Kan cassette, Western blot analysis did not detect a difference between the LEE4 substitution strain (ZAP636) and the Walla3 wild type strain. The

Walla3 LEE4<>*sac*/Kan strain was then used to absorb the antibody to reduce non specific binding, but this had little effect. Tricine gels were run which contained the wild type strain, the Walla3 LEE4<>*sac*/Kan strain and purified EscF, but no bands at the right size were detected. Fluorescence microscopy was also carried out with the anti EscF antibody; it showed discrete foci of fluorescence in the strains, which were present but more diffuse in the LEE4 substitution strain and not as bright in the Walla3 *escRSTU*<>*sac*/Kan strain. Interestingly the Walla3 *escU*<>$escU_{cc::gfp+}$ strain had an average bacterial fluorescence that was over 6 times higher than the Walla3 strain, with rings of fluorescence around the bacteria. This confirmed the Western blot analysis, which showed a higher amount of protein being detected in the supernatant when using this antibody.

Chapter 6
General Discussion

6. General Discussion

The project's objective was to label the basal apparatus of the T3SS of EHEC O157:H7 with variants of the fluorescent protein GFP or the immunogenic haemagglutinin (HA) tag. This was to create a tool to help answer questions concerning timing, regulation and location of T3SS proteins. The approach required the introduction of REase sites at the 3' end of the genes for predicted inner membrane proteins of the basal apparatus. The tag sequences were introduced using these sites. Allelic exchange was used to replace the wild type copy of the gene from the bacterial chromosome to avoid problems associated with artificial promoters, genetic context and fluorescent artefacts from over expression.

The cloning strategy was designed, in detail, for six proteins; EscR, S, T, U, V and N, all predicted to be part of the inner membrane basal apparatus (apart from EscN, which is predicted to be associated with the inner membrane). The cloning was carried out for EscR and EscU and tags were introduced. EscR and EscU tags were used to create five derivatives of EHEC O157:H7 Walla3, two of which were strains containing EscU that had been labelled in a naturally occurring REase site before the predicted NPTH cleavage sequence (Table 7).

Table 7. Table showing the different fusion proteins and the corresponding strain.

Wild Type Protein	Fusion Protein	Strain Name
EscU	$EscU_{CC::eGFP}$	ZAP1141
EscU	$EscU_{CC::GFP+}$	ZAP1142
EscU	$EscU_{CN::HA}$	ZAP634
EscU	$EscU_{CN::GFP+}$	ZAP635
EscR	EscR::HA	ZAP637

Despite the use of the expand long template PCR system (Roche, Burgess Hill, UK), which contains a high fidelity DNA polymerase, there were base pair changes added by PCR error that created substitution mutations in some of the genes. Strains with two substitutions had them at ORF3: V107F and EscU: F167S, whilst strains with four substitutions had also acquired two at EscU: G235E and rORF3: T53A (Table 8).

Table 8. Table showing which mutant strains contained two substitutions and which contained four.

Strains with Two Substitutions	Strains with Four Substitutions
ZAP632	ZAP1141
ZAP633	ZAP1142
ZAP634	
ZAP635	
ZAP637	

Even with these amino acid substitutions the complemented strain (ZAP632) was able to secrete EspD to wild type levels, indicating it contained a functioning T3SS. This meant the strains Walla3 *escU*<>*escU*$_{\Delta cc}$, Walla3 *escRSTU*<>*sac*/Kan restored TTSS strain, Walla3 *escU*<>*escU*$_{cn::HA}$, Walla3 *escU*<>*escU*$_{cn::gfp+}$ and Walla3 *escR*<>*escR::HA* contained unintentional amino acid substitutions that did not effect the ability of the T3SS to secrete EspD and so were taken forward for further analysis. For the strains Walla3 *escU*<>*escU*$_{cc::egfp}$ and Walla3 *escU*<>*escU*$_{cc::gfp+}$, that contained two additional sequence errors, the ability for the strains to secrete EspD with these substitutions was partly confirmed by the secretion of small levels of EspD after some of the GFP+ was cleaved from the EscU$_{CC::GFP+}$ fusion. This demonstrated that the small amount of EscU that was now unlabelled, yet still in the background with all four substitutions, was able to form a functioning T3SS apparatus. However, it is acknowledged that to fully discount these substitutions as having an effect on the T3SS, a complement should be made containing all four PCR errors and screened for its ability to secrete EspD.

Strains containing EscU labelled with variants of GFP were examined by fluorescence microscopy to detect the fusion protein. With an exposure time of one second and contrast manipulation on the OpenLab software (Improvision, Coventry, UK) foci were observed. However, these foci were also observed in the wild type Walla3 strain and the Walla3 *escRSTU*<>*sac*/Kan strain, so they were attributed to autofluorescence of proteins, detected because of the long exposure time and contrast enhancement. This result was disappointing as the GFP labelled EscU strains had higher population fluorescence than the Walla3 wild type strain. Unfortunately the relative fluorescence units (rfu) for the strains, measured on the Flurostar fluorimeter (FLUOstar Optima, Bath, UK), did not exceed 5000rfu at a gain of 1750. This level,

especially when compared to strains containing protein fusion of GFP on plasmids, is extremely low and may explain the inability to visualize the proteins directly.

An attempt was made to increase the low level of fluorescence by increasing the expression from the LEE1 promoter. This was done by transforming the strains with a plasmid containing either the positive regulator *ler* or *grlA* under an inducible promoter. This was unsuccessful and further analysis of Walla3 with and without the *grlA* plasmid showed little effect on the level of EspD secretion. This may be because the Walla3 LEE regulation network is at a maximum level of secretion and the addition of extra Ler or GrlA cannot increase this further, or because high levels of Ler act as a negative regulator on LEE1 promoter expression (Berdichevsky, T., *et al* 2005).

Western blot analysis was used to try and detect the HA tagged fusions of EscR and EscU with commercial anti HA antibodies from two separate companies. Only when high levels of protein were loaded, coupled with low stringency Western blot conditions, was the $EscU_{CN::HA}$ fusion protein detected. The EscR::HA fusion was not detected in any of the Western blots.

At this stage it was clear that the initial aims of the project could not be fulfilled as the tagged fusions were not detectable at the single cell level. This indicated that the amount of EscU and EscR in the basal apparatus is likely to be low and certainly insufficient for direct detection. Interestingly the work to this point had shown that all the strains containing tagged proteins (except strain Walla3 $escU<>escU_{cc::gfp+}$) were unable to secrete detectable amounts of EspD. The inability to visualize the tags and their apparent disruption on the T3SS led to the decision to analyze the tagged proteins to determine the effect the presence of the tag was having on the function of EscU.

It was also noted during Western blot analysis that the EscU protein appeared to be cleaved into two fragments, a ~10kDa peptide and a ~30kDa peptide, both of which were independently localized to membrane fractions. Sequence alignments with the

previously studied homologues YscU and FlhB showed the presence of a conserved cleavage site (NPTH) in the EscU sequence. The cleavage of the YscU and FlhB homologues plays an important role in regulating the length of the needle and the secretion of hook proteins in the *Yersinia* T3SS and the flagellar system, respectively.

A cloning strategy was used to delete the portion of the *escU* gene that encodes the 10kDa cleaved peptide. This was allelic exchanged to replace the wild type *escU* sequence. This strain was added to the repertoire of mutants to be screened for their ability to secrete proteins via the T3SS. The strains were screened for the secretion of EspD and the effector protein Tir. None of the strains had detectable levels of Tir in the supernatants and only Walla3 *escU*<>$escU_{cc::gfp+}$ had a small amount of secreted EspD. This demonstrated that introducing the tags, at the C terminus of EscR and in EscU at either the C terminus or before the NPTH cleavage site, led to a T3SS that was not fully functional. This phenotype was also seen when the cleaved portion of the EscU protein ($EscU_{CC}$) was deleted. The strains were unable to secrete T3SS proteins but were still localized to the membrane fraction of the cell. This may not be surprising with the GFP tagged proteins as GFP is 27kDa and may interfere with the function and interactions of EscU. Indeed it was shown that when GFP+ was fused to EscU before the NPTH cleavage site (strain Walla3 *escU*<>$escU_{cn::gfp+}$) the fusion protein was cleaved at alternative sites, possibly due to conformational changes in the EscU protein. However, the HA tag at the same position in EscU was localized to the membrane at the correct size (without alternative cleavage), but this fusion protein was still not able to produce a functional T3SS. This implies that either the HA tag was located in a domain important in the formation of the basal apparatus or secretion of T3SS proteins or, despite its small size, it altered the conformation of EscU. All of the *escU* mutants (except strain Walla3 *escU*<>$escU_{cn::gfp+}$) were screened for the ability of the pJRE02 plasmid to complement EspD secretion. The plasmid contains the genes *escRSTU* and gave a small degree of complementation to the mutant strains, with some EspD detected in the supernatants. The low level of complementation could have been due to the lack of a full LEE1 promoter, however, their partial complementation added to the body of evidence that the observed

phenotypes were due to the sequence changes created by adding the tags to, or deleting portions of, the EscU protein. Attempts to clone the *escU* gene failed, possibly due to toxicity issues. This meant that complementing the mutants with only *escU* was not possible.

All the mutants had EscJ present in the membrane at wild type levels. This indicated that the basal apparatus proteins that require Sec-dependent insertion into the inner membrane were present (EscJ, EscV and EscC in the presence of EscN (Gauthier, A., *et al* 2003b)).

Plasmids containing the LEE promoters fused to *egfp* were transformed into the Walla3, Walla3 *escRSTU<>sac*/Kan and Walla3 *escU<>escU*$_{\Delta cc}$ strains. FLUOstar OPTIMA readings demonstrated that the level of expression from these promoters remained the same in the two mutant strains when compared to Walla3. However, the large amount of EspD seen in the Walla3 supernatant was not detected in the strains unable to secrete EspD. Because the expression from the LEE promoters was the same yet the total amount of EspD detected was different, it implied regulation at a posttranscriptional stage, if this is coupled with translocation (as previously described in Roe, A., *et al* 2003b) then the lack of a functioning T3SS basal apparatus (due to the interference caused by the tags) would explain the decrease in EspD translation.

The deletion of the cleaved EscU$_{CC}$ portion and the strains inability to form a functioning T3SS demonstrated the need for the peptide for the secretion of EspD, Tir and the formation of EspA filaments. Supplying the peptide *in trans* did not complement the strain, indicating the whole EscU protein is needed. In the homologous flagellar system the FlhB protein is needed for secretion of rod and hook proteins and its cleavage acts as a timing mechanism that slows down rod and hook protein secretion, allowing FlhB to interact with FliK. This causes a conformational change in FlhB and increases its affinity for filament proteins (Moriya, N., *et al* 2006). If this was the case for EscU then deleting the cleaved peptide would create a

strain that could not secrete of EscF. Without the formation of a needle structure the proteins EspD and Tir would not be translocated.

When the deleted $EscU_{CC}$ 10kDa peptide was supplied *in trans* it was only detected in strains where the peptide had been deleted from the chromosome (Walla3 *escU<>escU*$_{\Delta cc}$ and Walla3 *escRSTU<>sac*/Kan) and it was only detectable in the membrane fractions. This may be because in strains like Walla3 *escU<>escU*$_{cc::egfp}$, where an eGFP labelled version of the $EscU_{CC}$ peptide was produced from the chromosome and localized to the membrane, the plasmid copy of the peptide could not interact at the membrane and was degraded. The peptide's localization to the membrane in the Walla3 *escRSTU<>sac*/Kan strain was unexpected; this would indicate that the peptide does not localize to the membrane by interacting with the $EscU_{CN}$ domain of EscU or can localize to the membrane in the absence of EscU by another interaction that would not normally occur (possibly an interaction of lower affinity).

To see whether the EscU mutant strains effected the level of EscF export (the predicted needle protein) an anti EscF antibody was obtained from Prof. Abe (Osaka, Japan). This was a published anti EscF antibody used to detect levels of EscF in Western blot analysis (Ando, H., *et al* 2007). Preparations of cytoplasmic, membrane and supernatant proteins were made and tested with the antibody. At first the results were encouraging but a mutant strain with an *escF* deletion was needed to check the antibodies specificity. After the creation of this mutant it became clear that the initial enthusiasm for the specificity of the antibody was misplaced as little difference in the Western blot banding pattern was seen between the wild type and the mutant. Interestingly the strain Walla3 *escU<>escU*$_{cc::gfp+}$ had a higher intensity band in Western blot analysis and a higher level of fluorescence when using the anti EscF antibody in fluorescence microscopy. If this published anti EscF antibody was detecting EscF then it was also detecting another small protein(s) that masked the difference in the level of EscF in the supernatants. It is possible that this masking of EscF was overcome in the Walla3 *escU<>escU*$_{cc::gfp+}$ strain because the tagged $EscU_{CC}$ caused the EscU protein to function incorrectly; over secreting EscF and not

switching properly to the secretion of EspA filament proteins. This may have been observed in the GFP+ fusion and not in the eGFP fusion because of sequence differences between the two proteins. It may also have been due to the cleavage of GFP+ from some of the EscU molecules, creating a small number of functioning T3SS, which secreted increased amounts of EscF.

Two models exist for the role of FliK in substrate-specificity switching in the flagellar secretion system: a measuring-cup model and a tape-measure model (Ferris, H., *et al* 2006). In the measuring-cup model the FliK molecule cannot interact with FlhB (the EscU homologue) and switch substrate-specificity because the flagellar C-ring is blocked by hook protein. It is only when this hook protein has been exported that the FliK molecule can interact with FlhB. In the tape-measure theory the FliK is exported through the growing flagellar hook until the hook reaches the correct size to allow the C terminus of FliK to interact with FlhB and the N terminus to interact with the tip of the growing hook (Ferris, H., *et al* 2006). It is likely that a combination of these two models, along with the cleavage of FlhB acting as a molecular clock (Moriya, N., *et al* 2006), exist to ensure correct rod/hook secretion and substrate-specificity switching. If EscU in the EHEC T3SS has a similar role, then having a few functioning T3SSs in the strain Walla3 *escU<>escU*$_{cc::gfp+}$ could overflow the 'molecular-cup', not allowing the a homologous, yet still unknown, molecular ruler (FliK in flagellar system) access to the needle at the correct time, missing the period when the ruler is able to interact with the growing tip of the needle and the C terminus of EscU. Another possibility is that the GFP+ cleaved from a few EscU molecules allows EscU cleavage to happen but leaves an altered peptide that, although present in lower levels, results in the hyper secretion of EscF or GFP+ cleavage leaves EscU altered in the time it takes for EscU cleavage to occur, resulting in EscF hyper secretion.

It is clear that tagging the T3SS basal apparatus protein EscU interferes with the secretion of EspA, EspD and Tir. Using the experimental data from the project models can be created detailing the different mechanisms that may exist in the wild type strain and the effect of the EscU mutants on the function of EscU.

6.1 What Function does EscU Have in the Wild Type Strain?

From research into the function of the homologous proteins, the role of EscU in EHEC can be extrapolated into models where the cleavage of EscU is a timing mechanism involved in the switching between EscF and EspA secretion. Uncleaved EscU could bind EscF and secrete it through the basal apparatus. EscF has been shown to interact with EscJ, EscD and EscC (Ogino, T., *et al* 2006) and may contribute to the inner rod (shown in the diagram as being composed of EscD) as well as forming the needle structure. Possibly, its interaction with these proteins mediates its passage through the T3SS pore, to the needle where it polymerises. It could be that the first few molecules of EscF could interact with EscC, EscJ and EscD to stabilize the inner rod, with the subsequent molecules passing through the basal apparatus to the needle where they polymerise and extend. This is the simplest of models for EscF secretion, involving no chaperone for EscF or interaction with molecules such as SepL or SepD that mediate the hierarchy of secretion. It is unlikely that EscF does not have a chaperone as it would polymerise within the bacterial cell or be degraded.

In the second model (Fig.99) the EscF interacts with SepL and SepD (Fig.99, A) and then it is translocated (Fig.99, B). A recent hypothesis for the role of SepL and SepD is that they function as a gate at the T3SS. This gate initially allows translocator but not effector proteins to be secreted. Then the completion of the translocon is signalled (possibly by a drop in calcium levels) and the SepL-SepD complex dissociates or changes to allow effector proteins through (Deng, W., *et al* 2005). The SepL-SepD complex may be associated with the C terminus of EscU and EscF is brought to them via a chaperone. It is interesting to speculate that SepL and SepD may play a role in the secretion of EscF as a *sepD* or a *sepL* deletion does not secrete translocon proteins, indicating they are involved at this stage of secretion or the next (EspA secretion).

After EscF has been secreted and the needle has reached the required length, EscF secretion stops and EspA is secreted. In Fig.100, A, the needle length is measured by a protein homologous to the YscP protein in *Yersinia* (possibly Orf16 from the LEE).

This protein translocates through the T3SS and interacts with the tip of the needle. When the needle is of the correct size the interaction at the tip of the needle will place the C terminus of Orf16 (YscP homologue) in close enough proximity to interact with the $EscU_C$ domain, promoting cleavage of $EscU_{CC}$ and a change in substrate-specificity. After this cleavage has occurred the Orf16 protein leaves the T3SS (Fig.100, B). The cleaved portion remains at the basal apparatus interacting with the $EscU_{CN}$ peptide and allows the secretion of translocon proteins to proceed. The secretion of EspA may be linked to SepL and SepD, although no work to date has shown a direct interaction with SepL-SepD and EspA. However, the SepL-SepD complex could interact with *espADB* mRNA, in the presence of a ribosome (Fig.100, C).

Alternatively the cleavage of EscU may happen auto-catalytically, after a set period of time, acting as a timing mechanism. This is independent of a molecular ruler molecule such as Orf16/YscP (Fig.101, A and B). The cleavage alters the substrate-specificity and allows the secretion of EspA via SepD and SepL in a coupled translation and translocation step (Fig.101, C and D). Of course a combination of both models could be possible, the cleavage of EscU could slow down the secretion of the needle proteins giving a molecular ruler time to enter the T3SS and measure the needle. When the needle is of the correct length the molecular ruler interacts with the already cleaved EscU molecule and alters its substrate-specificity, increasing its affinity for filament proteins.

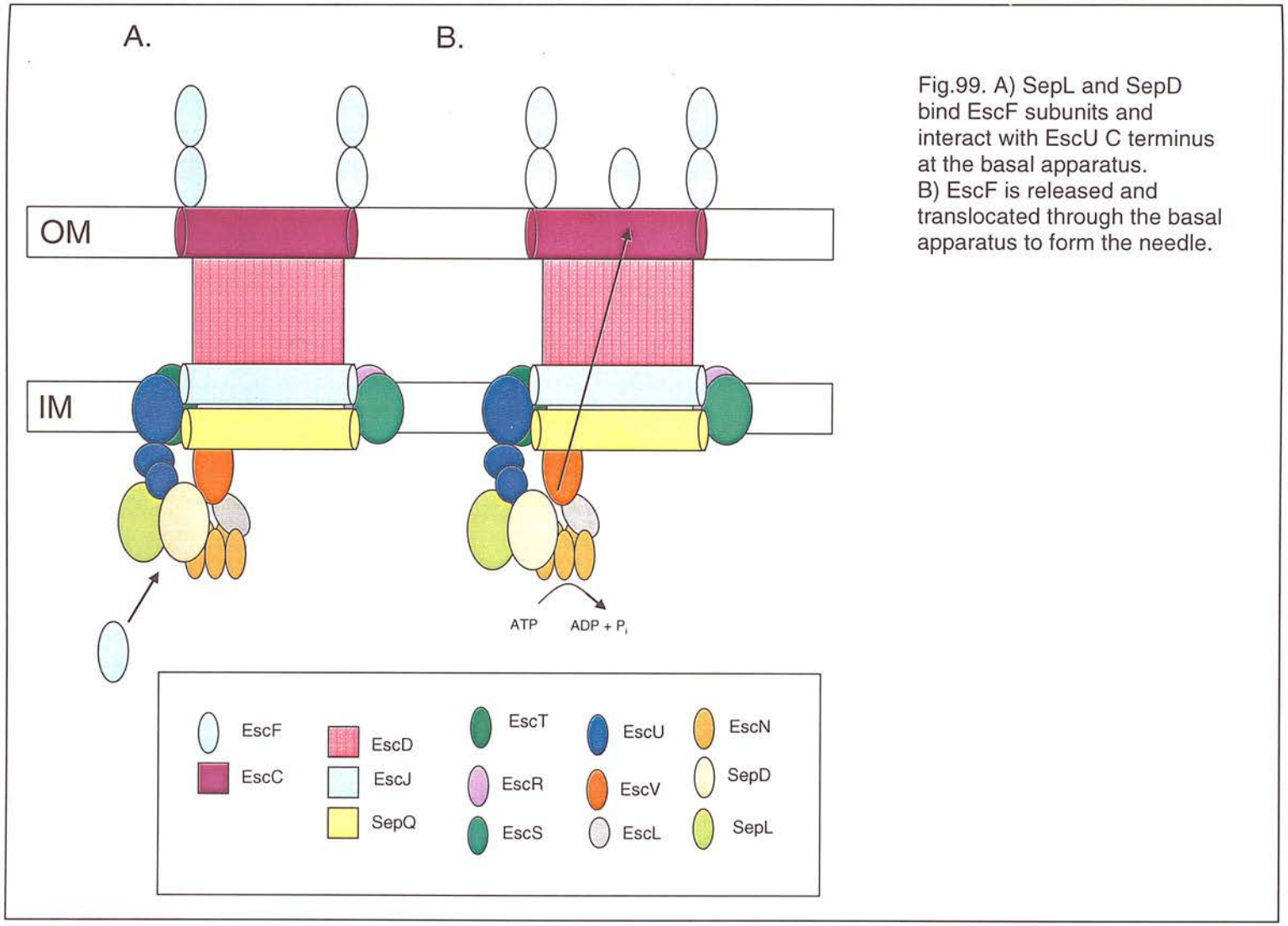

Fig.99. A) SepL and SepD bind EscF subunits and interact with EscU C terminus at the basal apparatus.
B) EscF is released and translocated through the basal apparatus to form the needle.

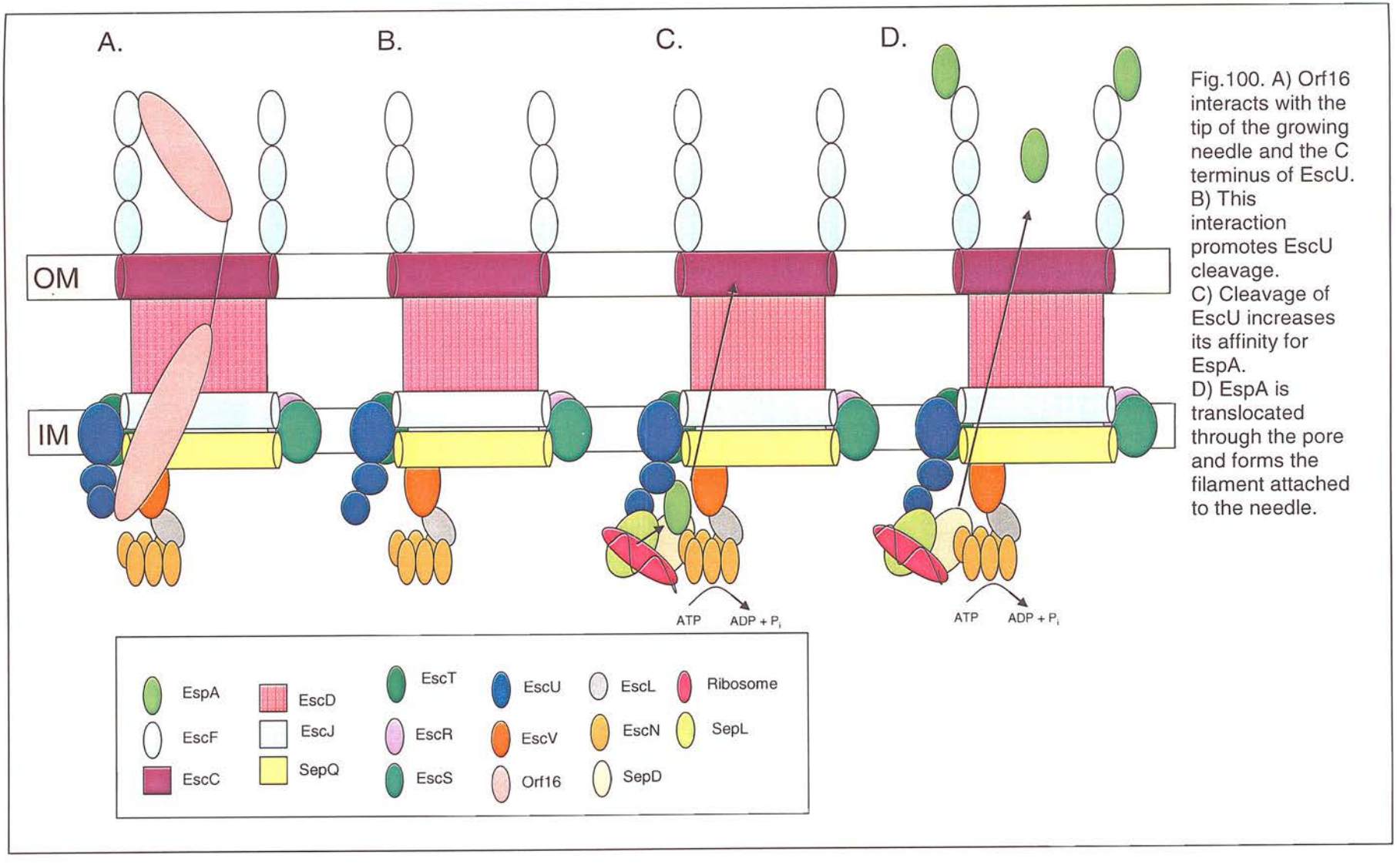

Fig.100. A) Orf16 interacts with the tip of the growing needle and the C terminus of EscU. B) This interaction promotes EscU cleavage. C) Cleavage of EscU increases its affinity for EspA. D) EspA is translocated through the pore and forms the filament attached to the needle.

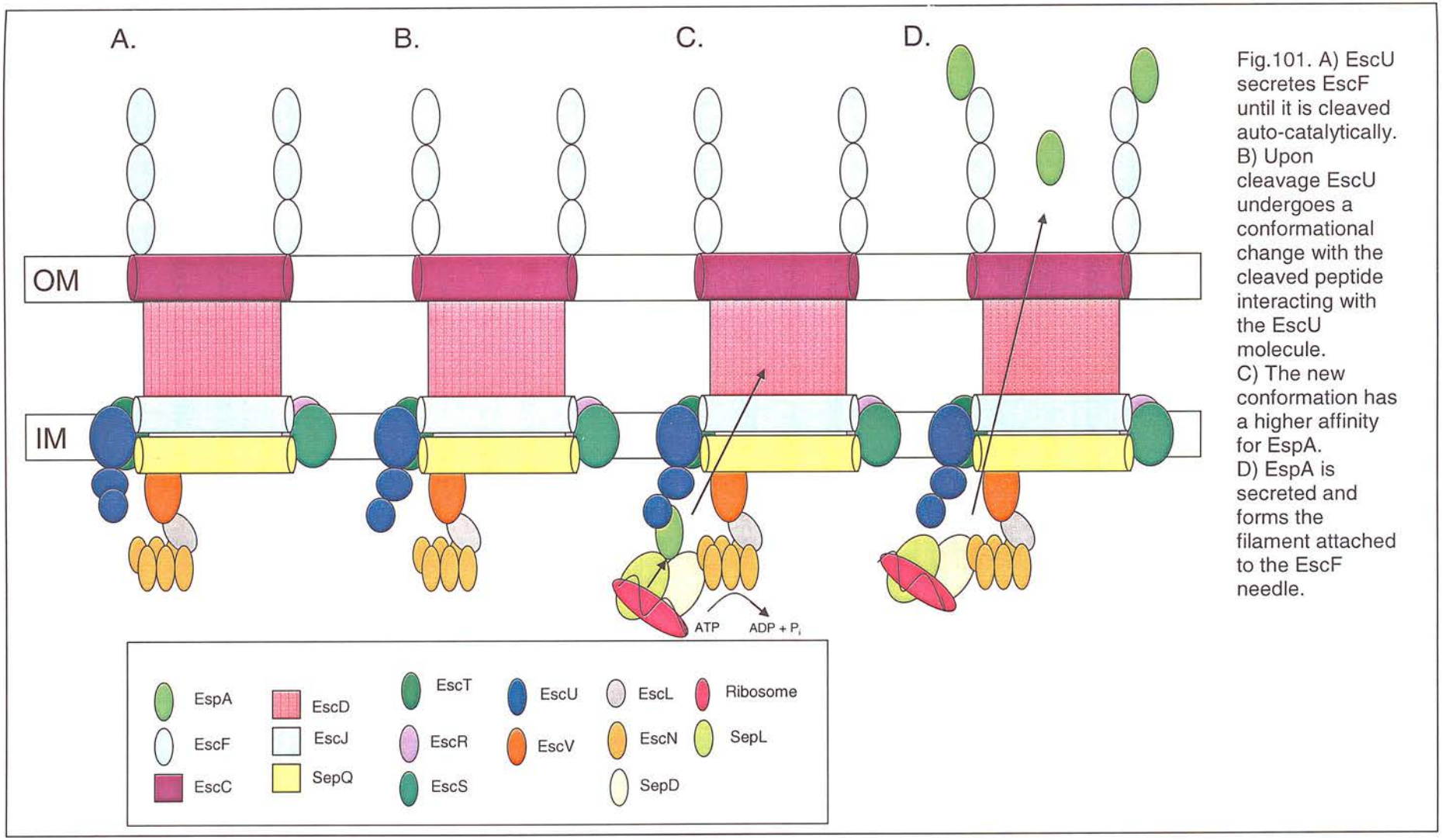

Fig.101. A) EscU secretes EscF until it is cleaved auto-catalytically. B) Upon cleavage EscU undergoes a conformational change with the cleaved peptide interacting with the EscU molecule. C) The new conformation has a higher affinity for EspA. D) EspA is secreted and forms the filament attached to the EscF needle.

The next step in T3S is the secretion of effector proteins. From unpublished work in our laboratory, SepL was shown to directly bind Tir, independent of its binding to SepD and that Tir could potentially be displaced from SepL by EscD. This means that SepL, whilst required for the secretion of EspA, B and D, is also potentially holding back Tir secretion at this stage. LEE4 and LEE5 seem to be expressed at the same time (Roe, A., *et al* 2004) in the same cells and this mechanism may exists to stop Tir secretion before the secretion of EspA, B and D. Following a drop in calcium levels, once a conduit has opened with the host cell (Deng, W., et al 2005) the SepL-SepD complex may dissociate and release Tir for secretion. If SepL can bind Tir with its chaperone CesT then all the effector proteins relying on CesT as a chaperone for export will not be secreted until the SepL-SepD complex dissociates.

6.2 What is the Effect of Tagging EscU?

It is hard to understand what is happening in the mutant strains without an accurate measure of EscF. It is clear that tags, which remain attached to the C terminus of EscU protein, even after cleavage at NPTH, are localised to the membrane. Even so strains containing these fusions do not secrete EspA, EspB, EspD and Tir. Possible explanations for this include:

1) The tags do not allow the correct assembly of the T3SS, auto-catalytic cleavage still occurs but no proteins are secreted. However, proteins that are inserted into the membrane in a Sec-dependent, T3SS independent, manner will be present in the membrane. These include EscV in the inner membrane and EscC in the periplasm. It has also been demonstrated that EscJ and EscU are localised to the membrane in the tagged mutants. In the presence of EscN the EscC molecules can be inserted into the outer membrane. This would indicate that EscN, EscV, EscJ, EscC and EscU are all localized correctly implying that the basal apparatus is formed. The presence of some secretion in the GFP+ tagged strain (Walla3 *escU<>escU*$_{cc::gfp+}$) adds evidence to this assumption
2) The tags are interfering with the function of EscU in the secretion of EscF. Conformational changes in EscU from the addition of the tag do not allow

EscF to be secreted. If EscF is not secreted then the substrate-specificity of EscU cannot be changed, so EscU does not interact with filament proteins and the SepL-SepD complex.

3) EscF is secreted onto the cell surface but cleavage of EscU does not happen normally, either earlier or later, and the resulting strain cannot interact with the molecular ruler to increase its affinity for filament proteins.
4) EscF is secreted onto the cell surface and cleavage happens normally, but the presence of the tags interferes with the ability of EscU to interact with filament proteins and the SepL-SepD complex.

It is apparent that a number of check points exist for the T3SS and multiple protein interactions occur with varying and changeable affinities to control sequential secretion. The T3SS has evolved to be tightly regulated and timed so that the basal apparatus are in place before the needle is formed, then the filament proteins secreted followed by the effector proteins. Proteins that regulate expression, chaperones, gating proteins and calcium signals all aid to form the T3SS in logical steps. It is not surprising that EscU may function as a switch and timing mechanism in this process, as it is important for the bacteria to form the complete T3SS in a precise manner at the right time and correct place.

This project was unsuccessful in realising its initial aims. Instead it went on to demonstrate that the amount of EscR and EscU in the basal apparatus of the T3SS is too low to make GFP+, eGFP and HA fusions a viable approach for microscopy or single cell work. It also highlighted the fact that even a nine amino acid addition into one of these proteins is enough to disrupt function. This may not be an unexpected result when considering how conserved the basal apparatus genes are amongst T3SSs in Gram negative bacteria. The project evolved to look at the tagged strains containing *escU* mutants, which has interesting homologues in the flagellar system and *Yersinia* T3SS. However, even this analysis was rife with problems including antibody specificity and complementation issues. The results can be interpreted to form models where EscU may act in a similar manner to its homologues but more work is needed to validate its role.

6.3 Future Work

The work with EscU and its role in the secretion of EscF inspires most of the future work for this project and is ongoing in the ZAP lab.

The anti EscF antibody did not function as hoped, even after attempts to absorb it against the *escF* deletion. Although previous published attempts to make anti EscF antibodies have failed (Wilson, R., *et al* 2001); it remains an avenue to consider as a good anti EscF antibody would be invaluable to this work. A His tag fusion to EscF has been created in the ZAP laboratory, with the intention to use it for the production of antibodies. Also an anti EscF antibody, published by Cook, S., *et al* 2007, will hopefully be acquired for use in the ZAP laboratory. The antibody will be used to see whether tagging EscU or EscU deletions have an effect on the amount of EscF secreted into the supernatant. It would be good to verify that the increase seen in Walla3 *escU<>escU*$_{cc::gfp+}$ is EscF. If the protein is not EscF it would be interesting to find out what protein has been effected so dramatically. It may be possible to MALDI-TOF the band from an SDS PAGE gel to identify the protein, or run samples on two dimensional SDS PAGE gels to better clarify its mass and pI. Obviously the antibodies, if successful will be used for microscopy. This would give an insight into whether the formation of the EscF needle is phase variable, only happening in a subset of bacteria, or whether all the bacteria, in T3SS permissive conditions, contain EscF needles.

Unfortunately, research in our laboratory (by Mr. Dai Wang) has shown that when EscF is fused to a His tag and artificially expressed it cannot be detected. The EscF fusion was not detected in the cytoplasm or the supernatant of strains with the plasmid, indicating the mRNA was unstable and not translated. Fusions to *bla* were also created with an identical outcome. If a plasmid fusion to EscF could be constructed and the protein detected, it could be expressed in the wild type strain to see if there is an increase in secretion of EscF from the cell. It would be interesting to see whether increasing the amount of EscF in the cell has the same phenotype as secreting wild type levels of EscF through fewer T3SS (as may be the case for Walla3 *escU<>escU*$_{cc::gfp+}$). This would help determine whether there is a timing

mechanism that stops EscF secretion no matter how much EscF is in the bacterial cell, or whether the controls for the EscF secretion can be by-passed with increased cellular EscF. If EscF continues to be secreted from a wild type strain with an EscF plasmid and no switching occurs to filament proteins then it may indicate that EscF is secreted until the 'pool' of EscF runs out. However, in the strain Walla3 *escU<>escU*$_{cc::gfp+}$ the 'pool' of EscF is the same as in the wild type, yet EscF secretion is higher, indicating a more complex mechanism than this.

Our laboratory's inability to create an EscF plasmid fusion that works may indicate the need for a single copy approach; however, personal communication with Prof. Gad Frankel's group in Imperial College, London indicated that tagging EscF disrupts its ability to polymerise and form the needle structure. This may not be surprising, given the effect of the HA tag on EscU, combined with the small size of EscF. This needs to be kept in mind when manipulating the gene and stresses the need for a working antibody.

If the Walla3 *escU<>escU*$_{cc::gfp+}$ strain is secreting more EscF, forming longer needles and secreting some EspA/D/B, then it could be possible to stain the ZAP1142 strain with anti EspA antibody (Crepin, V., *et al* 2005) and use gold conjugated secondary antibody for electron microscopy. If there were T3SSs with long needles and small filaments the T3SS could be detected by the EspA antibody and the needle distinguished from the filament by the lack of gold labelling. However, if the strain produced long needles without EspA filaments then the needles would still have to be identified as T3SS associated, which would be difficult with the current antibodies available. Alternatively the method for basal apparatus preparations (Ogino, T *et al* 2006) could be used to isolate the basal apparatus and compare needle length with electron microscopy.

Creating defined EscF mutants that polymerised slower than wild type EscF and exchanging the genes for these mutants onto the chromosome, replacing the wild type sequence, could help answer questions about the timing mechanism of EscF secretion. If EscU cleavage acts as a molecular clock then the slower polymerising

EscF would lead to shorter needles, a phenotype that may be overcome by over expressing the mutant EscF from a plasmid.

Fusions to *escU* could be created on a plasmid and the autoradiogram method (described in Minamino, T., *et al* 2000) used to see if the fusions effect the timing of the cleavage, a possible explanation for the potential increase in the amount of EscF secreted in Walla3 *escU*<>*escU*$_{cc::gfp+}$. This method requires making the fusion gene on a plasmid under an inducible promoter and expressing it in the presence of radioactively labelled amino acids for a set length of time. Determining what proportion of the protein is in the uncleaved form compared to the cleaved form indicates the time it takes for the protein to undergo cleavage.

His tag protein column purification experiments could be carried out with the cleaved peptide EscU$_{CC}$, running whole cell preparations of the Walla3 strain, the Walla3 *escU*<>*escU*$_{\Delta cc}$ strain (without the EscU$_{CC}$ peptide) and the Walla3 *escRSTU*<>*sac*/Kan strain through the column. The proteins eluted from the column that interact with the EscU$_{CC}$ peptide could help explain its observed membrane localisation. SepD and SepL localize to the membrane independent of *escRSTU* (work carried out by Mr. Dai Wang). It could be the case that SepD and SepL mediate EspA secretion in conjunction with EscU by interacting with the EscU$_{CC}$ peptide and in the absence of the EscU molecule the EscU$_{CC}$ peptide is localised to the membrane by an interaction with SepD and SepL. The co-purification experiments, in the absence of the genes *escRSTU,* may shed light on the process of the EscU switching from EscF to EspA secretion by identifying other proteins the EscU$_{CC}$ domain is capable of interacting with.

As mentioned in the introduction, the LEE encoded gene *orf16* may be the EHEC O157:H7 homologue to YscP and FliK (the molecular rulers that interact with YscU and FlhB, respectively) (Pallen, M., *et al* 2005). If this was the case then the Orf16 protein would be expected to interact with EscF and EscU. It would be interesting to see whether the Orf16 protein is expressed and where it localizes during T3S. Orf16 could also be used in His tag protein column purifications to see what proteins co-

purify with the His tagged Orf16. If Orf16 is a molecular ruler then can it be lengthened to created longer needles in EHEC? This was carried out with great success in *Yersinia* T3SS, proving a direct link between YscP length and the length of the needle (Journet, L., *et al* 2003). It would be assumed that an *orf16* deletion would not secrete EspA and carry on secreting EscF, if it acted as a molecular ruler, as there would be no mechanism for substrate-specificity switching. Deleting *orf16* and characterising the mutant phenotype, especially if an anti EscF antibody was available, would be an interesting experiment to carry out to determine its role in needle length.

The literature for FlhB and YscU contain numerous examples of defined mutants that helped clarify FlhB and YscU as molecular timers and switches in secretion (see section 1.3.5.9). This literature could be used to create similar mutants in EscU and observe the effect these have on EscF secretion and needle formation, once a measure for EscF secretion has been devised. Some of the most interesting mutants used in YscU work substituted amino acids in the NPTH cleavage site and altered the proteins ability to cleave (Lavander, M., *et al* 2002).

It is possible that other tags could be used to label the basal apparatus, or alternative positions found to place the tags. For example, an HA tag fused to the C terminus of the EscU protein may be able to secrete, as a similar plasmid construct in *Yersinia* was able to exert an effect on the *Yersinia* T3SS (Lavander, M., *et al* 2002). Other tags that exist include a tag that binds specifically to a CC-XX-CC motif in a protein (where C is a cysteine and X is any amino acid) (Selvin, P., 2002) and the Flash and ReAsh tagging method (Lebrasseur, N., *et al* 2002). However, the results from this project indicate that all tags added to the basal apparatus would interfere with T3S.

Possibly a more productive route would be using the basal apparatus proteins, or parts of them, to create antibodies. A good repertoire of antibodies raised against soluble fractions or small peptides from the basal apparatus proteins may lead to a more efficient tagging method without interfering with secretion.

Chapter 7
References

Abe, A., de Grado, M., Pfuetzner, R. A., Sanchez-Sanmartin, C., *et al.* (1999). Enteropathogenic Escherichia coli translocated intimin receptor, Tir, requires a specific chaperone for stable secretion. *Mol Microbiol, 33*(6), 1162-1175.

Abe, A., Heczko, U., Hegele, R. G., & Brett Finlay, B. (1998). Two enteropathogenic Escherichia coli type III secreted proteins, EspA and EspB, are virulence factors. *J Exp Med, 188*(10), 1907-1916.

Agrain, C., Sorg, I., Paroz, C., & Cornelis, G. R. (2005). Secretion of YscP from Yersinia enterocolitica is essential to control the length of the injectisome needle but not to change the type III secretion substrate specificity. *Mol Microbiol, 57*(5), 1415-1427.

Ahmer, B. M. (2004). Cell-to-cell signalling in Escherichia coli and Salmonella enterica. *Mol Microbiol, 52*(4), 933-945.

Ahmer, B. M., van Reeuwijk, J., Timmers, C. D., Valentine, P. J., *et al.* (1998). Salmonella typhimurium encodes an SdiA homolog, a putative quorum sensor of the LuxR family, that regulates genes on the virulence plasmid. *J Bacteriol, 180*(5), 1185-1193.

Allaoui, A., Schulte, R., & Cornelis, G. R. (1995). Mutational analysis of the Yersinia enterocolitica virC operon: characterization of yscE, F, G, I, J, K required for Yop secretion and yscH encoding YopR. *Mol Microbiol, 18*(2), 343-355.

Allaoui, A., Woestyn, S., Sluiters, C., & Cornelis, G. R. (1994). YscU, a Yersinia enterocolitica inner membrane protein involved in Yop secretion. *J Bacteriol, 176*(15), 4534-4542.

Ando, H., Abe, H., Sugimoto, N., & Tobe, T. (2007). Maturation of functional type III secretion machinery by activation of anaerobic respiration in enterohaemorrhagic Escherichia coli. *Microbiology, 153*(Pt 2), 464-473.

Andrade, A., Pardo, J. P., Espinosa, N., Perez-Hernandez, G., *et al.* (2007). Enzymatic characterization of the enteropathogenic Escherichia coli type III secretion ATPase EscN. *Arch Biochem Biophys, 468*(1), 121-127.

Auvray, F., Ozin, A. J., Claret, L., & Hughes, C. (2002). Intrinsic membrane targeting of the flagellar export ATPase FliI: interaction with acidic phospholipids and FliH. *J Mol Biol, 318*(4), 941-950.

Barba, J., Bustamante, V. H., Flores-Valdez, M. A., Deng, W., *et al.* (2005). A positive regulatory loop controls expression of the locus of enterocyte effacement-encoded regulators Ler and GrlA. *J Bacteriol, 187*(23), 7918-7930.

Bauer, M. E., & Welch, R. A. (1996). Characterization of an RTX toxin from enterohemorrhagic Escherichia coli O157:H7. *Infect Immun, 64*(1), 167-175.

Beery, J. T., Doyle, M. P., & Schoeni, J. L. (1985). Colonization of chicken cecae by Escherichia coli associated with hemorrhagic colitis. *Appl Environ Microbiol, 49*(2), 310-315.

Beltrametti, F., Kresse, A. U., & Guzman, C. A. (1999). Transcriptional regulation of the esp genes of enterohemorrhagic Escherichia coli. *J Bacteriol, 181*(11), 3409-3418.

Berdichevsky, T., Friedberg, D., Nadler, C., Rokney, A., *et al.* (2005). Ler is a negative autoregulator of the LEE1 operon in enteropathogenic Escherichia coli. *J Bacteriol, 187*(1), 349-357.

Beutin, L., Gleier, K., Kontny, I., Echeverria, P., *et al.* (1997). Origin and characteristics of enteroinvasive strains of Escherichia coli (EIEC) isolated in Germany. *Epidemiol Infect, 118*(3), 199-205.

Bielaszewska, M., Friedrich, A. W., Aldick, T., Schurk-Bulgrin, R., *et al.* (2006). Shiga toxin activatable by intestinal mucus in Escherichia coli isolated from humans: predictor for a severe clinical outcome. *Clin Infect Dis, 43*(9), 1160-1167.

Blaylock, B., Riordan, K. E., Missiakas, D. M., & Schneewind, O. (2006). Characterization of the Yersinia enterocolitica type III secretion ATPase YscN and its regulator, YscL. *J Bacteriol, 188*(10), 3525-3534.

Blocker, A., Komoriya, K., & Aizawa, S. (2003). Type III secretion systems and bacterial flagella: insights into their function from structural similarities. *Proc Natl Acad Sci U S A, 100*(6), 3027-3030.

Blomfield, I. C., Vaughn, V., Rest, R. F., Eisenstein, B. I., *et al.* (1991). Allelic exchange in Escherichia coli using the Bacillus subtilis sacB gene and a temperature-sensitive pSC101 replicon. *Mol Microbiol, 5*(6), 1447-1457.

Boerlin, P., McEwen, S. A., Boerlin-Petzold, F., Wilson, J. B., *et al.* (1999). Associations between virulence factors of Shiga toxin-producing Escherichia coli and disease in humans. *J Clin Microbiol, 37*(3), 497-503.

Bongaerts, R. J., Hautefort, I., Sidebotham, J. M., & Hinton, J. C. (2002). Green fluorescent protein as a marker for conditional gene expression in bacterial cells. *Methods Enzymol, 358*, 43-66.

Borczyk, A. A., Karmali, M. A., Lior, H., & Duncan, L. M. (1987). Bovine reservoir for verotoxin-producing Escherichia coli O157:H7. *Lancet, 1*(8524), 98.

Brady, M. J., Campellone, K. G., Ghildiyal, M., & Leong, J. M. (2007). Enterohaemorrhagic and enteropathogenic Escherichia coli Tir proteins trigger a common Nck-independent actin assembly pathway. *Cell Microbiol, 9*(9), 2242-2253.

Brewster, D. H., Brown, M. I., Robertson, D., Houghton, G. L., *et al.* (1994). An outbreak of Escherichia coli O157 associated with a children's paddling pool. *Epidemiol Infect, 112*(3), 441-447.

Brothers, S. P., Janovick, J. A., & Conn, P. M. (2003). Unexpected effects of epitope and chimeric tags on gonadotropin-releasing hormone receptors: implications for understanding the molecular etiology of hypogonadotropic hypogonadism. *J Clin Endocrinol Metab, 88*(12), 6107-6112.

Campellone, K. G., Brady, M. J., Alamares, J. G., Rowe, D. C., *et al.* (2006). Enterohaemorrhagic Escherichia coli Tir requires a C-terminal 12-residue peptide to initiate EspF-mediated actin assembly and harbours N-terminal sequences that influence pedestal length. *Cell Microbiol, 8*(9), 1488-1503.

Campellone, K. G., & Leong, J. M. (2003). Tails of two Tirs: actin pedestal formation by enteropathogenic E. coli and enterohemorrhagic E. coli O157:H7. *Curr Opin Microbiol, 6*(1), 82-90.

Campellone, K. G., Rankin, S., Pawson, T., Kirschner, M. W., *et al.* (2004). Clustering of Nck by a 12-residue Tir phosphopeptide is sufficient to trigger localized actin assembly. *J Cell Biol, 164*(3), 407-416.

Carrillo, C. D., Taboada, E., Nash, J. H., Lanthier, P., *et al.* (2004). Genome-wide expression analyses of Campylobacter jejuni NCTC11168 reveals coordinate regulation of motility and virulence by flhA. *J Biol Chem, 279*(19), 20327-20338.

Castillo, A., Eguiarte, L. E., & Souza, V. (2005). A genomic population genetics analysis of the pathogenic enterocyte effacement island in Escherichia coli: the search for the unit of selection. *Proc Natl Acad Sci U S A, 102*(5), 1542-1547.

Cha, H. J., Srivastava, R., Vakharia, V. N., Rao, G., *et al.* (1999). Green fluorescent protein as a noninvasive stress probe in resting Escherichia coli cells. *Appl Environ Microbiol, 65*(2), 409-414.

Chiu, H. J., & Syu, W. J. (2005). Functional analysis of EspB from enterohaemorrhagic Escherichia coli. *Microbiology, 151*(Pt 10), 3277-3286.

Clarke, S. C., Haigh, R. D., Freestone, P. P., & Williams, P. H. (2003). Virulence of enteropathogenic Escherichia coli, a global pathogen. *Clin Microbiol Rev, 16*(3), 365-378.

Cobbold, R. N., Hancock, D. D., Rice, D. H., Berg, J., *et al.* (2007). Rectoanal junction colonization of feedlot cattle by Escherichia coli O157:H7 and its association with supershedders and excretion dynamics. *Appl Environ Microbiol, 73*(5), 1563-1568.

Cook, S. R., Maiti, P. K., DeVinney, R., Allen-Vercoe, E., *et al.* (2007). Avian- and mammalian-derived antibodies against adherence-associated proteins inhibit host cell colonization by Escherichia coli O157:H7. *J Appl Microbiol, 103*(4), 1206-1219.

Creasey, E. A., Delahay, R. M., Daniell, S. J., & Frankel, G. (2003). Yeast two-hybrid system survey of interactions between LEE-encoded proteins of enteropathogenic Escherichia coli. *Microbiology, 149*(Pt 8), 2093-2106.

Creasey, E. A., Friedberg, D., Shaw, R. K., Umanski, T., *et al.* (2003b). CesAB is an enteropathogenic Escherichia coli chaperone for the type-III translocator proteins EspA and EspB. *Microbiology, 149*(Pt 12), 3639-3647.

Crepin, V. F., Shaw, R., Abe, C. M., Knutton, S., *et al.* (2005). Polarity of enteropathogenic Escherichia coli EspA filament assembly and protein secretion. *J Bacteriol, 187*(8), 2881-2889.

Daniell, S. J., Delahay, R. M., Shaw, R. K., Hartland, E. L., *et al.* (2001). Coiled-coil domain of enteropathogenic Escherichia coli type III secreted protein EspD is involved in EspA filament-mediated cell attachment and hemolysis. *Infect Immun, 69*(6), 4055-4064.

Daniell, S. J., Takahashi, N., Wilson, R., Friedberg, D., *et al.* (2001b). The filamentous type III secretion translocon of enteropathogenic Escherichia coli. *Cell Microbiol, 3*(12), 865-871.

Day, J. B., Guller, I., & Plano, G. V. (2000). Yersinia pestis YscG protein is a Syc-like chaperone that directly binds yscE. *Infect Immun, 68*(11), 6466-6471.

Day, N. P., Scotland, S. M., Cheasty, T., & Rowe, B. (1983). Escherichia coli O157:H7 associated with human infections in the United Kingdom. *Lancet, 1*(8328), 825.

Dean, P., Maresca, M., Schuller, S., Phillips, A. D., *et al.* (2006). Potent diarrheagenic mechanism mediated by the cooperative action of three enteropathogenic Escherichia coli-injected effector proteins. *Proc Natl Acad Sci U S A, 103*(6), 1876-1881.

Deng, W., Li, Y., Hardwidge, P. R., Frey, E. A., *et al.* (2005). Regulation of type III secretion hierarchy of translocators and effectors in attaching and effacing bacterial pathogens. *Infect Immun, 73*(4), 2135-2146.

Deng, W., Puente, J. L., Gruenheid, S., Li, Y., *et al.* (2004). Dissecting virulence: systematic and functional analyses of a pathogenicity island. *Proc Natl Acad Sci U S A, 101*(10), 3597-3602.

DeVinney, R., Stein, M., Reinscheid, D., Abe, A., *et al.* (1999). Enterohemorrhagic Escherichia coli O157:H7 produces Tir, which is translocated to the host cell membrane but is not tyrosine phosphorylated. *Infect Immun, 67*(5), 2389-2398.

Dipineto, L., Santaniello, A., Fontanella, M., Lagos, K., *et al.* (2006). Presence of Shiga toxin-producing Escherichia coli O157:H7 in living layer hens. *Lett Appl Microbiol, 43*(3), 293-295.

Donnenberg, M. S., & Kaper, J. B. (1992). Enteropathogenic Escherichia coli. *Infect Immun, 60*(10), 3953-3961.

Dziva, F., Mahajan, A., Cameron, P., Currie, C., *et al.* (2007). EspP, a Type V-secreted serine protease of enterohaemorrhagic Escherichia coli O157:H7, influences intestinal colonization of calves and adherence to bovine primary intestinal epithelial cells. *FEMS Microbiol Lett, 271*(2), 258-264.

Dziva, F., van Diemen, P. M., Stevens, M. P., Smith, A. J., *et al.* (2004). Identification of Escherichia coli O157 : H7 genes influencing colonization of the bovine gastrointestinal tract using signature-tagged mutagenesis. *Microbiology, 150*(Pt 11), 3631-3645.

Ebel, F., Podzadel, T., Rohde, M., Kresse, A. U., *et al.* (1998). Initial binding of Shiga toxin-producing Escherichia coli to host cells and subsequent induction of actin rearrangements depend on filamentous EspA-containing surface appendages. *Mol Microbiol, 30*(1), 147-161.

Edqvist, P. J., Olsson, J., Lavander, M., Sundberg, L., *et al.* (2003). YscP and YscU regulate substrate specificity of the Yersinia type III secretion system. *J Bacteriol, 185*(7), 2259-2266.

Elliott, S. J., Krejany, E. O., Mellies, J. L., Robins-Browne, R. M., *et al.* (2001). EspG, a novel type III system-secreted protein from enteropathogenic Escherichia coli with similarities to VirA of Shigella flexneri. *Infect Immun, 69*(6), 4027-4033.

Elliott, S. J., O'Connell, C. B., Koutsouris, A., Brinkley, C., *et al.* (2002). A gene from the locus of enterocyte effacement that is required for enteropathogenic Escherichia coli to increase tight-junction permeability encodes a chaperone for EspF. *Infect Immun, 70*(5), 2271-2277.

Elliott, S. J., Sperandio, V., Giron, J. A., Shin, S., *et al.* (2000). The locus of enterocyte effacement (LEE)-encoded regulator controls expression of both LEE- and non-LEE-encoded virulence factors in enteropathogenic and enterohemorrhagic Escherichia coli. *Infect Immun, 68*(11), 6115-6126.

Elliott, S. J., Wainwright, L. A., McDaniel, T. K., Jarvis, K. G., *et al.* (1998). The complete sequence of the locus of enterocyte effacement (LEE) from enteropathogenic Escherichia coli E2348/69. *Mol Microbiol, 28*(1), 1-4.

Elliott, S. J., Yu, J., & Kaper, J. B. (1999). The cloned locus of enterocyte effacement from enterohemorrhagic Escherichia coli O157:H7 is unable to confer the attaching and effacing phenotype upon E. coli K-12. *Infect Immun, 67*(8), 4260-4263.

Emmerson, J. R., Gally, D. L., & Roe, A. J. (2006). Generation of gene deletions and gene replacements in Escherichia coli O157:H7 using a temperature sensitive allelic exchange system. *Biol Proced Online, 8*, 153-162.

Fadouloglou, V. E., Tampakaki, A. P., Glykos, N. M., Bastaki, M. N., *et al.* (2004). Structure of HrcQB-C, a conserved component of the bacterial type III secretion systems. *Proc Natl Acad Sci U S A, 101*(1), 70-75.

Fan, F., Ohnishi, K., Francis, N. R., & Macnab, R. M. (1997). The FliP and FliR proteins of Salmonella typhimurium, putative components of the type III flagellar export apparatus, are located in the flagellar basal body. *Mol Microbiol, 26*(5), 1035-1046.

Feng, P. (1995). Escherichia coli serotype O157:H7: novel vehicles of infection and emergence of phenotypic variants. *Emerg Infect Dis, 1*(2), 47-52.

Ferris, H., & Minamino, T. (2006). Flipping the switch: bringing order to flagellar assembly. *Trends in Micro*, **14**(12), 519-526.

Finlay, B. B., Ruschkowski, S., Kenny, B., Stein, M., *et al.* (1996). Enteropathogenic E. coli exploitation of host epithelial cells. *Ann N Y Acad Sci, 797*, 26-31.

Frankel, G., Phillips, A. D., Rosenshine, I., Dougan, G., *et al.* (1998). Enteropathogenic and enterohaemorrhagic Escherichia coli: more subversive elements. *Mol Microbiol, 30*(5), 911-921.

Fraser, M. E., Fujinaga, M., Cherney, M. M., Melton-Celsa, A. R., *et al.* (2004). Structure of shiga toxin type 2 (Stx2) from Escherichia coli O157:H7. *J Biol Chem, 279*(26), 27511-27517.

Friedberg, D., Umanski, T., Fang, Y., & Rosenshine, I. (1999). Hierarchy in the expression of the locus of enterocyte effacement genes of enteropathogenic Escherichia coli. *Mol Microbiol, 34*(5), 941-952.

Galletta, B. J., Chuang, D. Y., & Cooper, J. A. (2008). Distinct Roles for Arp2/3 Regulators in Actin Assembly and Endocytosis. *PLoS Biol, 6*(1), e1.

Garcia-Aljaro, C., Muniesa, M., Jofre, J., & Blanch, A. R. (2004). Prevalence of the stx2 gene in coliform populations from aquatic environments. *Appl Environ Microbiol, 70*(6), 3535-3540.

Gauthier, A., & Finlay, B. B. (2003). Translocated intimin receptor and its chaperone interact with ATPase of the type III secretion apparatus of enteropathogenic Escherichia coli. *J Bacteriol, 185*(23), 6747-6755.

Gauthier, A., Puente, J. L., & Finlay, B. B. (2003b). Secretin of the enteropathogenic Escherichia coli type III secretion system requires components of the type III apparatus for assembly and localization. *Infect Immun, 71*(6), 3310-3319.

Ghosh, P. (2004). Process of protein transport by the type III secretion system. *Microbiol Mol Biol Rev, 68*(4), 771-795.

Goffaux, F., China, B., Janssen, L., Pirson, V., *et al.* (1999). The locus for enterocyte effacement (LEE) of enteropathogenic Escherichia coli (EPEC) from dogs and cats. *Adv Exp Med Biol, 473*, 129-136.

Goffaux, F., China, B., & Mainil, J. (2001). Organisation and in vitro expression of esp genes of the LEE (locus of enterocyte effacement) of bovine enteropathogenic and enterohemorrhagic Escherichia coli. *Vet Microbiol, 83*(3), 275-286.

Goosney, D. L., DeVinney, R., & Finlay, B. B. (2001). Recruitment of cytoskeletal and signaling proteins to enteropathogenic and enterohemorrhagic Escherichia coli pedestals. *Infect Immun, 69*(5), 3315-3322.

Green, N., Alexander, H., Olson, A., Alexander, S., *et al.* (1982). Immunogenic structure of the influenza virus hemagglutinin. *Cell, 28*(3), 477-487.

Gruenheid, S., & Finlay, B. B. (2003). Microbial pathogenesis and cytoskeletal function. *Nature, 422*(6933), 775-781.

Grys, T. E., Siegel, M. B., Lathem, W. W., & Welch, R. A. (2005). The StcE protease contributes to intimate adherence of enterohemorrhagic Escherichia coli O157:H7 to host cells. *Infect Immun, 73*(3), 1295-1303.

Haddad, J. E., & Jackson, M. P. (1993). Identification of the Shiga toxin A-subunit residues required for holotoxin assembly. *J Bacteriol, 175*(23), 7652-7657.

Hardwidge, P. R., Deng, W., Vallance, B. A., Rodriguez-Escudero, I., *et al.* (2005). Modulation of host cytoskeleton function by the enteropathogenic Escherichia coli and Citrobacter rodentium effector protein EspG. *Infect Immun, 73*(5), 2586-2594.

Hartland, E. L., Daniell, S. J., Delahay, R. M., Neves, B. C., *et al.* (2000). The type III protein translocation system of enteropathogenic Escherichia coli involves EspA-EspB protein interactions. *Mol Microbiol, 35*(6), 1483-1492.

Hensel, M., Shea, J. E., Raupach, B., Monack, D., *et al.* (1997). Functional analysis of ssaJ and the ssaK/U operon, 13 genes encoding components of the type III secretion apparatus of Salmonella Pathogenicity Island 2. *Mol Microbiol, 24*(1), 155-167.

Hilborn, E. D., Mshar, P. A., Fiorentino, T. R., Dembek, Z. F., *et al.* (2000). An outbreak of Escherichia coli O157:H7 infections and haemolytic uraemic syndrome associated with consumption of unpasteurized apple cider. *Epidemiol Infect, **124***(1), 31-36.

Hirano, T., Yamaguchi, S., Oosawa, K., & Aizawa, S. (1994). Roles of FliK and FlhB in determination of flagellar hook length in Salmonella typhimurium. *J Bacteriol, **176***(17), 5439-5449.

Hoey, D. E., Currie, C., Else, R. W., Nutikka, A., *et al.* (2002). Expression of receptors for verotoxin 1 from Escherichia coli O157 on bovine intestinal epithelium. *J Med Microbiol, **51***(2), 143-149.

Hoey, D. E., Sharp, L., Currie, C., Lingwood, C. A., *et al.* (2003). Verotoxin 1 binding to intestinal crypt epithelial cells results in localization to lysosomes and abrogation of toxicity. *Cell Microbiol, **5***(2), 85-97.

Holden, N., Totsika, M., Dixon, L., Catherwood, K., *et al.* (2007). Regulation of P-fimbrial phase variation frequencies in Escherichia coli CFT073. *Infect Immun, **75***(7), 3325-3334.

Honda, T. (1999). Factors influencing the development of hemolytic uremic syndrome caused by enterohemorrhagic Escherichia coli infection: from a questionnaire survey to in vitro experiment. *Pediatr Int, **41***(2), 209-212.

Hrudey, S. E., Payment, P., Huck, P. M., Gillham, R. W., *et al.* (2003). A fatal waterborne disease epidemic in Walkerton, Ontario: comparison with other waterborne outbreaks in the developed world. *Water Sci Technol, **47***(3), 7-14.

Hueck, C. J. (1998). Type III protein secretion systems in bacterial pathogens of animals and plants. *Microbiol Mol Biol Rev, **62***(2), 379-433.

Hurley, B. P., Jacewicz, M., Thorpe, C. M., Lincicome, L. L., *et al.* (1999). Shiga toxins 1 and 2 translocate differently across polarized intestinal epithelial cells. *Infect Immun, **67***(12), 6670-6677.

Ide, T., Laarmann, S., Greune, L., Schillers, H., *et al.* (2001). Characterization of translocation pores inserted into plasma membranes by type III-secreted Esp proteins of enteropathogenic Escherichia coli. *Cell Microbiol, **3***(10), 669-679.

Iizumi, Y., Sagara, H., Kabe, Y., Azuma, M., *et al.* (2007). The enteropathogenic E. coli effector EspB facilitates microvillus effacing and antiphagocytosis by inhibiting myosin function. *Cell Host Microbe, **2***(6), 383-392.

Iyoda, S., Koizumi, N., Satou, H., Lu, Y., *et al.* (2006). The GrlR-GrlA regulatory system coordinately controls the expression of flagellar and LEE-encoded type III protein secretion systems in enterohemorrhagic Escherichia coli. *J Bacteriol, **188***(16), 5682-5692.

Jacewicz, M. S., Acheson, D. W., Binion, D. G., West, G. A., *et al.* (1999). Responses of human intestinal microvascular endothelial cells to Shiga toxins 1 and 2 and pathogenesis of hemorrhagic colitis. *Infect Immun, **67***(3), 1439-1444.

Jarvik, J. W., & Telmer, C. A. (1998). Epitope tagging. *Annu Rev Genet, **32***, 601-618.

Jepson, M. A., Pellegrin, S., Peto, L., Banbury, D. N., *et al.* (2003). Synergistic roles for the Map and Tir effector molecules in mediating uptake of enteropathogenic Escherichia coli (EPEC) into non-phagocytic cells. *Cell Microbiol, 5*(11), 773-783.

Jerse, A. E., Yu, J., Tall, B. D., & Kaper, J. B. (1990). A genetic locus of enteropathogenic Escherichia coli necessary for the production of attaching and effacing lesions on tissue culture cells. *Proc Natl Acad Sci U S A, 87*(20), 7839-7843.

Jobichen, C., Li, M., Yerushalmi, G., Tan, Y. W., *et al.* (2007). Structure of GrlR and the implication of its EDED motif in mediating the regulation of type III secretion system in EHEC. *PLoS Pathog, 3*(5), e69.

Journet, L., Agrain, C., Broz, P., & Cornelis, G. R. (2003). The needle length of bacterial injectisomes is determined by a molecular ruler. *Science, 302*(5651), 1757-1760.

Jung, G., Wiehler, J., & Zumbusch, A. (2005). The photophysics of green fluorescent protein: influence of the key amino acids at positions 65, 203, and 222. *Biophys J, 88*(3), 1932-1947.

Kanack, K. J., Crawford, J. A., Tatsuno, I., Karmali, M. A., *et al.* (2005). SepZ/EspZ is secreted and translocated into HeLa cells by the enteropathogenic Escherichia coli type III secretion system. *Infect Immun, 73*(7), 4327-4337.

Kandel, G., Donohue-Rolfe, A., Donowitz, M., & Keusch, G. T. (1989). Pathogenesis of Shigella diarrhea. XVI. Selective targetting of Shiga toxin to villus cells of rabbit jejunum explains the effect of the toxin on intestinal electrolyte transport. *J Clin Invest, 84*(5), 1509-1517.

Kaper, J. B., Nataro, J. P., & Mobley, H. L. (2004). Pathogenic Escherichia coli. *Nat Rev Microbiol, 2*(2), 123-140.

Karmali, M. A., Petric, M., Lim, C., Fleming, P. C., *et al.* (1983). Escherichia coli cytotoxin, haemolytic-uraemic syndrome, and haemorrhagic colitis. *Lancet, 2*(8362), 1299-1300.

Karmali, M. A., Steele, B. T., Petric, M., & Lim, C. (1983b). Sporadic cases of haemolytic-uraemic syndrome associated with faecal cytotoxin and cytotoxin-producing Escherichia coli in stools. *Lancet, 1*(8325), 619-620.

Kawagishi, I., Homma, M., Williams, A. W., & Macnab, R. M. (1996). Characterization of the flagellar hook length control protein fliK of Salmonella typhimurium and Escherichia coli. *J Bacteriol, 178*(10), 2954-2959.

Kaye, S. A., Louise, C. B., Boyd, B., Lingwood, C. A., *et al.* (1993). Shiga toxin-associated hemolytic uremic syndrome: interleukin-1 beta enhancement of Shiga toxin cytotoxicity toward human vascular endothelial cells in vitro. *Infect Immun, 61*(9), 3886-3891.

Kelly, M., Hart, E., Mundy, R., Marches, O., *et al.* (2006). Essential role of the type III secretion system effector NleB in colonization of mice by Citrobacter rodentium. *Infect Immun, 74*(4), 2328-2337.

Kenny, B., DeVinney, R., Stein, M., Reinscheid, D. J., *et al.* (1997). Enteropathogenic E. coli (EPEC) transfers its receptor for intimate adherence into mammalian cells. *Cell, **91***(4), 511-520.

Kenny, B., Ellis, S., Leard, A. D., Warawa, J., *et al.* (2002). Co-ordinate regulation of distinct host cell signalling pathways by multifunctional enteropathogenic Escherichia coli effector molecules. *Mol Microbiol, **44***(4), 1095-1107.

Kenny, B., & Finlay, B. B. (1997b). Intimin-dependent binding of enteropathogenic Escherichia coli to host cells triggers novel signaling events, including tyrosine phosphorylation of phospholipase C-gamma1. *Infect Immun, **65***(7), 2528-2536.

Kenny, B., & Jepson, M. (2000). Targeting of an enteropathogenic Escherichia coli (EPEC) effector protein to host mitochondria. *Cell Microbiol, **2***(6), 579-590.

Kihara, M., Minamino, T., Yamaguchi, S., & Macnab, R. M. (2001). Intergenic suppression between the flagellar MS ring protein FliF of Salmonella and FlhA, a membrane component of its export apparatus. *J Bacteriol, **183***(5), 1655-1662.

Kimmitt, P. T., Harwood, C. R., & Barer, M. R. (2000). Toxin gene expression by shiga toxin-producing Escherichia coli: the role of antibiotics and the bacterial SOS response. *Emerg Infect Dis, **6***(5), 458-465.

Kitova, E. N., Daneshfar, R., Marcato, P., Mulvey, G. L., *et al.* (2005). Stability of the homopentameric B subunits of shiga toxins 1 and 2 in solution and the gas phase as revealed by nanoelectrospray fourier transform ion cyclotron resonance mass spectrometry. *J Am Soc Mass Spectrom, **16***(12), 1957-1968.

Knutton, S., Baldwin, T., Williams, P. H., & McNeish, A. S. (1989). Actin accumulation at sites of bacterial adhesion to tissue culture cells: basis of a new diagnostic test for enteropathogenic and enterohemorrhagic Escherichia coli. *Infect Immun, **57***(4), 1290-1298.

Knutton, S., Rosenshine, I., Pallen, M. J., Nisan, I., *et al.* (1998). A novel EspA-associated surface organelle of enteropathogenic Escherichia coli involved in protein translocation into epithelial cells. *Embo J, **17***(8), 2166-2176.

Kohler, B., Karch, H., & Schmidt, H. (2000). Antibacterials that are used as growth promoters in animal husbandry can affect the release of Shiga-toxin-2-converting bacteriophages and Shiga toxin 2 from Escherichia coli strains. *Microbiology, **146 (Pt 5)***, 1085-1090.

Kolodziej, P. A., & Young, R. A. (1991). Epitope tagging and protein surveillance. *Methods Enzymol, **194***, 508-519.

Konowalchuk, J., Speirs, J. I., & Stavric, S. (1977). Vero response to a cytotoxin of Escherichia coli. *Infect Immun, **18***(3), 775-779.

Koster, M., Bitter, W., de Cock, H., Allaoui, A., *et al.* (1997). The outer membrane component, YscC, of the Yop secretion machinery of Yersinia enterocolitica forms a ring-shaped multimeric complex. *Mol Microbiol, **26***(4), 789-797.

Kresse, A. U., Beltrametti, F., Muller, A., Ebel, F., *et al.* (2000). Characterization of SepL of enterohemorrhagic Escherichia coli. *J Bacteriol, **182***(22), 6490-6498.

Laaberki, M. H., Janabi, N., Oswald, E., & Repoila, F. (2006). Concert of regulators to switch on LEE expression in enterohemorrhagic Escherichia coli O157:H7: interplay between Ler, GrlA, HNS and RpoS. *Int J Med Microbiol, 296*(4-5), 197-210.

Lai, L. C., Wainwright, L. A., Stone, K. D., & Donnenberg, M. S. (1997). A third secreted protein that is encoded by the enteropathogenic Escherichia coli pathogenicity island is required for transduction of signals and for attaching and effacing activities in host cells. *Infect Immun, 65*(6), 2211-2217.

Lathem, W. W., Grys, T. E., Witowski, S. E., Torres, A. G., *et al.* (2002). StcE, a metalloprotease secreted by Escherichia coli O157:H7, specifically cleaves C1 esterase inhibitor. *Mol Microbiol, 45*(2), 277-288.

Lavander, M., Sundberg, L., Edqvist, P. J., Lloyd, S. A., *et al.* (2002). Proteolytic cleavage of the FlhB homologue YscU of Yersinia pseudotuberculosis is essential for bacterial survival but not for type III secretion. *J Bacteriol, 184*(16), 4500-4509.

Law, D. (2000). Virulence factors of Escherichia coli O157 and other Shiga toxin-producing E. coli. *J Appl Microbiol, 88*(5), 729-745.

Law, D., & Kelly, J. (1995). Use of heme and hemoglobin by Escherichia coli O157 and other Shiga-like-toxin-producing E. coli serogroups. *Infect Immun, 63*(2), 700-702.

Li, M., Rosenshine, I., Yu, H. B., Nadler, C., *et al.* (2006). Identification and characterization of NleI, a new non-LEE-encoded effector of enteropathogenic Escherichia coli (EPEC). *Microbes Infect, 8*(14-15), 2890-2898.

Li, Z., Bell, C., Buret, A., Robins-Browne, R., *et al.* (1993). The effect of enterohemorrhagic Escherichia coli O157:H7 on intestinal structure and solute transport in rabbits. *Gastroenterology, 104*(2), 467-474.

Lim, J. Y., Sheng, H., Seo, K. S., Park, Y. H., *et al.* (2007). Characterization of an Escherichia coli O157:H7 plasmid O157 deletion mutant and its survival and persistence in cattle. *Appl Environ Microbiol, 73*(7), 2037-2047.

Lingwood, C. A. (1996). Role of verotoxin receptors in pathogenesis. *Trends Microbiol, 4*(4), 147-153.

Low, A. S., Dziva, F., Torres, A. G., Martinez, J. L., *et al.* (2006). Cloning, expression, and characterization of fimbrial operon F9 from enterohemorrhagic Escherichia coli O157:H7. *Infect Immun, 74*(4), 2233-2244.

Low, A. S., Holden, N., Rosser, T., Roe, A. J., *et al.* (2006b). Analysis of fimbrial gene clusters and their expression in enterohaemorrhagic Escherichia coli O157:H7. *Environ Microbiol, 8*(6), 1033-1047.

Low, J. C., McKendrick, I. J., McKechnie, C., Fenlon, D., *et al.* (2005). Rectal carriage of enterohemorrhagic Escherichia coli O157 in slaughtered cattle. *Appl Environ Microbiol, 71*(1), 93-97.

Makino, K., Ishii, K., Yasunaga, T., Hattori, M., *et al.* (1998). Complete nucleotide sequences of 93-kb and 3.3-kb plasmids of an enterohemorrhagic Escherichia coli O157:H7 derived from Sakai outbreak. *DNA Res, 5*(1), 1-9.

Marches, O., Wiles, S., Dziva, F., La Ragione, R. M., *et al.* (2005). Characterization of two non-locus of enterocyte effacement-encoded type III-translocated effectors, NleC and NleD, in attaching and effacing pathogens. *Infect Immun, 73*(12), 8411-8417.

Margolin, W. (2000). Green fluorescent protein as a reporter for macromolecular localization in bacterial cells. *Methods, 20*(1), 62-72.

Matthews, L., Low, J. C., Gally, D. L., Pearce, M. C., *et al.* (2006). Heterogeneous shedding of Escherichia coli O157 in cattle and its implications for control. *Proc Natl Acad Sci U S A, 103*(3), 547-552.

Mead, P. S., Slutsker, L., Dietz, V., McCaig, L. F., *et al.* (1999). Food-related illness and death in the United States. *Emerg Infect Dis, 5*(5), 607-625.

Mellies, J. L., Elliott, S. J., Sperandio, V., Donnenberg, M. S., *et al.* (1999). The Per regulon of enteropathogenic Escherichia coli : identification of a regulatory cascade and a novel transcriptional activator, the locus of enterocyte effacement (LEE)-encoded regulator (Ler). *Mol Microbiol, 33*(2), 296-306.

Menard, L. P., Lussier, J. G., Lepine, F., Paiva de Sousa, C., *et al.* (2004). Expression, purification, and biochemical characterization of enteroaggregative Escherichia coli heat-stable enterotoxin 1. *Protein Expr Purif, 33*(2), 223-231.

Minamino, T., Gonzalez-Pedrajo, B., Yamaguchi, K., Aizawa, S. I., *et al.* (1999). FliK, the protein responsible for flagellar hook length control in Salmonella, is exported during hook assembly. *Mol Microbiol, 34*(2), 295-304.

Minamino, T., & Macnab, R. M. (2000). Domain structure of Salmonella FlhB, a flagellar export component responsible for substrate specificity switching. *J Bacteriol, 182*(17), 4906-4914.

Minamino, T., Saijo-Hamano, Y., Furukawa, Y., Gonzalez-Pedrajo, B., *et al.* (2004). Domain organization and function of Salmonella FliK, a flagellar hook-length control protein. *J Mol Biol, 341*(2), 491-502.

Moriya, N., Minamino, T., Hughes, K. T., Macnab, R. M., *et al.* (2006). The type III flagellar export specificity switch is dependent on FliK ruler and a molecular clock. *J Mol Biol, 359*(2), 466-477.

Mullineaux, C. W., Nenninger, A., Ray, N., & Robinson, C. (2006). Diffusion of green fluorescent protein in three cell environments in Escherichia coli. *J Bacteriol, 188*(10), 3442-3448.

Muniesa, M., Jofre, J., Garcia-Aljaro, C., & Blanch, A. R. (2006). Occurrence of Escherichia coli O157:H7 and other enterohemorrhagic Escherichia coli in the environment. *Environ Sci Technol, 40*(23), 7141-7149.

Munro, S., & Pelham, H. R. (1984). Use of peptide tagging to detect proteins expressed from cloned genes: deletion mapping functional domains of Drosophila hsp 70. *Embo J, 3*(13), 3087-3093.

Murray, M. G., & Thompson, W. F. (1980). Rapid isolation of high molecular weight plant DNA. *Nucleic Acids Res, 8*(19), 4321-4325.

Nadler, C., Shifrin, Y., Nov, S., Kobi, S., *et al.* (2006). Characterization of enteropathogenic Escherichia coli mutants that fail to disrupt host cell spreading and attachment to substratum. *Infect Immun, 74*(2), 839-849.

Nagai, T., Abe, A., & Sasakawa, C. (2005). Targeting of enteropathogenic Escherichia coli EspF to host mitochondria is essential for bacterial pathogenesis: critical role of the 16th leucine residue in EspF. *J Biol Chem, 280*(4), 2998-3011.

Nagano, K., Taguchi, K., Hara, T., Yokoyama, S., *et al.* (2003). Adhesion and colonization of enterohemorrhagic Escherichia coli O157:H7 in cecum of mice. *Microbiol Immunol, 47*(2), 125-132.

Nataro, J. P., & Kaper, J. B. (1998). Diarrheagenic Escherichia coli. *Clin Microbiol Rev, 11*(1), 142-201.

Nataro, J. P., Kaper, J. B., Robins-Browne, R., Prado, V., *et al.* (1987). Patterns of adherence of diarrheagenic Escherichia coli to HEp-2 cells. *Pediatr Infect Dis J, 6*(9), 829-831.

Naylor, S. W., Gally, D. L., & Low, J. C. (2005). Enterohaemorrhagic E. coli in veterinary medicine. *Int J Med Microbiol, 295*(6-7), 419-441.

Naylor, S. W., Low, J. C., Besser, T. E., Mahajan, A., *et al.* (2003). Lymphoid follicle-dense mucosa at the terminal rectum is the principal site of colonization of enterohemorrhagic Escherichia coli O157:H7 in the bovine host. *Infect Immun, 71*(3), 1505-1512.

Naylor, S. W., Nart, P., Sales, J., Flockhart, A., *et al.* (2007). Impact of the direct application of therapeutic agents to the terminal recta of experimentally colonized calves on Escherichia coli O157:H7 shedding. *Appl Environ Microbiol, 73*(5), 1493-1500.

Naylor, S. W., Roe, A. J., Nart, P., Spears, K., *et al.* (2005b). Escherichia coli O157 : H7 forms attaching and effacing lesions at the terminal rectum of cattle and colonization requires the LEE4 operon. *Microbiology, 151*(Pt 8), 2773-2781.

Neves, B. C., Mundy, R., Petrovska, L., Dougan, G., *et al.* (2003). CesD2 of enteropathogenic Escherichia coli is a second chaperone for the type III secretion translocator protein EspD. *Infect Immun, 71*(4), 2130-2141.

Neves, B. C., Shaw, R. K., Frankel, G., & Knutton, S. (2003b). Polymorphisms within EspA filaments of enteropathogenic and enterohemorrhagic Escherichia coli. *Infect Immun, 71*(4), 2262-2265.

Niman, H. L., Houghten, R. A., Walker, L. E., Reisfeld, R. A., *et al.* (1983). Generation of protein-reactive antibodies by short peptides is an event of high frequency: implications for the structural basis of immune recognition. *Proc Natl Acad Sci U S A, 80*(16), 4949-4953.

Niswender, K. D., Blackman, S. M., Rohde, L., Magnuson, M. A., *et al.* (1995). Quantitative imaging of green fluorescent protein in cultured cells: comparison of microscopic techniques, use in fusion proteins and detection limits. *J Microsc, 180*(Pt 2), 109-116.

O'Brien A D, L. T. A., Chen M E, Rothman S W, Formal S B. (1983). Escherichia coli O157:H7 strains associated with haemorrhagic colitis in the United States produce a Shigella dysenteriae 1 (Shiga) like cytotoxin. *Lancet*, 702.

O'Brien, A. D., & Holmes, R. K. (1987). Shiga and Shiga-like toxins. *Microbiol Rev, 51*(2), 206-220.

O'Brien, A. D., LaVeck, G. D., Thompson, M. R., & Formal, S. B. (1982). Production of Shigella dysenteriae type 1-like cytotoxin by Escherichia coli. *J Infect Dis, 146*(6), 763-769.

Ogino, T., Ohno, R., Sekiya, K., Kuwae, A., *et al.* (2006). Assembly of the type III secretion apparatus of enteropathogenic Escherichia coli. *J Bacteriol, 188*(8), 2801-2811.

Ohnishi, K., Fan, F., Schoenhals, G. J., Kihara, M., *et al.* (1997). The FliO, FliP, FliQ, and FliR proteins of Salmonella typhimurium: putative components for flagellar assembly. *J Bacteriol, 179*(19), 6092-6099.

Orskov, I., Orskov, F., Jann, B., & Jann, K. (1977). Serology, chemistry, and genetics of O and K antigens of Escherichia coli. *Bacteriol Rev, 41*(3), 667-710.

Ostroff, S. M., Griffin, P. M., Tauxe, R. V., Shipman, L. D., *et al.* (1990). A statewide outbreak of Escherichia coli O157:H7 infections in Washington State. *Am J Epidemiol, 132*(2), 239-247.

Pacheco-Gil, L., Ochoa, T. J., Flores-Romo, L., DuPont, H. L., *et al.* (2006). Enteroinvasive Escherichia coli severe dysentery complicated by rotavirus gastroenteritis. *J Infect, 53*(5), e211-213.

Pallen, M. J., Beatson, S. A., & Bailey, C. M. (2005). Bioinformatics analysis of the locus for enterocyte effacement provides novel insights into type-III secretion. *BMC Microbiol, 5*(1), 9.

Papatheodorou, P., Domanska, G., Oxle, M., Mathieu, J., *et al.* (2006). The enteropathogenic Escherichia coli (EPEC) Map effector is imported into the mitochondrial matrix by the TOM/Hsp70 system and alters organelle morphology. *Cell Microbiol, 8*(4), 677-689.

Paton, J. C., & Paton, A. W. (1998). Pathogenesis and diagnosis of Shiga toxin-producing Escherichia coli infections. *Clin Microbiol Rev, 11*(3), 450-479.

Paul, K., & Blair, D. F. (2006). Organization of FliN subunits in the flagellar motor of Escherichia coli. *J Bacteriol, 188*(7), 2502-2511.

Paul, K., Harmon, J. G., & Blair, D. F. (2006b). Mutational analysis of the flagellar rotor protein FliN: identification of surfaces important for flagellar assembly and switching. *J Bacteriol, 188*(14), 5240-5248.

Perna, N. T., Mayhew, G. F., Posfai, G., Elliott, S., *et al.* (1998). Molecular evolution of a pathogenicity island from enterohemorrhagic Escherichia coli O157:H7. *Infect Immun, 66*(8), 3810-3817.

Perna, N. T., Plunkett, G., 3rd, Burland, V., Mau, B., *et al.* (2001). Genome sequence of enterohaemorrhagic Escherichia coli O157:H7. *Nature, 409*(6819), 529-533.

Phan, J., Austin, B. P., & Waugh, D. S. (2005). Crystal structure of the Yersinia type III secretion protein YscE. *Protein Sci, 14*(10), 2759-2763.

Prasher, D. C., Eckenrode, V. K., Ward, W. W., Prendergast, F. G., *et al.* (1992). Primary structure of the Aequorea victoria green-fluorescent protein. *Gene, 111*(2), 229-233.

Pruimboom-Brees, I. M., Morgan, T. W., Ackermann, M. R., Nystrom, E. D., *et al.* (2000). Cattle lack vascular receptors for Escherichia coli O157:H7 Shiga toxins. *Proc Natl Acad Sci U S A, 97*(19), 10325-10329.

Quitard, S., Dean, P., Maresca, M., & Kenny, B. (2006). The enteropathogenic Escherichia coli EspF effector molecule inhibits PI-3 kinase-mediated uptake independently of mitochondrial targeting. *Cell Microbiol, 8*(6), 972-981.

Reilly, A. (1998). Prevention and control of enterohaemorrhagic Escherichia coli (EHEC) infections: memorandum from a WHO meeting. WHO Consultation on Prevention and Control of Enterohaemorrhagic Escherichia coli (EHEC) Infections. *Bull World Health Organ, 76*(3), 245-255.

Remington, S. J. (2006). Fluorescent proteins: maturation, photochemistry and photophysics. *Curr Opin Struct Biol, 16*(6), 714-721.

Riley, L. W., Remis, R. S., Helgerson, S. D., McGee, H. B., *et al.* (1983). Hemorrhagic colitis associated with a rare Escherichia coli serotype. *N Engl J Med, 308*(12), 681-685.

Ritchie, J. M., & Waldor, M. K. (2005). The locus of enterocyte effacement-encoded effector proteins all promote enterohemorrhagic Escherichia coli pathogenicity in infant rabbits. *Infect Immun, 73*(3), 1466-1474.

Roberts, R. J., Belfort, M., Bestor, T., Bhagwat, A. S., *et al.* (2003). A nomenclature for restriction enzymes, DNA methyltransferases, homing endonucleases and their genes. *Nucleic Acids Res, 31*(7), 1805-1812.

Rock, G., Clark, W., Sternbach, M., Kolajova, M., *et al.* (2005). Haemolytic uraemic syndrome is an immune-mediated disease: role of anti-CD36 antibodies. *Br J Haematol, 131*(2), 247-252.

Roe, A. J., Hoey, D. E., & Gally, D. L. (2003). Regulation, secretion and activity of type III-secreted proteins of enterohaemorrhagic Escherichia coli O157. *Biochem Soc Trans, 31*(Pt 1), 98-103.

Roe, A. J., Naylor, S. W., Spears, K. J., Yull, H. M., *et al.* (2004). Co-ordinate single-cell expression of LEE4- and LEE5-encoded proteins of Escherichia coli O157:H7. *Mol Microbiol, 54*(2), 337-352.

Roe, A. J., Tysall, L., Dransfield, T., Wang, D., *et al.* (2007). Analysis of the expression, regulation and export of NleA-E in Escherichia coli O157 : H7. *Microbiology, 153*(Pt 5), 1350-1360.

Roe, A. J., Yull, H., Naylor, S. W., Woodward, M. J., *et al.* (2003b). Heterogeneous surface expression of EspA translocon filaments by Escherichia coli O157:H7 is controlled at the posttranscriptional level. *Infect Immun, 71*(10), 5900-5909.

Rose, R. E. (1988). The nucleotide sequence of pACYC184. *Nucleic Acids Res, **16**(1)*, 355.

Saijo-Hamano, Y., Imada, K., Minamino, T., Kihara, M., *et al.* (2005). Crystallization and preliminary X-ray analysis of the C-terminal cytoplasmic domain of FlhA, a membrane-protein subunit of the bacterial flagellar type III protein-export apparatus. *Acta Crystallogr Sect F Struct Biol Cryst Commun, **61***(Pt 6), 599-602.

Sambrook, J., Fritsch, E. F., and Maniatis, T. (2001). *Molecular Cloning: A laboratory Manual.* 3rd Edition, Cold Spring Harbor, NY: Cold Spring Harbor Press.

Sandvig, K., Garred, O., Prydz, K., Kozlov, J. V., *et al.* (1992). Retrograde transport of endocytosed Shiga toxin to the endoplasmic reticulum. *Nature, **358***(6386), 510-512.

Sani, M., Allaoui, A., Fusetti, F., Oostergetel, G. T., *et al.* (2007). Structural organization of the needle complex of the type III secretion apparatus of Shigella flexneri. *Micron, **38***(3), 291-301.

Savarino, S. J., Fasano, A., Watson, J., Martin, B. M., *et al.* (1993). Enteroaggregative Escherichia coli heat-stable enterotoxin 1 represents another subfamily of E. coli heat-stable toxin. *Proc Natl Acad Sci U S A, **90***(7), 3093-3097.

Schmidt, H., Beutin, L., & Karch, H. (1995). Molecular analysis of the plasmid-encoded hemolysin of Escherichia coli O157:H7 strain EDL 933. *Infect Immun, **63***(3), 1055-1061.

Schmidt, H., Henkel, B., & Karch, H. (1997). A gene cluster closely related to type II secretion pathway operons of gram-negative bacteria is located on the large plasmid of enterohemorrhagic Escherichia coli O157 strains. *FEMS Microbiol Lett, **148***(2), 265-272.

Schoeni, J. L., & Doyle, M. P. (1994). Variable colonization of chickens perorally inoculated with Escherichia coli O157:H7 and subsequent contamination of eggs. *Appl Environ Microbiol, **60***(8), 2958-2962.

Scotland, S. M., Smith, H. R., & Rowe, B. (1985). Two distinct toxins active on Vero cells from Escherichia coli O157. *Lancet, **2***(8460), 885-886.

Sekiya, K., Ohishi, M., Ogino, T., Tamano, K., *et al.* (2001). Supermolecular structure of the enteropathogenic Escherichia coli type III secretion system and its direct interaction with the EspA-sheath-like structure. *Proc Natl Acad Sci U S A, **98***(20), 11638-11643.

Sharp, F. C., & Sperandio, V. (2007). QseA directly activates transcription of LEE1 in enterohemorrhagic Escherichia coli. *Infect Immun, **75***(5), 2432-2440.

Shaw, R. K., Cleary, J., Murphy, M. S., Frankel, G., *et al.* (2005). Interaction of enteropathogenic Escherichia coli with human intestinal mucosa: role of effector proteins in brush border remodeling and formation of attaching and effacing lesions. *Infect Immun, **73***(2), 1243-1251.

Shibata, S., Takahashi, N., Chevance, F. F., Karlinsey, J. E., *et al.* (2007). FliK regulates flagellar hook length as an internal ruler. *Mol Microbiol, **64***(5), 1404-1415.

Sinclair, J. F., & O'Brien, A. D. (2004). Intimin types alpha, beta, and gamma bind to nucleolin with equivalent affinity but lower avidity than to the translocated intimin receptor. *J Biol Chem, 279*(32), 33751-33758.

Sorg, I., Wagner, S., Amstutz, M., Muller, S. A., *et al.* (2007). YscU recognizes translocators as export substrates of the Yersinia injectisome. *Embo J, 26*(12), 3015-3024.
Southward, C. M., & Surette, M. G. (2002). The dynamic microbe: green fluorescent protein brings bacteria to light. *Mol Microbiol, 45*(5), 1191-1196.

Sperandio, V., Mellies, J. L., Nguyen, W., Shin, S., *et al.* (1999). Quorum sensing controls expression of the type III secretion gene transcription and protein secretion in enterohemorrhagic and enteropathogenic Escherichia coli. *Proc Natl Acad Sci U S A, 96*(26), 15196-15201.

Stevens, M. P., Roe, A. J., Vlisidou, I., van Diemen, P. M., *et al.* (2004). Mutation of toxB and a truncated version of the efa-1 gene in Escherichia coli O157:H7 influences the expression and secretion of locus of enterocyte effacement-encoded proteins but not intestinal colonization in calves or sheep. *Infect Immun, 72*(9), 5402-5411.

Stricklett, P. K., Hughes, A. K., Ergonul, Z., & Kohan, D. E. (2002). Molecular basis for up-regulation by inflammatory cytokines of Shiga toxin 1 cytotoxicity and globotriaosylceramide expression. *J Infect Dis, 186*(7), 976-982.

Strockbine, N. A., Marques, L. R., Newland, J. W., Smith, H. W., *et al.* (1986). Two toxin-converting phages from Escherichia coli O157:H7 strain 933 encode antigenically distinct toxins with similar biologic activities. *Infect Immun, 53*(1), 135-140.

Sullivan, K., Kay., S. (1999). *Methods in Cell Biology, Volume 58: Green Fluorescent Proteins* **(Vol. 58)**. San Diego: Academic Press.

Sussman, M. (1997). *Escherichia coli and human disease. In Escherichia coli mechanisms of virulence*. Cambridge: Cambridge University Press.

Swerdlow, D. L., Woodruff, B. A., Brady, R. C., Griffin, P. M., *et al.* (1992). A waterborne outbreak in Missouri of Escherichia coli O157:H7 associated with bloody diarrhea and death. *Ann Intern Med, 117*(10), 812-819.

Tamblyn, S., deGrosbois, J., Taylor, D., & Stratton, J. (1999). An outbreak of Escherichia coli O157:H7 infection associated with unpasteurized non-commercial, custom-pressed apple cider--Ontario, 1998. *Can Commun Dis Rep, 25*(13), 113-117; discussion 117-120.

Tatsuno, I., Horie, M., Abe, H., Miki, T., *et al.* (2001). toxB gene on pO157 of enterohemorrhagic Escherichia coli O157:H7 is required for full epithelial cell adherence phenotype. *Infect Immun, 69*(11), 6660-6669.

Tauxe, R. V. (1997). Emerging foodborne diseases: an evolving public health challenge. *Emerg Infect Dis, 3*(4), 425-434.

Tauxe, R. V. (2001). Food safety and irradiation: protecting the public from foodborne infections. *Emerg Infect Dis, 7*(3 Suppl), 516-521.

Thomas, J. D., Daniel, R. A., Errington, J., & Robinson, C. (2001). Export of active green fluorescent protein to the periplasm by the twin-arginine translocase (Tat) pathway in Escherichia coli. *Mol Microbiol, 39*(1), 47-53.

Thomas, N. A., Deng, W., Puente, J. L., Frey, E. A., *et al.* (2005). CesT is a multi-effector chaperone and recruitment factor required for the efficient type III secretion of both LEE- and non-LEE-encoded effectors of enteropathogenic Escherichia coli. *Mol Microbiol, 57*(6), 1762-1779.

Torres, A. G., Giron, J. A., Perna, N. T., Burland, V., *et al.* (2002). Identification and characterization of lpfABCC'DE, a fimbrial operon of enterohemorrhagic Escherichia coli O157:H7. *Infect Immun, 70*(10), 5416-5427.

Torres, A. G., Kanack, K. J., Tutt, C. B., Popov, V., *et al.* (2004). Characterization of the second long polar (LP) fimbriae of Escherichia coli O157:H7 and distribution of LP fimbriae in other pathogenic E. coli strains. *FEMS Microbiol Lett, 238*(2), 333-344.

Torres, A. G., Zhou, X., & Kaper, J. B. (2005). Adherence of diarrheagenic Escherichia coli strains to epithelial cells. *Infect Immun, 73*(1), 18-29.

Toth, I., Cohen, M. L., Rumschlag, H. S., Riley, L. W., *et al.* (1990). Influence of the 60-megadalton plasmid on adherence of Escherichia coli O157:H7 and genetic derivatives. *Infect Immun, 58*(5), 1223-1231.

Tu, X., Nisan, I., Yona, C., Hanski, E., *et al.* (2003). EspH, a new cytoskeleton-modulating effector of enterohaemorrhagic and enteropathogenic Escherichia coli. *Mol Microbiol, 47*(3), 595-606.

Turner, S. M., Scott-Tucker, A., Cooper, L. M., & Henderson, I. R. (2006). Weapons of mass destruction: virulence factors of the global killer enterotoxigenic Escherichia coli. *FEMS Microbiol Lett, 263*(1), 10-20.

Van Arnam, J. S., McMurry, J. L., Kihara, M., & Macnab, R. M. (2004). Analysis of an engineered Salmonella flagellar fusion protein, FliR-FlhB. *J Bacteriol, 186*(8), 2495-2498.

Viswanathan, V. K., Koutsouris, A., Lukic, S., Pilkinton, M., *et al.* (2004). Comparative analysis of EspF from enteropathogenic and enterohemorrhagic Escherichia coli in alteration of epithelial barrier function. *Infect Immun, 72*(6), 3218-3227.

Wainwright, L. A., & Kaper, J. B. (1998). EspB and EspD require a specific chaperone for proper secretion from enteropathogenic Escherichia coli. *Mol Microbiol, 27*(6), 1247-1260.

Wang, R. F., & Kushner, S. R. (1991). Construction of versatile low-copy-number vectors for cloning, sequencing and gene expression in Escherichia coli. *Gene, 100*, 195-199.

Wasteson, Y. (2001). Zoonotic Escherichia coli. *Acta Vet Scand Suppl, 95*, 79-84.

Weintraub, A. (2007). Enteroaggregative Escherichia coli: epidemiology, virulence and detection. *J Med Microbiol, 56*(Pt 1), 4-8.

Wickham, M. E., Lupp, C., Vazquez, A., Mascarenhas, M., *et al.* (2007). Citrobacter rodentium virulence in mice associates with bacterial load and the type III effector NleE. *Microbes Infect, 9*(3), 400-407.

Wieler, L. H., McDaniel, T. K., Whittam, T. S., & Kaper, J. B. (1997). Insertion site of the locus of enterocyte effacement in enteropathogenic and enterohemorrhagic Escherichia coli differs in relation to the clonal phylogeny of the strains. *FEMS Microbiol Lett,* ***156***(1), 49-53.

Wilson, R. K., Shaw, R. K., Daniell, S., Knutton, S., *et al.* (2001). Role of EscF, a putative needle complex protein, in the type III protein translocation system of enteropathogenic Escherichia coli. *Cell Microbiol,* ***3***(11), 753-762.

Yamada, H., Muramatsu, S., & Mizuno, T. (1990). An Escherichia coli protein that preferentially binds to sharply curved DNA. *J Biochem,* ***108***(3), 420-425.

Yip, C. K., Kimbrough, T. G., Felise, H. B., Vuckovic, M., *et al.* (2005). Structural characterization of the molecular platform for type III secretion system assembly. *Nature,* ***435***(7042), 702-707.

Yoh, M., & Honda, T. (1997). The stimulating effect of fosfomycin, an antibiotic in common use in Japan, on the production/release of verotoxin-1 from enterohaemorrhagic Escherichia coli O157:H7 in vitro. *Epidemiol Infect,* ***119***(1), 101-103.

Yoshioka, K., Yagi, K., & Moriguchi, N. (1999). Clinical features and treatment of children with hemolytic uremic syndrome caused by enterohemorrhagic Escherichia coli O157:H7 infection: experience of an outbreak in Sakai City, 1996. *Pediatr Int,* ***41***(2), 223-227.

Yu, X. J., Liu, M., & Holden, D. W. (2004). SsaM and SpiC interact and regulate secretion of Salmonella pathogenicity island 2 type III secretion system effectors and translocators. *Mol Microbiol,* ***54***(3), 604-619.

Yuste, M., De La Fuente, R., Ruiz-Santa-Quiteria, J. A., Cid, D., *et al.* (2006). Detection of the astA (EAST1) gene in attaching and effacing Escherichia coli from ruminants. *J Vet Med B Infect Dis Vet Public Health,* ***53***(2), 75-77.

Zahrl, D., Wagner, M., Bischof, K., Bayer, M., *et al.* (2005). Peptidoglycan degradation by specialized lytic transglycosylases associated with type III and type IV secretion systems. *Microbiology,* ***151***(Pt 11), 3455-3467.

Zarivach, R., Vuckovic, M., Deng, W., Finlay, B. B., *et al.* (2007). Structural analysis of a prototypical ATPase from the type III secretion system. *Nat Struct Mol Biol,* ***14***(2), 131-137.

Zhang, X., McDaniel, A. D., Wolf, L. E., Keusch, G. T., *et al.* (2000). Quinolone antibiotics induce Shiga toxin-encoding bacteriophages, toxin production, and death in mice. *J Infect Dis,* ***181***(2), 664-670.

Zhao, T., Doyle, M. P., & Besser, R. E. (1993). Fate of enterohemorrhagic Escherichia coli O157:H7 in apple cider with and without preservatives. *Appl Environ Microbiol,* ***59***(8), 2526-2530.

Chapter 8
Publications from the Thesis

oced. Online 2006; 8(1): 153-162.
1251/bpo123
mber 27, 2006

Generation of gene deletions and gene replacements in *Escherichia coli* O157:H7 using a temperature sensitive allelic exchange system

James R. Emmerson[1], David L. Gally[1] and Andrew J. Roe[1]*

e for Infectious Diseases, University of Edinburgh. The Chancellors Building, 49 Little France Crescent, EH16 4SB. United Kingdom.

esponding Author: Andrew J. Roe, Centre for Infectious Diseases, University of Edinburgh. The Chancellors Building, 49 Little France Crescent, EH16 nited Kingdom. Email: aroe@vet.ed.ac.uk

ted: July 5, 2006; Revised: August 15, 2006; Accepted: September 12, 2006.

g terms: Gene Deletion; Escherichia coli O157:H7.

ABSTRACT

s work we describe protocols for the generation of gene deletions and gene replacements using a temperature ive plasmid in *Escherichia coli* O157:H7. This technology requires flanking DNA to be cloned into a temperature ive vector but the resulting clone allows great flexibility for further modification of the target sequence. It is fore highly suited to the study of genes in which several rounds of changes are envisaged. A number of examples ed to illustrate the flexibility of the system which has been used to create novel gene replacements including s for protein localisation work and reporters for transcriptional analyses. In this paper we describe protocols can be used with a high degree of success when applied to *E. coli* O157. The deletion and replacement of the operon of *E. coli* O157 is detailed to show the advantages and limitations of the technology.

INTRODUCTION

ability to generate directed gene deletions and replacements is a central technique used to nstrate gene function and fulfil Molecular Koch's lates in any study (1). The past two decades have the development of a variety of molecular iques to achieve such chromosomal modifications *coli* K-12, including F' homogenotization, the ation and resolution of ColE1 plasmid cointegrates olA1 background, transformation and mating via fr cross, and the use of temperature sensitive ids with selection for homologous recombination More recently, the phage λ red recombinase has successfully applied to allow rapid, one step ration of genes (4). However, these techniques uffer from the requirement of specific genetic grounds (often mutants themselves), and are ized for efficient use in *E. coli* K-12 laboratory s. The application of these techniques to "wild- strains including pathotypes of *E. coli* is, fore, often problematic. Furthermore, using erature sensitive plasmids provides a number of dvantages compared with other methods. Firstly, although lambda red is probably the most rapid system for inactivation of genes it does suffer from the fact that transient expression of the recombinase system enhances the frequency of unwanted genetic rearrangements. Secondly, the lambda red approach is also highly suited to creation of gene deletions, delivery of gene replacements, as we describe for the temperature sensitive based system, is less straightforward. Additionally, as the temperature sensitive allelic exchange system does not rely on any conjugation step, for example when using lambda Pir-dependent iroR6K plasmids, strains that produce bacteriocins or capsule can also be successfully modified.

In the case of *E. coli* O157, the complete genome sequencing of two strains has revealed an additional 1.4MB of DNA when compared with the *E. coli* K-12 genome (5). These sequences include numerous putative adhesin clusters, the complete LEE pathogenicity island, shiga-like toxins encoded on prophages and other putative virulence factors (6). Genetic manipulation of *E. coli* O157 to selectively disrupt these factors is therefore highly desirable. Two approaches have been widely adopted to achieve this goal: a modified lambda red protocol and the use of temperature sensitive plasmids

and selection for allelic exchange (7, 8). Here we describe a modified protocol for use with temperature sensitive plasmids. This protocol reliably yields allelic exchange constructs, works well to replace large DNA fragments (we have deleted/modified up to 7KB), and gives excellent flexibility for further modifications. This flexibility is demonstrated by our use of the system to: 1) knockout a specific operon and then complement the knockout by allelic exchange back at the site of deletion. 2) Engineer whole gene or sequence deletions. 3) Introduce marker genes for single copy reporter fusions. 4) Introduce specific tags to track or visualise the resultant recombinant proteins.

OUTLINE OF ALLELIC EXCHANGE METHODOLOGY

In this paper we describe a modified allelic exchange method that allows the exchange of genetic information into a wild-type *E. coli* strain background. Firstly an intermediate strain is constructed in which the wild-type chromosomal sequence is replaced by a DNA cassette. This *sacB-kan* cassette contains the *sacB* gene from *Bacillus subtilis* and the neomycin (kanamycin) gene from Tn5. The method has two distinct rounds of allelic exchange. The *sacB-kan* cassette is cloned into a temperature sensitive chloramphenicol resistant plasmid in between homologous flanking regions of DNA. This is used in the first round of allelic exchange to create an intermediate strain containing the cassette on the chromosome in replace of wild-type sequence (Fig. 1). The selection for plasmid integration occurs at 42°C in the presence of chloramphenicol while plasmid excision occurs at 28°C in the presence of kanamycin. In the second round of allelic exchange, for example to create a complete deletion, the temperature sensitive plasmid containing only the homologues flanking regions is used (Fig. 2). Alternatively DNA cloned in between the flanking regions can be exchanged onto the chromosome e.g. to complement the mutant or to introduce different alleles. During this allelic exchange the plasmid is transformed into the intermediate strain. Growth at 42°C in chloramphenicol selects for plasmid integration, whilst growth at 28°C in the presence of sucrose selects for bacteria in which the inserted cassette has been exchanged for the target sequence and then the plasmid lost through lack of selective pressure. The selective pressure results from the action of the *sacB* gene that encodes levansucrase, an enzyme that cleaves sucrose resulting in toxic levels of levans in many *E. coli* strains.

MATERIALS AND METHODS

The allelic exchange method has been used for a number of studies in which defined deletions or gene replacements were made. In this paper, the deletion and complementation of the *LEE4* operon of *Escherichia coli* O157 is used as a specific example to illustrate the technique. A number of further examples are used to illustrate how the technology can be used in other applications.

Creation of the *LEE4* deletion and complemented strains

The allelic exchange method was used to delete and then repair the entire *LEE4* operon from *E. coli* O157:H7 (ZAP198), generating strains ZAP984 and ZAP985, respectively. A step by step protocol for the allelic exchange procedure is listed under the protocols section of this work. These methods were used to create ZAP984 (Δ*LEE4*), using plasmid pHY10 and the complemented strain, ZAP985, using plasmid pAJR162. The detailed construction of these plasmids and strains including oligonucleotide sequences are covered in Naylor *et al.*, 2005 (9). In this work, we aim to provide an overview of the steps involved in the cloning, the allelic exchange methodology and our experience with the technology.

RESULTS AND DISCUSSION

Factors affecting co-integrate formation

Two key factors play a role in determining the frequency of co-integrate formation: 1) degree of DNA homology and 2) size of the flanking regions. We have observed a dramatic reduction in efficiency of primary integrate formation with even a few base pair mismatched between flanking region DNA and target region on the chromosome. This is a drawback as sometimes it results in the requirement of cloning specific flanking regions for each strain being studied. For example, we have used an allelic exchange system at the *lac* locus in several wild-type O157:H7 strains that created a number of promoter-*lacZ* fusions (8). However, we observed extremely low

uencies of allelic exchange when plasmids were with any strain other than the one from which the ting regions were cloned.

key reagent we use for the knockout strategy is the mid pIB307. The replicon from this plasmid is ed from the large antibiotic resistance plasmid R6-). This replicon and a tetracycline resistance gene manipulated to form a smaller plasmid termed 101. pSC101 has undergone *in vitro* mutagenesis hydroxylamine, creating distinct mutants that d in their temperature dependent replication (11). e included pH01, a pSC101 replicon mutant that unable to replicate at 42°C but could replicate ally at 28°C. The replicon from pH01 was ved and ligated to the chloramphenicol resistance from pBR325. The resulting plasmid, pMAK705, modified by the addition of the *lacZ* gene and its oter (to facilitate screening) and the polylinker np19 as a multiple cloning site (12). At a later date majority of the *lac* sequences were removed to ease the plasmid's size and homology with mosomal DNA, thereby creating pIB307 (13).

lanking regions we routinely use between 600bp 1000bp of DNA, and find it is important to have ar sizes of left and right hand flanking regions to mise the efficiency of exchange. Grossly differing ing regions will favour recombination at one ing region thereby reducing frequency of the le crossover event that is required for successful exchange. The deletion of *LEE4* used a left hand ing region of 958 bp and a right hand flanking of 610 bp. Smaller flanking regions (200-300bp) work but will reduce the efficiency of exchange. flanking region for the *LEE4* knockout was PCR ified and cloned into the temperature sensitive pIB307 creating pHY3. A *sacB-kan* cassette was between the flanking regions at the *Bam*HI tion site to create plasmid pHY10 (8). Again, the ement of cloning three separate DNA fragments e creation of the allelic exchange vector is a antage compared with the lambda red approach. ow subsequent 'repair' of any deletion, the *LEE4* n was amplified by long-range PCR and cloned IB307 to create construct pAJR162.

An alternative method is to amplify the whole region including the flanking regions and the gene(s) to be deleted using long-range PCR. This can be cloned into the pIB307 vector and restricted by endonucleases at naturally occurring restriction sites to replace the gene(s) to be deleted with the *sacB-kan* cassette. This plasmid can then be used in the allelic exchange process.

Optimising conditions for generation of large deletions

For large deletions of several kilobases or problematic deletions we have found that increasing the temperature from 42°C to 44°C will aid the selection of primary integrates. Furthermore, we also find it useful to plate out dilutions of the primary integrates on LBC plates at 44°C, enabling single colonies to be analysed for the primary integration event by PCR. This "primary positive" colony can then be cultured at the lower, permissive temperature of 28°C to allow the generation of resolution products. This approach is particularly useful if any construct results in low levels of primary integrates at 42°C, often indicated by a subsequent failure to culture at 28°C.

Location of the *sacB* gene

The *sacB* gene offers a powerful tool for the selection of allelic exchange events that do not occur frequently. The stage at which the *sacB* gene carries out this function in the allelic exchange strategy can vary depending on its location on the exchange plasmid. For the creation of the *LEE4* deletion strain the exchange plasmid contained the *sacB* gene as part of a cassette that was situated in between the homologous flanking regions. For the complementation of *LEE4* the *sacB* gene was used to select for bacteria that had lost the *sacB-kan* cassette from the chromosome after it was used to replace the genetic material, i.e. on the second round of allelic exchange. If the *sacB* gene is located outwith the homologous flanking regions then it can be used as a negative selective marker for the loss of the plasmid during the first round of allelic exchange. The colonies that do not contain the *sacB* gene successfully grow in the presence of sucrose and can then be screened for the correct resistance profiles (if any) and verified by PCR. In one study the *sacB* gene was situated on the allelic exchange plasmid outside the flanking regions. In between the flanking regions was a cassette that replaced the genetic material of interest for a genetic element containing *lacZ*, the *aph* gene (encoding resistance

to kanamycin) and the *lac* promoter. This cassette was flanked by FRT sites, so it could be excised from the chromosome by the Flp recombinase provided in *trans*, creating a clean deletion (14).

Exchange frequencies

During the first round of allelic exchange when the *sacB-kan* cassette is inserted into the chromosome, we have found that >80% of colonies plated on LBC after 48 hours selection are primary integrants suitable for resolution (ascertained by PCR). Following culture at 28°C, the success of the allelic exchange can vary widely, from 5-90%. Therefore, we typically replica plate about 100 colonies and expect to find a successful exchange clone. The removal of the *sacB-kan* cassette during the second round of exchange has a higher frequency of success due to the negative selective screening offered by the *sacB* gene.

Construct validation

Following the allelic exchange process and, assuming a clone has been obtained with the correct antibiotic resistance profile; two key checks should be carried out on any construct. Firstly, the loss of the plasmid is verified using PCR primers designed to amplify the pIB plasmid (Table 1). Secondly, the region that has been exchanged is PCR amplified (usually in 2 or more sections) including DNA that is outside the flanking region, i.e. was unmodified during the exchange process. This shows that the allelic exchange is indeed at the target site and that the cloned DNA does not contain any sequence errors.

Table 1: Strains and oligonucleotide primers used in the study.

Strains	**Description**
ZAP198	*E. coli* O157:H7 (Walla3) VT1-VT2-
ZAP984	ZAP198 Δ LEE4
ZAP985	ZAP784 LEE4 complement
Primers	**Primer Sequence**
PIB sp.5	AGACAAATGGATCTCGTAAGCG
PIB sp.3	GCTGTAACAAGTTGTCTCAGGTGT
Plasmids	**Description**
pIB307	pMAK705 based plasmid for allelic exchange. Temperature sensitive replicon.
pAJR162	pIB307 vector with cloned LEE4

APPLICATION OF THE METHOD

Examination of EspD secretion phenotype in wild-type, deletion and complemented strains

The ability of strains to secrete EspD protein in the wild-type, and *LEE4* deletion strain (ZAP984) and the complement (ZAP985) was confirmed by Western analysis. As expected, deletion of *LEE4*, the operon that encodes EspD, leads to a loss of secretion phenotype. Complementation of the deletion mutant by allelic exchange using the *LEE4* operon resulted in restoration of the secretion phenotype. Clearly, complementation using plasmids is far easier than the approach described. However, the approach has a number of limitations, including plasmid stability and copy number. We subsequently used the *LEE4* deletion strain and complement to assess the importance of this operon during colonization of the terminal rectum of cattle (9). The *LEE4* complement strain was capable of adhering to bovine epithelium *in vitro* and colonising the terminal rectum of cattle, indicating that the type III secretion system plays a key role in the animal host. In such an animal model, plasmid selection using antibiotics is not always possible and many studies therefore avoid performing any form of complementation. We consider that single-copy chromosomal complementation is more desirable, as it can replace the region of interest into its original site thereby fulfilling molecular Koch's postulates (1).

Further applications

We are currently using the described allelic exchange system to deliver a number of hybrid protein fusions into the structural components of the type three secretion system. This approach includes delivery of an EscU::eGFP fusion (EscU being a type three secretion apparatus protein) into the chromosome and subsequent hybrid protein localisation using fluorescence microscopy and Western analyses. Ongoing work is also replacing the eGFP protein with brighter variants such as GFP+ and alternative tags such as haemagglutinin (HA) to determine the most appropriate detection system in terms of sensitivity and stability. Again, the flexibility of the system allows easy replacement of the *sacB-kan* cassette with any construct cloned between the flanking region DNA.

have made extensive use of the described system to te chromosomal *lacZ* fusions to fimbrial genes, type secretion genes and regulators (15-17). In these ies we observed that once the *sacB-kan* cassette is grated into the chromosome, it is straightforward to duce single copy fusions at this target site

ntial problems areas

ur experience, there are two inherent problems the method. Firstly, the pSC101 replicon based mid vector can be susceptible to loss of perature sensitivity. Care must be taken to ensure all initial cloning steps, transformation recoveries cultures are carried out at 30°C or less. Loss of perature sensitivity will result in the inability to the strain of the plasmid. We have even untered this problem following particularly hot mer days when the temperature of the laboratory reach >28°C. Secondly, the copy-number of the mid is approximately 6 to 10 per cell. For certain s it is possible that this could result in gene dosage lems. This may explain our observation when we pted to delete a DNA methylase gene but found itial transformants cultured very slowly in LBC and did not produce primary integrates (data not m). With regards to which strains of *E. coli* the nique can be applied to, we have successfully pulated several *E. coli* O157 strains, opathogenic *E. coli* (EPEC), uropathogenic *E. coli* C) and K-12 strains. The only strain-specific factor may limit the application of the technique is if the carries a sucrose utilisation system that has been ibed in certain isolates of *E. coli* (18). Clearly the nce of such loci would negate the selective bility of the *sacB* gene used in the allelic exchange ocol.

also important to appreciate that unintended dary mutations can occur when using suicide nids to create a deletion (19). Before a phenotypic ge is attributed to the deleted gene the strain ld be checked. PFGE has been shown to be a useful for detecting these unwanted changes and thern blotting is also advisable to show that no angements have occurred proximal to the site of rgeted modification. Alternatively, reverse allelic nge can restore the wild-type allele to the genome; if the phenotype is restored then the changes observed can be attributed to the deletion.

Summary

Allelic exchange is an invaluable tool for creating defined deletions of chromosomal DNA sequences. In this paper we describe protocols that ensure a high degree of success when using temperature sensitive plasmids for generating deletions in *Escherichia coli* O157:H7. Our experience in creating defined knockouts and complements at several loci is discussed as are potential problem areas. Further applications of the technology are covered including the creation of chromosomal gene fusions to markers such as green fluorescent protein and haemagglutinin.

FIGURES

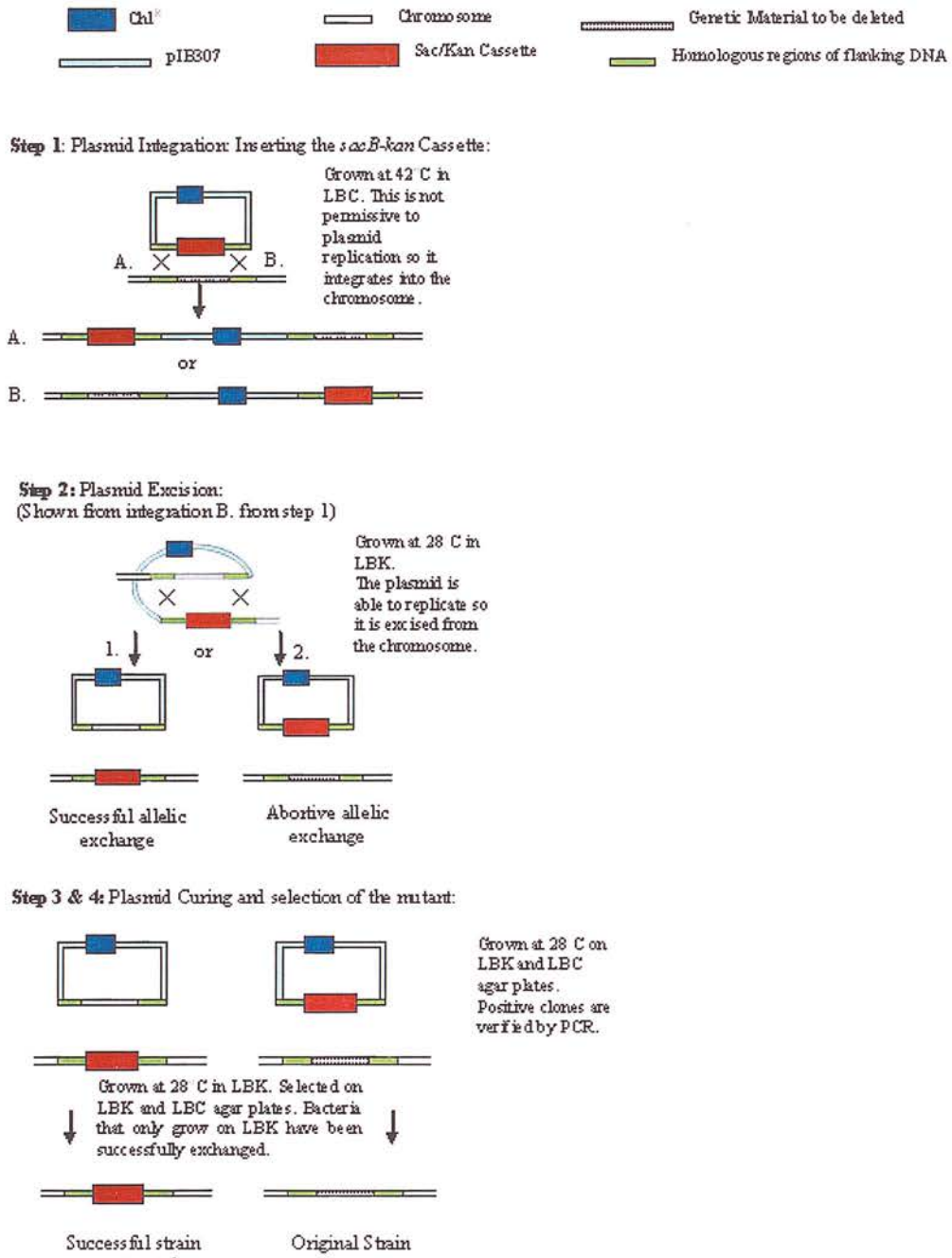

Fig. 1: (Adapted from Blomfield *et al.* 1991). The transfer of the *sacB-kan* cassette into the chromosome requires two recombination events leading to plasmid integration followed by plasmid excision. Step 1: plasmid integrates into the wild-type strain at the non permissive temperature for plasmid replication (42°C). Steps 2 and 3: plasmid integrates are grown at 28°C in the presence of kanamycin to enrich for bacteria that have excised and cured the plasmid, leaving the cassette on the chromosome. Step 4: Growth on media containing LBC or LBK. Bacteria that can only grow on LBK are successful constructs of the intermediate strain.

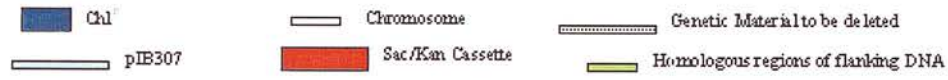

Step 1: Plasmid Integration: Removing the *sacB-kan* Cassette:

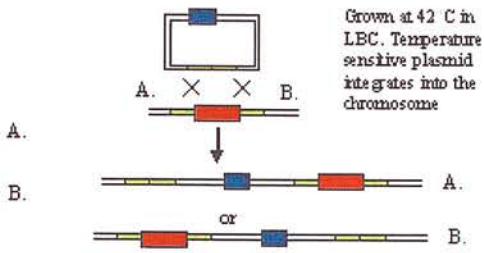

Step 2: Plasmid Excision:
(Shown from integration B. from step 1)

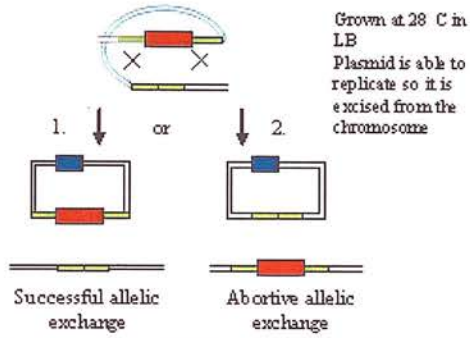

Step 3 & 4: Plasmid Curing and selection of the mutant:

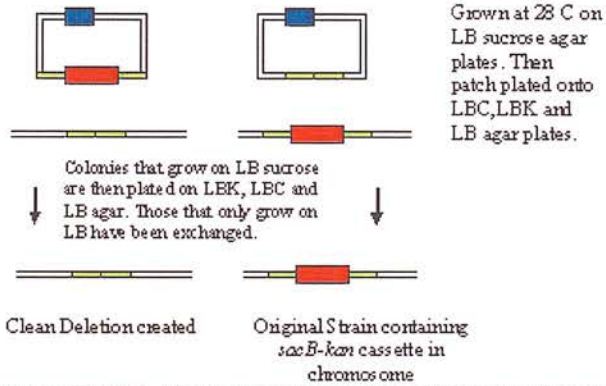

(Adapted from Blomfield *et al.* 1991). Step 1: Plasmid integration in the intermediate strain is selected at the non permissive temperature for replication (42°C). Steps 2 and 3: Plasmid integrates are grown at 28°C in the absence of antibiotics to enrich for bacteria that have excised and later cured (Step 3) the integrated plasmid. Step 4: Growth on media containing sucrose selects for successful strain constructs.

ading to
plasmid
d cured
LBK are

xchange

ACKNOWLEDGMENTS

J.R.E. is supported by a BBSRC funded studentship. D.L.G. and A.J.R. are supported by funding from the Department of Environment, Food and Rural Affairs (DEFRA) VTRI Fellowship. The authors have no conflicts of interest to declare related to this publication.

REFERENCES

1. Falkow S. Molecular Koch's postulates applied to bacterial pathogenicity - a personal recollection 15 years later. *Nat Rev Microbiol* 1994; 2:67-72.
2. Miller JH. Experiments in Molecular Genetics. New York: Cold Spring Harbour Laboratory Press; 1972.
3. Parker B, Marinus MG. A simple and rapid method to obtain substitution mutations in *Escherichia coli*: isolation of a dam deletion/insertion mutation. *Gene* 1988; 73:531-535.
4. Datsenko KA, Wanner BL. One-step inactivation of chromosomal genes in *Escherichia coli* K-12 using PCR products. *Proc Natl Acad Sci USA* 2000; 97:6640-6645.
5. Perna NT *et al.* Genome sequence of enterohaemorrhagic *Escherichia coli* O157:H7. *Nature* 2001; 409:529-533.
6. Spears KJ, Roe AJ, Gally DL. A comparison of enteropathogenic and enterohaemorrhagic *Escherichia coli* pathogenesis. *FEMS Microbiol Letts* 2005; 255:187-202.
7. Campellone KG, Robbins D, Leong JM. EspF(U) is a translocated EHEC effector that interacts with Tir and N-WASP and promotes nck-independent actin assembly. *Dev Cell* 2004; 7:217-228.
8. Roe AJ *et al.* Heterogeneous surface expression of EspA translocon filaments by *Escherichia coli* O157:H7 is controlled at the posttranscriptional level. *Infect Immun* 2003; 71:5900-5909.
9. Naylor SW *et al.* *Escherichia coli* O157:H7 forms attaching and effacing lesions at the terminal rectum of cattle and colonization requires the LEE4 operon. *Microbiol* 2005; 151:2773-2781.
10. Cohen SN, Chang ACY. Revised Interpretation of the Origin of the pSC101 Plasmid. *J Bacteriol* 1997; 132:734-737.
11. Hashimoto-Gotoh TSM, Sekiguchi M. Mutations to Temperature Sensitivity in R Plasmid pSC101. *J Bacteriol* 1977; 131:405-412.
12. Hamilton CM *et al.* New method for generating deletions and gene replacements in *Escherichia coli*. *J Bacteriol* 1989; 171:4617-4622.
13. Blomfield IC *et al.* Allelic exchange in *Escherichia coli* using the *Bacillus subtilis sacB* gene and a temperature-sensitive pSC101 replicon. *Mol Microbiol* 1991; 5:1447-1457.
14. Merlin C *et al.* Tools for characterization of *Escherichia coli* genes of unknown function. *J Bacteriol* 2002; 184:4573-4581.
15. Low AS *et al.* Analysis of fimbrial gene clusters and their expression in enterohaemorrhagic *Escherichia coli* O157:H7. *Env Microbiol* 2006; 8:1033-1047.
16. Roe AJ *et al.* Co-ordinate single-cell expression of LEE4- and LEE5-encoded proteins of *Escherichia coli* O157:H7. *Mol Microbiol* 2004; 54:337-352.
17. Porter ME *et al.* The LEE1 promoters from both enteropathogenic and enterohemorrhagic *Escherichia coli* can be activated by PerC-like proteins from either organism. *J Bacteriol* 2005; 187:458-472.
18. Tsunekawa H *et al.* Acquisition of a sucrose utilization system in *Escherichia coli* K-12 derivatives and its application to industry. *Appl Environ Microbiol* 1992; 58:2081–2088.
19. Johnson JR *et al.* High-Frequency Secondary Mutations after Suicide-Driven Allelic Exchange Mutagenesis in Extraintestinal Pathogenic *Escherichia coli*. *J Bacteriol* 2003; 185:5301-5305.

PROTOCOLS

exchange process relies on a series of sub-culturing steps. Each time 100 µl of the culture is used to inoculate 100 of fresh media. The old culture is discarded and the new inoculated media is incubated for 8 or 16 hours.

ting the *sacB-kan* cassette into the chromosome:

One:
Transform the exchange plasmid into the appropriate strain
Plate 250 µl of the recovered transformation onto LB (Luria-Bertani) agar plates containing chloramphenicol (25 µg/ml)
Recover at 28°C in a static incubator for ~48 hours

Three:
Inoculate 100ml of LBC broth (Luria-Bertani broth containing 25 µg/ml of chloramphenicol) with ~10 colonies from the recovered transformation plate
Incubate at 42°C and 200 RPM in a shaking incubator for ~16 hours

Four:
Sub the culture into 100 ml LBC broth, incubate for ~8 hrs at 42°C and 200 RPM
After 8 hrs repeat the sub-culturing step into LBC and incubate for ~16 hrs at 42°C and 200 RPM

Five:
Duplicate the sub-culturing step into LBC broth and incubate for ~8 hrs at 42°C and 200 RPM
After 8 hrs sub the culture into 100 ml of LBK (Luria-Bertani broth containing 25 µg/ml of kanamyacin) and incubate for ~16 hrs at 28°C and 200 RPM
Before discarding the culture used for the LBK sub create serial dilutions and plate 250 µl of the 10^{-4} and 10^{-5} dilutions onto LBC agar plates. Incubate at 28°C in the static incubator for 16 hours. These can be used to screen for primary integrants if later steps in the allelic exchange process fails

Six:
Sub the culture into 100 ml of the LBK broth and incubate for ~8 hrs at 28°C and 200 RPM
Repeat the sub-culturing step into LBK broth and incubate for ~16 hrs at 28°C and 200 RPM

Seven:
Repeat the sub-culturing step into LBK broth and incubate for ~8 hrs at 28°C and 200 RPM
After 8 hrs create serial dilutions of the culture and plate out 250 µl of the 10^{-3}, 10^{-4}, 10^{-5} and 10^{-6} dilutions onto LBK agar plates and incubate for ~16 hrs in a static incubator at 28°C

Eight:
Use the colonies from the serial dilution LBK agar plates to create patch plates. Each colony screened should be patched on an LBC agar plate first followed by an LBK plate. Only those colonies that grow on LBK and not LBC will be correct. On average 100 – 200 colonies are screened.
The colonies that can only grow on the LBK patch plate are further checked by PCR. They can be screened by using pIB specific primers. Primers that sit inside the deleted genetic material can also be used. The correct strain should only grow on kanamyacin.

Removing the *sacB-kan* cassette from the chromosome, leaving a clean deletion:

Day 1:

- Transform the exchange plasmid (containing the flanking regions and no *sacB-kan* cassette) into the intermediate strain with the *sacB-kan* cassette in the chromosome
- Plate 250 µl of the recovered transformation onto LB (Luria-Bertani) agar plates containing chloramphenicol (25 µg/ml).
- Recover at 28°C in a static incubator for ~48 hours

From this the steps are identical to inserting the *sacB-kan* cassette into the chromosome, up until day four, where the subs go from LBC to LB (not LBK). This is grown and sub-cultured (into LB) in the same way until day seven when the dilutions are plated onto LB agar plates containing 6% sucrose and no NaCl. This is a selective media where any bacteria still containing the *sacB-kan* cassette will not be able to grow; the colonies that do grow are patched onto LBK, LBC and LB (or replica plated). Only those colonies that grow on LB and not LBK or LBC are correct and can be verified by PCR.

Appendix 1

9 Cloning Strategies not Taken Forward

9.1 Strategy for *escN*

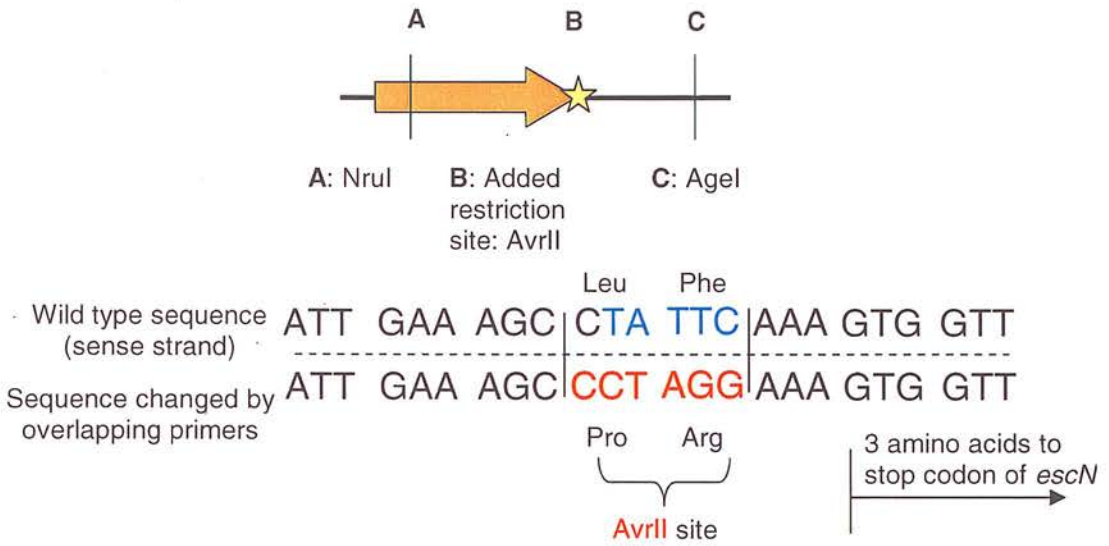

Fig.7 Diagram showing the REases to be used in the strategy for *escN* to add an AvrII recognition site. The nucleotides in blue will be changed in the wild type sequence to form the recognition sequence for AvrII (shown in red).

For the gene *escN* primer 1 (primer F_1 from Fig.5) sits over the REase recognition site NruI, whilst primer 2 sits over AgeI (primer R_2 from Fig.5) and primers 3, 4 add the AvrII site (Fig.7). AgeI is not unique; it is also present in the pIB307 vector. This means that either a partial digest will have to be carried out or the AgeI site in the pIB307 vector will have to be removed. Removal of this site is an option as it is in non essential pIB307 sequence. The site chosen to manipulate is 4 amino acids from the stop codon of the *escN* gene. This position was chosen as it is 17bp from the start of the next gene in the operon, allowing this distance means the addition of a restriction site and a tag will hopefully not interfere with the ribosome binding site for the downstream gene. The non complementary sequence in the 5' primer used to amplify the tag will contain the sequence for the four amino acids from the AvrII site to the stop codon of *escN*. This means that when the tag is cloned into the AvrII site the whole of the *escN* coding sequence (without the stop codon) will be transcribed before the start of the fused tag.

9.2 Strategy for *escV*

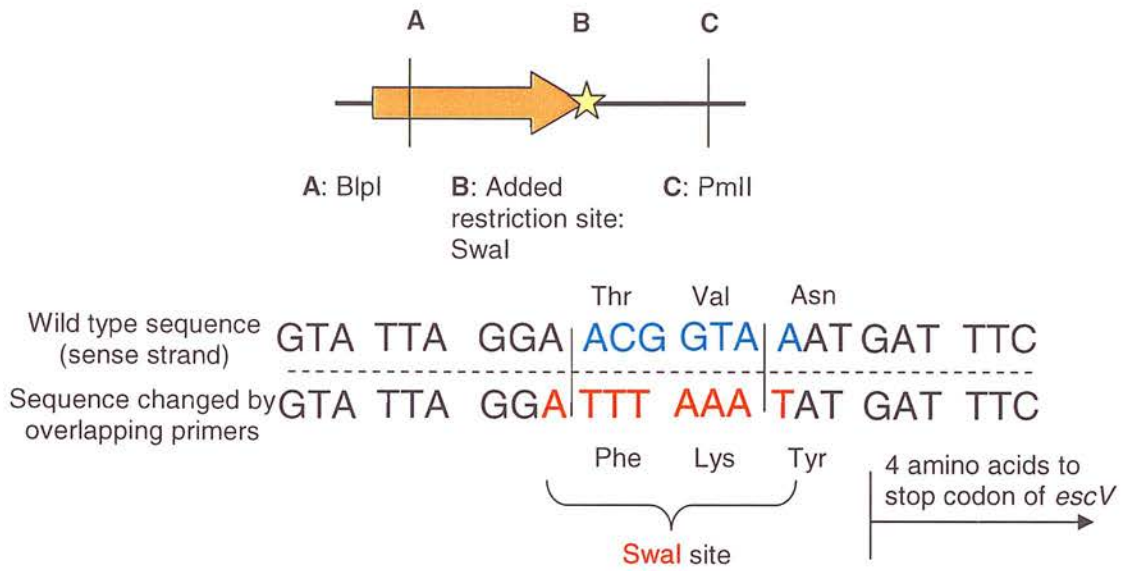

Fig.8 Diagram showing the REases to be used in the strategy for *escV* to add a SwaI recognition site. The nucleotides in blue will be changed in the wild type sequence to form the recognition sequence for SwaI (shown in red).

The strategy for *escV* has primer 5 (primer F_1) situated over the BlpI recognition site and primer 6 (primer R_2) over the PmlI site with primers 7, 8 overlapping to add a SwaI recognition site (Fig.8). The strategy is made slightly more complicated as the ATG start of *escN* is 15bp before the 3' end of *escV*. This means that the 5' primer for the tag will contain the sequence for the 5 amino acids from the added SwaI site to the 3' end of *escV*. The 3' primer for the tag will also contain 9bp after the stop codon for the tag and before the SwaI site in the 3'primer, which will recreate the sequence that may contain the ribosome binding site for *escN*. When the tag is cloned into the SwaI recognition site the 9bp in the 3' primer tail for the tag will be repeated; once naturally in the coding region for *escV* before the added SwaI site and then again after the stop codon for the tag as non-coding DNA before the start codon of *escN*.

9.3 Strategy for *escS*

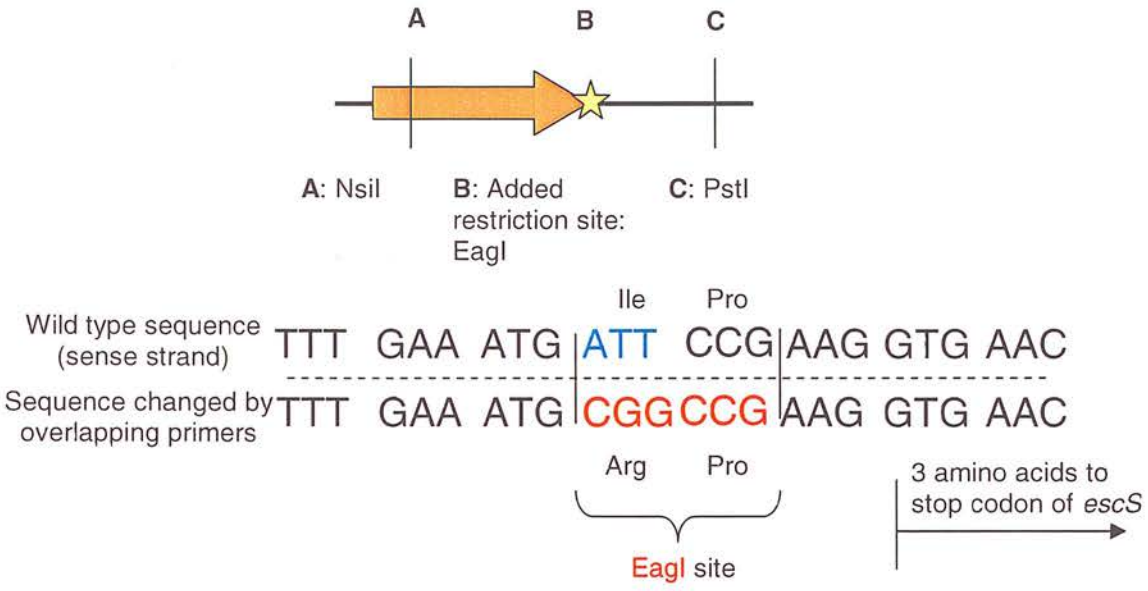

Fig.10 Diagram showing the REase to be used in the strategy for *escS* to add an EagI recognition site. The nucleotides in blue will be changed in the wild type sequence to form the recognition sequence for EagI (shown in red).

The primers over the unique restriction sites for *escS* are the same as the primers for *escR* (primers 9, 10) (Fig.10). To tag both *escR* and *escS* in the same strain either one of *escS* or *escR* would have to be made first and cloned into the pIB307 plasmid containing the *escRSTU* genes. This plasmid would then be used as the DNA template for the PCR reactions needed to create the second tagged gene. When this is cloned the plasmid will contain tagged versions of both *escS* and *escR*. The ATG start codon of *escT* is 14bp from where primers 13, 14 overlap to add an EagI REase site and the site is 4 amino acids from the stop codon of *escS*. The 5' primer tail for the PCR of the tag should contain the 12bp for these 4 amino acids.

9.4 Strategy for *escT*

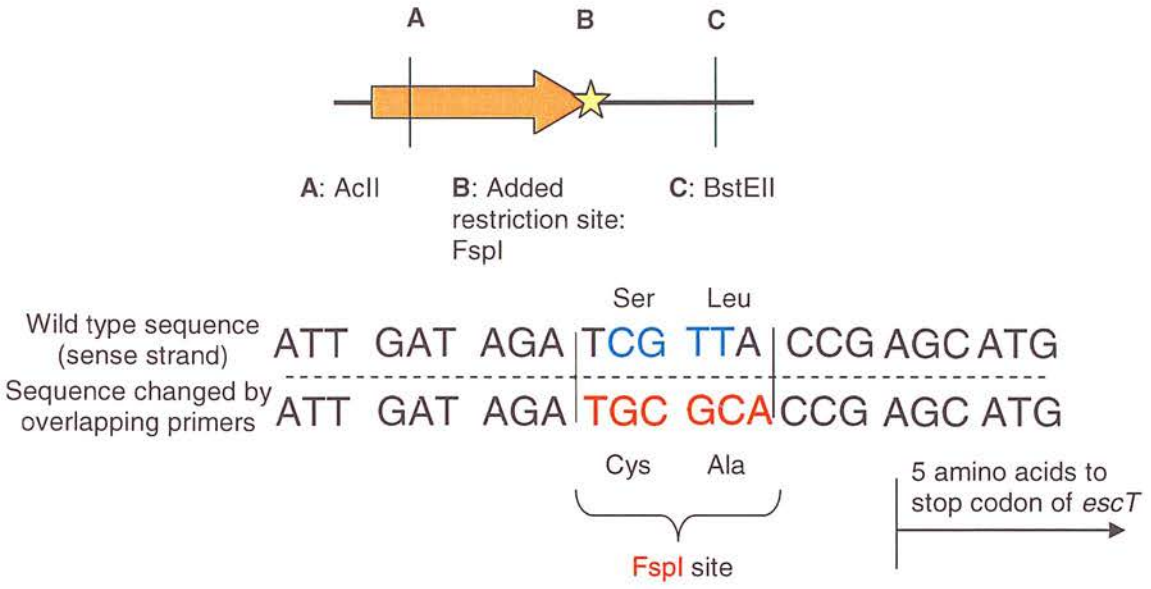

Fig.11 Diagram showing the REases to be used in the strategy for *escT* to add an FspI recognition site. The nucleotides in blue will be changed in the wild type sequence to form the recognition sequence for FspI (shown in red).

Primer 15 for *escT* is over the unique REase recognition site AcII, and primer 16 over BstEII. The added REase recognition site is FspI, added by primers 17, 18 and is 6 amino acids from the stop codon of *escT* (Fig.11). The ATG of *escU* is 5bp upstream from the stop codon for *escT*. This means there are 13bp from the ATG of *escU* and the added restriction site. These six amino acids will be added in the non complementary sequence in the tail of the 5' primer used in the PCR for the tag that will be added at the FspI site. The distance on the chromosome between the added REase recognition site and the start of *escU* should be enough not to interfere with the ribosome binding site for *escU*.

9.5 Table of Primers Designed for Cloning Strategies, but not Taken Forward

Primer No.	PCR Product Name	Sequence	Paired primer	PCR size	T_a (°C)	5' / 3' primer	Additional Information
Primer 1	*escN* PCR 1	GAACGTGG***tcgcga***AGTAAATGAATTCCTCG	4	~730bp	NU	5'	Situated over *Nru*I site
Primer 2	*escN* PCR 2	GCTAATATAGAGGCG***accggt***TCCG	3	~850bp	NU	3'	Situated over *Age*I site
Primer 3	*escN* PCR 2	CGATTGAAAGC***cctagg***AAAGTGGTGC	2	~850bp	NU	5'	Addition of *Avr*II
Primer 4	*escN* PCR 1	GCAACCACTTT***cctagg***GCTTTCAATCG	1	~730bp	NU	3'	Addition of *Avr*II
Primer 5	*escV* PCR 1	CTAATAGCCAAAACATCTCACCGGGC***g***	8	~980bp	NU	5'	Situated over *Blp*I site
Primer 6	*escV* PCR 2	CGATGCAAGCCCAACAT***cacgtg***C	7	~840bp	NU	3'	Situated over *Pml*I site
Primer 7	*escV* PCR 2	GTATTAGG***atttaaat***ATGATTTC	6	~840bp	NU	5'	Addition of *Swa*I site
Primer 8	*escV* PCR 1	GAAATCAT***atttaaat***CCTAATAC	5	~980bp	NU	3'	Addition of *Swa*I site